

This electronic thesis or dissertation has been downloaded from the King's Research Portal at <https://kclpure.kcl.ac.uk/portal/>

## Evaluation of the role of odontoblasts in dental pain

Egbuniwe, Obi

*Awarding institution:*  
King's College London

The copyright of this thesis rests with the author and no quotation from it or information derived from it may be published without proper acknowledgement.

### END USER LICENCE AGREEMENT



Unless another licence is stated on the immediately following page this work is licensed

under a Creative Commons Attribution-NonCommercial-NoDerivatives 4.0 International

licence. <https://creativecommons.org/licenses/by-nc-nd/4.0/>

You are free to copy, distribute and transmit the work

Under the following conditions:

- Attribution: You must attribute the work in the manner specified by the author (but not in any way that suggests that they endorse you or your use of the work).
- Non Commercial: You may not use this work for commercial purposes.
- No Derivative Works - You may not alter, transform, or build upon this work.

Any of these conditions can be waived if you receive permission from the author. Your fair dealings and other rights are in no way affected by the above.

### Take down policy

If you believe that this document breaches copyright please contact [librarypure@kcl.ac.uk](mailto:librarypure@kcl.ac.uk) providing details, and we will remove access to the work immediately and investigate your claim.

This electronic theses or dissertation has been downloaded from the King's Research Portal at <https://kclpure.kcl.ac.uk/portal/>

**Title:** Evaluation of the role of odontoblasts in dental pain

**Author:** Obi Egbuniwe

The copyright of this thesis rests with the author and no quotation from it or information derived from it may be published without proper acknowledgement.

#### END USER LICENSE AGREEMENT



This work is licensed under a Creative Commons Attribution-NonCommercial-NoDerivs 3.0 Unported License. <http://creativecommons.org/licenses/by-nc-nd/3.0/>

You are free to:

- Share: to copy, distribute and transmit the work

Under the following conditions:

- Attribution: You must attribute the work in the manner specified by the author (but not in any way that suggests that they endorse you or your use of the work).
- Non Commercial: You may not use this work for commercial purposes.
- No Derivative Works - You may not alter, transform, or build upon this work.

Any of these conditions can be waived if you receive permission from the author. Your fair dealings and other rights are in no way affected by the above.

#### Take down policy

If you believe that this document breaches copyright please contact [librarypure@kcl.ac.uk](mailto:librarypure@kcl.ac.uk) providing details, and we will remove access to the work immediately and investigate your claim.

# Evaluation of the role of odontoblasts in dental pain

Obinna C Egbuniwe

**Thesis submitted for the degree of Doctor of Philosophy at King's College  
London**

**Biomaterials, Biomimetics and Biophotonics**

**Dental Institute, King's College London**

**July 2012**

## **Abstract**

Dental pain is a very common ailment affecting a large percentage of people and its mechanisms are not well understood, thus impairing the development of new therapies. The current paradigm of dental pain is that thermal or osmotic changes around a tooth produce movements within the dentine fluid, which are detected through mechanoreceptors on dental sensory neurons. However, initial studies have identified tentative links between TRP channels and dental pain, suggesting that TRP channels in dental nociceptive neurons may be directly activated by temperature changes and contribute to sensitivity to hot or cold foods. Certain structural and biochemical properties of odontoblasts suggest that they may also play a role in pain sensation.

The aim of this project was to investigate the expression of pain-related ion channels (TRP channels) in human pulp cells (odontoblasts). Dental pulp cells were isolated and cultured in conditioned medium to allow for differentiation following which they were characterized by demonstrating the expression of odontoblast phenotypic markers. This cell culture model was optimized and a viable immortalised cell line established, and then used to determine the responsiveness of these odontoblast-like cells to TRP channel agonists and antagonists following the identification of their expression. The data obtained from this study will serve as a template for the better understanding of the function of TRP channels in human odontoblasts.

## Publications and posters

Egbuniwe O, Koller G, Grant A, Renton T, Di Silvio L (2011). *P16/P53 expression and telomerase activity in immortalized human dental pulp cells*. Cell Cycle. 10: 3912 - 3919.

Egbuniwe O, Grant A, Renton T, Di Silvio L (2010). *Characterization of isolated populations of human dental pulp stem cells*. European Society for Biomaterials Conference, Tampere, Finland (poster).

Egbuniwe O, Koller G, Grant A, Renton T, Di Silvio L (2009). *The role of human dental pulp cells in tissue repair*. United Kingdom Society for Biomaterials Conference, Ulster, Ireland (poster).

Egbuniwe O, Grant A, Renton T, Di Silvio L (2009). Investigating the role of odontoblasts in dental pain (Establishing culture techniques for pulpal precursor cells). Bone Stem Cells - A European Science Foundation Workshop: "Regenerative Medicine" (REMEDI) Research Networking Programme, Bertinoro (Forlì), Italy (Oral presentation)

Egbuniwe O, Grant A, Renton T, Di Silvio L (2009). *In vitro culture and characterization of odontoblast cells from adult human pulp tissue*. European Society for Biomaterials Conference, Lausanne (poster).

## Grants

Central Research Fund (University of London Scholarship Fund), 2009

Polymer and Drug Delivery Grant (Institute of Polymer Science and Technology, Madrid- Spain), 2009

Doctoral Student Sponsorship (Primer Design UK), 2010

## Acknowledgements

I would like to start off by thanking my supervisors Professor Lucy Di Silvio, Dr Andrew Grant and Professor Tara Renton for providing the opportunity for the development of the body of work presented in this thesis. I am most grateful to all three of my supervisors for the academic, technical and moral support and guidance I received from them over the last three and three-quarter years - Dr Grant for painstakingly teaching me the basics of several bench-side research techniques as well as helping me improve my scientific writing; Professor Di Silvio for her academic mentoring and her constant accessibility and Professor Renton whose infectious enthusiasm for dental research shared with me one fine July afternoon in 2008 and subsequent well founded advice and tutelage all through the course of my time at King's College.

I would also like to thank a number of people without whose assistance I would have been lost. My thanks go to Aneesha Shah, Kiran Benang and George Paolinelis for their invaluable clinical assistance in obtaining the human teeth samples used in this study, Garritt Koller and Carl Hobbs for all their help with the immunocytochemical and immunohistochemical work, Borvornwut Buranawat (BB) for showing me how to perform ALP and DNA assays, my sister Isy Egbuniwe for her invaluable advice on FACS analysis, Jack Bircher for his generosity with his CHO cells, Hannes Keisewetter for teaching me all I know about qPCR assays, John Dawes for taking time out of writing his thesis to help me with running micro array assays as well as the occasional five-side football game, Sowmya Shetty for her help with the statistical studies and Sibani Grover for her help with TRP calcium assays . I would also like to thank all members of the Floor 17 Biomimetics, Biophotonics and Biomaterials (B3) group as well as members of the Mac Lab who provided an amenable working environment. To Stefania Mazzetelli, Almas Waqar, Elisa Fiorentini, Paula Coward, Neelam Gurav, I am grateful for the kind words and advice and, to Pete Pilecki and Richard Mallet for all the technical assistance (and pints of beer).

And finally a special thanks to my family, whose support has been indescribable and, to Isi and Aby who have been my pillars of strength, putting up with my hang-ups and tantrums over the last four years. I am indebted to you all.

# Table of Contents

<b>ABSTRACT</b>	<b>2</b>
<b>PUBLICATIONS AND POSTERS</b>	<b>3</b>
<b>ACKNOWLEDGEMENTS</b>	<b>4</b>
<b>TABLE OF CONTENTS</b>	<b>6</b>
<b>LIST OF FIGURES</b>	<b>10</b>
<b>LIST OF TABLES</b>	<b>16</b>
<b>ABBREVIATIONS</b>	<b>17</b>
<b>LITERATURE REVIEW</b>	<b>20</b>
<b>1.1 PAIN AND PAIN SIGNALLING</b>	<b>20</b>
<b>1.2 OROFACIAL PAIN</b>	<b>21</b>
<b>1.3 ANATOMY OF THE TOOTH</b>	<b>23</b>
<b>1.4 AN OVERVIEW OF TOOTH FORMATION</b>	<b>25</b>
1.4.1 THE DENTINE – PULP COMPLEX	29
1.4.2 ODONTOBLASTS	31
1.4.3 ODONTOBLAST DIFFERENTIATION	32
1.4.4 CONTROL AND REGULATION OF ODONTOBLAST DIFFERENTIATION	33
1.4.5 DENTINE MATRIX FORMATION	34
1.4.6 MINERALISATION OF DENTINE	38
1.4.7 DENTAL PULP STEM CELLS	38
1.4.7.1 METHODS OF ISOLATING DENTAL PULP STEM CELLS	42
<b>1.4.8 PAIN PHYSIOLOGY AND THE MECHANICS OF SOMATIC PAIN</b>	<b>43</b>
<b>1.5 AN OVERVIEW OF DENTAL PULP PHYSIOLOGY</b>	<b>44</b>
1.5.1 INNERVATION OF THE DENTAL PULP	44
1.5.2 PULPAL NEUROPEPTIDES AND THE RESPONSE TO INJURY	45
<b>1.6 THE SKIN AS A MODEL SENSORY ORGAN</b>	<b>48</b>
<b>1.7 SENSORY MECHANISMS IN THE DENTAL PULP AND THE HYDRODYNAMIC THEORY</b>	<b>50</b>
<b>1.8 ODONTOBLASTS AND SENSORY TRANSDUCTION</b>	<b>54</b>
<b>1.9 TRANSIENT RECEPTOR POTENTIAL (TRP) CHANNELS</b>	<b>56</b>
1.9.1 TRANSIENT RECEPTOR POTENTIAL (TRP) CHANNELS – AN OVERVIEW	56
1.9.2 TRANSIENT RECEPTOR POTENTIAL (TRP) CHANNELS IN THE DENTAL PULP	60
1.9.3 CALCIUM SIGNALLING AND TRANSIENT RECEPTOR POTENTIAL (TRP) CHANNELS	62
<b>1.10 AIMS AND OBJECTIVES</b>	<b>64</b>
<b>GENERAL MATERIALS AND METHODS</b>	<b>69</b>
<b>2.1 ESTABLISHMENT OF PRIMARY CELL CULTURES</b>	<b>69</b>



<b>2.2</b>	<b>CELL VIABILITY COUNTS</b>	<b>69</b>
<b>2.3</b>	<b>PREPARATION OF CELL LYSATES</b>	<b>70</b>
<b>2.4</b>	<b>DNA QUANTIFICATION ASSAY</b>	<b>70</b>
<b>2.5</b>	<b>ALKALINE PHOSPHATASE ACTIVITY ASSAY</b>	<b>71</b>
<b>2.6</b>	<b>CELL PROLIFERATION ASSAY</b>	<b>71</b>
<b>2.7</b>	<b>IMMUNOCYTOCHEMISTRY</b>	<b>72</b>
<b>2.8</b>	<b>RNA EXTRACTION AND ANALYSIS</b>	<b>73</b>
<b>2.9</b>	<b>CDNA SYNTHESIS</b>	<b>73</b>
<b>2.10</b>	<b>PRIMERS FOR REVERSE TRANSCRIPTION-POLYMERASE CHAIN REACTION</b>	<b>74</b>
<b>2.11</b>	<b>AGAROSE GEL ELECTROPHORESIS</b>	<b>77</b>
<b>2.12</b>	<b>GEL IMAGING</b>	<b>77</b>
<b>2.13</b>	<b>REVERSE TRANSCRIPTION-QUANTITATIVE POLYMERASE CHAIN REACTION</b>	<b>78</b>
2.13.1	REFERENCE GENES	78
2.13.2	QRT-PCR WORKFLOW	78
2.13.3	QRT-PCR DATA ANALYSIS	79
<b>2.13.4</b>	<b>DESIGNING THE PRIMERS FOR QRT-PCR EXPERIMENTS</b>	<b>80</b>
2.13.5	SENSITIVITY AND SPECIFICITY OF DESIGNED PRIMER SETS	80
<b>2.14</b>	<b>TAQMAN MICROARRAY ANALYSIS</b>	<b>81</b>
<b>2.15</b>	<b>SAMPLE STORAGE</b>	<b>82</b>
2.15.1	CRYOPRESERVATION	82
2.15.2	RESUSCITATION OF CRYOPRESERVED DPSCs	82
<b>ISOLATION OF DENTAL PULP CELLS</b>		<b>85</b>
<b>3.2</b>	<b>MATERIALS AND METHODS</b>	<b>86</b>
3.2.1	ESTABLISHMENT OF PRIMARY CELL CULTURES	86
3.2.2	CELL VIABILITY COUNTS	89
3.2.3	CELL PROLIFERATION ASSAY	89
3.2.4	ALKALINE PHOSPHATASE ACTIVITY ASSAY	90
3.2.5	IMMUNOCYTOCHEMISTRY	90
3.2.6	RNA EXTRACTION FROM ISOLATED PULP TISSUE	90
3.2.7	RNA EXTRACTION FROM ESTABLISHED HUMAN PULP TISSUE CELL CULTURES	92
3.2.9	CRYOPRESERVATION	94
3.2.10	STATISTICAL METHODS	94
<b>3.3</b>	<b>RESULTS</b>	<b>96</b>
3.3.1	CELL ISOLATION METHODS	96
3.3.2	CELL PROLIFERATION ASSAY	97
3.3.3	ALP ACTIVITY FINDINGS	98
3.3.4	CELL MORPHOLOGY AND CHARACTERISATION	99
3.3.5	RNA EXTRACTION	100
3.3.6	EXPRESSION OF ODONTOBLASTIC PHENOTYPE MARKERS	103
<b>3.4</b>	<b>DISCUSSION</b>	<b>107</b>
<b>OPTIMIZATION OF THE ODONTOBLAST CELL CULTURE MODEL</b>		<b>114</b>
<b>4.1</b>	<b>INTRODUCTION</b>	<b>114</b>
<b>4.2</b>	<b>MATERIALS AND METHODS</b>	<b>119</b>

4.2.1	POPULATION DOUBLING STUDIES	119
4.2.2	SERUM CONTENT OF CELL CULTURE MEDIA	119
4.2.3	GLUCOSE CONTENT OF CELL CULTURE MEDIA	120
4.2.4	RT-PCR TO DEMONSTRATE MULTI-LINEAGE POTENTIAL OF DPCs	120
4.2.5	DPC TRANSDUCTION	121
4.2.6	TRAP (TELOMERE REPEAT AMPLIFICATION PROTOCOL) ASSAY	122
4.2.7	BETA-GALACTOSIDASE STAINING	122
4.2.8	GENE DETECTION USING REVERSE TRANSCRIPTION POLYMERASE CHAIN REACTION	123
4.2.9	DNA CONTENT ASSAY	123
4.2.10	ALKALINE PHOSPHATASE ASSAY	124
4.2.11	IMMUNOCYTOCHEMISTRY	124
4.2.12	FLUORESCENCE ACTIVATED CELL SORTING (FACS)	125
4.2.13	REVERSE TRANSCRIPTION-QUANTITATIVE POLYMERASE CHAIN REACTIONS	126
4.2.14	STATISTICAL ANALYSIS	126
<b>4.3</b>	<b>RESULTS</b>	<b>127</b>
4.3.1	POPULATION DOUBLING STUDIES	127
4.3.2	SERUM CONTENT AND GLUCOSE CONCENTRATION STUDIES	128
4.3.3	RT-PCR ANALYSIS OF DPCs: BEFORE AND AFTER TRANSDUCTION	130
4.3.4	TRAP ASSAY READINGS	132
4.3.5	BETA GALACTOSIDASE STAINING	133
4.3.6	EVALUATION OF DNA CONTENT AND ALP ACTIVITY AFTER TRANSDUCTION	135
4.3.7	ANALYSIS OF CYTOSKELETAL STRUCTURE BY FLUORESCENCE MICROSCOPY	136
4.3.8	STEM CELL MARKERS	138
4.3.9	QUANTITATIVE REAL TIME PCR RESULTS	146
4.3.10	EXPRESSION OF ODONTOBLASTIC AND ONCOGENIC MARKERS	149
<b>4.4</b>	<b>DISCUSSION</b>	<b>152</b>
<b><u>TRANSIENT RECEPTOR CHANNEL EXPRESSION AND FUNCTION IN ODONTOBLASTS</u></b>		<b>160</b>
<b>5.1</b>	<b>INTRODUCTION</b>	<b>160</b>
<b>MATERIALS AND METHODS</b>		<b>164</b>
5.2.1	(A) DETECTION OF TRP CHANNELS IN HUMAN WHOLE PULP SAMPLES	164
5.2.1	(B) IDENTIFICATION OF TRP CHANNELS AND NEUROPEPTIDE RECEPTORS IN NDPSCs AND TDPSCs	164
5.2.2	INVESTIGATION OF LONG-TERM TRP CHANNEL EXPRESSION	165
5.2.3	MEASUREMENT OF INTRACELLULAR $[Ca^{2+}]_i$ IN CULTURED ODONTOBLASTS	165
5.2.4	MEASUREMENT OF ATP RELEASE	167
<b>5.3</b>	<b>RESULTS</b>	<b>169</b>
5.3.1	RT-PCR ANALYSIS OF TRP CHANNEL EXPRESSION	169
5.3.2	QUANTITATIVE GENE EXPRESSION OF TRP CHANNELS AND NEUROPEPTIDE RECEPTORS	171
5.3.3	IDENTIFICATION OF ODONTOBLAST TRP CHANNELS THROUGH $Ca^{2+}$ IMAGING	174
5.3.4	TRP CHANNEL INDUCED ATP RELEASE	181
5.3.5	EFFECTS OF SP ON TRP CHANNEL EXPRESSION AND ACTIVITY	182
<b>5.4</b>	<b>DISCUSSION</b>	<b>184</b>
5.4.1	TRP CHANNEL EXPRESSION	184
5.4.2	ANALYSIS OF TRP CHANNEL FUNCTION BY SINGLE CELL IMAGING	185
5.4.3	TDPSC $K^+$ CHANNEL EXPRESSION	188

5.4.4	ANALYSES OF TRP CHANNEL ACTIVATION AND INHIBITION	188
5.4.5	TRP CHANNEL-EVOKED ATP RELEASE	190
5.4.6	TDPSC EXPRESSION OF TACHYKININ RECEPTORS	191
5.4.8	SUMMARY	192
<b>GENERAL DISCUSSIONS AND CONCLUSIONS</b>		<b>195</b>
<hr/>		
6.1	SUMMARY	195
6.2	SUGGESTED MODIFICATIONS TO EXPERIMENTAL TECHNIQUES	196
6.3	PAIN ASSOCIATED GENE EXPRESSION IN PAINFUL AND NON PAINFUL PULPS	198
6.3B	MICROARRAY FINDINGS	199
6.4	CONCLUSIONS	204
<b>REFERENCES</b>		<b>206</b>
<hr/>		

## List of Figures

Figure 1: 1 Schematic cross section of a human tooth (adapted from intranet.tdmu.edu.ua) .....	24
Figure 1:2 Modified photomicrograph images of a tooth bud from Ten Cate's Oral Histology (Nanci and Cate 2008). The developing tooth bud is composed of the enamel organ, dental papilla and dental follicle. Differentiation within the enamel organ will yield 4 cell types: outer enamel (dental) epithelium, stellate reticulum, stratum intermedium and the inner enamel (dental) epithelium. With the loss of the middle 2 layers of the enamel organ, both inner and outer enamel (dental) epithelial layers will appose each other at the cervical loop and grow downwards into the dental papilla to yield the root sheath of Hertwig that determines the shape of the root of the tooth.....	27
Figure 1:3 A modified schematic overview of human tooth development showing tooth germ derivatives and their secretory products (Nanci and Cate 2008).....	28
Figure 1:4 Hematoxylin and Eosin (H&E; x 400µm) staining of the dentin and pulp tissues. 1: odontoblast cell bodies; 2: dentinal tubules; 3: odontoblast processes in the dentinal tubules. Adapted from (Wu and Schwartz 2008) and <a href="http://www.sciencephoto.com">http://www.sciencephoto.com</a> .....	31
Figure 1: 5 Architecture of a TRP channel. The region between the fifth and sixth domains forms the region, which contains the selectivity filter. The cytoplasmic N and C terminals contain regulatory complexes and enzymes and the relevance of their function to that of the TRP channels are not entirely clear (Clapham 2003; Voets, Janssens et al. 2004). .....	57
Figure 3:1: A schematic workflow chart of the three different methods of dental pulp cell isolation used. The teeth were aseptically held in place on the mount on an Isomet 1000 Precision Saw (Buehler) using dental wax (Kemdent) and were then cut along the cervical margin or the longitudinal axis as indicated by the black arrows in Figure 3.1 (A - C).....	87
Figure 3:2: Phase contrast image of a 4mm area of the counting chamber showing live and dead cells 30 seconds after staining with TC10™ trypan blue dye. A= SCi-derived cells; B= ICi-derived cells; C=PEX-derived cells. The live cells are the green circles and the dead cells appear as the red circles. The black speckles are cellular debris, which took up the blue dye. The graph shows effect of the different isolation methods on cell viability. The cell numbers are representative of cells/ml. The error bars demonstrate the standard error from the mean (technical replicates). .....	97
Figure 3:3: Cell proliferation rates as determined by means of an MTS assay. There was a significantly higher level of activity seen in the SCi-derived cells compared to the PEX-group. The results shown are expressed as the mean ± S.E of triplicate experiments (technical replicates) with significance differences measured between the 3 cell groups at the different time points by one-way ANOVA and post hoc Bonferroni's test, (* <i>p</i> < 0.05, ** < 0.01, *** < 0.001). .....	98
Figure 3:4: Rates of cell mineralization as determined by means of alkaline phosphatase enzyme activity. Optical density (OD) absorbance readings at 490nm are represented by arbitrary values as denoted by the scale on the x-axis. The data shows that ALP activity is significantly higher in the SCi-derived cells compared to the PEX-group at days 3 and 7. The results shown are expressed as the mean ± S.E of triplicate experiments (technical replicates) with significance differences measured between the 3 cell groups at the different time points by one-way ANOVA and post hoc Bonferroni's test, n=12 (* <i>p</i> < 0.05, ** < 0.01, *** < 0.001).....	99
Figure 3:5: A representation of the cytoskeletal characterization of the isolated cells from the 3 groups (SCi, ICi and PEX) by confocal microscopy. The cells were cultured for 14 days (passages 3 and 4) and analyzed. Green = actin filaments, Blue = cell nuclei, Scale bar = 400µm. The merged images are composites of the FITC and DAPI images. The images labelled PCI are phase contrast images of the appropriately labelled cell groups at day 14. The spindle shape observed on confocal microscopy was once again evident in all 3 of the cell groups. Scale bar = 40 µm .....	100

- Figure 3:6: The influence of cell isolation and extraction methods on the quality of RNA extracted assessed by Nanodrop spectrophotometry. The values represent mean concentrations (ng/μl), absorbance ratios (A260/A280 and A260/A230) of three independently processed cell isolates and are represented by arbitrary values as denoted by the scale on the x-axis. The data was analysed using one-way ANOVA and post hoc Bonferroni's test: \* $p < 0.05$ , \*\*  $< 0.01$ , \*\*\*  $< 0.001$ . Pure RNA gives an A260/A280 ratio of approximately 1.9 – 2.2 and an A260/A230 absorbance ratio of approximately 1.6 to 1.8. Cell isolation method and RNA extraction method significantly affected the concentration of RNA obtained (\*\* $p < 0.001$ )..... **102**
- Figure 3:7:** Representative agarose gels containing RT-PCR products that show the expressions of genes associated with the odontoblastic phenotype in the SCi-, ICi- and PEx-derived cell isolates analyzed at day 14 of cell culture. These included alkaline phosphatase (ALP), collagen type-I (Col-I), dentine sialophosphoprotein (DSPP), and dentine matrix protein-1 (DMP1). The housekeeping gene GAPDH was expressed in all samples. The vertical array of bands on the left side of each gel image represents a PCRSizer 1000bp ladder (Norgen, Biotek Corporation) and was used to determine product size. .... **103**
- Figure 3:8:** Standard curves of the real time RT-PCR assays for CD44 (A) and CD45 (B). Ten-fold dilutions of plasmid DNA prior to amplification were used ranging from  $1 \times 10^0$  to  $1 \times 10^4$  copies (indicated on the y-axis) with the CT values represented on the x-axis. The co-efficient of determination ( $R^2$ ) is indicated on the graphs. The CT values for the primers were: CD44 (32.204) and CD45 (35.232). .... **105**
- Figure 3:9:** Expression of mesenchymal surface markers CD45 (A) and CD44 (B), odontoblast differentiation markers DMP-1(C) and DSPP (D) ALP (E) and COL-1 (F) was determined by real-time qPCR. Values are reported as relative fold change in cDNA concentration, which was normalised to the housekeeping gene. The data are represented as the mean  $\pm$  S.E of triplicate experiments (technical replicates) with significance differences measured between the 3 cell groups by one-way ANOVA and post hoc Bonferroni's test (\* $p < 0.05$ , \*\* $p < 0.01$ , \*\*\* $p < 0.001$ ). ..... **106**
- Figure 4:1: The map of the pBABE-puro-hTERT gene designed for use in humans. The hTERT insert size is 3500 base pairs (bp) and the pBABE-puro backbone size is 5169 base pairs (bp). The 5' sequencing primer is pBABE 5' and the 3' sequencing primer is pBABE-3'. The 5'- and 3' cloning sites are *EcoRI* and *SalI* respectively. The plasmid was designed to confer resistance to ampicillin, and the selection marker to determine its uptake was puromycin (Counter, Hahn et al. 1998). ..... **121**
- Figure 4:2 Population doubling assessed in DPSCs cultured in media containing 1.0mM and 4.5mM concentrations of glucose over six culture passages spanning a 56-day period (n=5). Scale bars in A, B, D, E = 40 microns. C, F = 100 microns..... **127**
- Figure 4:3 Cell populations of DPCs exposed to 1.0mM and 4.5mM glucose concentrations were counted over 21 days. In each of the experimental groups, the cells in different sub-groups were cultured in 5%, 10% and 20% concentrations of fetal calf serum (FCS). (n=7 per sub-group)..... **129**
- Figure 4:4 Analysis of the influence of glucose concentrations (1.0mM and 4.5mM) on cell proliferation over a 21-day period in DPCs. Mesenchymal controls (\*D0) were used. The values are means of the optical absorbance readings at 490nm  $\pm$  SE and the data was analysed using one-way ANOVA and post hoc Bonferroni's test: \* $p < 0.05$ , \*\*  $< 0.01$ , \*\*\*  $< 0.001$ . (n = 7,\*d0 Vs d14 - \*\* $< 0.01$ ; \*D0 Vs D14 - \*\* $< 0.01$ ). ..... **129**
- Figure 4:5 RT-PCR was used to identify the expression of non-odontoblastic and transcription factors in human dental pulp cell populations (A). Mesenchymal cells were run as a control (B) GAPDH served as an internal control. .... **130**
- Figure 4:6: The identification of the hTERT expression profile in tDPSCs (B) following retroviral transduction. No hTERT band was visible in the nDPSCs (A). GAPDH was used as an internal control. No visible bands were observed in mesenchymal controls (MyhTERT)..... **131**

Figure 4: 7: The cells maintained an odontoblastic phenotype as evidenced by the presence of mRNA expression for DMP-1, DSPP and Cbfa-1 in nDPCs (A) and tDPCs (B). There was no visible expression of DSPP in mesenchymal controls (MyDSPP). GAPDH was used as an internal control. ....	<b>132</b>
Figure 4:8. Following the introduction of hTERT, relative fluorescent readings were used to analyse telomerase expression in early (EtDPSCs) and late (LtDPSCs) passage cells and nDPSCs. Telomerase positive cells (TM+) provided in the assay kit, were used as controls The data was analysed using one-way ANOVA and post hoc Bonferroni's test: (Mean $\pm$ SD, n=4; * $p$ < 0.05, ** < 0.01, *** < 0.001). ....	<b>133</b>
Figure 4:9a. Beta-galactosidase staining in cultured nDPSCs and tDPSCs. Scale bar in A and C = 100x magnification; B and D = x200 microns magnification. Figure 4:9b shows graphical representation of early passage nDPSCs (passage 6) that showed > 80% positive beta galactosidase staining. This positive staining was only seen in the tDPSCs at passage 30, with < 10% positivity. Positive staining was absent after re-plating tDPSCs.....	<b>134</b>
Figure 4:10. Analyses of cell proliferation (B – DNA assay) and cell mineralization (A- ALP assay) in cultured tDPSCs and nDPSCs. Mesenchymal controls (*D0) were used in all experiments. The values are means of the optical density absorbance readings at 490nm. The data was analysed using one-way ANOVA and post hoc Bonferroni's test: (Mean $\pm$ SD, n=4; * $p$ < 0.05, ** < 0.01, *** < 0.001; <u>Figure 4:10A</u> : *d0 Vs d7 - *<0.05; *D0 Vs D7 - **<0.01; <u>Figure4: 10B</u> : *d0 Vs d7 - *<0.05; *D0 Vs D7 - **<0.01). ....	<b>135</b>
Figure 4:11. Optical phase contrast images showing the spindle-like structure of the tDPSCs and nDPSCs with centrally placed DAPI-positive nuclei under phase contrast microscopy (x400 microns).....	<b>137</b>
Figure 4:12 Collagen-1/DAPI staining of cultured nDPSCs and tDPSCs. The pattern of expression in both cell groups is almost identical. The heterogeneous spindle-shape morphology of both cell groups consists of: 1-Proximal pole, 2-Nuclear region 3-Sub nuclear area, 4-Intercellular process, and 5- High density of intercellular processes. (Scale bar = x400 microns).....	<b>138</b>
Figure 4:13: Isolation of CD13-positive tDPSCs by FACS. Forward scatter – AmCyan gate was applied on early passage (A, B) and late passage (C, D) tDPSCs to discriminate viable tDPSCs. A forward scatter-CD13 gate was applied on the viable tDPSCs to detect tDPSCs positive for this stem cell marker. Forward scatter – CD13 gate was applied on a commercial isotype control (E) to establish baseline criteria for selective gating. The number of events in (B) 100% and (D) 99.99% is representative of encircled area of cell staining seen in (A) 68.44% and (C) 68.97%. ....	<b>140</b>
Figure 4:14: Isolation of CD44-positive tDPSCs by FACS. Forward scatter – AmCyan gate was applied on early passage (A, B) and late passage (C, D) tDPSCs to discriminate viable tDPSCs. Forward scatter-CD44 gate was applied on the viable tDPSCs to detect CD44-positive tDPSCs. Forward scatter – CD44 gate was applied on a commercial isotype control (E) to establish gating parameters used. The number of events in (B) 94.80% and (D) 91.90% is representative of encircled area of cell staining seen in (A) 67.35% and (C) 71.66%. ....	<b>141</b>
Figure 4:15: Isolation of CD73-positive tDPSCs by FACS. Forward scatter – AmCyan gate was applied on early passage (A, B) and late passage (C, D) tDPSCs to discriminate viable tDPSCs. Forward scatter-CD73 gate was applied on the viable tDPSCs to detect CD73-positive tDPSCs. Forward scatter – CD73 gate was applied on a commercial isotype control (E) to establish gating parameters used. The number of events in (B) 93.57% and (D) 75.22% is representative of encircled area of cell staining seen in (A) 66.04% and (C) 74.07%. ....	<b>142</b>
Figure 4:16: Isolation of CD90-positive tDPSCs by FACS. Forward scatter – AmCyan gate was applied on early passage (A, B) and late passage (C, D) tDPSCs to discriminate viable tDPSCs. Forward scatter-CD90 gate was applied on the viable tDPSCs to detect CD90-positive tDPSCs. Forward scatter – CD90 gate was applied on a commercial isotype control (E) to establish	

- gating parameters used. The number of events in (B) 99.69% and (D) 98.27% is representative of encircled area of cell staining seen in (A) 67.83% and (C) 64.27%. ..... **143**
- Figure 4:17: Isolation of CD146-positive tDPSCs by FACS. Forward scatter – AmCyan gate was applied on early passage (A, B) and late passage (C, D) tDPSCs to discriminate viable tDPSCs. Forward scatter-CD146 gate was applied on the viable tDPSCs to detect CD146-positive tDPSCs. Forward scatter – CD146 gate was applied on a commercial isotype control (E) to establish gating parameters used. The number of events in (B) 11.21% and (D) 1.85% is representative of encircled area of cell staining seen in (A) 70.40% and (C) 75.36%. ..... **144**
- Figure 4:18: Isolation of CD166-positive tDPSCs by FACS. Forward scatter – AmCyan gate was applied on early passage (A, B) and late passage (C, D) tDPSCs to discriminate viable tDPSCs. Forward scatter-CD166 gate was applied on the viable tDPSCs to detect CD166-positive tDPSCs. Forward scatter – CD166 gate was applied on commercial isotype control (E) to establish gating parameters used. The number of events in (B) 68.38% and (D) 23.72% is representative of encircled area of cell staining seen in (A) 64.83% and (C) 71.01%. ..... **145**
- Figure 4: 19: Standard curve of the real time RT-PCR assays for B-actin (A), ALP (B), COL-1 (C). Ten-fold dilutions of plasmid DNA prior to amplification were used ranging from  $1 \times 10^0$  to  $1 \times 10^4$  copies (indicated on the y-axis) with the CT values represented on the x-axis. Sensitivity of the primers against the tDPSCs was tested in duplicates as demonstrated by the gel at the bottom left of Figure 4.21. The co-efficient of determination ( $R^2$ ) is indicated on the graphs. The CT values for the primers were: B-actin (27.842), ALP (30.798) and COL-1 (25.178). ..... **146**
- Figure 4:20: Standard curve of the real time RT-PCR assays for DMP-1 (D) and DSPP-1(E). Ten-fold dilutions of plasmid DNA prior to amplification were used ranging from  $1 \times 10^0$  to  $1 \times 10^4$  copies (indicated on the y-axis) with the CT values represented on the x-axis. Sensitivity of the primers against the tDPSCs was tested in duplicates as demonstrated by the gel at the bottom left of Figure 4.21. The co-efficient of determination ( $R^2$ ) is indicated on the graphs. The CT values for the primers were: DMP-1 (24.807) and DSPP (29.050). ..... **147**
- Figure 4:21: Standard curve of the real time RT-PCR assays for p16 (F) and p53 (G). Ten-fold dilutions of plasmid DNA prior to amplification were used ranging from  $1 \times 10^0$  to  $1 \times 10^4$  copies (indicated on the y-axis) with the CT values represented on the x-axis. Sensitivity of the primers against the tDPSCs was tested in duplicates as demonstrated by the gel (I) at the bottom right of the figure. The co-efficient of determination ( $R^2$ ) is indicated on the graphs. The CT values for the primers were: p16 (27.833) and p53 (27.892). ..... **148**
- Figure 4:22 Expression of odontoblast mineralization markers ALP (A) and COL-1 (B), odontoblast differentiation markers DMP-1(C) and DSPP (D) and, oncogenic markers p16 (E) and p53 (F) in nDPSC (passage n5 and tDPSCs, passage 10 – 60) was determined by real-time qPCR. Values are reported as relative fold change in cDNA concentration, which were normalised to the housekeeping gene. The data are represented as the mean  $\pm$  S.E of triplicate experiments (technical replicates) with significance differences measured between the cell groups by one-way ANOVA and post hoc Bonferroni's test ( $*p < 0.05$ ,  $**p < 0.01$ ,  $***p < 0.001$ ). ..... **150**
- Figure 5:1: A shows the order of application of test compounds allyl isothiocyanate (AITC), a TRPA1 agonist and GSK1016790A, a commercial TRPV4 agonist (Thorneloe, Sulpizio et al. 2008). The preceding bath phases represent cell response baselines periods during which the cultured cells were perfused for 30 seconds with Hanks buffered solution (HBBS). B shows the application of test compounds icilin, a TRP A1/M8 agonist and capsaicin, a TRPV1 agonist. **166**
- Figure 5:2: The gel shows the identification of TRPV1 and DSPP expression in the whole pulp lysate. GAPDH was used as an internal control. Arrows indicate predicted size of TRPV4 mRNA. .... 169**
- Figure 5:3: (A) demonstrates the identification of the TRP (A1, V1, M8 and V4) expression profile in nDPSCs before retroviral transduction. (B) Shows positive bands for TRPA1, V1 and V4 in tDPSCs at passages 6 (first group of TRP bands) and 30 (second group of TRP bands). GAPDH was used as an internal control. The encircled genes have been discussed in Chapter 4. The

underlined mesenchymal stem cells were run in gel B as part of an unrelated experiment to test a beta actin primer. ....	<b>169</b>
Figure 5:4: The identification of the substance P receptors NK1R and NK2R in nDPSCs (A) and tDPSCs (B). The efficacy of the TRP M8 primer was confirmed as positive bands were seen with control Chinese hamster ovary (CHO) cell RNA. ALP and COL-1 were run as controls. .	<b>170</b>
Figure 5:5: Standard curves of the real time RT-PCR assays for TRPA1 (A), TRPV1 (B), TRPV4(C), NK1R (D) and NK2R (E). Ten-fold dilutions of plasmid DNA prior to amplification were used ranging from $1 \times 10^0$ to $1 \times 10^4$ copies (indicated on the y-axis) with the CT values represented on the x-axis. Sensitivity of the primers against the tDPSCs was tested in duplicates as demonstrated by the gel (F) above. The co-efficient of determination ( $R^2$ ) is indicated on the graphs. Beta actin was run as a housekeeping gene. The encircled genes in the gel have been discussed in Chapter 4. ....	<b>172</b>
Figure 5:6: Gene expression levels of TRP channels TRPA1 (A), TRPV1 (B) and TRPV4 (C) and substance P receptors NK1R (E) and NK2R (F) in WPL, nDPSC (passage n5) and tDPSCs, (passage 10 – 60) was determined by real-time qPCR. Values are reported as relative fold change in cDNA transcription which were normalised to the housekeeping gene. The data is represented as mean $\pm$ S.E, with significance differences measured between WPL (control) and the different time points (P5 – P60) by one-way ANOVA and post hoc Bonferroni's test. ( $***p < 0.001$ , $**p < 0.01$ ). ....	<b>173</b>
Figure 5:7: $[Ca^{2+}]_i$ imaging by the application of chemical stimuli (agonists) for thermosensitive and mechanosensitive TRP channels in the cultured tDPSCs. There were no spikes observed following the application of capsaicin while two consecutive sets of spikes were evoked in response to AITC and GSK1016790A respectively. tDPSCs in which the application of these two agonists produced a change in $[Ca^{2+}]_i$ are highlighted by the red arrows in images below the graph. ....	<b>175</b>
Figure 5:8: (A) Percentage of responders (cells that showed a ratio change $\geq 0.2$ from the averaged baseline) to changes in $[Ca^{2+}]_i$ following the application of selective TRP channels agonists in the cell populations tested. (B) Mean ratio changes demonstrated by the responders in this study. Error bars demonstrate the standard error from the mean. ....	<b>177</b>
Figure 5:9: Dose-response curves for (A) GSK1016790A, (B) hypotonic solution, (C) allyl isothiocyanate, AITC, (D) cinnamaldehyde, CA, (E) capsaicin, CAPS, (F) icilin, ICI measured in cultured tDPSCs. The data points in each response plot are representative of mean responses (measurements of the emission ratios of Fura-2 as indicators of $[Ca^{2+}]_i$ transients, n=6) at tested concentrations for each agonist. The tDPSCs showed very poor responses to the TRPV1 agonist, capsaicin (E) and TRPM8, agonist icilin (F) in contrast to the responses seen with the other agonists (TRPA1 – AITC and CA, and TRPV4 – GSK1016790A). There is also a concentration-dependent effect of hypotonicity on tDPSC-TRPV4 as evidenced by the observed $[Ca^{2+}]_i$ responses, (n=4, VHC = isotonic solution) (B). The column plot data points are represented as mean $\pm$ S.E, with significance differences measured between VHC (control) and the different percentages of hypotonic solution by one-way ANOVA and post hoc Bonferroni's test. ( $***p < 0.001$ , $**p < 0.01$ and $*p < 0.05$ ). ....	<b>179</b>
Figure 5:10: Concentration-dependent inhibition of $[Ca^{2+}]_i$ responses by TRPV4 antagonist HC067047 to 200nM GSK1016790A, (n=4) (A), TRPA1 antagonist HC030031 to 200 $\mu$ M AITC, (n=4) (C) and 200 $\mu$ M cinnamaldehyde, (n=4) (D). Exposure to TRPV4 antagonist does not significantly inhibit the effect of tDPSC pre-exposure to 40% hypotonic solution, (n=3, VHC = isotonic solution) (B). The data points in each of the response plots are representative of mean responses at tested concentrations for each antagonist. The column plot data points are represented as mean $\pm$ S.E, with significance differences measured between VHC (control) and the different percentages of hypotonic solution by one-way ANOVA and post hoc Bonferroni's test. ( $***p < 0.001$ , $**p < 0.01$ and $*p < 0.05$ ). ....	<b>180</b>



- Figure 5:11: TRP channel agonist evoked ATP release by tDPSCs. Significant increases in ATP release was induced by (A) AITC (n=5), while (C) cinnamaldehyde (n=5), TRPV4 agonists GSK1016790A (n=5) (B) and (D) hypotonic solution (n=4) failed to induce significant increases in ATP release. The data is represented as mean  $\pm$  S.E and a Student t test was performed to compare for significant differences between the vehicle (control) and the respective TRP agonists ( $*p < 0.05$ )..... **181**
- Figure 5:12: The relationship between TRP channel expression levels and variations in concentrations of SP added to tDPSC cell cultures at passage 12 (tDPSC-p12/SP<sup>+</sup>). Expression levels of tDPSC mRNA at passage 12 cultures unexposed to SP (tDPSC-p12/SP<sup>-</sup>) were used as comparative baselines. (B, C). The addition of 10<sup>-8</sup>M SP showed a significant increase in mRNA expression levels in TRPA1 and V4. The data is represented as mean  $\pm$  S.E, with significance differences measured between SP free samples (control) and the respective concentrations of SP, by one-way ANOVA and post hoc Bonferroni's test ( $***p < 0.001$ ,  $**p < 0.01$  and  $*p < 0.05$ ). ..... **182**
- Figure 5:13: Validation of up-regulated transcripts as measured by the microarray cards with real-time qPCR. Values are reported as relative fold change in cDNA transcription, which were normalised to the housekeeping gene. The data is represented as mean  $\pm$  S.E and a Student t test was performed to compare for significant differences between the non-painful pulps (control) and the painful pulps for the respective transcripts ( $*p < 0.05$ ,  $**p < 0.01$ , n=3)..... **203**

## List of Tables

Table 1:1 Odontoblast growth factors and associated receptor families.....	34
Table 1:2: An overview of stem cells in dental tissues. Adapted from (Orenuga and da Costa 2006; Dhima, Petropoulos et al. 2012) .....	41
Table 1:3 A modified overview of the functional characteristics of myelinated (*) and unmyelinated pulpal sensory nerve fibres (Olgart 1974; Bender 2000; Byers, Suzuki et al. 2003; Ikeda and Suda 2003; Yu 2007).....	53
Table 1:4 Activating stimuli for mammalian TRP channels of interest.....	57
Table 1:5 Mammalian chemo-sensitive TRP channels and their chemical agonists.....	59
Table 1:6 The role of TRP channels in calcium signalling. Ca <sup>2+</sup> influx across the TRP channels activates Cn-NFAT (Calcineurin nuclear factor of activated T cells) and CaMK (calmodulin-dependent kinases). .....	64
Table 2:1 Sequences of the primers designed to recognise genes of interest which were alkaline phosphatase, beta-3-tubulin (β3T), core binding factor 1 (CBFA-1), collagen type I (Col I), dentine matrix protein 1 (DMP1), dentine sialophosphoprotein (DSPP), enolase 2 (EN-2), human telomerase reverse transcriptase (hTERT), Homeobox protein NANOG (NANOG), nestin, substance P receptors – neurokinin-1 and -2 (NK1R and NK2R), peroxisome proliferator activated receptor gamma (PPARγ), senescence associated proteins p16 and p53, RNA exonuclease 1 (REX-1), runt-related transcription factor 2 (RUNX2), sex determining region Y-box 9 (SOX9) and transient receptor potential channel receptors (TRPA1, M8, V1 and V4). Glyceraldehyde 3-phosphate dehydrogenase (GAPDH) was used as the housekeeping gene. ....	76
Table 2:2: Sequences of the primers designed to recognise genes of interest which were CD44 and CD45, alkaline phosphatase (ALP), collagen type I (Col I), dentine matrix protein 1 (DMP1), dentine sialophosphoprotein (DSPP), neurokinin receptors – neurokinin-1 and -2 (NK1R and NK2R), transient receptor potential channels (TRPA1, V1 and V4), senescence associated proteins p16 and p53. Beta actin (β-actin) was used as the housekeeping gene. ....	81
Table 4:1: Conjugated antibodies used in the fluorescence-activated cell sorting of the tDPSCs. PE – Phycoerythrin; FITC – Fluorescein isothiocyanate. All the antibodies used showed cross-reactivity for human protein. ....	126
Table 4:2: Stem marker expression in tDPSCs over 60 passages. * - CD markers tested as negative controls for the odontoblastic phenotype. ....	139
Table 5-1: Tested TRP channel agonists and antagonists. ....	167

## Abbreviations

ALP – Alkaline phosphatase	DSPP – Dentine sialophosphoprotein
ATP – Adenosine triphosphate	DRG – Dorsal root ganglion
BDNF – Brain-derived neurotrophic factor	DP – Dental pulp
BK – Bradykinin	DPC – Dental pulp cell
BrdU - 5-bromo-2'-deoxyuridine	DPSC – Dental pulp stem cell
BSA – Bovine serum albumin	EGFR – Epidermal growth factor receptor
C5a – Complement component 5a	EO – Enamel organ
cAMP – Cyclic adenosine monophosphate	FC – Fold change
CaMK - Calmodulin-dependent kinases	FON – First order neurons
CCI – Chronic constriction injury	G-CSFR – Granulocyte-colony stimulating factor receptor
CCL – Chemokine C-C motif ligand	GFAP – Glial fibrillary acidic protein
CHO – Chinese hamster ovary	GAPDH - Glyceraldehyde 3-phosphate dehydrogenase
CGRP – Calcitonin gene-related peptide	GPCR – G-protein coupled receptor
CNS – Central nervous system	GDNF – Glial cell-derived neurotrophic factor
Cn-NFAT - Calcineurin nuclear factor of activated T cells	HBSS – Hank's balanced salt solution
CT – Cycling time	hTERT – human telomerase reverse transcriptase
COX - cyclooxygenase	HEPES -4-(2-hydroxyethyl)-1-piperazineethanesulfonic acid
COL-1 – collagen type 1	HIV – Human immunodeficiency virus
CXCL – Chemokine C-X-C motif ligand	HK – Housekeeping gene
CX3CL – Chemokine C-X3-C ligand	IEE – Internal enamel epithelium
DEJ – Dentine-enamel junction	IFN – Interferon
DMEM – Dulbecco's modified Eagle's medium	IL – Interleukin
DMP1 – Dentine matrix protein 1	

IGF – Insulin growth factor	PKA – Protein kinase A
LIF – Leukemia inhibitory factor	PKC – Protein kinase C
LIX – Lipopolysaccharide-induced	PLC – Phospholipase C
CXC - chemokine	PMN – Polymorphonuclear
LPS - Lipopolysaccharide	PNS - Peripheral nervous system
LTB4 – Leukotriene B4	qPCR – Quantitative polymerase chain reaction
MAPK – Mitogen activated protein kinase	SE – Standard error
MMP – Matrix metalloproteinase	SD – Standard deviation
nDPSC – non-transformed dental pulp stem cell	SEM – Standard error of the mean
NFkB - nuclear factor kappa-light-chain-enhancer of activated B cells	SON – Second order neurons
NGF – Nerve growth factor	SR – Stellate reticulum
NK – Natural Killer	tDPSC – transformed dental pulp stem cell
P2X3 – Purinergic receptor P2X ligand-gated ion channel 3	TGF – transforming growth factor
PAR4 – Proteinase activated receptor 4	TLR – Toll-like receptor
PBS – Phosphate-buffered saline	TNFa – Tumour necrosis factor alpha
PCR – Polymerase chain reaction	TrK – Tyrosine kinase receptor
PFA - Para formaldehyde	TRP – Transient receptor potential channel
PIP2 - phosphatidylinositol bisphosphate	

# Literature review and general introduction

---

**1**

## Literature review

### 1.1 Pain and pain signalling

The understanding of pain has evolved over time. Greek philosophers conceptualised pain as an emotional expression of the controlling presence of deities. The Romans had a different viewpoint and thought that the brain of the individual controlled the pain experience. This was the premise on which the 17<sup>th</sup> century philosopher Rene Descartes sought to explain pain. He proposed that pain served as an expression of a physical activity. This suggested that in the absence of an injury, there was no pain. Since that time, the analysis of pain has broadened, making way for anatomical and physiological concepts of transmission pathways through nerve tracts and fibres to specific end organs. Presently, pain is considered as an unpleasant emotional experience associated with potential or actual tissue damage; a learned response subserved by the nervous system (IASP 1994). While the processing of pain is a function shared by different loci within the brain, pain does occur in different forms and has been categorised based on cause, with the occasional overlap between these different forms – such as that between physical and social pain; pain overlap theory (Eisenberger and Lieberman 2004). Nociceptive pain is the normal response to tissue damage. It is usually short lived and occurs in response to stimuli such as tissue trauma, chemicals or changes in pH or temperatures. In the presence of certain disease conditions, inflammation arises leading in some cases to inflammatory pain. When there is dysfunction of the peripheral or central nervous system, neuropathic pain sometimes occurs. It is of a chronic nature and is known to persist even after the repair of damaged tissues (Niv and Devor 2006).

Following the detection of noxious stimuli, impulses are sent to higher centres in the brain through peripheral nerves, where they are processed. The pain signal is first generated at the peripheral end of a primary sensory (afferent) neuron. The noxious stimuli act on a range of receptors present in the different organs (skin for example). The activation of these receptors leads to the opening of ion channels, which allow the

entry of ions that change the membrane potential and cause the opening of more ion channels eventually leading to the generation of an action potential. Depending on the combination of several action potentials spread along the axons of the afferent neurons, amount of central neurotransmitter released and, the electrical current generated within these neurons is strong enough, a pain signal is generated. A theory (gate control theory) put forward in 1965 by Melzack and Wall, proposed that the spinal cord has a gate which filters pain signals, either blocking or permitting them to pass on to the brain (Melzack and Wall 1965). In the brain, the pain signals are modulated in a “pain matrix” (a composite of brain structures such as somatosensory cortex, gyrus and limbic system) and it has been suggested that this pain signal modulation is dependent on external psychophysical variables such as emotion, environment and memory (Melzack and Wall 1965; Melzack,Coderre et al. 1999; Tracey and Mantyh 2007). This is an abridged summary of the central mechanisms involved in pain perception as the focus of the work described in this thesis is on peripheral dental pain perception.

## 1.2 Orofacial pain

A large proportion of the world population has suffered from toothaches or tooth-associated pain. Early studies estimated that 64% of the UK population and 80% of Americans have experienced some form of tooth pain and sensitivity (Bonica 1981). Two decades later, the literature shows that almost half of dentate adults in the UK (40%) have experienced some form of dental pain, with a percentage of these individuals (8%) suffering adverse effects such as gum infections and tooth loss as a result (Nuttall, Steele et al. 2001). This decline was attributed to an increase use of preventive dental health care measures such as the use of fluoridated toothpastes and a rise in dental health awareness. A few years later, another study estimated that close to 40% of community-dwelling adults are affected by dental pain (Pau, Croucher et al. 2005). The group of individuals studied here was unequally distributed by age, gender and sex, but consisted mainly of a young population. A report published a few years

later suggested that while visits to the dentist by adults was on the increase, there was a small minority of adults who would only do so if in pain (2011). This was in keeping with earlier suggestions that an aversion for dental treatment in most cases was borne out of a previous “unpleasant” experience of dental care, thus increasing the likelihood of a visit to the dentist only occurring as a last ditch attempt to relieve pain (Gold, Belmont et al. 2007). An interesting observation was that this attitude was exhibited to a greater extent in older adults, who were less likely to report episodes of pain than younger patients. Only 17% of adults over 65 reported aching in the previous 12 months, compared to 30% of 25-34 year olds (Pau, Croucher et al. 2007). The ability or lack thereof to access dental treatment by this percentage of non-reporting individuals (both young and old) may be influenced by a number of factors such as education, economic conditions and apathy due to the presence of very few standing teeth (Pau and Allen 2011; 2011). Despite improvement in dental health care regimes, the description of 40% of the UK population as dental pain sufferers (Nuttall, Steele et al. 2001), is representative of millions of people. It is this high number of “pain sufferers” that informs the need for a better understanding of dental pain sensation and effective treatment remedies.

The primary origin of innervation of the structures in the orofacial region is the trigeminal nerve. It is the fifth of twelve cranial nerves and is divided into three divisions (ophthalmic, maxillary and mandibular) on the basis of the cutaneous distribution of the divisions. Damage to any of these divisions can cause neuropathic pain, similar in its mechanism of development as would be found in other regions in the body (Polycarpou, Ng et al. 2005). The trigeminal nerves are not able to sprout sympathetic nerve endings in the face of external insults which would cause neuropathic pain, suggesting that an alternate mechanism for the generation of pain signals may exist in this region (Fried, Bongehiell et al. 2001).

The current mechanistic explanations of dental hypersensitivity and approaches to pain management are based around the hydrodynamic hypothesis put forward by Brännstrom which proposed that tooth sensitivity secondary to stimulation was due to the combined effects of movements of fluid within dentinal tubules and the



sensitization of sensory nerve fibres present in the tubules (Brannstrom and Astrom 1972; Brannstrom 1986). Current management of dental pain is primarily based on the use of restorative fillings (deep and surface fillings as the clinical picture may dictate) and extractions of painful teeth. The focus of this study is the examination of an alternative hypothesis, which is slowly gaining prominence, and suggests that in addition to dental sensory neurons, odontoblasts within the tooth play a functional role in dental pain sensation. These odontoblasts may do so via their expression of certain members of the sensory Transient Receptor Potential (TRP) family of cation channels. Some groups have suggested that the TRPs are involved in the transduction of dental pain as they are expressed in both the odontoblasts as well as the trigeminal nerve fibres and are directly activated by the same stimuli that produce tooth pain (Morgan, Rodd et al. 2005; Rodd 2007; El Karim, Linden et al. 2010). Before considering these hypotheses, a brief overview of the anatomy and development of the human tooth is necessary.

### **1.3 Anatomy of the tooth**

The primary function of teeth in mammals is the mastication of food. In humans they are also required for the production of speech as well as contributing to aesthetic definitions of the face. The human tooth is divided into two parts: the root, which anchors the tooth to the jaw, and the crown, which projects into the mouth above the jaw (Figure 1.1).

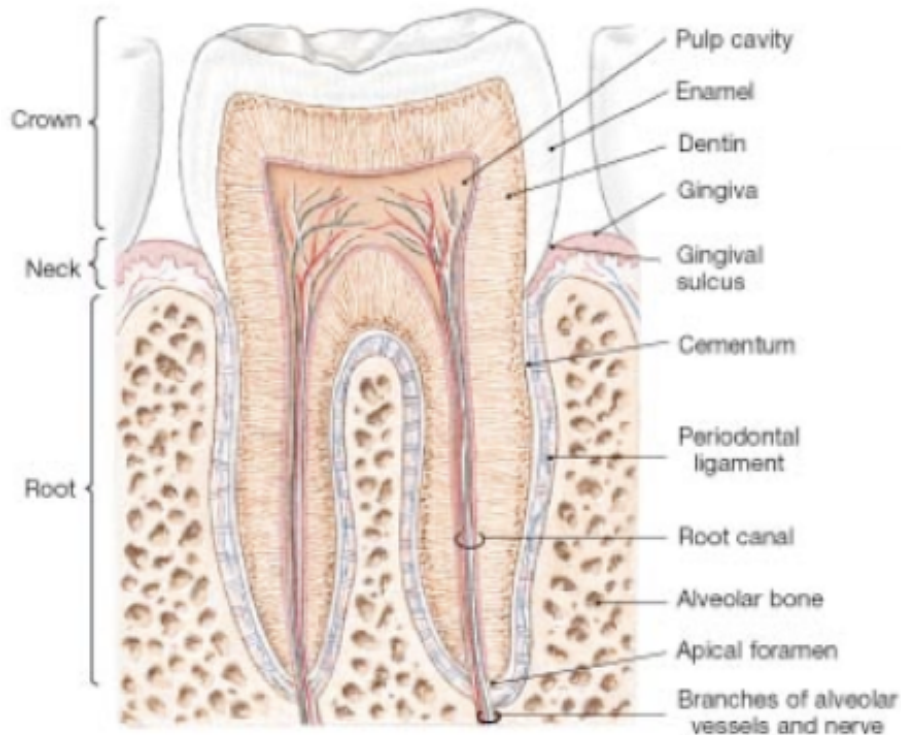


Figure 1: 1 Schematic cross section of a human tooth (adapted from intranet.tdmu.edu.ua)

The anatomic crown is the portion of tooth that is visible in the oral cavity and its' size can vary as the teeth erupt or with recession of the gingiva (Woelfel 1990). Covering the crown is an outer protective hull of enamel. Beneath this lies the root that is covered by cementum, a yellowish layer of bone-like tissue. Dentine is usually completely covered by enamel and cementum (in the crown and root areas respectively). The anatomical root is defined as the portion of the tooth that is usually covered by cementum and the clinical root is defined as the portion of the tooth in the oral cavity that is covered by gingiva (Woelfel 1990). The tooth sits suspended in a socket within the alveolar bone of the jaw by Sharpey's fibres, which lie within connective tissue called the periodontal ligament. The cementum serves as an anchorage point for the collagenous Sharpey's fibres on the tooth side, while alveolar bone within the tooth socket is the second point of attachment (Nanci and Cate 2008). This provides a stable support base for the tooth.

The nerve supply of the tooth is through maxillary and mandibular branches of the trigeminal nerve. The nerves access the tooth in a neurovascular bundle through

the apical foramen (Figure 1.1). These neurovascular bundles gain entry into the pulp through the foramen and serve as a source of nutrition and sensation. The foramen is not always located at the very tip of the root, but may be offset one to three millimetres towards the crown of the tooth. The nerves run in an occlusal (upward) direction through the pulp with each fibre giving off terminal branches. The branches of these nerve fibres anastomose in the top corners of the coronal pulp (the pulp horns) to form a plexus of nerves. This plexus lies below the cell bodies of the odontoblasts (which are dentine-producing cells and are described in greater detail in Section 1.4.2) and is referred to as the Plexus of Raschkow. Free nerve endings from this plexus synapse onto and into the odontoblast cell layer (approximately 100–200  $\mu\text{m}$  deep in the dentinal tubules) and the odontoblastic cell processes (Johnsen, Harshbarger et al. 1983). The plexus contains small myelinated A-delta ( $A-\delta$ ), large myelinated A-beta ( $A-\beta$ ) fibres (2-5 $\mu\text{m}$  in diameter) and smaller unmyelinated C fibres (0.3-1.2  $\mu\text{m}$ ) (Yu 2007). These nerves play a major role in the control of pulpal vasculature and influence the defensive functions of the dental pulp.

#### 1.4 An overview of tooth formation

Embryologically the human tooth is formed by a series of interactions between the ectoderm and ectomesenchyme of the oral mucosal tissue (Couve 1986; Nanci and Cate 2008). The ectomesenchymal cells are products of neural crest cell migration from the cephalic region to the first brachial arch where teeth develop (Imai, Osumi-Yamashita et al. 1996; Ohtani, Zebedee et al. 2001). The aggregation of these cells forms what is known as a tooth bud (tooth germ), which consists of three parts (Figure 1.2) as outlined below.

1. A depression forms in the deepest part of each tooth bud and this is the **enamel organ (EO)**, which is made up of the outer enamel (dental) epithelium (OEE), inner enamel (dental) epithelium (IEE), stellate reticulum (SR) and stratum intermedium (SI). The IEE cells differentiate into pre-ameloblasts

(which become ameloblasts and produce the future enamel. The OEE and IEE layers appose each other at a region referred to as the cervical loop. The growth of cervical loop cells in this region gives rise to an epithelial root sheath of Hertwig, which determines the shape of the root of tooth. This only occurs after the loss of the middle layers. The SR and SI cells synthesize glycosaminoglycans, which are involved in the production of enamel. The water contained in these cells is lost during this exhaustive process and both cell layers collapse, usually after the first layer of enamel is secreted.

2. Below this cap is a condensing mass of mesenchymal tissue called the **dental papilla** (DP) which undergoes differentiation (under the influence of the pre-ameloblasts) and produces two types of cells (Linde and Goldberg 1993; Chai, Jiang et al. 2000):

(a) An outer layer of cells which forms the dentine-secreting cells (pre-odontoblasts), and

(b) A central zone of cells, which are “non-neural crest” derived cells that form the primordium of the pulp.

This distinction suggests a group-specific response of these cells to epigenetic differentiation signals. Opinion is still divided and while the neural crest derived cells potentially yield the odontoblasts, there is a chance of these cells forming part of the pulp primordium (Beguekirn, Smith et al. 1992; Ruch, Lesot et al. 1995).

In concert with the IEE, the DP also determines the shape of the crown of the tooth, and

3. The mesenchymal tissue that remains surrounds the enamel organ and condenses to form the **dental follicle**.

The membrane separating the dental (enamel) organ and the dental papilla becomes the future site for the **dentine-enamel junction** (DEJ). The process of formation and mineralisation of each structural layer of the tooth is tailored to the specific requirements of each layer.

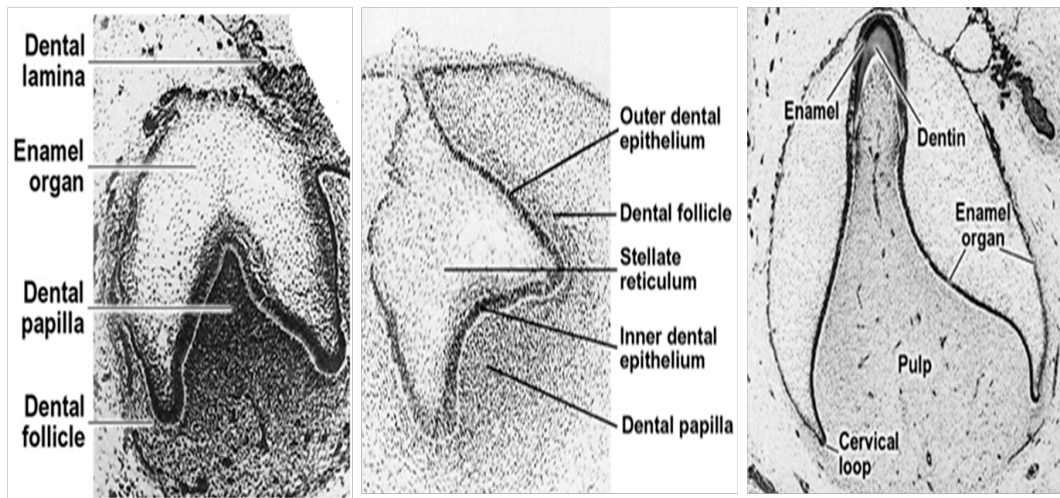


Figure 1:2 Modified photomicrograph images of a tooth bud from Ten Cate's Oral Histology (Nanci and Cate 2008). The developing tooth bud is composed of the enamel organ, dental papilla and dental follicle. Differentiation within the enamel organ will yield 4 cell types: outer enamel (dental) epithelium, stellate reticulum, stratum intermedium and the inner enamel (dental) epithelium. With the loss of the middle 2 layers of the enamel organ, both inner and outer enamel (dental) epithelial layers will appose each other at the cervical loop and grow downwards into the dental papilla to yield the root sheath of Hertwig that determines the shape of the root of the tooth.

Origin	Components of tooth bud	Cells derived from the tooth bud	Secretory products
Ectomesenchyme from 1 <sup>st</sup> brachial arch	Enamel organ	Outer enamel epithelium	Root sheet of Hertwig
		Stratum intermedium	Reduced enamel epithelium
		Stellate reticulum	Ameloblasts
		Inner enamel epithelium	
		Cervical loop	
Tooth germ	Dental papilla	Odontoblasts	Crown form
		Undifferentiated mesenchymal cells	Dentin
			Pulp
Ectomesenchyme from neural crest cells	Dental follicle	Cementoblasts	Cementum
		Fibroblasts	Periodontal ligament
		Osteoblasts	Alveolar bone

Figure 1:3 A modified schematic overview of human tooth development showing tooth germ derivatives and their secretory products (Nanci and Cate 2008).

### 1.4.1 The dentine – pulp complex

The pulp shares a similar embryology and has been regarded as a singular entity with the dentine (dentine-pulp complex) (Hume and Massey 1990; Massey, Romberg et al. 1993). The dentine forms the bulk of the tooth and its formation occurs concurrently with that of enamel (Nanci and Cate 2008). It is formed by a group of mesodermally derived cells (odontoblasts), which lie at the junction between the pulp and the dentine (during its formative process, these odontoblasts line its pulpal surface) (Linde and Goldberg 1993). Dentine continues to be laid down throughout life, with collagen serving as the focus for further mineralization (Butler and Ritchie 1995; Butler 1998). Its mineralization is synonymous with its maturation (from predentine to dentine, now called primary dentine which contains tubular structures that radiate outwards from the pulp to the enamel or cementum (Nanci and Cate 2008). These multiple closely packed dentinal tubules that traverse the entire thickness of the dentine contain the cytoplasmic extensions of odontoblasts (odontoblastic processes) and dentinal fluid, forming a mineralised meshwork of cell processes and nerve endings (See Figure 1.4) (Nanci and Cate 2008). It has been suggested that the composition of the dentinal fluid is determined by the odontoblasts (Özok, Wu et al. 2002).

Encased within the core of the dentine is the dental pulp. It is enclosed within the pulp cavity with its only opening to the exterior located in the region of the apical foramen through which blood vessels and nerves pass (Figure 1.1). This mass of non-calcified soft tissue is responsible for maintaining the viability of the living tooth and it is believed to play a significant role in tooth repair secondary to external insults (C. Yu 2007; Nanci and Cate 2008; Schoenebeck, Hartschen et al. 2009). The pulp is mesodermally derived and has a rich network of blood vessels and nerves (Nanci and Cate 2008). The nerve endings, which transmit dental pain, are found primarily in the pulp, although a small portion of these nerve endings penetrate the dentine for a very short distance. While the pulp lies in the middle of the tooth, it is still able to respond to external insults (such as mechanical trauma), as would any other connective tissue in the body, the primary difference being that it is much better protected than any

other connective tissue. Possible reasons for this type of response by these cells, which are believed to be odontoblast-like, are suggested in Section 1.4.4. Pulp tissue is a matrix of different components. It consists primarily of two types of collagen (types I and III collagen - there is a greater proportion of type I). There is a ground substance made up of glycosaminoglycans, glycoproteins and water which provides a means of support for the cells and also serves as to transport nutrients to, and metabolites from, the cells (Nanci and Cate 2008). The pulp tissue provides nutritional support for the odontoblasts. The cell population within the pulp is heterogeneous and consists of undifferentiated mesenchymal cells, cells involved in defence (macrophages and other immunocompetent cells) and fibroblasts (Massey, Romberg et al. 1993). Other structures present are collagen fibres, blood vessels and lymphatics, nerves and free sensory nerve endings. The most abundant cell population of the pulp tissue, occurring in the cell-rich zone are the fibroblasts (Nanci and Cate 2008). If the odontoblasts die following deleterious stimuli such as caries or trauma, there is a replacement of the dead cells by odontoblast-like cells from the pulpal ectomesenchymal tissues (Massey, Romberg et al. 1993; Torneck, Titley et al. 1993). These cells are responsible for the secretion of a form of "replacement" dentine (reparative dentine) (Linde and Goldberg 1993). These replacement cells also have the potential to differentiate into fibroblasts (Massey, Romberg et al. 1993).



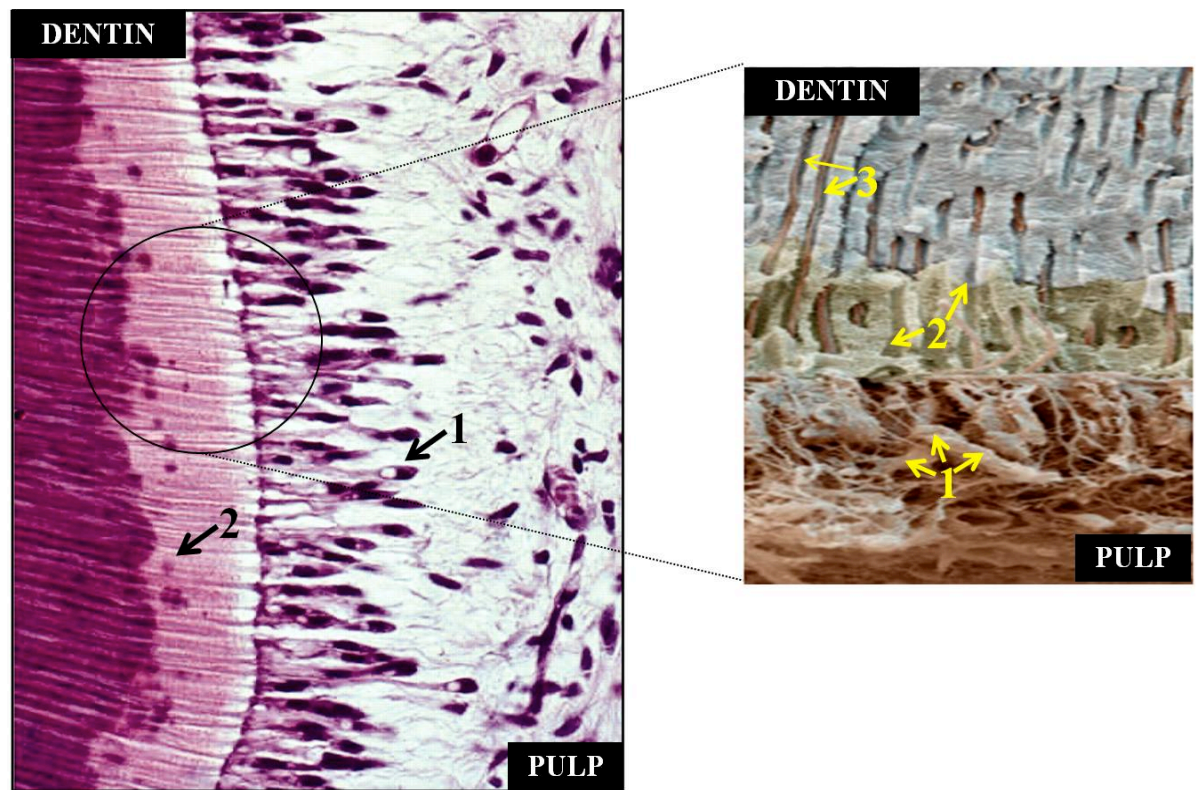


Figure 1:4 Hematoxylin and Eosin (H&E; x 400 $\mu$ m) staining of the dentin and pulp tissues. 1: odontoblast cell bodies; 2: dentinal tubules; 3: odontoblast processes in the dentinal tubules. Adapted from (Wu and Schwartz 2008) and <http://www.sciencephoto.com>.

### 1.4.2 Odontoblasts

The odontoblast is a cell of neural crest origin, which secretes predentine and eventually dentine, when fully, mature (Linde and Goldberg 1993; Zartman, McWhorter et al. 2002). The process of maturation from a pre-odontoblast to a mature odontoblast prepares for this secretory role (Goldberg and Smith 2004). The mature odontoblast is a fully functional and terminally differentiated post mitotic cell, which is characterised by a long, polarized cell body that contains a structured granular endoplasmic reticulum, mitochondria, Golgi apparatus, a nucleus, well established network of microtubules and microfilaments and several secretory vesicles (Linde and Goldberg 1993; Torneck, Titley et al. 1993). There are junctional complexes on the distal (pulpal) ends of the cell bodies of the odontoblasts which may allow for communication through the cell layer (Ushiyama 1989). Also in a supranuclear location

is a network of primary cilia involved in odontoblast responses to external stimuli (Magloire, Couble et al. 2004).

The orientation of the odontoblasts is such that the cells lie with their cell bodies in the direction of the pulp tissue on the inner surface of predentine-dentine into which their cell processes extend and lie in dentinal tubules (Linde and Goldberg 1993). This arrangement is maintained throughout the life of the tooth by the production of dentine by the odontoblasts in opposition to occlusal forces (the forces exerted on opposing teeth when the jaws are brought into approximation in everyday function) (Ortega, Malumbres et al. 2002). As the secretion of the matrix progresses, the odontoblast cell body withdraws in a pulpal direction but the process within the dentinal tubule remains intact. The odontoblast process occupies just over a third of the length of the fluid-filled dentinal tubule (Brannstrom and Astrom 1972).

### **1.4.3 Odontoblast differentiation**

The initiation of odontoblast differentiation relies on a combination of two things: the interaction of pre-odontoblasts with the inner dental (enamel) epithelium through a basement membrane, and the presence of growth factors in the extracellular matrix (Ruch, Lesot et al. 1995; Thesleff and Sahlberg 1996). The growth factors are expressed by the inner dental epithelium and are held within the basement membrane in close proximity to the pre-odontoblasts (Ruch, Lesot et al. 1995). Terminal odontoblast differentiation runs as a sequence of events (Ruch, Lesot et al. 1995; Tziafas 1995; Lesot, Lisi et al. 2001):

1. Pre-odontoblasts withdraw from the cell cycle and during the last round of cell division, the mitotic spindles align close to basement membrane (between the enamel organ and dental papilla),
2. The newly formed daughter cells, which lie in contact with the basement membrane, elongate and then become aligned in a polarized fashion (the nuclei are positioned basally). This cytological polarization is affected by a

re-organization (mechanisms are still undefined) of microtubules and microfilaments present in the cytoskeleton of the cell. There is also flattening of the cells making them parallel to long axis of the basement membrane as well as the development of granular endoplasmic reticular system of the cells.

3. The cells are then ready for secretion of predentine-dentine.

#### **1.4.4 Control and regulation of odontoblast differentiation**

The terminal differentiation of these cells is thought to be controlled by the primary dental epithelium which has been shown to regulate the number of cell cycles (Ruch, Lesot et al. 1995). There is literature to suggest that the pre-odontoblasts must complete a certain number of cell cycles to attain competence to respond to epigenetic signals that herald the start of differentiation. While the number of cycles has been determined in some animals (for example, mice = 15 cycles, 10 hours per cycle) (Holyfield, Bolin et al. 2005), it has been suggested that this is not of importance in human cells and the primary concern is the attainment of a terminal differentiation state which ultimately prepares the odontoblast cell to respond to inductive signalling (Beguekirn, Smith et al. 1992). There is no clear explanation at present, but suggestions are that competence of the cells might be due to serine/threonine kinase receptors present in the cell membranes interacting with growth factors secreted by the inner dental epithelium (for example transforming growth factor- $\beta$  (TGF- $\beta$ )) (Beguekirn, Smith et al. 1992).

The extracellular matrix of the inner dental epithelium contains a complex of proteins with mitogenic properties, as well as growth factors which are responsible for odontoblast differentiation and polarization (Tziafas 1995). Animal studies showed that combinations of some of these growth factors such as members of the transforming growth factor- $\beta$  (TGF- $\beta$ ) superfamily (TGF- $\beta$ 1-3 are the most commonly associated), fibroblast growth factors (FGF) and mitogenic proteins (dentine matrix proteins, bone morphogenic proteins, BMP-2, -4 and -7) (Beguekirn, Smith et al. 1992;

Thesleff, Keranen et al. 2001; Oka, Oka et al. 2007) can cause the differentiation of dental pulp cells to yield odontoblasts (See Table 1-1). The TGF- $\beta$  family of proteins were believed to control odontoblast function (secretion of dentine matrix) (Beguekirn, Smith et al. 1992; Lesot, Lisi et al. 2001). The effects of an isoform of TGF- $\beta$  (TGF- $\beta$ 1) on TGF- $\beta$ 1 receptors in a study using mice (knock-out, over-expression and wild type variants) showed that it was required for the secretion of dentine matrix proteins (dentine sialophosphoprotein proteins, DSPP, and Collagen-1, COL-1) as the dentine matrix and dentine tubules produced in the knock-outs was reduced in volume and as well as being malformed (Oka, Oka et al. 2007). The exogenous introduction of another isoform, TGF- $\beta$ 2 caused similar effects in TGF- $\beta$ 2 receptors in wild-type cells (D'Souza, Cavender et al. 1997; Thyagarajan, Sreenath et al. 2001). *In vitro* studies have also considered the role of insulin-like growth factors in combination with the other growth factors. The differentiated odontoblasts exposed to IGF-1 and IGF-2 showed an increased expression of odontoblastic phenotypic markers (for example, DSPP), suggesting interactions between growth factors (Caton, Bringas et al. 2007).

Growth factor	Cell type	Receptor family
<b>Fibroblast growth factors (FGF-1)</b>	Differentiated and secretory odontoblasts  (Kettunen, Karavanova et al. 1998)	Tyrosine kinase
<b>Transforming growth factors (TGF-<math>\beta</math>1, TGF-<math>\beta</math>3)</b>	Polarised odontoblasts  (Beguekirn, Smith et al. 1992)	Serine/Threonine kinase
<b>Insulin-like growth factors (IGF-1, IGF-2)</b>	Differentiated odontoblasts  (Caton, Bringas et al. 2007)	Tyrosine kinase

Table 1:1 Odontoblast growth factors and associated receptor families

#### 1.4.5 Dentine matrix formation

Following the initial secretion of predentine as an unmineralised matrix by the odontoblasts, the predentine undergoes a transformation to dentine ( $\approx 20\mu\text{m}$  from the

cell border) and the odontoblasts move backwards towards the pulp while still secreting more predentine (Linde and Goldberg 1993; Nanci and Cate 2008). This means that the newly secreted predentine lies close to the odontoblasts while the older mineralised dentine is distal from the secretory cells. A connection between the odontoblasts and the newly formed tissues of dentine is maintained by the presence of odontoblastic processes (MacDougall, Dong et al. 2006). The matrix secreted by the odontoblasts consists in the majority of collagen and the rest is made up of non-collagenous proteins (NCPs) and lipids (Linde and Goldberg 1993). The conversion of predentine to dentine is not well studied but the literature suggests that the process is centred on the combined effects of collagen and the NCPs (Butler and Ritchie 1995).

Collectively, the non-collagenous component of the dentine matrix is believed to be responsible for the mineral induction and growth regulation during dentinogenesis (Butler and Ritchie 1995; Butler 1998). The dentine matrix is mineralised with the deposition of hydroxyapatite (HA) crystals and following mineralization, the NCPs are bound to the HA crystals.

Besides these NCPs are fractional inclusions such as glycoproteins, phosphatases, phosphoproteins, proteoglycans, and sialoproteins (Butler 1998). The proteoglycans, PG, represent a major constituent of the dentine matrix (Oyarzun, Rathkamp et al. 2000). They are high molecular weight polyanionic carbohydrates with a polypeptide core and a few (1-2) glycosaminoglycan side chains (Goldberg and Takagi 1993; Okazaki, Embery et al. 1999). They form the ground substance in the matrix and are involved in transportation across the bulk of the matrix (Goldberg and Smith 2004). PGs are also involved in dentine mineralization as they serve as a reservoir for calcium cations and can induce HA formation (Linde 1989).

#### **1.4.5.1 Collagen**

Collagen secreted in dentine makes up a bulk of the matrix ( $\approx 90\%$ ) (Nanci and Cate 2008). Approximately 86% of the collagen present in the total dentine matrix is type I collagen (MacDougall, Dong et al. 2006), which serves as a scaffold to support the mineral content of dentine (Nanci and Cate 2008). Small amounts of types III and V

(and even smaller amounts of types IV and VI), make up the rest of the collagen in dentine and are neither uniformly nor ubiquitously expressed (Nanci and Cate 2008). Type IV is secreted at the very start of dentinogenesis for a short time while Type VI is found in very small amounts in predentine (Goldberg and Smith 2004). Type V is the most common of this group as it is seen in odontoblast cell cultures, accounting for 3% of collagen produced (Sodek and Mandell 1982).

#### **1.4.5.2 Non-collagenous proteins (NCPs)**

These make up the matrix proteins that fill the spaces between the collagen fibrils. They have been classified into two groups based on the specificity of their sites of expression. The common denominator to both groups is the presence of an Arg-Gly-Asp (RGD) motif that allows for cell attachment, cell differentiation and cell signalling (Kulkarni, Chen et al. 2000; Fisher and Fedarko 2003).

The first group consists of dentine specific proteins and these are dentine phosphoprotein (DPP) and dentine sialoprotein (DSP) (Butler and Ritchie 1995). DPP makes up ≈50% of the NCP fraction (Butler 1998). In man, both dentine phosphoprotein (DPP) and dentine sialoprotein (DSP) are products of the dentine sialophosphoprotein gene (DSPP), which is cleaved after translation (Boskey, Spevak et al. 2000). It is a polyanionic protein and plays a major role in the HA formation, affecting both rate of nucleation and the order of the HA crystals formed (Boskey, Spevak et al. 2000; Paine, Luo et al. 2005). This function is based on the presence of a repeat sequence of aspartate and serine (Asp-Ser-Ser) within the DPP sequence. This highly flexible and highly phosphorylated region serves as a binding site for calcium cations, with recent work showing that it can also recruit calcium phosphate without phosphorylation (Cross, Huq et al. 2005; Yarbrough, Hagerman et al. 2010).

Dentine sialoprotein (DSP) is a non-phosphorylated protein rich in sialic acid. It has little effect on mineralization and is expressed in the early stages of tooth development (Butler and Ritchie 1995; Butler 1998; Boskey, Spevak et al. 2000; Park, Cho et al. 2009). Some studies have suggested that it is also expressed elsewhere besides dentine, such as in human mandibular bone (Park, Cho et al. 2009). A third

protein, dentine matrix protein was believed to be part of this select group until its presence was demonstrated in bone (D'Souza, Cavender et al. 1997; Macdougall, Gu et al. 1998). A variant of dentine matrix protein, DMP-1 has been shown to be involved in the formation of apatite and mineralization of dentine (He and George 2004). It has been suggested to also be involved in the maintenance of the dentine after its formation (Orsini, Ruggeri et al. 2008).

The second group of NCPs consists of proteins that are not exclusive to dentine, but are found in bone and cementum as well. These include bone sialophosphoprotein (BSP), osteopontin (OSP), osteonectin (ON) and osteocalcin (OC), also known as bone Gla protein (BGP) (Butler and Ritchie 1995). **Bone sialophosphoprotein** (BSP) is glycosylated and promotes the formation of type 1 collagen fibres, and is involved in the initial stages of mineralization (Bosshardt, Zalzal et al. 1998). **Osteopontin** is a phosphoprotein seen only in young odontoblasts before the mineralisation of dentine begins and its possible role in dentine mineral formation is unclear (Beguekirn, Smith et al. 1992; Ruch, Lesot et al. 1995). The phosphorylated glycoprotein, **Osteocalcin** (OC) exhibits no direct effect on mineral formation but it is involved in the inhibition of hydroxyapatite growth. An early comparative bovine and human study showed that OC was not expressed in human dentine (Gorter de Vries, Coomans et al. 1988). This opinion has changed over time following the demonstration of OC expression in human dentine and pulpal tissues by other groups (Ranly, Thomas et al. 1997). Its high level of expression in bone has been well established (Price, Otsuka et al. 1976; Gorter de Vries, Coomans et al. 1988; Aubin, Liu et al. 1995). It has been suggested that its expression can be used as a means of distinguishing odontoblasts from osteoblasts (Papagerakis, Berdal et al. 2002). **Osteonectin** (ON) is another phosphorylated glycoprotein and it is also involved in the inhibition of HA growth, but it is actively involved in the binding of calcium and phosphate to denatured collagen (Martinek, Shahab et al. 2007). While it is expressed ubiquitously in human dentine and bone (Liao, Brandsten et al. 1998), its expression occurs at a much earlier stage of differentiation in bone cells than in odontoblasts (Papagerakis, Berdal et al. 2002).

#### 1.4.6 Mineralisation of dentine

Hydroxyapatite crystals  $[\text{Ca}_{10}(\text{OH})_2(\text{PO}_4)_6]$  form the mineral phase of dentine and are part of its crystalline structure (alongside carbonate and fluoride) (Nanci and Cate 2008). The mineral crystals in dentine are arranged with their c-axis (a vertically oriented crystal axis) in parallel to the collagen fibrils (Linde and Goldberg 1993). The first step of dentine mineralisation is the fragmentation of odontoblast cell plasma membranes (at the mineralisation front) to form matrix vesicles which contain a variety of enzymes and proteins including high levels of alkaline phosphatase, pyrophosphatase, adenosine triphosphatase, nucleotide triphosphate pyrophosphohydrolase and the phospholipid-dependent  $\text{Ca}^{2+}$  binding protein, annexin II (Goldberg, Septier et al. 1995; Sasaki and Garant 1996). The activity of these enzymes and protein causes an increased concentration of calcium ions and phosphates in the vesicles. These organelles thus serve as the initial nucleation sites. Progressively the calcium phosphate mineral crystals assume the hydroxyapatite crystal structure and this is dependent on the calcium and phosphate concentrations, as well as the pH ( $\approx 7.0$  at the mineralisation front of dentine) (Goldberg, Septier et al. 1995; Goldberg and Smith 2004).

#### 1.4.7 Dental pulp stem cells

The term “stem cell” is a fluid definition that encompasses the existence within niches of pluripotent (or multipotent) cells, with the ability to proliferate, yielding identical progeny that possess the potential for specialized differentiation, which leads to the growth of different cell types – a feature seen in mesenchymal stromal cells as first identified by Friedenstein and colleagues in rat bone marrow (Friedenstein, JF et al. 1976; Liu, Gronthos et al. 2006; Sloan and Waddington 2009; Atari, Gil-Recio et al. 2012). A broad classification of stem cells has been described based on their origin – embryonic and adult stem cells (Lakshmi pathy and Verfaillie 2005). The different stem cell types include totipotent stem cells, which are derived from embryonic tissues; pluripotent stem cells from which mesodermal, endodermal and ectodermal cells



arise; adult stem cells, which are post natal and multi-potent in nature as they give rise to cells of capable of multiple lineage differentiation (Lakshmiopathy and Verfaillie 2005).

The primary focus of stem cell research is the harnessing of this potential for self-renewal in the gaining of a better understanding of the processes underlying tissue repair and regeneration. In this context, the most ideal group of stem cells to study would be the embryonic stem cells as they have the ability to develop into almost any cell type in the human body. Asides from the huge challenges faced by researchers in answering ethical questions surrounding the use of human embryos for any stem cell based investigations, there are practical issues such as the likelihood of teratomas and carcinomas developing when used in *in vivo* experiments which detract from their use (Fry 2009). The other experimental option would be the use of adult stem cells, which are found in different tissues within the human body. These cells are capable of self-renewal and are able to generate new cells following tissue damage as well as in the absence of injury (Mason and Strike 2003). The teeth are one of these source tissues for stem cells. Work undertaken by Smith and colleagues demonstrated the initiation of a repair sequence in teeth (with damage extending past the enamel and dentine layers, into the pulp) where new odontoblasts were derived and involved in the formation of new dentine (Smith, Cassidy et al. 1995). This led to the suggestion put forward by the same author some years later that this might be due to the presence of mesenchymal stem cells in the pulp (Smith and Lesot 2001). Gronthos and colleagues isolated a population of dental pulp stem cells (DPSCs) from wisdom teeth which they described as a proliferative cell population with the ability for colony formation and the production of calcified nodules (Gronthos, Mankani et al. 2000). Further to that, characterization of the DPSCs has also described the possession of mesenchymal stem cell characteristics such as a fibroblast-like morphology and adherence to a plastic culture surface (About, Bottero et al. 2000). Work carried out by other groups on these DPSCs has since then characterized these cells as being able to differentiate *in vitro* into mesenchymal cell derivatives such as adipocytes, chondrocytes, melanocytes, odontoblasts, osteoblasts and neuronal cells (d'Aquino, Graziano et al. 2007; Stevens,

Zuliani et al. 2008; Yu, He et al. 2010). These findings give credence to the description of the vascularized dental pulp tissue as a “stem cell niche” (Newble and Jaeger 1983). To further aid the characterization of DPSCs, a panel of different cell surface antigens has used to identify these cells of mesenchymal origin. Comparative studies have shown that a similar expression pattern of mesenchymal and hematopoietic surface markers is found in both DPSCs and MSCs: a positive expression of the mesenchymal markers CD29, CD44, CD59, CD90, CD106 and CD146 and a negative expression for hematopoietic makers CD34, CD45 and CD11b (which are found in MSCs) (Arai, Ohneda et al. 2002; Huang, Gronthos et al. 2009; Alge, Zhou et al. 2010; Karaöz, Doğan et al. 2010). However, animal studies have demonstrated that the multi-lineage differentiation potential of the DPSCs is linked to the interaction of Notch receptors (Notch 1 -4) and ligands (Delta i – iii; Jagged 1 and 2) which are both expressed on the cell membranes (Nicol and Macfarlane, Dick 2006; Tigh 2012). Experiments on rat molars demonstrated that this receptor-ligand interaction is triggered by pulp tissue injury and leads to the transcription of Hairy and Enhancer of Split (HES) loci of target genes (Svinicki and McKeachie 2011), ultimately causing odontoblast (and perivascular) differentiation of dental pulp stem cells (Nicol and Macfarlane, Dick 2006). Since then, other groups have gone on to isolate other different stem cell populations from dental tissues (see Table 1). However, for the purposes of this thesis in which we consider the expression of transient receptor potential channels in odontoblast-like cells isolated from the dental pulp tissue, the focus shall be on the DPSCs.

<b>Stem cell type</b>	<b>Source</b>	<b>Differentiation potential</b>	<b>Tissue repair</b>
<b>Dental pulp stem cells (DPSCs)</b>	Permanent tooth pulp	Odontoblast, osteoblast, chondrocyte, myocytes, neurocyte, adipocyte, melanocyte	Bone regeneration, neuro-regeneration, pulp-dentine regeneration
<b>Stem cells from the apical papilla (SCAP)</b>	Developing root apical papilla	Odontoblast, osteoblast, neurocyte, adipocyte	Bone regeneration, neuro-regeneration, pulp-dentine regeneration
<b>Stem cells from the pulp of exfoliated deciduous teeth (SHED)</b>	Exfoliated deciduous tooth pulp	Odontoblast, osteoblast, chondrocyte, myocytes, neurocyte, adipocyte	Bone regeneration, neuro-regeneration, pulp-dentine regeneration
<b>Periodontal ligament stem cells (PDLSC)</b>	Periodontal ligament	Odontoblast, osteoblast, chondrocyte, cementoblast, neurocyte	Bone regeneration, root formation, periodontal regeneration
<b>Dental follicle precursor cells (DFPC)</b>	Dental follicle of developing tooth	Odontoblast, osteoblast, neurocyte	Bone regeneration, periodontal regeneration

Table 1:2: An overview of stem cells in dental tissues. Adapted from (Orenuga and da Costa 2006; Dhima, Petropoulos et al. 2012)

### 1.4.7.1 Methods of isolating dental pulp stem cells

There is at present, no standardised protocol for the isolation and purification of DPSCs. As outlined in a previous section (Section 1.4.7), the identity of these cells is dependent on the presence of demonstration of a wide array of morphological and phenotypic characteristics. Since the isolation of the DPSCs by Gronthos in 2000, there have been a number of methods developed by other researchers. These include:

- Isolation by sieving – This method employs the use of small size filters (20 – 70 micrometers in diameter) to separate cells from dental tissues digested in 3% solutions of collagenase. This allows for the purification of single cell suspensions and the underlying basis for this approach is that small diameter cells are more viable with greater chances of survival than larger cells (Gronthos, Mankani et al. 2000; Gronthos, Brahim et al. 2002). An effective method of ensuring the culture of these single “progenitor stem cells” is plating of the cells post-sieving on fibronectin-coated plates (Waddington, Youde et al. 2009) (Fibronectin has been described as a large, modular glycoprotein that generates a polymeric fibrillar network that may be used as a solid support for the attachment of adherent cells (Armstrong and Armstrong 1984)).
- Colony culturing - Following the disaggregation of the dental tissues after the collagenase solution digest phase, there is the possibility of not obtaining a homogenous cell population. The dilution of the obtained cell suspensions and re-seeding the cells over a period of time (2 – 4 weeks) allows for the selection of cell populations with the greatest potential for self-renewal and differentiation. The major disadvantage of this method is that it is time consuming and very much dependent of the rate of growth of the cell populations (Gronthos, Brahim et al. 2002; Gronthos, Arthur et al. 2011).
- Cell sorting – There are 2 ways of doing this. (1) Magnetic activated cell sorting involves separating the stem cells on the basis of expressed surface

antigens such as STRO-1 (Yu, He et al. 2010). Using immuno-magnetic beads coated with the marker specific secondary antibodies, single cell suspensions are placed in magnetic particle connectors. The target cells that bind to the beads are re-plated having being identified as subpopulations, which express for the tested markers (for example STRO-1 positive DPSC cell populations). It has however been criticised as not being a very good method for the stem cell isolation owing to a low degree of stem cell purity (Orenuga and da Costa 2006). (2) Fluorescence activated cell sorting (FACS) involves cell separation from cell suspensions using fluorescent dyes which target specific areas of the cells (nuclei, cell membranes or cytosol). A number of DPSC populations have been isolated using this technique such as STRO-1 and CD34 positive DPSCs (Laino, Graziano et al. 2006; Yang, van den Dolder et al. 2007). However, it is a very capital-intensive technique requiring the using of expensive equipment and the cells sorted by this method often lose viability owing to physiological stresses, which occur during processing.

A combination of all three methods was used to isolate cells from the dental pulp tissues in this thesis are and described in greater detail in Chapters 2 and 3.

#### **1.4.8 Pain physiology and the mechanics of somatic pain**

As highlighted in Section 1.1, pain is a complex experience that is modulated at different levels within the CNS. The detection and processing of nociceptive information is the function of the neural (pain) system (Willis 1985). This system consists of nociceptors, ascending pathways (which are made up of a number of parallel tracts such as the lateral spinothalamic tract and trigeminal tract) and higher processing centres in the brain (such as the thalamus and cerebral cortex). These nociceptors are high threshold polymodal receptors that have their cell bodies located in the dorsal root ganglia (DRG) (Julius and Basbaum 2001). Afferents from these first order neurons (FONs) within the DRGs and other cranial ganglia (apart from the

trigeminal ganglia - first order neurons from the head, face and intra-oral structures have somata in the trigeminal ganglia), project and synapse with second order neurons (SONs) in the dorsal horn of the spinal cord (lamina I and / II)(Light and Perl 1979; Todd 2010). These second order neurons extend projections to higher centres in the brain (thalamus and cerebral cortex).

There are different types of nociceptors but considered generally, they respond to chemical, mechanical and thermal stimulation. The distinguishing features are the size of their cell bodies and degree of myelination of their primary afferents. There is the A-delta, A- $\delta$  group of fibres, which are thinly myelinated and have fast conduction velocities ( $>2\text{m/s}$ ), and the unmyelinated C-fibres that have slow conduction velocities ( $<2\text{m/s}$ ). Both these groups arise from small (to medium) cell bodies and are responsible for the initial sharp and the delayed pain sensation following noxious stimulation respectively(Basbaum, Bautista et al. 2009). The A-delta fibres are subdivided into two groups – Type I A- $\delta$  fibres, which respond primarily to mechanical and chemical stimuli but can be sensitised to respond to thermal stimuli above normal noxious threshold levels, and Type II A- $\delta$  fibres that respond primarily to thermal stimuli. It has been proposed that both these groups of A-delta fibres contribute to the perception of mechanically and thermal noxious stimuli respectively (Treede 1999). Another group of fibres, A-beta fibres, A- $\beta$ , which have large diameters and are myelinated with fast conduction velocities, are not involved in pain perception (Truini, Padua et al. 2009).

## **1.5 An overview of dental pulp physiology**

### **1.5.1 Innervation of the dental pulp**

In the presence of a stimulus that elicits nervous activation in a tooth, pain is produced. The sensation experienced is described by the individual as uncomfortable, or painful, irrespective of the nature of the stimulus. There is no discrimination between modes of activation. The nerve supply of the tooth (See Section 1.3) is both sensory and autonomic. The sensory components are the trigeminal afferents

(maxillary and mandibular divisions) and the autonomic (sympathetic) component is the corresponding efferents, which regulate blood flow (Byers and Narhi 1999). The cell bodies of the pulpal sensory neurons are located in the trigeminal ganglion. Following the distribution of the vasculature of the tooth, the branches of maxillary and mandibular afferents run through the entirety of the pulp, eventually forming the Plexus of Raschkow as previously described (See Section 1.3). The myelinated sensory nerve fibres (A-fibres) are located at the dentine-pulp interface in the coronal region of the pulp. A majority of the A- $\delta$  fibres ( $\approx$ 90%) are localised in the pulpal horns (Byers 1984). The smaller non-myelinated C-fibres that make up 70 -90% of pulpal nerves are located in the core of the pulpal tissue and below the odontoblastic cell layer (Reader and Foreman 1981; Bender 2000). The cell bodies of pulpal non-myelinated sympathetic neurons originate in the cervical sympathetic ganglion and join the trigeminal ganglion. At this point they divide, some following either the course of the sensory nerves or the pulpal blood vessels (Kim and Dorscherkim 1989; Kim, Dorscherkim et al. 1989). Projections from the primary afferents of the cell bodies in the trigeminal ganglia are sent to SONs in the trigeminal brainstem sensory complex, which consists of a main sensory nucleus and a spinal tract nucleus (which is made up of 3 subnuclei – oralis, interpolaris and caudalis). Electrical stimulation studies in cats and rats have demonstrated that there is a high degree of afferent convergence in this sensory complex especially in the subnucleus caudalis, which receives most of the small diameter pulpal afferents as well as cranial nerve (VII – facial; IX – glossopharyngeal; X- vagus, and XII – hypoglossal) afferents (Dubner R 1978; Sessle 2000; Svensson P 2004). This has been proposed as a possible reason for the poor localisation and referral of pulpal (and oral musculature) pain (Sessle 2005) .

### **1.5.2 Pulpal neuropeptides and the response to injury**

Neuropeptides are neuromodulators made up of polypeptide chains of 3 -100 amino acids that are widely secreted in the human body and found in all parts of central nervous system (Caviedes-Bucheli, Muñoz et al. 2008). They function as neurotransmitters, hormones and signalling molecules of the immune system and as

such are involved in the response of tissues to injury and disease (Sacerdote and Levrini 2012). Tissue injury and the activation of pulpal sensory afferents to cause pain, also leads to vasodilatation (resulting in increased pulpal blood flow) and increased vascular permeability. Most of this increase is influenced by the C-fibres (C. Yu 2007). These vascular effects have been attributed to neuropeptides released by the neuronal fibres (Caviedes-Bucheli, Muñoz et al. 2008). Substance P (SP) and calcitonin gene-related peptide (CGRP) are perhaps the most commonly studied neuropeptides in the dental pulp (others include neurokinin A, neuropeptide Y and vasoactive intestinal polypeptide) (Olgart, Hokfelt et al. 1977; Brain, Williams et al. 1985; Jansen, Uddman et al. 1986; Helke, Sasek et al. 1991; Bellinger, Lorton et al. 1996; Beneng, Renton et al. 2010; Beneng, Renton et al. 2010; Sattari, Mozayeni et al. 2010; Caviedes-Bucheli, Azuero-Holguin et al. 2011; Caviedes-Bucheli, Moreno et al. 2011). The cell bodies of the trigeminal ganglia produce SP and CGRP which are transported to nerve terminals in the dental pulp and stored (Uddman, Grunditz et al. 1986; Wakisaka and Akai 1989). These nerve terminals are mainly C-type fibres (a few A- $\delta$  fibres as well), which closely follow pulpal vasculature and when these are stimulated, SP and any other co-stored neuropeptides are released (Awawdeh, Lundy et al. 2002). The receptors for SP, neurokinin-1 receptors and neurokinin-2 receptors have been identified in rat dental pulp fibroblasts (Fristad, Vandevska-Radunovic et al. 2003). There is evidence of the expression of NK-1 receptors in cytoplasmic processes of rat odontoblasts (Kido, Ibuki et al. 2005). Human pulp tissue has been found to express SP receptors, unfortunately a clear distinction between the two receptor types, and the cell populations within the pulp that express these receptors, is still unknown (Caviedes-Bucheli, Gutierrez-Guerra et al. 2007). It is a similar scenario with CGRP as well. There are two known receptors for CGRP, CGRP-1 receptor and CGRP-2 receptor. While there is no identification of a particular cell population or receptor isoform in human pulp tissue responsible for CGRP receptor expression (Caviedes-Bucheli, Arenas et al. 2005), an earlier detection of mRNA expression for the calcitonin-receptor-like receptor (CRLR) component of the CGRP-1 receptor in human dental pulp and trigeminal ganglia suggests that this might be the CGRP receptor present (Uddman, Kato et al. 1999).



Substance P has been described as an immuno-stimulatory factor as it controls the release of inflammatory mediators (Hahn and Liewehr 2007). It modulates the production of interleukin-2 (IL-2), -8 (IL-8), the expression of lipopolysaccharide-associated inflammatory factors by pulpal cells (Calvo, Chavanel et al. 1992; Patel, Park et al. 2003; Tokuda, Miyamoto et al. 2004) and, induces the release of inflammatory cytokines (IL-1, 6, 10 and 12) by human monocytes (Lotz, Vaughan et al. 1988; KincyCain and Bost 1997). Both SP and CGRP have been demonstrated to cause histamine release following interaction with mast cells, leading to increased interstitial pressure owing to increased vascular permeability (Hargreaves, Swift et al. 1994). The vasodilatation-promoting effects of these neuropeptides is not restricted to just inflammatory states as stimuli such as drilling, the application of ultrasound and application of occlusal and orthodontic force can also initiate their function (Matthews and Vongsavan 1994) or increase their release (Caviedes-Bucheli, Azuero-Holguin et al. 2011; Caviedes-Bucheli, Moreno et al. 2011). In addition, SP and CGRP have been shown to stimulate the growth of cells within the pulp (fibroblasts and odontoblast-like cells) (Bongenhillem, Hægerstrand et al. 1995; Trantor, Messer et al. 1995; Caviedes-Bucheli, Azuero-Holguin et al. 2011; Caviedes-Bucheli, Moreno et al. 2011). The mechanisms by which these neuropeptides influence cell growth are still unclear. SP is involved in the formation of inositol triphosphate, a product of hydrolysis of phosphatidylinositol 4-bisphosphate (into diacylglycerol and inositol triphosphate) which functions as a second messenger in the mobilization of intracellular calcium (Berridge and Irvine 1984). There have been studies showing that CGRP activates cyclic adenosine monophosphate (cAMP), which may be involved in encouraging cell proliferation (Haegerstrand, Dalsgaard et al. 1990; Kawanami, Morimoto et al. 2009). This has not been proven in dental pulp experiments however; *in vitro* work carried out by some groups has demonstrated that CGRP does stimulate the production of bone morphogenic protein-2 (bmp-2), which is involved in the formation of the dentine matrix (Calland, Harris et al. 1997; Caviedes-Bucheli, Moreno et al. 2011). While these findings highlight features, which could be of importance in the development of odontoblast-cell cultures, it shows the importance of SP and CGRP to the response of the dental pulp to damage. These neuropeptides function primarily to

potentiate an inflammatory response in the pulp as well as aid the process of pulp tissue repair. A probable sequence of events following dental pulp inflammation (considering that the pulp is enclosed within a non-yielding calcified pulp chamber) might be that the increase in vascular permeability as induced by histamine release and the subsequent increase in interstitial tissue pressure (Hargreaves, Swift et al. 1994; Cooper, Takahashi et al. 2010), could be sufficient enough to cause the dentinal tubule deformation as described in the Lin-model (which is discussed in greater detail in subsequent sections) (Lin, Liu et al. 2011) and trigger a response from mechanosensitive odontoblasts (or transduced to nociceptive sensory axons).

## 1.6 The skin as a model sensory organ

Most of the available knowledge about the sensory functions of the dental pulp is modelled around the sensory mechanisms of the skin, which is the most studied site of sensory transduction. The skin is able to respond to and discriminate between different external stimuli (mechanical, thermal and chemical stimuli). The sensory modalities in the skin are served by, in some cases, stimuli-specific sensory end organs (receptors) and in others, by polymodal (respond to more than one form of stimuli) receptors. These receptors in the skin respond to innocuous and noxious stimuli, with some degree of functional crossover (Schepers and Ringkamp 2010; Delmas, Hao et al. 2011). Mechanical sensations perceived by mechanoreceptors are touch, pressure and vibrations. Innocuous mechano-receptors in the skin such as Merkel complexes, hair follicles, free nerve endings, Meissner and Pacinian corpuscles are referred to as low threshold mechano-receptors (LTMs) and are connected primarily to A- $\beta$  nerve fibres (some hair follicles are served by A- $\delta$  fibres) through which perception of stimuli is transmitted (Munger and Ide 1988; Birder and Perl 1994; Lucarz and Brand 2007). The mechano-receptors which respond to noxious mechanical stimuli (high threshold mechano-receptors, HTMs) are connected to A- $\delta$  and C-fibres and are in some cases polymodal, also responding to noxious heat as well as chemical insult (Perl 1996). The distinction is not as clear-cut as there are C-fibres, which are LTMs and respond to “pleasant” tactile sensations (Loken, Wessberg et al. 2009; Morrison, Loken et al.

2011). However, these sensations can be perceived as painful if accompanied by trauma or inflammation (Seal, Wang et al. 2009). Thermal sensations are perceived in a similar fashion. Innocuous cold thermal stimuli are detected by “cold” fibres which when already in an active state (maximum activity is between 0 - 10°C), respond to menthol which increases the rate of action potential generation (Hensel and Zotterman 1951; McKemy, Neuhauser et al. 2002; Zanotto, Merrill et al. 2007). As with the mechano-receptors there is some functional crossover and a quick drop in temperatures is able to cause a negligible and transient sensitization of some C-fibres (LTMs) (Campero, Serra et al. 2001). However, they are not thought to be the main responders to innocuous cold temperatures. There is evidence from differential nerve block experiments in humans showing that innocuous cold sensations are perceived by A- $\delta$  fibres (Mackenzie, Burke et al. 1975). Noxious cold temperatures (0 - 20°C) are detected by A- $\delta$  and C-fibres and it is believed that the function of the C-fibres is dependent on the A- $\delta$  signals (Chéry-Croze 1983; Harrison and Davis 1999; Davis and Pope 2002). A nerve block of the A- $\delta$  fibres in the presence of noxious stimuli causes the perception of the noxious cold stimuli as hot (Davis 1998). Both A- $\delta$  and C-fibres detect innocuous and noxious warm stimuli. Warm stimuli ( $\geq 30^\circ\text{C}$ ) activate “warm” fibres which unlike the cold fibres are unresponsive to mechanical stimulation and menthol (Hensel and Zotterman 1951; Hensel and Iggo 1971). Animal studies in monkeys to determine the conduction speeds of these fibres have shown them to be C-fibres (Darian-Smith, Johnson et al. 1979). This has been supported by a loss of heat perception when these fibres are selectively blocked (Mackenzie, Burke et al. 1975). With increases in temperatures to noxious levels ( $> 53^\circ\text{C}$ ), there is a dual mechanism behind the pain sensations. A- $\delta$  fibres mediate a fast onset initial response while the second pain sensation is due to stimulation of the slower conducting C-fibres (Hallin, Torebjork et al. 1982; Gronroos, Reunala et al. 1996).

## 1.7 Sensory mechanisms in the dental pulp and the hydrodynamic theory

The dental pulp like other connective tissues (skin for example) in the body, responds to damage with a typical set of responses: inflammation, healing or death. The primary difference is that the different forms of noxious stimulation changes in pH, temperature and mechanical stimulation are perceived as a singular sensation, which is pain. The lack of an ability to discriminate between stimuli aside, the dental pulp possesses other unique features in comparison to other connective tissues - its confinement within the core of the tooth and its high degree of neurovascular supply. Drawing its blood supply from the maxillary artery, the larger of the two terminal branches of the external carotid artery, a complicated system of arterioles and venules is present in the dental pulp making it a highly vascularised region comparable to regions of the brain and tongue (Kishi, Shimozato et al. 1989). In the presence of a compromising infection, the early response of the pulp is inflammation and swelling secondary to dilation of blood capillaries and exudation of fluids, causing pressure on the nerve endings within the tissues and thus pain. Unfortunately, the pulp does not receive any collateral blood supply, meaning that in the presence of an overwhelming insult (such as would occur if there was an immune response to infection), this response may be inadequate owing to blockage of its singular blood supply by swelling (Yu 2007), causing pulpal ischaemia (self strangulation) and a resultant necrosis.

The nerve fibres (A- and C-fibres) that are described in the skin are also found in the dental pulp and, as in the skin, they maintain structural and functional differences (Byers 1984; Närhi, Yamamoto et al. 1994). Brannstrom suggested that nerve fibres extend into the dentinal tubules as part of the free nerve endings, lying in close proximity to the processes from the odontoblasts (Brannstrom and Astrom 1964). By making a cut across a tooth in a human subject and thus exposing dentine, the finding was that a fluid appeared on the cut surface, and the application of puffs of air and application of a dry filter paper on the cut surfaces caused painful responses. Their assumption was that mechanical stimulation caused an alteration of the level of dentinal fluid within the tubules and this movement stimulated nerve endings in the

tubules to yield a painful response. However, in that same experiment, the application of isotonic potassium chloride, which is a potent nerve stimulator, did not cause any pain. This suggested that there were no nerve fibres in the dentine or if there were any present, these nerve fibres did not reach the cut surface. This premise also applied to the observations made by Orchardson and colleagues in which, the direct application of the pain inducer bradykinin did not yield a painful response; neither did the application of local anaesthetic solution cause or prevent pain (Orchardson and Gillam 2006). The presence of sensory axons in dentinal tubules was demonstrated by Byers and Dong who injected radioactive proline isotopes into monkey trigeminal ganglia which over a 20-hour period, travelled through the teeth by axoplasmic transport in sensory fibres, and with radiographic evidence showed that the labeling dye had moved a distance of 120µm into the dentinal tubules (this only occurred in less than half the tubules) (Byers and Dong 1983). Later work has shown that the movement of fluid causes a mechanical deformation of the A-δ fibres, which increases the permeability to Na<sup>+</sup> ions, causing a depolarisation of the fibre membrane and initiation of an action potential (Brannstrom and Astrom 1972; Brannstrom 1986; Pashley 1990; Matthews and Vongsavan 1994). These findings support the hydrodynamic theory, which stated that the mechanism underlying the pain in response to thermal stimuli is the movement of the dentinal fluids under thermal expansion, or contraction would stimulate nociceptive fibres in the pulp (Brannstrom and Astrom 1972; Brannstrom 1986). The time-course of nerve fibre activation by cold stimuli was measured in cats and showed a slower rate of nerve fibre activity with the cooling in C-fibres than A-δ fibres (Jyvasjarvi and Kniffki 1987), alluding to a primary response to cold stimuli by the A-δ fibres. A study in humans (within temperature ranges of 25-5°C and 20 to minus 5°C) by another group showed similar results (Mengel, Stiefenhofer et al. 1993). They found a dual pain experience, with an initial sharp response after 5 secs followed by a dull response 27 secs after the start of the experiment. They attributed the initial response to an indirect mechanical movement of dentinal tubule fluids causing A-δ fibre stimulation at the dentine-pulp border and the latter slower response to the C-fibres. This was plausible owing to the peripheral location of the A-fibres, low excitability threshold and fast conduction speeds (synaptic transmission to the

thalamus); these fibres were believed to produce the initial response to external stimuli (Olgart 1974). The C-fibres have a much higher excitability threshold and slower conduction speed (indirect transmission to the thalamus with many modulating interneurons), and produce a slow response (Olgart 1974) (Table 1-4).

Direct mechanical stimulation experiments of exposed beagle dog pulps using (air blasts, probes and a von Frey hair) by Narhi and colleagues showed increased intradental A- $\delta$  nerve activity (Narhi, Hirvonen et al. 1982). This result which demonstrated the existence of mechanosensitive nerve fibres in mammalian teeth pulps, was shown by another group in cat canine dentine, using fine glass probes and also demonstrating increases in pulpal blood flow as well as (Matthews and Vongsavan 1994). Human dental pulp experiments carried out in human subjects in prepared dentinal cavities demonstrated that the function of the pulpal A- $\delta$  nerves system was dependent on the gradient of dentinal fluid flow thus providing further evidence supporting the hydrodynamic theory (Ahlquist, Franzen et al. 1994). Most recently, a mathematical model (a three-dimensional thermomechanical model) was designed to test the response of the pulp to thermal stimulation (in a single dentinal tubule) and the suggestions were that the deformation of the mineralised structure of the tubule is more important in determining the pain sensations experienced and the influence of dentinal fluid movement was secondary (Lin, Liu et al. 2011).

From the available literature, the hydrodynamic theory suggests that if the dental pulp does possess peripheral receptors capable of detecting noxious stimuli, that the responses would be dependent on activation by a mechanical component. The mechanical activation of the nerve endings within and around the dentinal tubules would lead to the generation of action potentials that would be conducted along the parent primary afferent nerve fibres in the pulp, into the dental nerve branches and then to the thalamus of the brain (Irvine 1988). However, Fried and colleagues in a recent review published last year proposed that the mechanical transmission of force through the dentinal fluids to the nociceptive nerve fibres in the dentine tubules would only be sufficient to induce nociceptive transduction in the absence of a rigid mineralised dentine structure, as would occur in acid-etched teeth or soft dentinal

caries. The detection of nociceptive stimuli would then be the purview of “algoneurons” that could detect innocuous stimuli such as air puffs (by a class of low threshold algoneurons) and noxious mechanical stimuli (by a group of high threshold algoneurons such as A- $\delta$  and C-fibres)(Fried, Sessle et al. 2011).

In our opinion, a major shortcoming of the “Fried concept” is that it is based solely on the sensation of mechanical stimuli by pulpal nociceptors and does not account for the detection of thermal stimuli. Conversely, the validated hydrodynamic theory does demonstrate that there is a direct response of pulpal neurons to temperature changes as well as to fluid movements following thermal expansion and contraction. However, we agree with proposition made by Ahlquist and colleagues that the fluid-based stimulation of the mechano-sensitive A- $\delta$  pulpal afferents would be dependent on the centrifugal force induced by the noxious stimuli (Ahlquist, Franzen et al. 1994). This would mean that a separate sensory transduction mechanism exists for the detection of mechanical stimuli.

	<b>Conduction velocity (Metres/second)</b>	<b>Character of pain</b>	<b>Stimulators</b>
<b>A-<math>\beta</math> fibres*</b>	30-70 m/s	<ul style="list-style-type: none"> <li>• Sharp pain</li> </ul>	Vibrations (causing dentinal fluid movements)
<b>A-<math>\delta</math> fibres*</b>	2-30m/s	<ul style="list-style-type: none"> <li>• Fast</li> <li>• Sharp</li> <li>• Localised</li> </ul>	Hydrodynamic stimuli (mechanical – drilling, probing; osmotic changes - hypertonic solutions) Ischemia
<b>C-fibres</b>	0-2m/s	<ul style="list-style-type: none"> <li>• Slow</li> <li>• Dull</li> </ul>	Direct pulp damage
<b>Sympathetic* fibres</b>	0-2m/s	<ul style="list-style-type: none"> <li>• Vasoconstriction</li> </ul>	Stress and painful stimuli

Table 1:3 A modified overview of the functional characteristics of myelinated (\*) and unmyelinated pulpal sensory nerve fibres (Olgart 1974; Bender 2000; Byers, Suzuki et al. 2003; Ikeda and Suda 2003; Yu 2007).

## 1.8 Odontoblasts and sensory transduction

Two key structural features of the human odontoblasts were highlighted in Section 1.4.6 – direct involvement in dentine production and their location at the interphase between the dentine and pulp. While dentine production is in some situations (such as carious lesions or trauma) a reparative response (secondary and tertiary dentinogenesis), we agree with the opinions of Smith and colleagues who proposed that this could not be regarded as a mechano-sensory response involving the odontoblasts (Smith, Scheven et al. 2012). This proposition is supported by data from a number of *in vitro* and *in vivo* studies on the response of animal (rat) and human pulpal cells to the application of mechanical (orthodontic) forces, which demonstrated increases in the expression of genes and biomarkers (such as osteocalcin, bone morphogenic proteins and collagen type I) as well as fibroblast proliferation as the primary features of the pulpal response (Dhopatkar, Sloan et al. 2005; Masella and Meister 2006; Alfaqeeh and Anil 2011).

With their cell processes extending into the dentinal fluid-containing dentinal tubules and, their cell bodies in the dental pulp, the suggestion that the odontoblasts are involved in the transduction of mechanical stimuli by virtue of their anatomical location has been made (Magloire, Couble et al. 2009). It was previously suggested that the odontoblasts acted as receptors to mechanical stimuli and conducted these signals to closely apposed nerve terminals (Avery and Rapp 1959). While the odontoblasts are in close proximity to the nerve terminals, there is at present little or no evidence to suggest any synaptic connections between them (Hildebrand, Fried et al. 1995). Reelin, a protein secreted by odontoblasts as part of the extracellular matrix as well as the neuro-regulatory molecule semaphorin 7A were suggested to provide a functional means of communication and adhesion between the cells and the nerve fibres (Maurin, Couble et al. 2004; Luukko, Kvinnsland et al. 2005). However, they both have been found to function only as guidance cues during development (odontogenesis) (Maurin, Couble et al. 2004; Luukko, Kvinnsland et al. 2005; Bleicher, Magloire et al. 2008). The most probable hypothesis would be an indirect mechanism for sensory perception in the tooth, a concept evident in other cell types in the body. It



involves the perception of the stimulus by a non-neuronal cell (for example, hair cells in the ear responding to vibrations), causing the release of a chemical mediator (glutamate) which then leads to depolarisation of the adjacent neuron(s) (Matthews and Vongsavan 1994). The perception of different tastes involves chemical activation of specialized epithelial cells in the taste buds, which activate neurons via release of a chemical mediator, probably 5-HT or ATP (Fried, Sessle et al. 2011). Mechanical stimulation of keratinocytes (Willis 1985) causes a release of ATP, which can depolarize nearby sensory neurons. Similarly, the mechanical stimulation of urothelial cells by bladder stretch modulates neuronal activity via release of ATP and NO (Dubner R 1978; Smith, Scheven et al. 2012). Hypothetically, it is possible that the odontoblast cells play a similar role detecting fluid movements in the dentinal tubules, releasing chemical mediators (such as adenosine triphosphate, ATP or nitric oxide, NO for example) that would in turn trigger adjacent sensory neurons. A stretch-activated  $\text{Ca}^{2+}$  influx is observed in odontoblasts following challenge with hypo-osmotic solution (Ahlquist, Franzen et al. 1994), indicating the presence of a mechanically-sensitive  $\text{Ca}^{2+}$  channel in addition to the calcium sensitive potassium channels,  $\text{K}_{\text{Ca}}$ . Thus an intermediate role for odontoblasts as detectors of temperature changes around a tooth, or fluid movement in dentine tubules, is possible. The odontoblast primary cilium has a 9+0 arrangement of microtubules, characteristic of sensory cilia as seen in other cell types that can detect fluid movements across the cell surface (Magloire, Couble et al. 2004; Magloire, Couble et al. 2009). The odontoblast functioning as a mechanotransducer and a thermosensitive “receptor” would through stretch-activated and thermosensitive ion channels present in its cell membrane (calcium sensitive potassium channels,  $\text{K}_{\text{Ca}}$  and TREK-1 potassium channels), detect these fluid movements and trigger an influx of calcium ions across the membrane, and releasing a transmitter substance thus effecting a response by activating sensory axons (Magloire, Lesage et al. 2003; Allard, Magloire et al. 2006; Magloire, Couble et al. 2009; El Karim, Linden et al. 2010).

## 1.9 Transient receptor potential (TRP) channels

In the preceding section we showed data in literature, which concurs with our views that the human odontoblast is capable of responding to mechanical and thermal stimuli. Evidence highlighted to support this hypothesis were that human odontoblasts were mechanosensitive and thermosensitive due to the presence of  $K^+$  channels ( $K_{Ca}$  and TREK-1) and  $Na^+$  channels expressed in their cell membranes (Magloire, Lesage et al. 2003; Allard, Magloire et al. 2006). Also expressed in the odontoblast cell membranes are classes of transient receptor (TRP) channels, which are both mechanosensitive and thermosensitive (Tominaga 2007; El Karim, Linden et al. 2010). For the purposes of this study, the primary area of interest was in the expression of these TRP channels in human odontoblasts. Before considering the role played by the odontoblast-TRP channels in sensory transduction, a brief overview of the structure and function of the TRP channel is necessary.

### 1.9.1 Transient receptor potential (TRP) channels – an overview

First discovered in *Drosophila* (Minke 1977), there are 28 TRP channels in mammals and these are subdivided into 6 subgroups: TRPC (canonical TRP), TRPV (vanilloid TRP), TRPM (melastatin TRP), TRPA (ankyrin TRP), TRPP (polycystin TRP) and TRPML (mucolipins TRP) (Montell, Birnbaumer et al. 2002). These divisions were based on the amino acid sequence homology of these cation channels as their functions were very different, and in some cases unknown (Clapham 2003). The TRP channels (Figure 1-5) consist of six transmembrane proteins domains (S1 – S6) with a gate and selectivity filter (formed by amino acids which cross the lipid bi-layer) between the fifth and sixth domains (Clapham 2003) and cytoplasmic N- and C- terminals (Ramsey 2006). The channel proteins in turn aggregate as homo- or heterotetramers to form ion channels selectively permeable to cations (Stucky, Dubin et al. 2009). The influx of cations causes the depolarisation of the cell by increasing the concentrations of intracellular calcium [ $Ca^{2+}$ ] and sodium [Na] (Ramsey 2006) (Figure 1-5). TRP channels have been described as polymodal, and as they are able to respond to different types of stimuli (such as temperature changes and osmolar stress) (Nilius and Voets 2005).

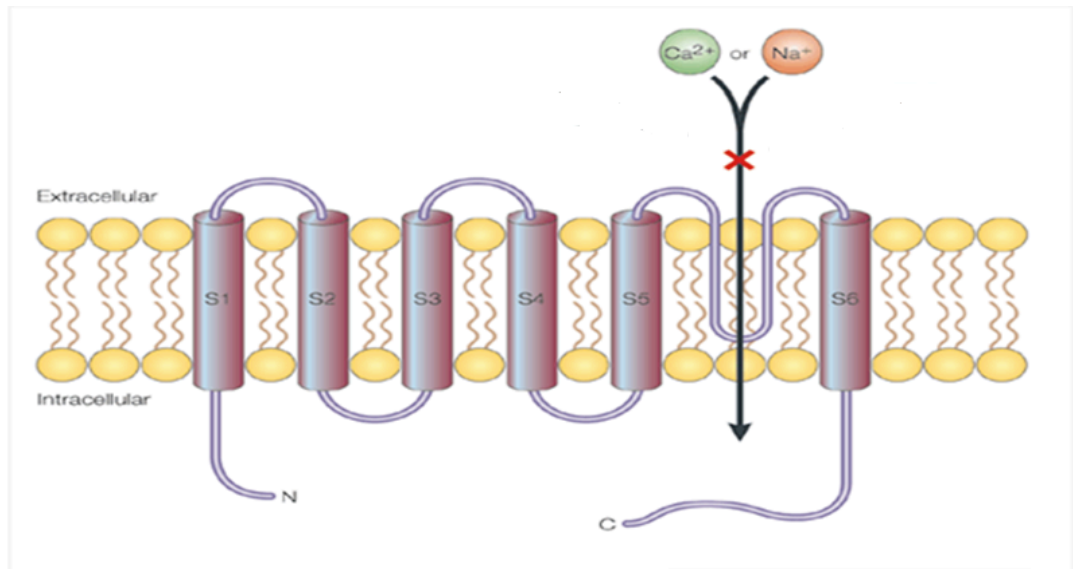


Figure 1: 5 Architecture of a TRP channel. The region between the fifth and sixth domains forms the region, which contains the selectivity filter. The cytoplasmic N and C terminals contain regulatory complexes and enzymes and the relevance of their function to that of the TRP channels are not entirely clear (Clapham 2003; Voets, Janssens et al. 2004).

TRP Channel	Activating stimuli
TRPA1	<ul style="list-style-type: none"> <li>• <math>\leq 17^{\circ}\text{C}</math>, cinnamaldehyde, allyl isothiocyanate (AITC), <math>\Delta^9</math>-Tetrahydrocannabinol, icilin, mechanical stress, <math>\text{Ca}^{2+}</math>, menthol, thymol</li> </ul>
TRPM8	<ul style="list-style-type: none"> <li>• <math>\leq 28^{\circ}\text{C}</math>, menthol, icilin, eucalyptol, <math>\text{Ca}^{2+}</math>, increased intracellular pH</li> </ul>
TRPV1	<ul style="list-style-type: none"> <li>• <math>\geq 42^{\circ}\text{C}</math>, capsaicin, camphor, nitric oxide, protons, arachidonic metabolites, endocannabinoids, resiniferatoxin</li> </ul>
TRPV4	<ul style="list-style-type: none"> <li>• <math>\geq 32^{\circ}\text{C}</math>, Osmolarity, shear stress, phorbol esters, low pH, citrate, nitric acid, arachidonic metabolites, endocannabinoids</li> </ul>

Table 1:4 Activating stimuli for mammalian TRP channels of interest

The first TRP channel identified as a thermal sensor was TRPV1 (sensitive to temperatures  $\geq 42^{\circ}\text{C}$ ) (Caterina, Schumacher et al. 1997). Other TRP channels sensitive to heating are TRPV2 (analogue of TRPV1) ( $\geq 52^{\circ}\text{C}$ ), TRPV3 ( $33\text{--}39^{\circ}\text{C}$ ) and TRPV4 ( $\geq 32^{\circ}\text{C}$ ) (Caterina, Rosen et al. 1999; Guler, Lee et al. 2002; Xu, Ramsey et al. 2002). The TRP channels, TRPA1 ( $\leq 17^{\circ}\text{C}$ ) and TRPM8 ( $\leq 28^{\circ}\text{C}$ ) are both responsive to cool temperatures less than 30 degrees (Peier, Moqrich et al. 2002; Story, Peier et al. 2003). TRP channels do show a temperature-dependent ionic response as demonstrated by cytosolic calcium measurements taken to investigate the function of TRPV1, TRPV3, TRPV4, TRPA1 and TRPM8 in human synovial fibroblasts (Kochukov, McNearney et al. 2006). The mechanisms underlying thermosensitivity of these channels are not entirely clear. In 2004 Voets et al using human kidney cells showed (by way of whole-cell patch clamp experiments) that the membranes of the cold-sensitive TRPM8 and heat-sensitive TRPV1 channels when depolarised, were activated by higher and lower physiological temperatures respectively; suggesting that perhaps there is a link between the function of these channels and the differences between activation energies across both channels (Voets, Droogmans et al. 2004). This proposed mechanism of voltage-dependent temperature sensitivity is not seen in the heat-sensitive TRPV4 channel as evidenced by earlier studies in mice (Watanabe, Vriens et al. 2002). The most likely explanation has been that temperature-controlled conformational changes occur in the TRP channel structure (TRPV1 and TRPM8) and its supporting lipid bi-layer (Liu, Hui et al. 2003; Zakharian, Cao et al. 2010). These thermo-sensitive TRP channels also show responses to a variety of chemical agonists (See Table 1:4). Work done by various groups has shown specific binding sites on the transmembrane domains of some of the TRP channels (See Table 1:5).

TRP Channel	Chemical agonist	Binding site
TRPA1	Allyl isothiocyanate	Modification of cysteines and lysines in terminal N-terminus (Bandell, Story et al. 2004; Hinman, Chuang et al. 2006)
TRPV1	Capsaicin	S2-S3 transmembrane domain link (Jordt and Julius 2002)
TRPV4	4 $\alpha$ -phorbol-12, 13didecanoate (phorbol ester)	S2-S3 transmembrane domain link (Vriens, Watanabe et al. 2004)
TRPM8	Icilin	S2-S3 transmembrane domain link (Chuang, Neuhausser et al. 2004)

Table 1:5 Mammalian chemo-sensitive TRP channels and their chemical agonists

There is no evidence in the literature of a singularly defined mechano-sensitive TRP channel. In 2004, Corey et al published evidence to show immuno-positive labelling of TRPA1 channels in mouse embryonic inner ear cells and a loss of its function following the transfection of these cells with adenoviruses containing small interfering RNAs (siRNA) targeted at the TRPA1 mRNA (whole-cell patch clamping experiments showed a reduction in transduction currents across these TRPA1 channels when compared to the non-transfected controls)(Corey, Garcia-Anoveros et al. 2004). Following this, however, studies in TRPA1 knockout mice showed an absence of impaired mechanosensitivity (there were no significant differences between the auditory brainstem responses of TRPA1<sup>+/+</sup> and TRPA1<sup>-/-</sup> mice to sound-pressure stimuli applied between 8 – 32kHz) suggesting that TRPA1 might be not solely responsible for this sensory modality (Bautista, Jordt et al. 2006). To investigate the possibility that more than one TRP channel might be involved in the detection of noxious mechanical stimuli, pain-related behaviour was tested in TRPA1 and TRPV4 knockout mice; showing an increased responsiveness to painful stimuli, more so in the TRPV4 knockouts

(Alessandri-Haber, Joseph et al. 2005). Expression of TRPV4 mRNA has been detected in mouse bladders and has been described as showing an association with stretch activated emptying of the bladder, supporting a mechano-sensitive influence of TRPV4 channels (Everaerts, Vriens et al. 2010; Janssen, Hoenderop et al. 2011). Mechano-sensitive TRP channels do not respond to stimulation through a defined mechanism. Conformational changes in the lipid bi-layer and associated cytochemical structures (similar to the mechanism described for the thermo-sensitive TRP channels earlier) following mechanical stimulation has been suggested as a possible mechanism (Corey, Garcia-Anoveros et al. 2004). This is supported by immunoprecipitation studies that have shown molecular connection between TRPV4 channels and the alpha catenin component of the adherence junctions in the mouse bladder cells (Janssen, Hoenderop et al. 2011).

### **1.9.2 Transient receptor potential (TRP) channels in the dental pulp**

Animal studies have demonstrated that some TRP channels (TRPV1, TRPA1 and TRPM8) are expressed in dental primary afferent neurones suggesting a possible role in the sensation of noxious thermal stimulation by these neurones (Park, Kim et al. 2006), contrary to the hydrodynamic theory. Some of the members of this family of cation channels (TRPV1, TRPA1 and TRPM8) have been described as transducers of dental pain and particularly temperature sensitivity as they are expressed in trigeminal nerve fibres and are (directly) activated by the same stimuli that produce tooth pain (Renton, Yiangou et al. 2003; Zanotto, Merrill et al. 2007). *In vitro* studies on cultured odontoblast-like cells have demonstrated the functional presence of these thermosensitive TRP channels (TRPV1, TRPA1 and TRPM8) (El Karim, Linden et al. 2010). As outlined in Table 1:5, these thermosensitive TRP channels also respond to a variety of chemical stimuli as well.

The presence of mechanosensitive TRP channels in the odontoblasts (and dental pulp) is an area in which a lot work still remains to be done. Mentioned in an earlier section, was the evidence to support the hypothesis that human odontoblasts were

mechanosensitive due to the presence of mechanosensitive K<sup>+</sup> channels (K<sub>Ca</sub> and TREK-1) and Na<sup>+</sup> channels expressed in their cell membranes (Magloire, Lesage et al. 2003; Allard, Magloire et al. 2006), with the most likely mechanosensitive TRP channels in human cells being TRPV4 (Tominaga 2007). At the start of our study in 2008, other than trigeminal neuron TRPV4 expression in mouse studies and in rat odontoblast cell cultures, the presence of TRPV4 in human teeth had not been described (Liedtke and Friedman 2003; Son, Yang et al. 2009). Most recently, immunohistochemical studies on human teeth sections by another group showed the presence of TRPV4-positive odontoblasts at the dentine-pulp border (Solé-Magdalena, Revuelta et al. 2011). This supports the theory that the odontoblasts might be capable of a mechano-sensory function. It has been suggested that some of the thermosensitive TRP channels (TRPA1) also respond to mechanical stimulation (Muraki, Iwata et al. 2003; Barritt and Rychkov 2005). A degree of functional overlap between the TRP channels in the dental pulp is possible. Studies performed to investigate this by considering the expression of TRPV1 and TRPV2 in rat trigeminal ganglia and rat pulp samples demonstrated (by means of retrograde labelling with a Fluoro-Gold tracer), that ≈ 50% of nerve fibres running to the trigeminal ganglia from the dental pulp expressed TRPV2 (compared to ≈ 15% of TRPV1-positive nerve fibres) (Gibbs, Melnyk et al. 2011). TRPV1 and TRPV2 are both thermosensitive responders with TRPV1 responding to temperatures lower down the spectrum (>43°C) than TRPV2 (>53°) (Caterina, Schumacher et al. 1997; Caterina, Rosen et al. 1999).

Changes in TRP channel expression with respect to tooth pathology is an area that has not been well studied. However, there is evidence supporting the functionality of some of the thermosensitive TRP channels. In studies where teeth with pulpitis were exposed to cold temperatures, there was a reduction in TRPM8 expression, suggesting that the TRPM8 channel may not show an increased response to cold sensitivity (Alvarado, Perry et al. 2007). Various groups have identified an increase in TRPV1 expression in conditions associated with pain of a trigeminal origin such as in burning mouth syndrome (Yilmaz, Renton et al. 2007), lingual and mandibular (both branches of the trigeminal nerve) nerve injuries (Biggs, Yates et al.

2007; Kim, Park et al. 2008). Capsaicin, cinnamaldehyde and menthol which are all agonists for TRPV1, TRPA1 and TRPM8 respectively, stimulate efferent lingual nerves which respond to cooling (Zanotto, Merrill et al. 2007). Carious teeth and hypomineralised teeth have been described as showing increases in pulpal TRPV1 expression (Morgan, Rodd et al. 2005; Rodd 2007).

One of the primary objectives of this thesis was to investigate the expression and function of the mechanosensitive TRPV4 in human odontoblast-like cells. Unlike the previously described thermosensitive TRPV1, TRPA1 and TRPM8 channels, there is still a huge gap in the information available regarding human odontoblasts and TRPV4 expression. While its presence in the human odontoblast has been demonstrated (Solé-Magdalena, Revuelta et al. 2011), the expression of proteins for this channel as shown by this study, is not evidence of its function. In the subsequent chapters, we shall describe the work carried out to investigate the link between the human odontoblast cell TRPV4 expression and function.

### **1.9.3 Calcium signalling and transient receptor potential (TRP) channels**

The role of the odontoblasts in the process of dentin formation and mineralisation is primarily dependent on the movement and accumulation of  $\text{Ca}^{2+}$  across the odontoblast cell membranes (Linde and Lundgren 1995). The balance between influx of  $\text{Ca}^{2+}$  into the odontoblasts and  $\text{Ca}^{2+}$  extrusion is mediated by the functions of calcium permeable channels. Some of the channels responsible for the maintenance of  $\text{Ca}^{2+}$  homeostasis in odontoblasts include plasma membrane store-operated  $\text{Ca}^{2+}$  channels (SOCE),  $\text{Ca}^{2+}$  release from intracellular inositol 1, 4, 5-trisphosphate receptors ( $\text{IP}_3\text{R}$ ), ryanodine receptors and the TRP family of cation channels (Linde 1995; Lundgren and Linde 1997; Shibukawa and Suzuki 2003). Animal studies using rat odontoblasts have also demonstrated the expression of plasma membrane  $\text{Na}^+-\text{Ca}^{2+}$  exchangers (NCX) such as NCX subtypes 1 and 3 which are thought to be involved in the extrusion of  $\text{Ca}^{2+}$  when there is an elevation of intracellular  $\text{Ca}^{2+}$  concentration in the odontoblasts (Lundquist, Lundgren et al. 2000; Tsumura, Okumura et al. 2010). The



signalling pathways involved in intracellular  $\text{Ca}^{2+}$  influx have been described in animal studies as being triggered by  $\text{Ca}^{2+}$  binding to the  $\text{Ca}^{2+}$  sensor protein, calmodulin (CaM)(Klee, Ren et al. 1998; Oshima and Watanabe 2012). The  $\text{Ca}^{2+}$ /CaM complex then activates the phosphatase calcineurin, which in its activated state dephosphorylates the transcription factor NFAT (Klee, Ren et al. 1998; Hirotsani, Tuohy et al. 2004). The activated NFAT then translocates into the cell nucleus and activates cell-specific gene transcription, which then regulate downstream terminal differentiation (Takayanagi 2007) (as seen bone cells such as the osteoblasts, osteoclasts and chondrocytes – see Table 2).

In preceding sections, the TRP channels considered in this study (TRPA1, V1, V4 and M8) have been described as non-selective cation channels that are primarily involved in thermo- and mechanosensation. With the well established fact that calcium ions are cellular secondary messengers, it was plausible to assume that TRP channels play a major role in cellular functions such as differentiation, growth and sensing of thermo mechanical stimuli (Berchtold, Brinkmeier et al. 2000). Animal studies have demonstrated this link, showing that some of these TRP channels are involved in the regulation of cell function and differentiation processes that are dependent on intracellular  $\text{Ca}^{2+}$  signalling (see table 2). In keeping with the focus of this thesis on the role of TRP channels in odontoblast sensitivity to stimuli, there is a shared opinion of the possibility that  $\text{Ca}^{2+}$  movements across the odontoblast cell membrane do play a very important part in possible cross talk between odontoblasts and adjacent sensory nerve fibres in the dentinal tubules (Tsumura, Okumura et al. 2010). Most recently, work carried out on rat odontoblasts demonstrated the cAMP-mediated cannabinoid receptor function as well as TRPV1-NCX coupled function following the application of TRPV1 agonist, capsaicin(Tsumura, Sobhan et al. 2012). This lends further support to the proposed role of TRP channels expressed by odontoblasts in response to external stimuli as well as the definition of odontoblasts as “sensory receptor cells”(Tsumura, Sobhan et al. 2012).

	Channel	Cell type	Function	Signalling cascade
INTRACELLULAR Ca <sup>2+</sup>	TRPV1	Osteoblasts, osteoclasts	Osteoblast and osteoclast differentiation (Entwistle, Tait et al. 2000)  Bone pain (Entwistle 1997; Buckley, Coleman et al. 2009)	Ca <sup>2+</sup> /Cn-NFAT; Ca <sup>2+</sup> /CaMK
	TRPV2	Osteoclasts	Osteoclastogenesis (Nicol and Macfarlane, Dick 2006)	Ca <sup>2+</sup> /Cn-NFAT; Ca <sup>2+</sup> /CaMK
	TRPV4	Osteoclasts, chondrocytes	Osteoclast and chondrocyte differentiation (Kolb 1984; Biggs 1999)  Chondrocyte osmo-sensitivity(Healey and Jenkins 2000)	Ca <sup>2+</sup> /Cn-NFAT; Ca <sup>2+</sup> /CaMK
EXTRACELLULAR Ca <sup>2+</sup>	TRPV5	Kidney cells, osteoclasts	Renal calcium reabsorption(Kolb and Kolb 2009)  Undefined role in osteoclast differentiation	Ca <sup>2+</sup> /Calbindin-D <sub>28k</sub>
	TRPV6	Intestinal cells, osteoblasts, osteoclasts	Intestinal calcium reabsorption(Hoad, Reddick and Theaker 2003)  No known role in osteoblast or osteoclast differentiation	Ca <sup>2+</sup> /Calbindin-D <sub>28k</sub>

Table 1:6 The role of TRP channels in calcium signalling. Ca<sup>2+</sup> influx across the TRP channels activates Cn-NFAT (Calcineurin nuclear factor of activated T cells) and CaMK (calmodulin-dependent kinases).

### 1.10 Aims and objectives

The previously described hydrodynamic theory proposed that dental pain was the product of the detection of dentine tubule fluid movements by dental sensory afferents (Brannstrom and Astrom 1972). It has been suggested that the TRP channels, which are expressed by dental pulp sensory neurons and odontoblasts, might respond to these fluid movements as either innocuous or noxious stimuli. However, there is no direct evidence available at present to explain how these trigeminal nerve fibres detect the movement of dentinal fluid within the tubules. The activation of these channels in the odontoblasts and sensory nerve fibres under the influence of mechanical, thermal or chemical stimuli may provide a more plausible mechanism by which nociceptive

stimuli in the pulp are detected and processed, independent of dentine fluid movements. There has not been, however, a systematic study of TRP channels expression and localisation within odontoblast cells of teeth, probably due to the difficulty in studying these cells *in situ*. Available literature highlights as one of the most important feature of human dental pulp cells, the multi-lineage potential for differentiation (odontoblast-like differentiation in this case). Human dental pulp cells can be induced *in vitro* to differentiate into cells demonstrating an odontoblastic phenotype, which is characterized by the presence of polarized cell bodies and the accumulation of mineralized nodules (Tsukamoto, Fukutani et al. 1992; About, Bottero et al. 2000; Couble, Farges et al. 2000). Present among these cells with this dentinogenic potential are subpopulations of human dental pulp cells with the capacity for adipogenic and neurogenic differentiation capacities demonstrated by the presence of adipocyte-like and neuronal-like cell morphologies and gene markers for the respective phenotypes (Gronthos, Brahim et al. 2002). Dental pulp stem cells have also been found to undergo chondrogenic, myogenic and osteogenic differentiation *in vitro* (Laino, d'Aquino et al. 2005; d'Aquino, Graziano et al. 2007). The demonstration of the multi-potent nature of these cells suggests that the induction and maintenance of an odontoblastic cell line is achievable. It is in this context we aimed to isolate DPSC populations from extracted human teeth. With the establishment of a viable odontoblast cell culture system, there is an increased potential for the analysis of peripheral dental pain mechanisms at the level of these nociceptive cells, an opinion shared by many research groups (Allard, Magloire et al. 2006; Magloire, Couble et al. 2009; Henry 2011). With the acquisition of this population of cells (odontoblasts), the next objective would be the analysis of the expression of pain-related cation channels (TRP channels) in these derivatives of human pulp cells (odontoblasts) by genetic methods, with an ultimate aim to establishing a correlation between protein expression and function of these TRP channels.

The aims of this study can be summarised as follows:

1. Establishment of human dental pulp cultures using teeth extracted from consenting dental patients with a primary aim to examine roles they play in dental pain.
  - a. To start this off, odontoblast cultures were grown from collected dental pulp cells (DPCs) to allow for study of individual odontoblast cell-induced activity.
  - b. Different culture media conditions were applied and optimised to trigger the induction of lineage specific odontoblast precursors, identified by functional differentiation markers (e.g. dentine sialophosphoprotein).
  - c. The odontoblast-like DPCs were observed through an odontoblast precursor phase to an odontoblast-like mature phenotype phase, spanning an average of 9 population doublings. Markers of cellular maturity and functional differentiation (for example, ALP and COL-1) were identified.
  
2. Examination of the expression of pain and inflammation-related receptors (TRP channels and SP-responsive tachykinin receptors) by genetic methods. The aim was to determine whether TRP channels were expressed in human dental tissues.
  - a. Following the validation of TRP channel expression by performing reverse transcription polymerase chain reaction (RT-PCR) and quantitative RT-PCR on samples of human pulpal tissue and human derived odontoblasts *in vitro*, we demonstrated the function of these TRP channels expressed by the odontoblast-like cells following the application of TRP channel agonists and antagonists using ratiometric Ca<sup>2+</sup> imaging techniques.
  - b. We also examined the release of chemical mediators such as ATP by the odontoblast-like cells in response to the tested TRP channel agonists.



# General materials and methods

---

2

## **General materials and methods**

In this chapter, a description is given of the general methods used in the course of this thesis. In subsequent chapters, references will be made as appropriate and the experimental details described in greater detail.

### **2.1 Establishment of primary cell cultures**

The primary human pulpal cell cultures used in this study were obtained from consented patients (with ethical approval – KCH REC REF 08/H0808/104) presenting for extractions at the Department of Oral Surgery, Dental Institute, King's College London. The details of the experimental procedures of isolation and expansion of these primary cell cultures are fully described in Chapter 3.

### **2.2 Cell viability counts**

Using a TC10™ Automated Cell Counter (Bio-Rad, USA) and a TC10™ trypan blue exclusion dye, counts for cell viability and proliferation were performed on cell cultures established from the isolated human pulpal tissues. Both counting chamber and coverslips were carefully cleaned with a solution of 70% industrial methylated spirit (IMS). 10µl volumes of cell suspensions (from post-centrifugation cell culture pellets) were aliquoted into 500µl Eppendorf tubes. An equal volume of trypan blue was added to achieve a 1:1 cell dilution. A 10µl volume of the cell mixture was pipetted into both chambers of the counting slide. The counting slide was then inserted into the slot and an automatic count of the cells of the viable cells was obtained. The counts were expressed as the total number of cells per ml of the suspension, number of live and dead cells, and are based on an imaged area of 4mm.

### 2.3 Preparation of cell lysates

In readiness for the analysis of the human pulpal tissue-derived cell phenotypes in culture (methods are explained in detail in subsequent sections) the cells were seeded in appropriate test conditions. At the designated time points, the membranes of the cells were disrupted by a series of 3 “freeze-thaw” cycles: The culture medium was removed and 1ml of sterile water added to each well. The culture plate was then placed in a freezer at -80°C for 20 mins, followed by a heating phase at 37°C in a sterile incubator (5% CO<sub>2</sub> in a humidified atmosphere) for 15 mins. At the end of the series, the lysate solution was collected, labelled and stored until required for use at -20°C.

### 2.4 DNA quantification assay

Cells from isolated human pulpal tissues, and mesenchymal stem cells (MSCs, which were used as cell controls), were seeded in 24-well plates at a density  $1 \times 10^4$  cells/well and cultured in Dulbecco’s modified Eagle’s media (DMEM)-based culture conditions. At designated time-points specific to the experiments described in subsequent chapters, the culture media was removed from culture plate wells and the cells were washed with phosphate buffered saline (PBS). Cell lysates were obtained as described in the previous section.

A calibration curve was prepared using a serial dilution of DNA in saline sodium citrate (SSC) buffer, pH 7.0. A 20 times working strength of SSC buffer (500ml volume) was made by dissolving 87.65g of sodium chloride (NaCl) and 44.1g of tri-sodium citrate in de-ionised water. The pH was adjusted to 7.0 using 1M sodium hydroxide (NaOH). A stock of DNA specific fluorimetric dye (1µg/ml Hoechst 33258; Sigma®) was thawed and serially diluted in a 1:20 ratio, in the SSC buffer. The concentrations of the serial dilutions were: 20, 10, 5, 2.5, 1.25, 0.625, and 0.315µg/ml. Where appropriate, approximations were made when pipetting the volumes to the closest 0.01. Using a 96 well plate, 100µl of each DNA dilution, Hoechst 33258 dye and cell lysate was pipetted into the appropriate well. The fluorescence readings (excitation at 355nm and emission at 460nm) were measured using a fluorimetric reader (Chameleon, Hidex, Finland).



## 2.5 Alkaline phosphatase activity assay

Human pulpal tissue-derived cells were seeded in 24-well plates at a density  $1 \times 10^4$  cells/well and cultured in DMEM-based growth media. At experiment-specific designated time points (which are described in subsequent sections), the growth media was removed from designated wells and the cells were washed with PBS. Cell lysates were collected for each time point as described in Section 2.4. Alkaline phosphatase, ALP, activity was measured using p-nitro phenyl phosphate (Sigma) as a substrate for the enzyme (Böker, Yin et al. 2008). ALP cleaves the phosphate group from p-nitro phenyl phosphate to yield p-nitro phenol, which is yellow at an alkaline pH (10.3). The activity of the enzyme in the cell lysates was measured by preparing a standard curve for the serial dilutions of the p-nitro phenyl phosphate in 0.1M glycine solution, pH 10.3. An alkaline phosphatase reaction buffer (1M diethanolamine (DEA) (Merck, USA), 10mM p-nitro phenyl phosphate (PNPP), 0.5mM  $MgCl_2$  and 0.22M NaCl at a pH of 9.8, was also prepared. Using a 96 well plate, 50 $\mu$ l of the cell lysates and the ALP reaction buffer was pipetted into an appropriate well. The absorbance was measured at a wavelength of 405nm with a spectrophotometer (Opsys MR Microplate reader) after 5 mins.

## 2.6 Cell proliferation assay

Using a CellTiter 96<sup>®</sup> AQ<sub>ueous</sub> Non-Radioactive Cell Proliferation Assay kit (Promega), 21ml stock solution of MTS [3-(4,5-dimethylthiazol-2-yl)-5-(3-carboxymethoxyphenyl)-2-(4-sulphonyl)-2H-tetrazolium] solution was prepared by adding 21ml of PBS to 42mg of MTS reagent powder in a light-protected falcon tube (BD Falcon). The pH of the MTS solution was adjusted to 6.5 using 1N HCl and then it was filter-sterilized [0.2 $\mu$ m filter (VWR, UK)]. A 100 $\mu$ l solution containing 0.92mg/ml phenazine methosulphate (PMS) in PBS was aseptically added to 2ml of MTS solution in a foil covered bijoux tube. The cells (DPSCs) were seeded as described in the previous section in 24-well plates (Cell Star<sup>®</sup>) at required densities (ranging from  $1 \times 10^2$  -  $1 \times 10^5$  cells/ml). At the designated time points, the growth media was removed from wells and the cells were washed with PBS. After gently mixing the MTS/PMS solution by swirling the holding tube, 20 $\mu$ l of the combined solution was added to each well of the plate at each designated time point, and then incubated for 2 hours in a humidified,

5% CO<sub>2</sub> incubator at 37°C. After this time, the plates were removed from the incubator and the MTS/PMS solution was pipetted out of each well and transferred individually into individual wells of a 96-well plate. The working principle of this assay relies on the bio-reduction of the MTS/PMS combination reagent by metabolically active cells (this occurs through the activities of dehydrogenase enzymes). The absorbance of the resultant formazan product from the cells of both experimental groups was read at 490nm using a spectrophotometric plate reader (FluroStar Optima: BMG Labtech).

## 2.7 Immunocytochemistry

To observe the spatial structure of, and the expression of phenotypic markers by the isolated human pulpal cells, immunocytochemistry was performed. The pulpal tissue-derived cells were cultured in T25 culture flasks up to a point of 80% confluence and were trypsinized and transferred to 6-well tissue culture plates 24 hours before the day of the experiment. Glass coverslips were sterilized by dipping in 80% ethanol before being left to dry for a few seconds. A single coverslip was placed in each well of the culture plates. 1ml of pulpal tissue-derived cell suspensions were placed over each of the coverslips in the 6 well culture plates and they were left to grow at 37°C in a humidified CO<sub>2</sub> incubator until 50-70% confluence was reached. At this point, the culture medium was aspirated from each well and the cells were rinsed twice with PBS at room temperature without letting the cells dry out. The cells were then fixed by incubation with 4% paraformaldehyde in PBS for 20 minutes at room temperature. The cells were rinsed thrice with PBS following this, and permeabilized using 0.1% Triton-X in PBS for 15 minutes at room temperature. The cells were rinsed again (thrice) with PBS. The cells then underwent a blocking step, submersed in 10% fetal bovine serum (FBS) for 1 hour at room temperature, to saturate non-specific binding sites. Following this step, visualization was performed using FITC-conjugated phalloidin (1/1000). This served as the primary antibody and was diluted at the appropriate concentration in 10% FBS to yield volumes that completely covered each coverslip within each well. The cells/ primary antibody mixture in the culture plates was then incubated at 4°C overnight. Control wells without primary antibodies were included in each batch of cells tested. At the end of the incubation period, the cells were rinsed in 1% FBS in PBS three times for 10 minutes. A nuclear marker, DAPI (4', 6-diamidino-2-phenylindole)

was diluted in 1% FBS and the cells were incubated in this solution for 10 minutes in a humidified CO<sub>2</sub> incubator at 37°C. The coverslips were then mounted on labelled glass slides with mounting medium and visualised using a fluorescent microscope, Leica DMRE upright confocal microscope (Leica Microsystems Heidelberg GmbH), equipped with appropriate filters for the visualization of nuclear and surface markers used in these experiments.

## 2.8 RNA extraction and analysis

Using modified experimental protocols, which are fully described in relevant sections of this thesis, RNA was obtained from isolated human pulpal tissues and established human pulpal cell cultures. Following this, a Nanodrop 1000 (Thermo Scientific®) spectrophotometer was used to quantify the yield and purity. For RNA samples previously stored at -80°C after extraction, a thawing process on ice was carried out prior to spectral measurements. The sample measurement pedestal was cleaned using a dry lint-free laboratory wipe and de-ionized water. A spectral measurement of 1µl of RNase-free water was made to initialise the experiment. After this the measuring pedestal was cleaned as previously described and 1µl of each sample was placed on the pedestal and measured. Ratios of readings at 260nm: 280nm and 260nm: 230nm were taken to determine the purity. Samples used in these studies were those with 260/280 ratios of between 1.9 to 2.2, and 260/230 ratios of 1.6 to 1.8 at pH of 7. These values showed an absence of genomic contamination and ethanol carry-over and are in keeping with the desirable requirements for the successful isolation and analysis of RNA (Wilfinger, Mackey et al. 1997).

## 2.9 cDNA synthesis

Using the quantified RNA (see section 2.8), stable cDNA was synthesized for polymerase chain reaction (PCR) amplification. The reaction required 1µg RNA, which was then diluted in 10µl in 0.5ml PCR tubes. The tubes used were thin walled to reduce insulation and allow for heat transfer. Oligo-dT primers made up 1µl of the total volume (25ng/µl), and the master mix made up the other 8µl. The mixture was placed on a heating block set at 65°C for 5 minutes to denature any secondary structures, thus

exposing the RNA sequence to oligo-dT primer adhesion. Following this, the tubes are placed on ice for 1 minute to allow for the primers to anneal. After centrifuging the contents of the PCR tube, a cDNA synthesis mix was added in the following order to the RNA/primer mix:

2µl 10X reverse transcriptase (RT) buffer; 4µl 25 mM MgCl<sub>2</sub>, 2µl 0.1 M dithiothreitol; a 1µl volume of an RNase inhibitor, RNaseOUT™ (40 U/µl), and a 1µl volume of SuperScript III RT™ (200 U/µl).

The mixes in the tubes were then incubated at 50°C for 50 minutes and then 85°C for 5 minutes in an Applied Biosystems® Thermocycler. At this point the reaction was terminated. During the first temperature cycle, the reverse transcriptase binds the oligo-dT primers and reverse transcribes the RNA sequence to form the cDNA. The high temperatures, to which the tubes are exposed to (85°C), denatured the reverse transcriptase and stopped cDNA synthesis. 1 µl of RNase H™ was added and the mixture left to stand at 37°C for 20 minutes. The resultant cDNA samples were then stored at -20°C.

## 2.10 Primers for reverse transcription-polymerase chain reaction

To design sequences specific to the DNA of the genes of interest, freeware programs were used. The first step was choosing the correct information for each gene of interest at the website, [www.ensembl.org](http://www.ensembl.org). Following the instructions on the home page, the name of the desired species (human) was typed in, followed by the gene of interest. From the drop down lists of genes that this action generated, the appropriate gene was selected and the exon information retrieved. On another website offering a freeware program, Primer3 (<http://frodo.wi.mit.edu/primer3/>), the exon codes were copied and pasted as directed by the program. Without changing any of the pre-set parameters on the primer3 page, the “pick primers” option was chosen. This generated a list of primer sequences in a drop down menu. The primer-pairs chosen had as closely matching T<sub>m</sub> (melting temperature) values as possible (differences of ± 1°C). Primers to human gene targets were designed using Primer3 (<http://frodo.wi.mit.edu/primer3/>) and checked for inappropriate binding using “Blastn” ([www.ncbi.nlm.nih.gov](http://www.ncbi.nlm.nih.gov)). Using another freeware program “OligoCalc”

([www.basic.northwestern.edu/biotools/oligocalc.html](http://www.basic.northwestern.edu/biotools/oligocalc.html)), the primers were designed to minimise hairpin formation.

Glyceraldehyde 3-phosphate dehydrogenase (GAPDH) was the housekeeping gene used to normalise for the RT-PCR experiments described in subsequent chapters. The table below (Table 2-1) outlines the sequences and sizes (in base pairs) of the designed primers used.

PRIMER	SEQUENCE PRODUCT	LENGTH (bp)	PRIMER	SEQUENCE PRODUCT	LENGTH (bp)
ALP	F: 5'-CCACGCTTCACATT TGGTG-3' R: 5'-AGACTGCGCTGGTAGTTGT-3'	196	NK2R	F: 5'-GGTATTGGCTATGCATACACC-3' R: 5'-TGACGGAACTGTCATTGAGG-3'	270
β3T	F: 5'-C-ATG GACAGTGTCCGCTCAG-3' R: 5'-CAGGCAGTCGCAAGTTTTCAC-3'	175	PPARγ	F: 5'-CAGTGGGGATGCTCATAA-3' R: 5'-CTTTTGGCATACTCTGTGAT-3'	422
CBFA-1	F: 5'-TGAGAGCCGCTTCTCAACC-3' R: 5'-GCGGAAGCATCTGGAAGGA-3'	270	p16	F: 5'-GACATCCCGATTGAAAAGAA-3' R: 5'-TTTACGGTAG TGGGGAAAGG-3'	198
COL-1	F: 5'-CCAAAATGCTCTCCCAAG-3' R: 5'-TCAAAAACGAAGGGAGAT-3'	213	p53	F: 5'-GGCCACATTCACCGTACTAA-3' R: 5'-GTGGTTTCAAGGCCAGATGT-3'	156
DMP-1	F: 5'-CAGGAGCACAGAAA AGGAG-3' R: 5'-CTGGTGTATCTTGGGCACT-3'	213	REX-1	F: 5'-GATCTCCCACTTCCCAAG-3' R: 5'-GCAGGTAGCACACCTCCTG-3'	104
DSPP	F: 5'-TCAAGGAGAGGGAATG-3' R: 5'-TGCCAT TTGCTG TGATGTTT-3'	489	RUNX2	F: 5'-CAGACCAGCAGCCTCCATA-3' R: 5'-CAGCGTCAACACCATCATTC-3'	177
DSPP	F: 5'-TCAAGGAGAGGGAATG-3' R: 5'-TGCCAT TTGCTG TGATGTTT-3'	201/489	SOX-9	F: 5'-TGAAGAAAGGAGCGAGGAA-3' R: 5'-GGGGCTGGTACTTGTAAATC-3'	348
EN-2	F: 5'-TTATTG GCATGGATG TTGCTGC-3' R: 5'-CCCGCTCAATAC GTTTTGGG-3'	269	TRPA1	F: 5'-TG GTGCACAAATAGACCAGT-3' R: 5'-TGCGCACCTTTAGAGAGTAGC-3'	318
GAPDH	F: 5'-ACCACAGTCATGCCATCAC-3' R: 5'-TCCACCACCTGTTGCTGTA-3'	452	TRPM8	F: 5'-GCACCAGATCAACCAAAAGT-3' R: 5'-CTTGGCCAAAACACAAATG-3'	681
hTERT	F: 5'-CCTCTG TGCTGGGCC TGGAGATA-3' R: 5'-ACGGCTGGAGGTC TGAAGGTAG-3'	282	TRPV1	F: 5'-GCCCTGGAGGCTTCAAGTTC-3' R: 5'-GCCTGAAACTCTGTTGACC-3'	452
NANOG	F: 5'- CCTCTTAAATTTTTCTCTCTTC-3' R: 5'-AAGTGGGTGTTGCTCTTG-3'	271	TRPV4	F: 5'-ACATGGGGAGTTCATTAAAC-3' R: 5'-CACAGCCAGCATCTGTGGGG-3'	512/692
NESTIN	F: 5'-CTCTGACCTGTCAGAAAGAAAT-3' R: 5'-GACGCTGACACTTACAGAAAT-3'	302			
NK1R	F: 5'-CGACAGCGACCAGATCAAGGAGG-3' R: 5'-TG CATTGCACCTCTTCAT-3'	312			
NK2R	F: 5'-GGTATTGGCTATGCATACACC-3' R: 5'-TGACGGAACTGTCATTGAGG-3'	270			

Table 2:1 Sequences of the primers designed to recognise genes of interest which were alkaline phosphatase, beta-3-tubulin (β3T), core binding factor 1 (CBFA-1), collagen type I (Col I), dentine matrix protein 1 (DMP1), dentine sialophosphoprotein (DSPP), enolase 2 (EN-2), human telomerase reverse transcriptase (hTERT), Homeobox protein NANOG (NANOG), nestin, substance P receptors – neurokinin-1 and -2 (NK1R and NK2R), peroxisome proliferator activated receptor gamma (PPARγ), senescence associated proteins p16 and p53, RNA exonuclease 1 (REX-1), runt-related transcription factor 2 (RUNX2), sex determining region Y-box 9 (SOX9) and transient receptor potential channel receptors (TRPA1, M8, V1 and V4). Glyceraldehyde 3-phosphate dehydrogenase (GAPDH) was used as the housekeeping gene.

## 2.11 Agarose gel electrophoresis

Agarose gels were prepared to separate and analyze the amplified DNA transcripts (of the genes of interest). To allow for good resolution, 2% agarose gels were made by mixing 4g multipurpose agarose in 200ml of Tris-Acetate-EDTA (TAE) buffer in a sterile glass bottle. While still molten, 8µl of Gel Red (Biotium™) was added per 200 ml, and swirled to get a good mix. TAE was chosen over Tris-Borate-EDTA (TBA) as it gave a better product resolution. By removing  $\text{Ca}^{2+}$  and  $\text{Mg}^{2+}$ , which regulate the activity of DNase enzymes, EDTA functions to reduce the loss of DNA. The solution was heated in a microwave for 3 minutes to boiling point to ensure the complete dissolution of the agarose in solution. The liquefied solution was then poured into a 15 x 10 cm multiSUB horizontal agarose gel flexicaster tray (Gentaur Molecular Products©) holding 2 20-tooth combs and sealed with rubber tray dams on either side. The gel was left to set at room temperature for 20 minutes. Once solidified, the gels were placed in the gel electrophoresis tank containing TAE buffer, which was topped up to submerge the agarose gel. The combs were removed and 10µl of amplified DNA sample (PCR product) was loaded into each well. The lid of the electrophoresis tank was sealed and it was connected to a power source through a gel electrophoresis power pack (Pharmacia LKB Biotechnology). The gels were run at 95 amperes and 100 volts for 30 minutes. The PCR master mix, GoTaq® DNA Polymerase (Promega™) used for the preparation of the cDNA contained two dyes (blue and yellow) that were designed to separate during electrophoresis, acting as visible colour indicators allowing for the monitoring of the migration progress.

## 2.12 Gel Imaging

At the end of the electrophoresis run, the gels were taken out of the gel tanks and drained of excess TAE buffer. The gels were then placed in the dark box of an Alpha Innotech Alpha-Imager 2000 (Alpha Innotech Corporation) for viewing. The imager was used to highlight the bands of the samples run. It did so by illuminating the gels with ultraviolet light, which excites the Gel Red dye, which had intercalated with the DNA bands. Black-and-white digital images were captured and saved in TIF format.

## 2.13 Reverse transcription-quantitative polymerase chain reaction

The reverse transcription-quantitative polymerase chain reaction (qRT-PCR) methodology used in these experiments was the Sybr Green I Dye detection system developed by Applied Biosystems™. This method employs the use of the Sybr Green dye, which has a high binding specificity for double stranded DNA. This allows for the detection and monitoring of amplified double stranded DNA (PCR products) over the course of the reaction. With the addition of the dye at the start of reaction, it binds to all double stranded DNA present resulting in fluorescence. As the PCR cycle progresses, a DNA polymerase yielding more PCR products amplifies the target sequences. This means there is an increase in the number of binding sites for the dye and this causes an increase in fluorescence in direct proportion to the PCR product yield. Primer sequences for genes of interest were designed for use in experiments employing this technique.

### 2.13.1 Reference genes

The primary importance of the addition of a reference gene to the qPCR setup is that it allows the normalization of data to eliminate errors borne out of biological variation of the samples being tested (Vandesompele, Kubista et al. 2009) or experimental errors such as a variation in instrumentation or pipetting techniques (Dheda, Huggett et al. 2005). Beta actin was used as a reference gene to normalise for RNA expression.

### 2.13.2 qRT-PCR workflow

Following the isolation of RNA as described in previous sections, first strand DNA synthesis was performed to yield cDNA (25µl) required for the qPCR. These cDNA samples are in a 1:1 ratio with the isolated RNA samples. To achieve a 20-fold dilution required to give appropriate volumes of cDNA needed for the qPCR, the appropriate amount of UltraPure™ DNase/RNase-Free Distilled water (Invitrogen™) was added (495µl). Following the instructions of the protocol, an appropriate volume of PCR master mix (4µl) containing SYBR Green dye, thermostable recombinant Taq DNA



Polymerase, ROX (a passive reference dye used for normalizing against non-PCR related fluorescence), and dNTPs (deoxynucleotides), was added to 9µl of UltraPure™ water. A separate stock mix of individual primer sets (2µl) and template cDNA (5µl) was also prepared. Pipetting (manually) both master and stock mixes into the appropriate reaction tubes (0.1ml strip tubes, Qiagen™) gave a total reaction volume of 20µl. To eliminate the possibility of non-specific fluorescent signals and cDNA contamination, controls where cDNA had been substituted with water were run. All samples were tested in triplicate and for a single primer at a time. The primers were run on a Rotor Gene™ 6000 PCR system. The PCR cycling parameters used were: (1) An initial “HOLD” step for 10 minutes at 95°C to activate the DNA polymerase, (2) a “CYCLING” phase consisting of 40 cycles of denaturing the cDNA at 95°C for 10 seconds, 60°C for 10 seconds and 72°C for 20 seconds and, (3) a “MELT” phase (annealing and extension) consisting of a step-wise increase in temperature from 72°C to 95°C, rising at 1°C per step, waiting 90 seconds of pre-melt conditioning on the first step and 5 seconds for every other step afterwards. The data showing the expression of the genes of interest (see table 2-2) relative to the internal control (Beta actin) was analysed using the Rotor-Gene 6000 Series Software (version 1.7.87) and GraphPad Prism®.

### 2.13.3 qRT-PCR data analysis

The experimental methods applied in these studies were aimed at the determination of fold changes in the expression levels of the genes of interest. The generated data was processed using the comparative  $C_T$  method ( $\Delta\Delta C_T$  method) which involved 3 steps (Livak and Schmittgen 2001). First, following the assay of samples for the chosen genes of interest and the chosen housekeeping gene, the  $C_T$  values (the threshold cycle during PCR when the level of fluorescence gives signal over the background and is in the linear portion of the amplified curve), were obtained using the Rotor-Gene 6000 Series Software (version 1.7.87). These values were normalized to the housekeeping gene to give the  $\Delta C_T$  value, ( $C_T$  gene of interest -  $C_T$  housekeeping gene =  $\Delta C_T$ ). These were then compared to a common reference gene (for all genes of interest) to give a  $\Delta\Delta C_T$  value, ( $C_T$  gene of interest -  $C_T$  reference gene =  $\Delta\Delta C_T$ ). This value was then imputed into the equation:  $2^{-\Delta\Delta C_T}$  (2 = fold change in PCR products

between cycles,  $\Delta\Delta C_T$  = normalized cycle changes between gene of interest and reference gene), to yield the fold changes observed. The means of the replicate samples used was normalized to the average  $C_T$  values obtained for the control samples. Quantification using this method was based on the assumption that the PCR amplification efficiencies of the genes of interest and the house keeping genes are relatively similar (Giulietti, Overbergh et al. 2001; Livak and Schmittgen 2001).

#### **2.13.4 Designing the primers for qRT-PCR experiments**

Using the freeware program “Refgene” available on the UCSC Genome Bioinformatics website (<http://genome.ucsc.edu/>), primers for genes of interest (see Table 2-1) that targeted dissimilar nucleotide sequences and would not cross-hybridize among one another were designed for use in real-time quantitative PCR experiments (Table 2-2). A primer for Beta actin was designed for use as the housekeeping gene to normalise for the qRT-PCR experiments, which is described in subsequent chapters.

#### **2.13.5 Sensitivity and specificity of designed primer sets**

The gene primer sets (Table 2-2) were tested in PCR assays against cDNA samples (see section 2.8). All assays and PCR amplifications were performed in keeping with the protocols described in Section 2.12.2. Ten–fold dilution series of the cDNA samples were prepared for each primer set (ranging in concentration from  $1 \times 10^0$  to  $1 \times 10^8$ ) and individual PCR assays were performed at each dilution using a reaction volume of 20 $\mu$ l (1 $\mu$ l of forward primer, 1 $\mu$ l of reverse primer, 4 $\mu$ l of PCR master mix, 9 $\mu$ l of water and 5 $\mu$ l of cDNA). Standard curves were generated for each of the tested primer sets, including the housekeeping gene (Beta actin) to demonstrate sensitivity of the primers (the results are further explained in Chapter 4 and 5). The amplified products were run on agarose gels to demonstrate the expression of bands, indicating the specificity of the primers (the gels are explained in Chapter 4 and 5).

PRIMER	SEQUENCE	PRODUCT	LENGTH (bp)	PRIMER	SEQUENCE	PRODUCT	LENGTH (bp)
CD44	F: 5'-CCAGAAGGAACAGTGGTTTGGC-3'		151	NK1R	F: 5'-GCAGAAGAAATAGGAGCCAAATG-3'		227
	R: 5'-ACTGTCCTCTGGCCTTG GTGT-3'				R: 5'-ACTGCTGAGGCTTGGGTCT-3'		
CD45	F: 5'-CTGACATCATCACCTAGCAG-3'		257	NK2R	F: 5'-CACCTATGCTGTCCACAACG-3'		72
	R: 5'-TGCTGTAGTCAATCCAGTGG-3'				R: 5'-CTGGAGGGGATGTATGATGG-3'		
ALP	F: 5'-GATCTGGCCATTGGCACCTG-3'		190	TRPA1	F: 5'-TCCTCTCCATCTGGCAGCAAAG-3'		115
	R: 5'-GCCGTCACTGTGGAGACACC-3'				R: 5'-GGACGCATGATGCAAAGCTGTC-3'		
β3T	F: 5'-CACCATGTACCCCTGGCATT-3'		117	TRPV1	F: 5'-GTGGACAGCTACAGTGAGATGC-3'		99
	R: 5'-CCGATCCACACGGAGTA-3'				R: 5'-GGAGCCACATACTCCTTGAGG-3'		
COL-1	F: 5'-CCCCTGGAAGAATGGAGAT-3'		61	TRPV4	F: 5'-TCACTCTCACCGCCTACTACCA-3'		110
	R: 5'-AATCCTCGAGCACCCCTGA-3'				R: 5'-CCAGTG AAGAGCGTAATGACC-3'		
DMP-1	F: 5'-TCACAAGGGAG AAGGGAATG-3'		168	p16	F: 5'-GACATCCCCGATTGAAAGAA-3'		150
	R: 5'-TGCCAT TTGCTGTGATGTTT-3'				R: 5'-TTTACG GTAGTGGG GGAAGG-3'		
DSPP	F: 5'-TCACAAGGGAG AAGGGAATG-3'		520	p53	F: 5'-GGCCCACTTCACCGTACTAA-3'		132
	R: 5'-TGCCAT TTGCTGTGATGTTT-3'				R: 5'-GTGGTTTCAAGGCCAGATGT-3'		

Table 2:2: Sequences of the primers designed to recognise genes of interest which were CD44 and CD45, alkaline phosphatase (ALP), collagen type I (Col I), dentine matrix protein 1 (DMP1), dentine sialophosphoprotein (DSPP), neurokinin receptors – neurokinin-1 and -2 (NK1R and NK2R), transient receptor potential channels (TRPA1, V1 and V4), senescence associated proteins p16 and p53. Beta actin (β-actin) was used as the housekeeping gene.

## 2.14 TaqMan microarray analysis

First strand DNA synthesis was performed on isolated RNA samples from human pulpal tissue to yield single-stranded cDNA required for the micro array analysis. The cDNA (in sterile Eppendorf tubes) and TaqMan master mix (Applied Biosystems) were kept on ice and the 96-well TaqMan custom-made microfluidics array card (<http://www.appliedbiosystems.com>) was at room temperature. The array card contained 96 genes and the house keeping genes included were glyceraldehyde 3-phosphate dehydrogenase (GAPDH), 18s RNA, beta actin and beta-2-microglobulin. The cDNA samples were diluted using PCR grade water to total volumes of 100µl, at a concentration of 200ng. An equal volume of master mix (100 µl) was added to each sample tube and mixed gently by gently pipetting up and down. A volume of 100 µl of the mixture of sample and master mix was then loaded into appropriate ports on the array card. The card was placed in a Sorval/Heraeus custom bucket, which was placed in a centrifuge and spun using the parameters outlined in Table 2-3. The card was sealed using a TaqMan Array Sealer (Applied Biosystems) to close the fluid channels.

With the cards sealed the ports were trimmed off using a pair of scissors. The cards were placed in an Applied Biosystems 7900HT Instrument and run through 40 cycles of amplification (which lasted for approximately 2 hours). The generated data (normalised to the geometric mean of the housekeeping genes using the R package NormqPCR (<https://r-forge.r-project.org/projects/qpcr/>)) was analysed using the comparative  $C_T$  method ( $\Delta\Delta C_T$  method) (Livak and Schmittgen 2001) described in Section 2.13.3.

## 2.15 Sample storage

### 2.15.1 Cryopreservation

To allow for further experiments the cell stocks ( $\geq 250,000$  cells) were stored in cryovials (BD Falcon) holding 1ml of a 1:1 freezing mixture; 10% dimethyl sulphoxide, DMSO (Sigma®) and fetal bovine serum, FBS (Sigma®). The cryovials are left overnight in a  $-70^\circ\text{C}$  freezer for the first stage of the preservation process. The next day the cryovials were transferred to a liquid nitrogen storage container.

### 2.15.2 Resuscitation of cryopreserved DPSCs

Previously cryopreserved cell stocks, stored in cryovials ( $\geq 250,000$  cells), were retrieved from the liquid nitrogen storage facility. The cryovials were disinfected with 70% ethanol and placed in a sterile Class II laminar cell culture cabinet to thaw. The thawed cells in 10% DMSO solution were transferred to sterile 15ml tubes (BD Falcon) and resuspended in 10ml of Minimal Essential Medium alpha ( $\alpha$ -MEM). The tubes were centrifuged at 2000 rpm for 5 mins at room temperature. The supernatant media was discarded and the cell pellets resuspended in a fresh 10ml of  $\alpha$ -MEM. The centrifugation process was repeated as previously described. The cell pellets were resuspended in 1ml of  $\alpha$ -MEM and counted using a TC10™ Automated Cell Counter (Bio-Rad) as described in Section 2.2.

Depending on the cell count, an appropriate cell density was selected for seeding the cells in cell culture flasks containing the previously described supplemented media (see Section 2.1) (Dulbecco's modified Eagle's medium DMEM (Pharmakine®) supplemented with 10% fetal bovine serum, FBS,  $2.5 \times 1000$  U/ml penicillin and 2.5mg/ml streptomycin and then conditioned for 12 – 24 hrs. by adding 50 $\mu\text{g/ml}$

ascorbic acid, 10mM  $\beta$ -glycerol phosphate and  $10^{-7}$ M dexamethasone). The cultures were incubated at 37°C in an atmosphere of 95% O<sub>2</sub> and 5% CO<sub>2</sub>. These served as stocks for the subsequent experiments.

# Isolation of dental pulp cells

---

**3**

## Isolation of dental pulp cells

Cell culture systems are designed primarily to mimic *in situ* cellular events in mature tissues. As mentioned earlier in Chapter 1, the experimental interest of this thesis is in a potential signalling role for the odontoblasts in the dental pain transmission pathway. The methodology adapted in this study relied on the isolation of dental pulp cells, induced to differentiate into and proliferate as cells of an odontoblast lineage. Achieving a primary culture of mature odontoblasts, isolated from human teeth is difficult as the odontoblasts remain firmly attached to dentine tubules by their processes and do not exist in isolation, surrounded by a variety of cell types such as dendritic cells and fibroblasts. The odontoblasts are also post-mitotic, terminally differentiated cells incapable of proliferation. This suggests that even if the odontoblasts could be isolated from the dentine, the cell damage that occurs following separation between the odontoblast cell body and processes, would severely reduce the number of surviving odontoblast cells (Tjäderhane, Salo et al. 1998). The dental pulp tissue however, contains a population of multipotent stem (progenitor) cells which can be isolated by proteolytic dispersal of the pulp tissue, to yield progeny of an identical phenotype (Arthur, Rychkov et al. 2008). These progenitor cells can be induced to differentiate into cells of an odontoblastic phenotype and initiate mineralisation following exposure to defined combinations of media and growth factors including  $\beta$ -glycerophosphate, 10% fetal bovine serum (FBS), Dulbecco's modified Eagle's medium (DMEM) and ascorbic acid, allowing for *in vitro* studies (Maurin, Couble et al. 2004; Huang, Shagramanova et al. 2006; Liu, Gronthos et al. 2006).

The method by which the pulp tissue is isolated is important, as it affects the type of cell populations that eventually grow from the tissue (Huang, Sonoyama et al. 2006) and the behaviour of these cells in growth media. The more invasive the nature of a method is, the greater the chance of low yields of harvested cells. Dental pulp stem cells used in culture can be obtained by the outgrowth of cells from intact pulpal explants, release of cells from pulpal explants through enzymatic digestion or by the outgrowth of cells from the pulp chamber following the extirpation of the pulp (Tjäderhane, Salo et al. 1998; About, Bottero et al. 2000; Gronthos, Mankani et al.

2000; Gronthos, Brahim et al. 2002). In this chapter, details of how all three methods were performed and comparisons made to determine the most efficient means of cell isolation are described.

Following this, the next step was the identification of markers of the odontoblast phenotype (ALP, COL-1, DMP-1 and DSPP) and mesenchymal expression markers (CD44 and CD45) (see section 1.4.7), following culture media induced differentiation. Once a viable cell isolation and culture methodology was established, the cells were cryopreserved and used for the further experimental studies explained in further detail in subsequent sections of this thesis.

## **3.2 Materials and methods**

### **3.2.1 Establishment of primary cell cultures**

Teeth were obtained from adult patients presenting for third molars extractions at the Department of Oral Surgery, Dental Institute, King's College London (Section 2.1 - Ethical approval), and the dental pulpal cells were isolated. The teeth specimens were washed with 70% ethanol to remove all blood and tissue debris. The specimens were transported in ice-cold phosphate-buffered saline (PBS) (Sigma – Aldrich UK) containing a supplement of 1mg/ml penicillin-streptomycin. In sterile conditions, the crowns and roots of the teeth were separated aseptically by making horizontal and vertical indentations (along the cervical margin and longitudinal axis) using a low speed circular diamond saw (Agar Scientific Ltd) fitted on an Isomet 1000 Precision Saw (Buehler) using a commercial dental wax (Kemdent) and the pulp tissue retrieved (See Figure 3.1).



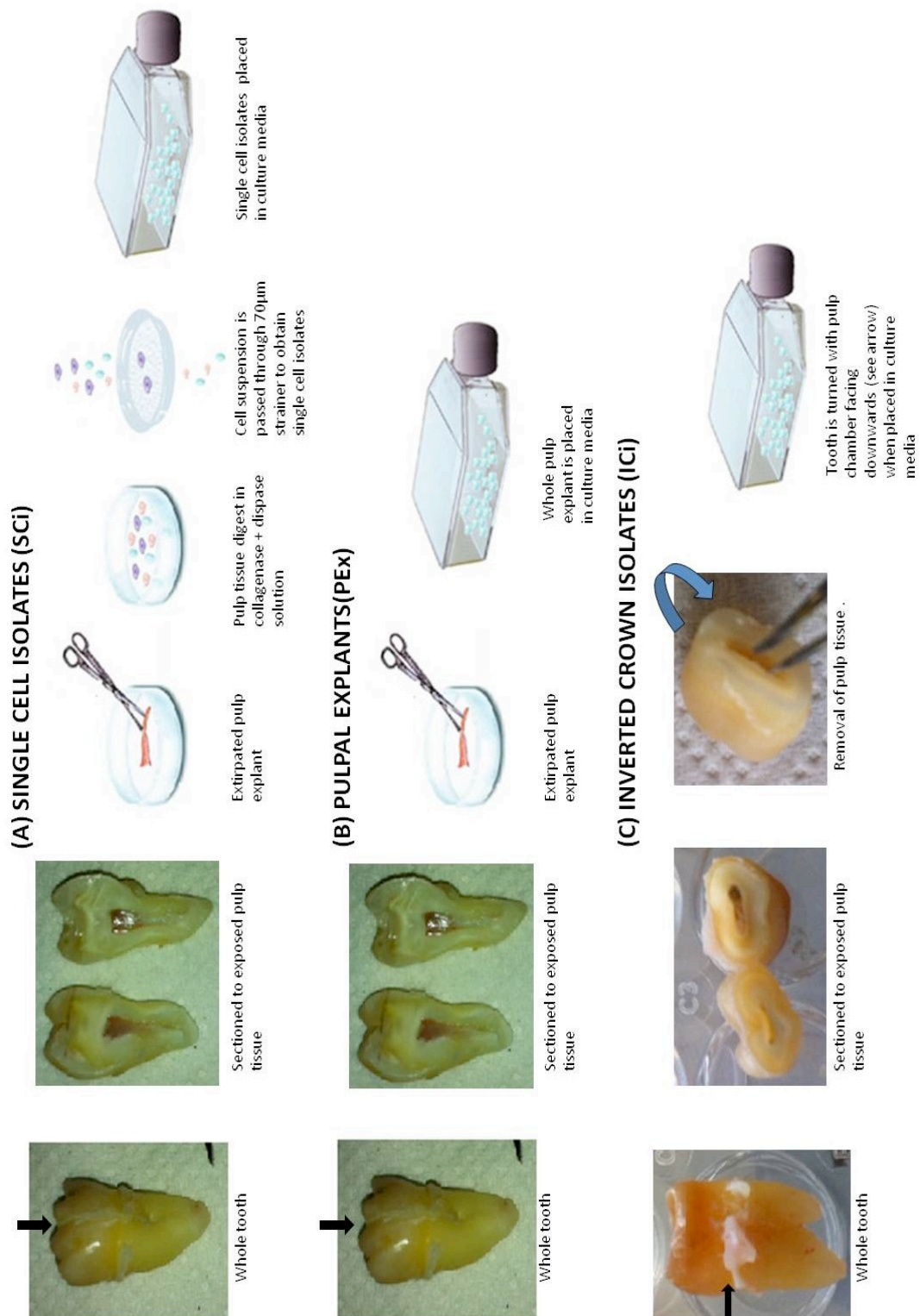


Figure 3:1: A schematic workflow chart of the three different methods of dental pulp cell isolation used. The teeth were aseptically held in place on the mount on an Isomet 1000 Precision Saw (Buehler) using dental wax (Kemdent) and were then cut along the cervical margin or the longitudinal axis as indicated by the black arrows in Figure 3.1 (A - C).

The pulp tissue was then cut into small pieces measuring (3-4mm) and placed in a solution of 3mg/ml collagenase type I and 4mg/ml dispase (Sigma-Aldrich UK) for 30 minutes at 37°C. The enzymatic solutions were prepared in filter-sterilised PBS using a 0.2µm filter (VWR, UK). This step was to digest the pulp tissues and so allow the release of pulp cells from within the tissue. Two volumes of minimal essential medium alpha (α-MEM) was added to the reaction to end digestion, and the pulp cell-containing supernatant was centrifuged at 2000 revolutions per minute (rpm) for 5 mins at 4°C. The pulp tissue-cell suspension was passed through a cell strainer with a pore size, 70µm (VWR, UK) to obtain single-cell suspensions. The suspensions of cells were washed twice with α-MEM to ensure the complete elimination of all traces of the digestive solution and resuspended in a volume of 500µl of α-MEM and counted using a TC10™ Automated Cell Counter (Bio-Rad). An appropriate cell density was selected for seeding the cells in cell culture plates containing Dulbecco's modified Eagle's medium DMEM (Pharmakine®) supplemented with 10% fetal bovine serum, FBS, 2,500 U/ml penicillin and 2.5mg/ml streptomycin. The cultures were incubated at 37°C in an atmosphere of 95% O<sub>2</sub> and 5% CO<sub>2</sub>. All undigested pulpal tissue explants, which remained present in the cell strainers, were also washed in like manner and placed into culture flasks under the same conditions. The crowns of the teeth from which the pulp explants had been extruded (now with empty pulp chambers save for the odontoblasts still embedded in the walls of the chamber) were washed out with α-MEM. The crowns were then inverted in cell culture plates in the same media conditions as described for the pulpal explants and single cell isolates. The reference nomenclature for the cells from the different isolation methods runs thus: single cell isolates, SCi, pulpal explants, PEx and inverted crown isolates, ICi. The media in the cell culture plates and flasks was changed every 48 hours to remove non-adherent cells and cellular debris subsequently up until the point was reached where the cells were 80% confluent. At confluence, the adherent cells from the culture plates and flasks were washed in sterile PBS, trypsinized (using 1% trypsin) and passaged in T25 flasks. These cells (SCi, PEx and ICi) were designated Passage 2. The cells were maintained for 3 passages before using a supplemented media to induce differentiation. Conditioning the culture media with 50µg/ml ascorbic acid, 10mM β-glycerophosphate and 100nM dexamethasone effected this supplementation. The culture media for the three groups

of cells was changed to a low glucose (1mM) DMEM supplemented with 10% FBS, 5000 U/ml penicillin, 5mg/ml streptomycin and 0.11g/L sodium pyruvate (Sigma Aldrich UK), DMEM/R. The cell-rich supernatants were then centrifuged in the same conditions as described above and the resulting cell pellets were resuspended in culture flasks for continued expansion to use in further experiments.

### 3.2.2 Cell viability counts

Using a TC10™ Automated Cell Counter (Bio-Rad, USA) and a TC10™ trypan blue exclusion dye, counts for cell viability and proliferation were performed on cell cultures established from the SCi-group, PEx-group and ICi-group as described in Section 2.2.

### 3.2.3 Cell proliferation assay

Using a CellTiter 96® AQueous Non-Radioactive Cell Proliferation Assay kit (Promega), 21ml stock solution of MTS [3-(4,5-dimethylthiazol-2-yl)-5-(3-carboxymethoxyphenyl)-2-(4-sulphonyl)-2H-tetrazolium] solution was prepared by adding 21ml of PBS to 42mg of MTS reagent powder in a light-protected falcon tube (BD Falcon). The pH of the MTS solution was adjusted to 6.5 using 1N HCl and then filter-sterilized [0.2µm filter (VWR, UK)]. A 100µl solution containing 0.92mg/ml phenazine methosulphate (PMS) in PBS was aseptically added to 2ml of MTS solution in a foil covered bijou tube. Cells from the 3 cell groups were seeded in 96-well plates at a density  $1 \times 10^4$  cells/well. On days 1, 3, and 7, the growth media was removed from designated wells and the cells were washed with PBS. After gently mixing the MTS/PMS solution by swirling the holding tube, 20µl of the combined solution was added to each well of the plate at each designated time point, and then incubated for 2 hours in a humidified, 5% CO<sub>2</sub> at 37°C. After this time, the absorbance of the resultant formazan product from the cells of the experimental groups was read at 490nm using a spectrophotometric plate reader (FluroStar Optima: BMG Labtech).

### 3.2.4 Alkaline phosphatase activity assay

Cells from the SCi, PEx, and ICi cell groups cultured in DMEM/R (low glucose media) and passaged over a 28-day culture period. Cells from the 3 cell groups were seeded in 96-well plates at a density  $1 \times 10^4$  cells/well. On days 1, 3, and 7 the growth media was removed from designated wells and the cells were washed with PBS. Cell lysates were collected for each time point as described in Section 2.3. The methodology outlined in Section 2.5 was used to demonstrate ALP activity in these cell groups. Equal volumes of cell-free media were used as negative controls. The absorbance values were measured at a wavelength of 405nm with a spectrophotometer (Opsys MR Microplate reader) after 5 mins.

### 3.2.5 Immunocytochemistry

To observe the spatial structure of actin in the isolated cells, immunocytochemistry was performed. The SCi-, ICi- and PEx-derived cells were cultured in T25 culture flasks up to a point of 80% confluence and were trypsinized and transferred to 6-well tissue culture plates containing sterile glass coverslips 24 hours before the day of the experiment. Following the experimental protocols described in section 2.6, the cells were fixed with 4% paraformaldehyde in PBS and incubated overnight with primary antibody, FITC-conjugated phalloidin. Thereafter, the cells were incubated with nuclear marker, DAPI (4', 6-diamidino-2-phenylindole) for 10mins. Images were taken using a confocal microscope. Plates to which no primary antibodies were added served as negative controls.

### 3.2.6 RNA extraction from isolated pulp tissue

In the initial stages of this study, two methods of RNA extraction were tested to optimise the purity of RNA obtained from the samples for downstream applications.

### 3.2.6.1 RNA extraction from isolated human pulp tissues - modified Trizol/RNeasy/Phase-Lock tube extraction protocol

Previously obtained pulpal tissues (See section 2.1) were placed in 1.5ml flat bottomed falcon tubes (BD Falcon) containing 800µl of TRIzol reagent. The pulpal tissues were disintegrated and homogenized for 1 min in an IKA® T-25 Digital High-Speed Homogenizer. The resulting homogenates were then moved to clean RNase-free 1.5ml round bottomed falcon tubes and 200µl of chloroform was added to each tube and the mixture (homogenates/chloroform) was left to stand at room temperature for 5 mins. The homogenate/chloroform mix was transferred to Phase Lock gel heavy tubes (5Prime Inc.) and placed in a centrifuge, which was spun at 13,000 (rpm) for 15 mins at 2-8°C. The clear aqueous phase, (a volume of approximately 900µl) at the top of the contents of the tube after centrifugation was transferred by pipetting into a clean tube. The gel barrier in the Phase Lock tube prevented the contamination of the nucleic acid solution. The aqueous phase were diluted by adding 500µl of 80% ethanol and mixed by pipetting, then transferred to RNeasy MinElute spin column in a 2ml collection tube (Qiagen). These tubes were spun in a centrifuge at 10,000 rpm for 15 secs. The flow through was discarded and the spin columns placed in clean RNase-free 2ml collection tubes. A second wash of the columns was performed by adding 500 µl of RPE buffer (Qiagen) prior to centrifugation for 15 secs at 10,000 rpm. Once again, the flow through was discarded. The spin columns were placed in clean RNase-free 2ml collection tubes and 500µl of 80% ethanol was pipetted into each column prior to centrifugation at 10,000 rpm for 2 mins. The collection tubes were discarded and the spin columns placed in fresh collection tubes as described previously. The lids of the spin columns were left open and spun for 5 mins in the centrifuge at 13,000 rpm. The flow through and collection tubes were discarded. The spin columns were placed in clean RNase-free 1.5ml collection tubes and 24µl of RNase-free water was pipetted directly on the membrane in the centre of the spin column. This was left to incubate for 5 mins at room temperature. The tubes were spun at 13,000 rpm for 1 min to elute the RNA. Once eluted, the RNA concentration and quality was measured (see section 2.6) and the samples stored at -80°C.

### **3.2.6.2 RNA extraction from isolated human pulp tissues - Trizol extraction protocol**

Batches of pulpal tissue samples were placed in 1.5ml flat bottomed falcon tubes (BD Falcon) containing 1000µl of TRIzol reagent. The samples were homogenized as described in the previous section. The resulting homogenates were incubated for 5 mins at 15-30°C. Two hundred µl of chloroform solution per 1000µl of TRIzol was added to each sample tube. The tubes were capped and shaken vigorously by hand for 15 secs and incubated at 15-30°C for 2-3mins. The samples were centrifuged for 15mins at 11,600 rpm at 2-8°C. The clear, colourless aqueous phase, which appeared at the top of the tube, was transferred to a fresh tube. Mixing with 500µl of isopropanol precipitated the RNA present in this aqueous phase out. The samples were incubated for a further 10 mins at 15-30°C and centrifuged for 10mins at 11,600 rpm at 2-8°C. The RNA precipitate at this point had formed a gel-like sludge on the bottom of the tube. The supernatant was discarded and the RNA pellet was washed twice in 1000µl of 80% ethanol. After the third addition of the ethanol solution, the mixture was mixed by pipetting and centrifuged for 7,250 rpm at 2-8°C for 5 mins. The resulting RNA pellet was left to air-dry in the sample tube for 5 mins without being left to completely dry out (to prevent a loss of solubility). Twenty-four µl of RNase-free water was pipetted directly on the RNA pellet to dissolve it, following which the RNA concentration and quality was measured (see section 2.6) and the samples stored at -80°C.

### **3.2.7 RNA extraction from established human pulp tissue cell cultures**

Following the removal of the growth media in the culture flasks, the adherent DPCs on the culture surfaces of the flasks, were washed with Dulbecco's phosphate buffered saline (PBS). The cells were then detached using TRIzol reagent (1000µl of TRIzol reagent in a 25ml culture flask) and a sterile cell scraper. Pipetting to an RNase free 1.5ml round-bottomed falcon tubes transferred the resulting lysate and 200µl of chloroform was added to each tube and the mixture (lysates/chloroform) was left to stand at room temperature for 5 mins. 24µl of RNase-free water was pipetted directly on the membrane in the centre of the spin column. This was left to incubate for 5 mins

at room temperature. The tubes were spun at 13,000 rpm for 1 min to elute the RNA. The extraction of RNA from the lysates was completed (in two separate groups). Once eluted, the RNA concentration and quality was measured (see section 2.6) and the samples stored at -80°C.

### **3.2.8 Amplification of cDNA and agarose gel electrophoresis**

Following the extraction procedures, the concentration for each of the RNA samples was quantified using methodologies described in Section 2.7. The cDNA products derived by means of reverse transcriptase reactions as detailed in Section 2.9 were thawed on ice. They were used as templates for polymerase chain reactions (PCR) to amplify target sequences.

The primer sequences designed for use in this section of experimentation were chosen to test the odontoblastic phenotype of the cells by determining the expression of mRNA for dentine matrix protein-1 (DMP-1) and dentine sialophosphoprotein (DSPP). This would corroborate the typical features of odontoblasts in culture (McCabe, Davis et al. 2005; Allard, Magloire et al. 2006; Gold, Belmont et al. 2007; Ohtani, Mann et al. 2009). In addition to this, the genetic expression of alkaline phosphatase (ALP) and collagen-1 (COL-1) would be further evidence to show the mineralising potential of the cells. Glyceraldehyde 3-phosphate dehydrogenase (GAPDH) was the housekeeping gene used as a control in this series of experiments. The sequences and melting temperatures for these primers are listed in Table 2-1 in Chapter 2.

The reaction volume for all PCRs performed was 25µl. To make up this volume, 12.5µl of 2x Go Taq®Green master mix was added to each 0.2ml PCR reaction tube, along with 1µl (10µM) of both forward and reverse primers and 1µl of the template cDNA. Nuclease-free water was added to make up the rest of the reaction volume. The tubes were sealed and the contents were mixed by centrifugation. The amplification program chosen to run the PCR reaction was as follows: a denaturation step at 95°C for 5 minutes which involved the breaking down of the single stranded cDNA RT products (ssDNA) to single stranded DNA (ssDNA), an annealing and Taq polymerase driven extension phase consisting of 35 cycles of 94°C for 30 seconds, 60°C for 45

seconds and 72°C for 60 seconds and a final extension phase at 72°C for 5 minutes. The resulting amplified DNA transcripts were stored at -20°C. Following this, agarose gels were prepared as described in Section 2.11 and DNA products were retrieved from storage. They were then separated by agarose gel electrophoresis on a 2% gel, and visualised using Gel Red (Biotium™) in an Alpha Innotech Alpha-Imager 2000.

Following this, to quantitatively demonstrate the expression of these odontoblastic markers, qPCR analysis was performed. Cells from the SCi, PEx, and ICI cell groups cultured to Passage 5 were used. Also tested was the expression of mRNA for CD44 (a mesenchymal surface marker typically expressed by odontoblasts(Jo, Lee et al. 2007; Karaöz, Doğan et al. 2010)), and CD45 (haemopoietic cell surface marker expressed by mesenchymal stem cells and typically absent in odontoblasts(Atari, Gil-Recio et al. 2012)) in all 3 of the cell groups. A commercial mesenchymal stem line was used as a control in these qPCR experiments. The RT-qPCR methodology used in these experiments has been described in section 2.12. The list of primer sequences (including sizes in base pairs) used in the qPCR analysis is provided in Table 2-2 (See Section 2.13). Beta actin was used as a reference gene to normalise for RNA expression.

### 3.2.9 Cryopreservation

To allow for further experiments the cell stocks ( $\geq 250,000$  cells) were stored in cryovials (BD Falcon) holding 1ml of a 1:1 freezing mixture; 10% dimethyl sulphoxide, DMSO (Sigma Aldrich UK) and fetal bovine serum, FBS (Sigma Aldrich UK). The cryovials are left overnight in a -70°C freezer for the first stage of the preservation process. The next day the cryovials were transferred to a liquid nitrogen storage container.

### 3.2.10 Statistical methods

The data was expressed as a means of standard error ( $\pm$  S.E). Normal distribution of data sets was assessed using the Shapiro-Wilk test. The statistical significance between enzymatic and proliferative activities of isolated human dental pulp cells and mesenchymal control cells was determined using one-way ANOVA. The ANOVA



analyses were examined post hoc by Bonferroni's post-test. GraphPad Prism® was used to carry out statistical analysis. The  $p$  value for statistical significance was set at  $*p < 0.05$ ,  $**p < 0.01$  and  $***p < 0.001$ .

### 3.3 Results

#### 3.3.1 Cell isolation methods

The isolation of DPCs from the tooth samples was done in three ways to yield three cell culture groups. The viability of the isolated cells was determined by performing cell counts as described in Section 2.2 and taking phase contrast images of the cells being counted (Figure 3.2). The numbers of cells present after a 2-week culture period in 1ml of culture media were:  $1.14 \times 10^7$  cells (PEX-derived cells),  $1.02 \times 10^7$  cells (ICi—derived cells) and  $1.0 \times 10^7$  cells (SCi-derived cells). However, the percentages of these total cell populations that were live cells were 83% (PEX-derived cells), 87% (ICi-derived cells) and 88.7% (SCi-derived cells). There were no statistically significant differences between the cell groups ( $P = 0.071$ ).

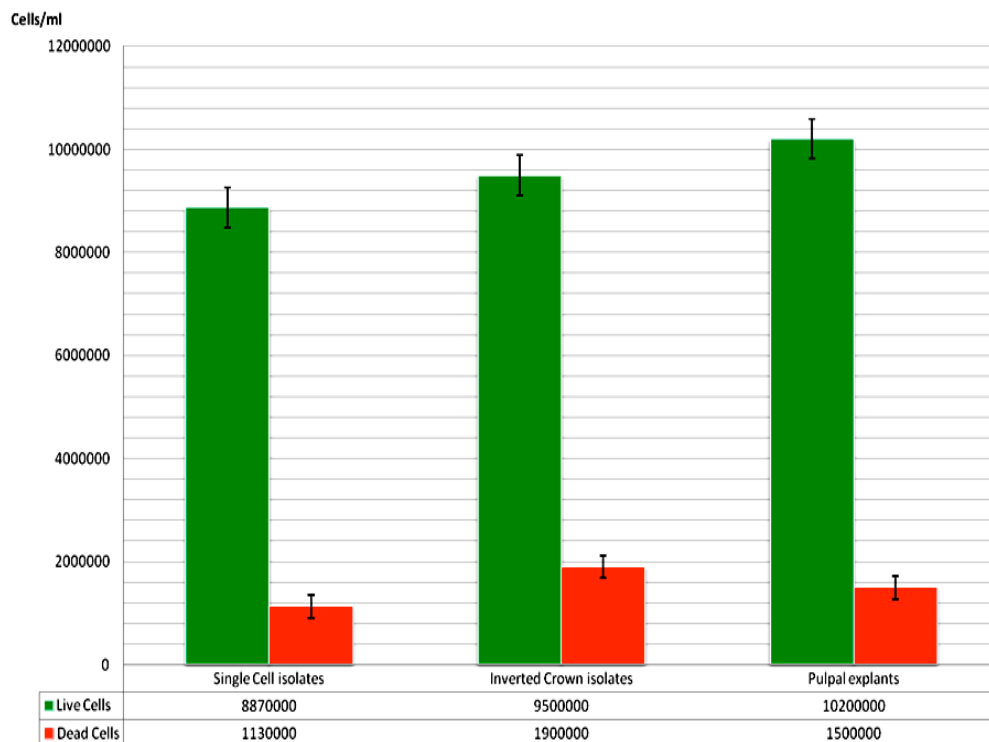
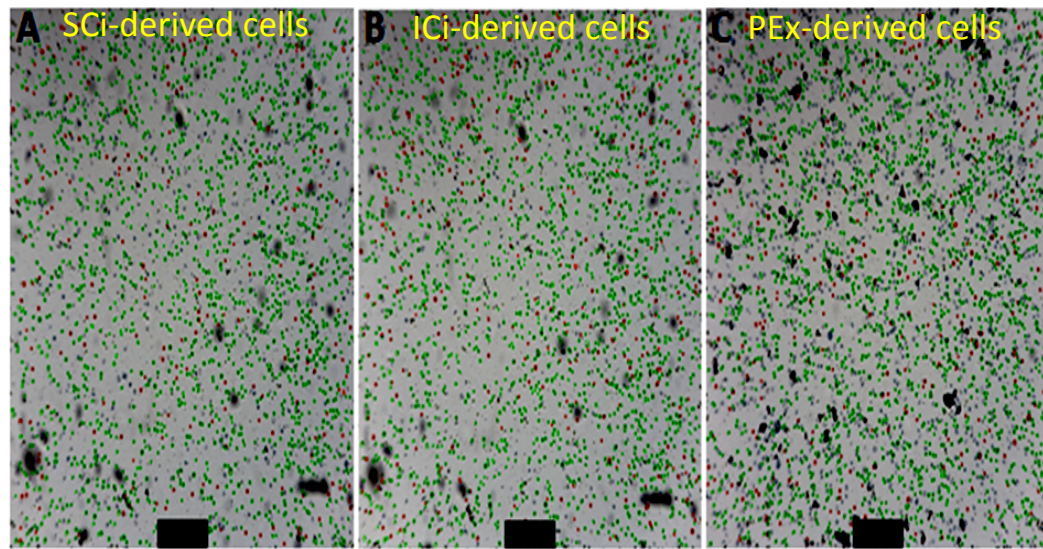


Figure 3:2: Phase contrast image of a 4mm area of the counting chamber showing live and dead cells 30 seconds after staining with TC10™ trypan blue dye. A= SCI-derived cells; B= ICI-derived cells; C=PEX-derived cells. The live cells are the green circles and the dead cells appear as the red circles. The black speckles are cellular debris, which took up the blue dye. The graph shows effect of the different isolation methods on cell viability. The cell numbers are representative of cells/ml. The error bars demonstrate the standard error from the mean (technical replicates).

### 3.3.2 Cell proliferation assay

To quantitatively analyse the proliferation of the different cell groups, the isolated cells were cultured in DMEM/S growth medium for 28 days, spanning over 4

passages (Passage 3 – 6). Following this 28-day culture period, cells from the different groups were seeded in 96-well plates. At different time points (days 1, 3 and 7) an MTS assay was run. The optical absorbance (OD) values were obtained and are represented graphically (Figure 3.3). The data showed a statistically significant difference in the proliferation rates of SCi-derived cells in comparison to those of the PEx-cell groups (\*\* $p < 0.01$ ).

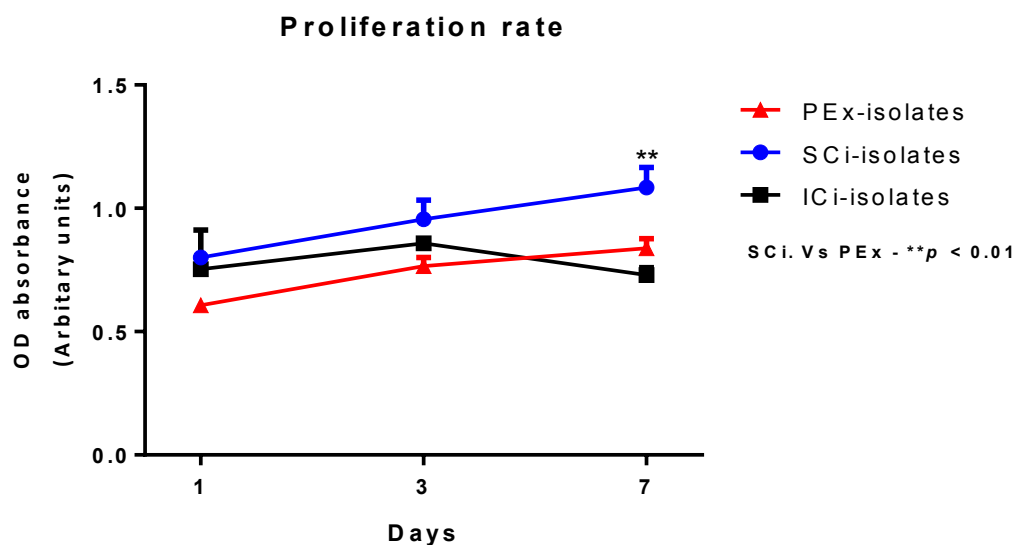


Figure 3:3: Cell proliferation rates as determined by means of an MTS assay. There was a significantly higher level of activity seen in the SCi-derived cells compared to the PEx-group. The results shown are expressed as the mean  $\pm$  S.E of triplicate experiments (technical replicates) with significance differences measured between the 3 cell groups at the different time points by one-way ANOVA and post hoc Bonferroni's test, (\* $p < 0.05$ , \*\* $p < 0.01$ , \*\*\* $p < 0.001$ ).

### 3.3.3 ALP activity findings

ALP activity is an important indicator of odontoblast function. The cells cultured in differentiation medium were assessed for 7 days, as shown in Figure 3.4. For all 3 of the cell groups, the ALP activity was highest on day 7. The SCi-derived cells show a significant increase on day 3 and 7 (Figure 3.4A) compared to the PEx-group (\*\* $p < 0.01$ ) and a non-significant increase when compared to the ICi-group.

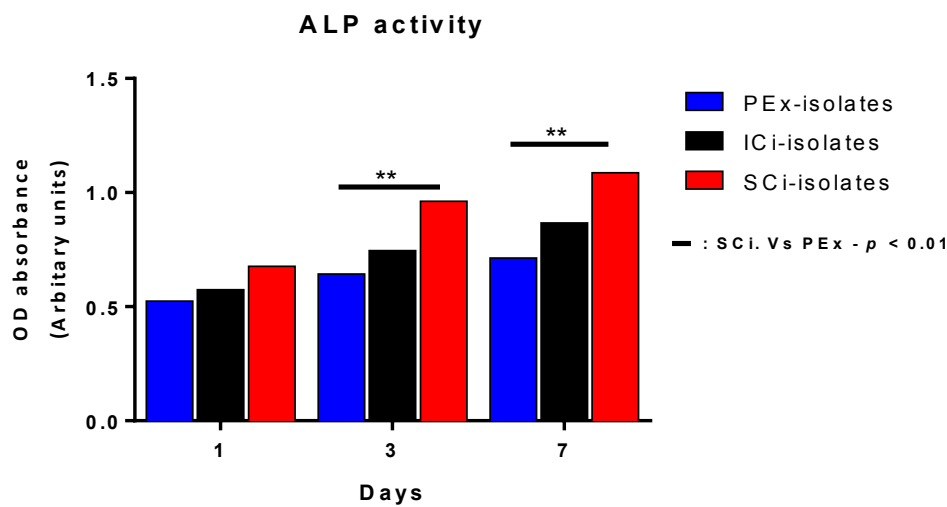


Figure 3:4: Rates of cell mineralization as determined by means of alkaline phosphatase enzyme activity. Optical density (OD) absorbance readings at 490nm are represented by arbitrary values as denoted by the scale on the x-axis. The data shows that ALP activity is significantly higher in the SCi-derived cells compared to the PEx-group at days 3 and 7. The results shown are expressed as the mean  $\pm$  S.E of triplicate experiments (technical replicates) with significance differences measured between the 3 cell groups at the different time points by one-way ANOVA and post hoc Bonferroni's test,  $n=12$  ( $*p < 0.05$ ,  $** < 0.01$ ,  $*** < 0.001$ ).

### 3.3.4 Cell morphology and characterisation

The morphology of the SCi-, ICi- and PEx-derived cells was analysed microscopically (Figure 3.5). All the cells, as depicted by the optical phase contrast microphotograph reported in Figure 3.5, spread along the surface of the culture plates, showing a rapid phase of growth within the first 6 days. By Day 7, the cells had assumed a heterogeneous morphology typified by the appearance of spindle-like shaped cells with cellular processes and this phenotype was seen as the cells (SCi-, ICi- and PEx-) grew to confluence (Figure 3:5). This spindle-like phenotype was maintained beyond day 7, through further culture passages, in keeping with the normal growth morphology as observed by other groups (Huang, Sonoyama et al. 2006; Mesgouez, Oboeuf et al. 2006; Kitagawa, Ueda et al. 2007; Karaöz, Doğan et al. 2010).

Using a fluorescent-labelled phalloidin, the actin filaments (stained green) of the SCi-, ICi- and PEx-derived cells were also observed. In all of the cell groups, there was an identical pattern of parallel fibre orientation (Figure 3:5). This was mainly in the

cytoplasmic areas of the visualised cells, transversing the cell nuclei (stained blue by the fluorescent DAPI) of the spindle-like cells. A similar pattern was observed in all 3 of the cell groups.

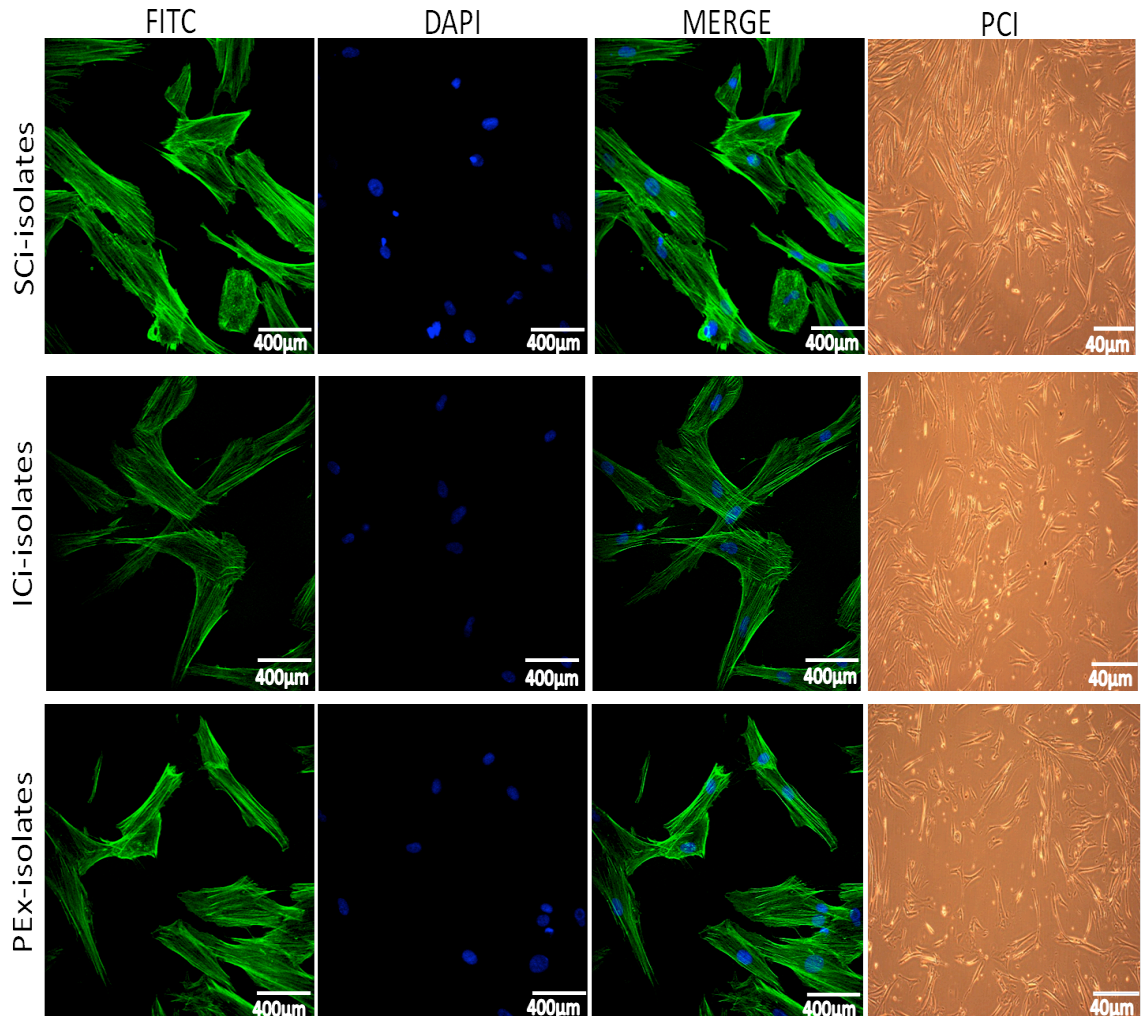


Figure 3:5: A representation of the cytoskeletal characterization of the isolated cells from the 3 groups (SCi, ICi and PEx) by confocal microscopy. The cells were cultured for 14 days (passages 3 and 4) and analyzed. Green = actin filaments, Blue = cell nuclei, Scale bar = 400µm. The merged images are composites of the FITC and DAPI images. The images labelled PCI are phase contrast images of the appropriately labelled cell groups at day 14. The spindle shape observed on confocal microscopy was once again evident in all 3 of the cell groups. Scale bar = 40 µm

### 3.3.5 RNA extraction

The methods chosen for the processing of isolated cells affected the concentrations of the RNA obtained in all the samples tested (Figure 3:6). In the SCi-,

ICi- and PEx-derived cells isolates; the Trizol extraction method produced much lower RNA concentrations in comparison to the Hybrid extraction method (Figure 3.6A). The  $A_{260}/A_{230}$  ratio (range in this study of 0.5 – 2.11) is used as a secondary measure of nucleic acid purity and the data obtained showed significant differences between the hybrid extraction and TRIzol extraction groups (Figure 3.6C), and among the hybrid groups (Figure 3.6D). There were no significant variations in the RNA quality ( $A_{260}/A_{280}$  absorbance readings with a range of 1.72 – 2.00) for all 3 samples (using both the Trizol and Hybrid methods) (Figure 3.6E).

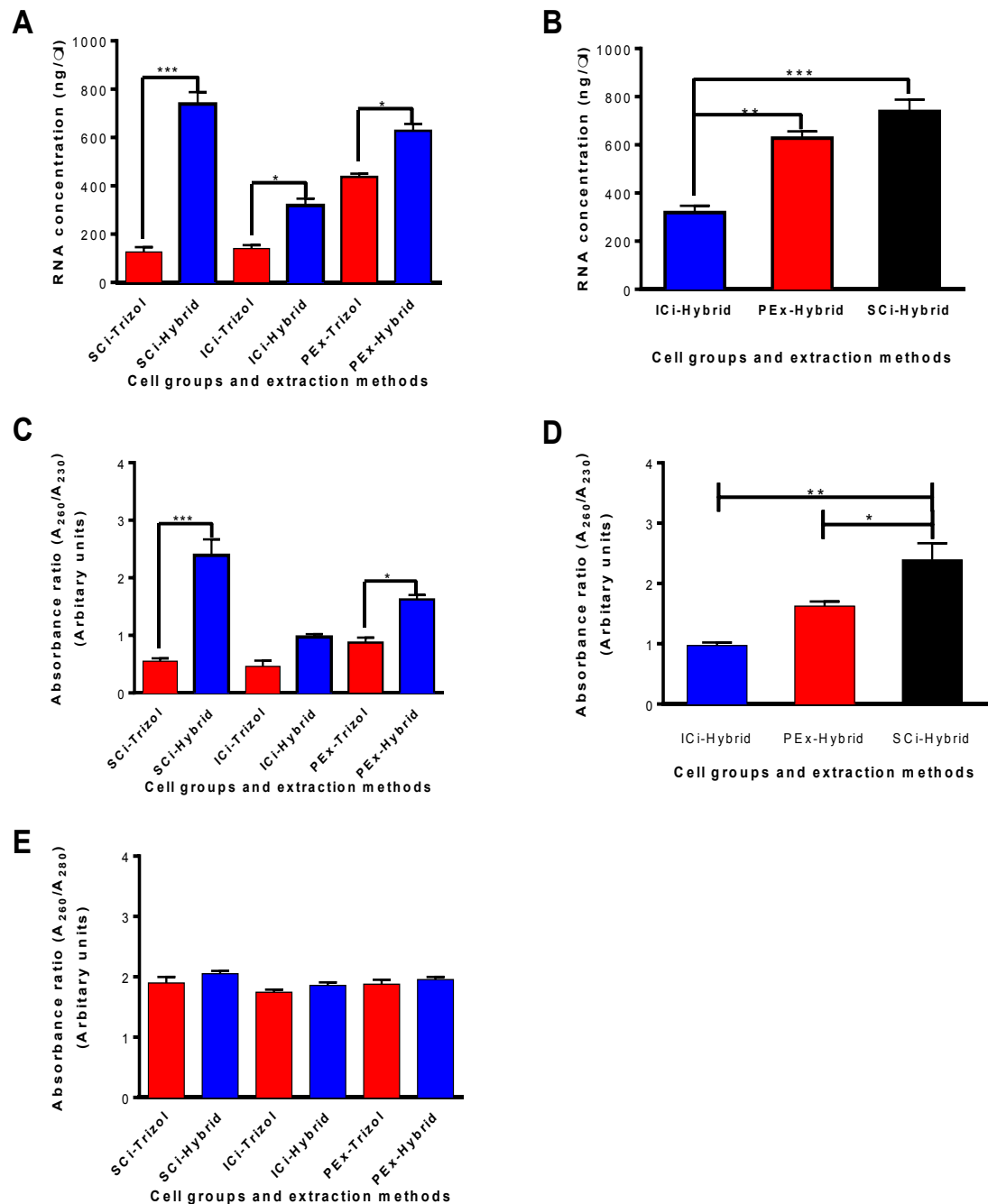
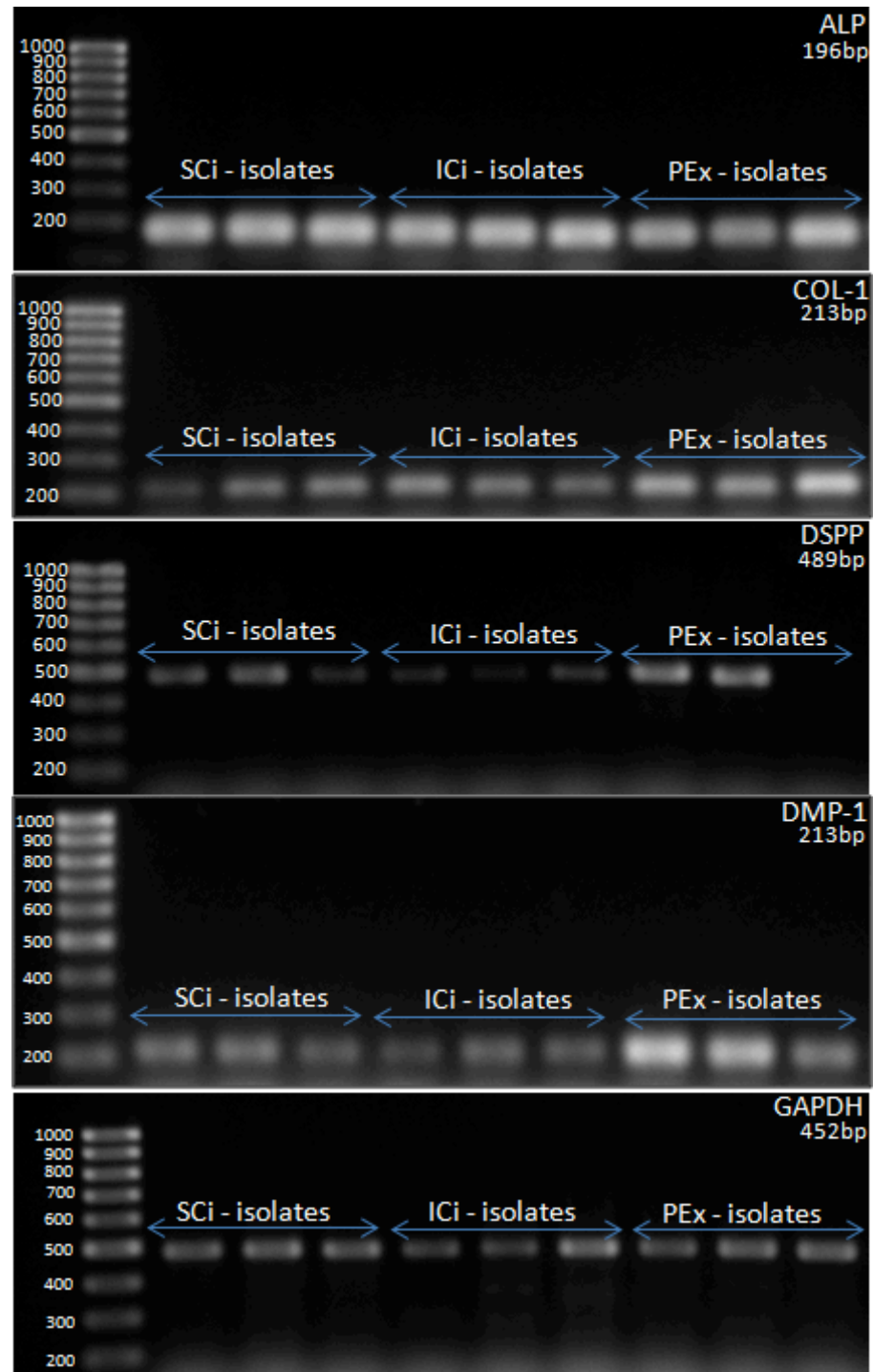


Figure 3:6: The influence of cell isolation and extraction methods on the quality of RNA extracted assessed by Nanodrop spectrophotometry. The values represent mean concentrations (ng/μl), absorbance ratios (A<sub>260</sub>/A<sub>280</sub> and A<sub>260</sub>/A<sub>230</sub>) of three independently processed cell isolates and are represented by arbitrary values as denoted by the scale on the x-axis. The data was analysed using one-way ANOVA and post hoc Bonferroni's test: \* $p < 0.05$ , \*\*  $< 0.01$ , \*\*\*  $< 0.001$ . Pure RNA gives an A<sub>260</sub>/A<sub>280</sub> ratio of approximately 1.9 – 2.2 and an A<sub>260</sub>/A<sub>230</sub> absorbance ratio of approximately 1.6 to 1.8. Cell isolation method and RNA extraction method significantly affected the concentration of RNA obtained (\*\*\* $p < 0.001$ ).



### 3.3.6 Expression of odontoblastic phenotype markers



**Figure 3:7:** Representative agarose gels containing RT-PCR products that show the expressions of genes associated with the odontoblastic phenotype in the Sci-, ICI- and PEx-derived cell isolates analyzed at day 14 of cell culture. These included alkaline phosphatase (ALP), collagen type-I (Col-I), dentine sialophosphoprotein (DSPP), and dentine matrix protein-1 (DMP1). The housekeeping gene GAPDH was expressed in all samples. The vertical array of bands on the left side of each gel image represents a PCR Sizer 1000bp ladder (Norgen, Biotek Corporation) and was used to determine product size.

The presence of bands for dentine matrix protein-1 (DMP-1), dentine sialophosphoprotein (DSPP), collagen type I (COL-1), and alkaline phosphatase (ALP) were compared by RT-PCR analysis of RNA extracted (Figure 3:7) from the SCi-, ICi- and PEx-derived cell isolates after 14 days of culture. The gel revealed bands showing the presence of odontogenic differentiation markers DMP-1 and DSPP. There was also evidence of strong ALP and COL-1 (markers associated with mineralization in differentiated cells) expression in all of the samples tested. GAPDH was used as an internal control.

To further quantitatively evaluate the phenotype of the cells from the different groups, the expression of mesenchymal surface markers was examined alongside the previously tested odontoblastic markers. The standard curves for CD44 and CD45, were generated using serially diluted cDNA ranging from  $1 \times 10^0$  to  $1 \times 10^4$  copies. The standard curves generated detected cDNA expression down to  $10^3$  copies and demonstrated linear regressions ( $R^2$ ), which ranged between 0.97700 (CD44) and 0.96062 (CD45) (Figures 3.8a). The cycle threshold values obtained in these experiments demonstrated moderately ( $C_T$  between 30 and 37) positive results, indicating the presence of the target nucleic acids. The standard curves for the odontoblastic markers are discussed in

CD44 mRNA expression was significantly higher in the SCi- and ICi- groups in comparison to the MSC controls (Figure 3.8b -B). While PEx-CD44 mRNA levels were higher than those of the MSC-CD44 mRNA, the observed values were not statistically significant (Figure 3.7b - B). MSC-CD45 mRNA expression was significantly lower in the SCi- and ICi- groups in comparison to the MSC controls (Figure 3.7b -A). The expression of odontoblastic markers, DMP-1 and DSPP mRNA was significantly lower in MSC controls compared to the SCi- and ICi- groups (Figure 3.7b – C, D). The ALP and COL-1 mRNA expression levels in all of the 3 cell groups, showed a similar trend (but with an absence of any statistical indications of significance) (Figure 3.7b – E, F).

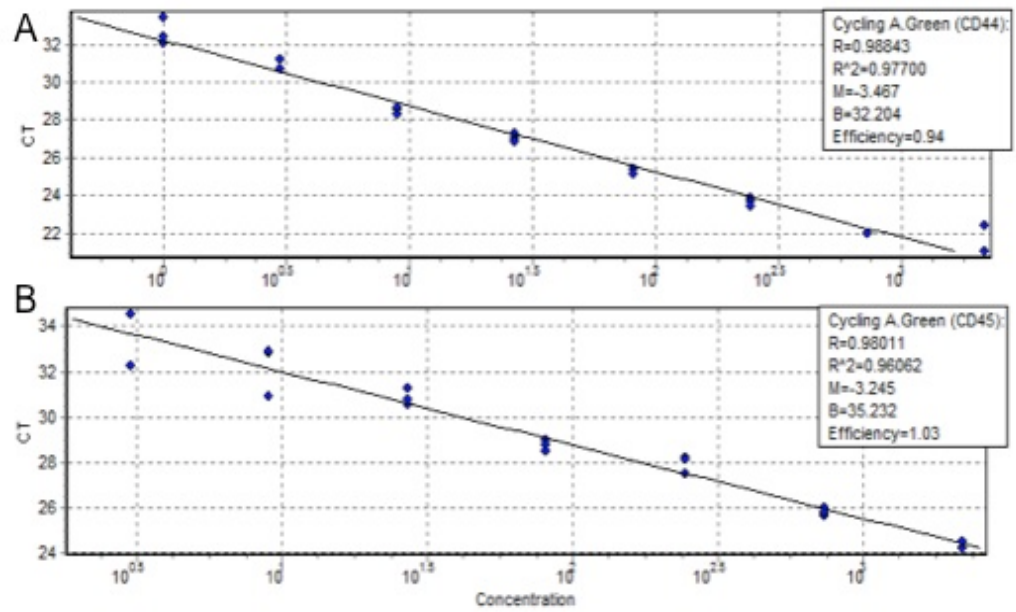


**Figure 3:8:** Standard curves of the real time RT-PCR assays for CD44 (A) and CD45 (B). Ten-fold dilutions of plasmid DNA prior to amplification were used ranging from  $1 \times 10^0$  to  $1 \times 10^4$  copies (indicated on the y-axis) with the CT values represented on the x-axis. The co-efficient of determination (R<sup>2</sup>) is indicated on the graphs. The CT values for the primers were: CD44 (32.204) and CD45 (35.232).

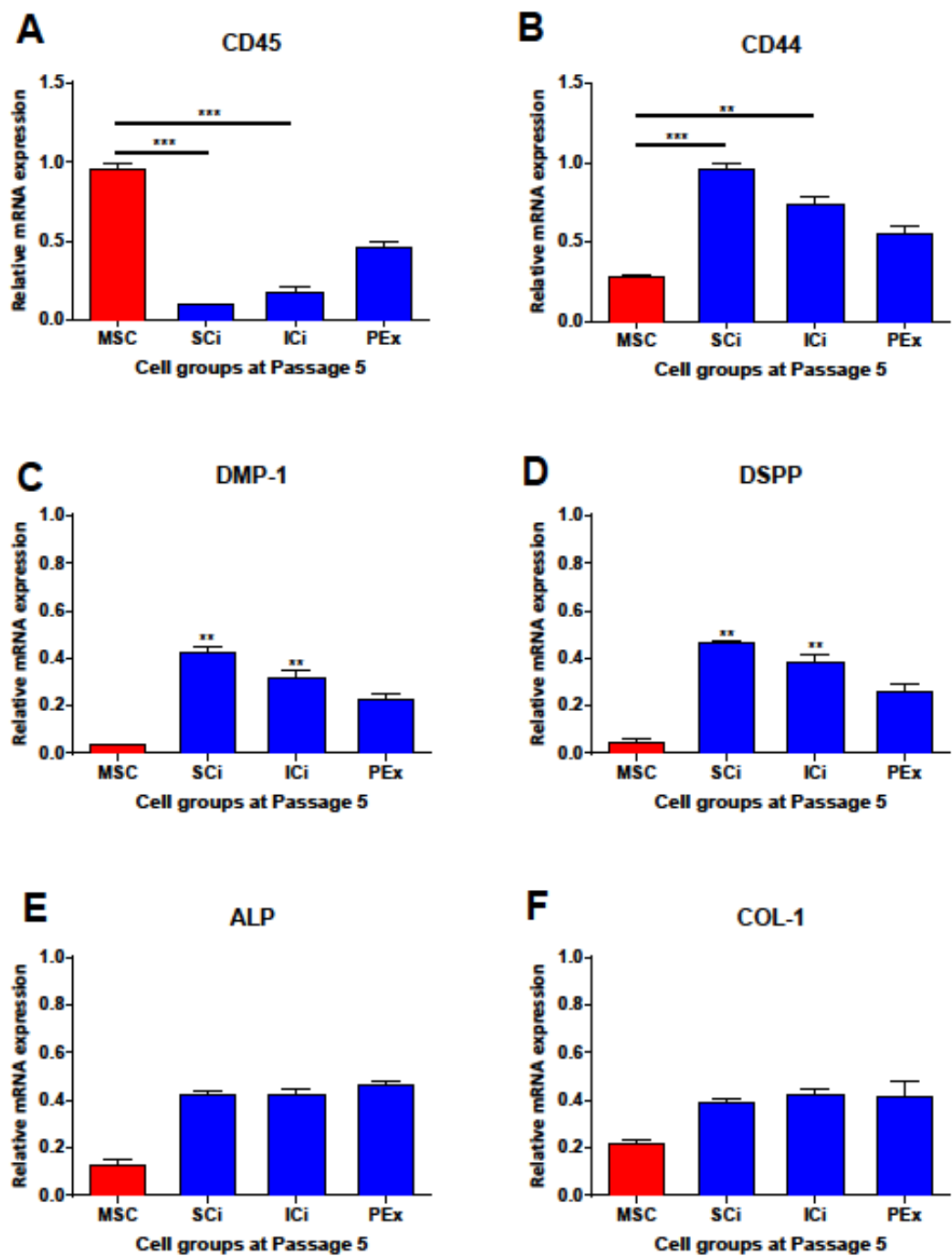


**Figure 3:9:** Expression of mesenchymal surface markers CD45 (A) and CD44 (B), odontoblast differentiation markers DMP-1(C) and DSPP (D) ALP (E) and COL-1 (F) was determined by real-time qPCR. Values are reported as relative fold change in cDNA concentration, which was normalised to the housekeeping gene. The data are represented as the mean  $\pm$  S.E of triplicate experiments (technical replicates) with significance differences measured between the 3 cell groups by one-way ANOVA and post hoc Bonferroni's test (\* $p < 0.05$ , \*\* $p < 0.01$ , \*\*\* $p < 0.001$ ).

### 3.4 Discussion

The experiments described thus far have been performed with the objective of identifying an effective means of isolating cells with a potential for odontogenic differentiation from human dental pulp tissue. These cells can be induced to differentiate along the odontogenic pathway, one of the other possible differentiation lineages (such as adipogenic, chondrogenic and neural lineages). The pulp, as has been described in Chapter 1, contains a heterogeneous cellular population and the isolation of the odontoblast and odontoblast-progenitor cell populations for the purposes of *in vitro* experimentation has been demonstrated by other groups (Tjäderhane, Salo et al. 1998; Gronthos, Mankani et al. 2000; Gronthos, Brahim et al. 2002; Huang, Sonoyama et al. 2006; Huang, Chen et al. 2008; Huang, Chen et al. 2009). For the purposes of this study, we examined three methods of physically isolating the odontoblast cells

- I. Single cell isolation technique following an enzyme digest of the pulpal tissues (Gronthos, Mankani et al. 2000; Gronthos, Brahim et al. 2002; Batouli, Miura et al. 2003; Huang, Chen et al. 2009).
- II. Using the de-coronated tooth (aseptic removal of the tooth crown) as a crucible for cell culture; referred to in this study as the Inverted crown cell isolation (Tjäderhane, Salo et al. 1998)
- III. Cell growth from pulpal explants (About, Bottero et al. 2000; Couble, Farges et al. 2000)

The use of these techniques is not entirely novel as all three techniques have been used independently by various investigators. However, to our knowledge there has never been a comparison of the efficacy of all three methods. The objective was to determine the most efficient means of isolating an odontoblast cell population that would remain viable in culture and mirror as closely as possible the phenotype of odontoblasts *in situ* by comparing all three methods.

The starting point was the choice of tooth samples from which the pulp was to be obtained. The third molar teeth are the last teeth to erupt in a human adult (17 -25

years). The third molar tooth germ begins development around the sixth year of life. Until this time, embryonic tissues of dental lamina remain quiescent and undifferentiated within the jaw of the child. Although crown mineralization begins during the eighth year of life, often third molar roots are still incomplete at the age of 18. This means that the structures of these teeth are still immature at this age and a conspicuous pool of undifferentiated cells, resident within the “cell rich zone” of the dental germ pulp, are needed for development. This suggests that the cell population in the tooth (dental pulp for our purposes) are developmentally young and would provide a good source of progenitor cells (Gronthos, Mankani et al. 2000; Liu, Gronthos et al. 2006; Tirino, Paino et al. 2011). After the extirpation of the pulp, its physical preparation was performed by the three methods (SCi-isolates, ICi-isolates and PEx-isolates) described in Section 3.1.1. The data obtained showed that all three methods were successful for the isolation of the cells. The initial cell counts after a 2-week cell culture period showed a live cell count range of 8800000- 10200000 cells/ml, with the PEx-isolates generating the most cells. The exposure of the SCi- and PEx-isolates to an enzymatic digest phase (a modification to reported methods for the outgrowth methodology) which causes the release of cells from the tissues is probably accountable for the high cell numbers seen. It was interesting to note that the ICi-isolate method also recorded the highest dead cell count (1900000). An issue with this method is that it is aimed at encouraging the growth of odontoblasts, which line the walls of the pulp chamber (attached to the dentine) and would not be completely extruded during the removal of the pulpal tissue. A probable reason might be the destruction (damage) of the odontoblast cell bodies during the sectioning of the teeth leading to a reduction in their viability. Another reason might be the age of the odontoblasts. As they are post-mitotic at this point, the potential for proliferation may have been lost (Tjäderhane, Salo et al. 1998).

With the isolation phase complete, we proceeded to analyse the proliferative potential of the three groups of cells by performing MTS assays. The results showed that the rate of proliferation of the SCi-isolates was higher than those of ICi- and PEx-isolates and significantly more so on day 7 (Figure 3.3). These higher levels suggest that this method produces a greater number of cells with a potential for proliferation.

While SCi- and PEx-isolates showed an increase in proliferation from days 1 - 7, the ICi-isolates showed a slight drop at day 7. A possible explanation for the increased viability of the SCi-group might be that with the enzymatic digestion of the SCi-isolates there is the generation of a greater number of cell colonies (Gronthos, Brahim et al. 2002; Huang, Sonoyama et al. 2006). It is likely that the ICi- and PEx-isolates may have generated lower yields owing to the presence of a higher amount of particulate cellular material from non viable cells or clumps of poorly disaggregated tissue. The observations in this study indicate that the SCi-isolates have a greater potential for proliferation *in vitro*, a finding supported by work by other groups (Huang, Sonoyama et al. 2006).

One of the key features of odontoblasts is the expression of ALP. The ALP assay results showed significantly higher levels of ALP activity in SCi-isolates at days 3 and 7 and all 3 of the cell groups showing peak activity at day 7. In animal studies using rabbits, odontoblasts have been described as having a much higher ALP activity than mesenchymal cells (Shiba, Mouri et al. 2003). It is important to note that these differences in cell proliferation and ALP activity, in all three groups at this point suggest differences in cell populations across the groups.

To analyze these differences, we decided to take a look at the morphology of the cells in culture at the peak of the proliferative and mineralising potential. There were no discernible differences in the structure of the cells from the three groups on phase contrast microscopy. The cells spread across the culture plates and at confluence assumed a heterogeneous elongated morphology typified by the appearance of spindle-like shaped cells with extensive cellular processes, an appearance maintained all through the cell culture period. A further consideration of the cytoskeletal structure of the cells was carried out by fluorescence microscopy. Using a fluorescent-labelled phalloidin, the actin filaments that are typically abundant in the cytoplasm and periphery of the cell in a longitudinal fashion, were visualized. The labelling of this structural protein provided further evidence of the shape of these cells (spindle). The fibres appeared to run in a perinuclear fashion sparing the cell nucleus. This typifies the description of odontoblasts in culture (Nishikawa and Kitamura 1987; Bluteau, Luder et al. 2008).

The expression of markers of an odontoblast phenotype was also analyzed. We investigated the expression of alkaline phosphatase (ALP), collagen type I (Col I), dentine sialophosphoprotein (DSPP) and, dentine matrix protein 1 (DMP-1). All three of the cell groups showed expression of these markers suggesting that the mRNA for an odontoblastic phenotype was present. The bands seen for DSPP, however, were not as pronounced in all the samples. Studies in rats have suggested that alkaline phosphatase and collagen expression occurs first (Bleicher, Couble et al. 1999) with the expression of DMP-1 and DSPP following afterward. It has been proposed that this expression pattern is linked with the formation of the dentine matrix only after the formation of a collagenous predentine matrix (Beguekirn, Smith et al. 1992; Ruch, Lesot et al. 1995; Macdougall, Gu et al. 1998; Gronthos, Brahim et al. 2002). This would suggest that DMP-1 and DSPP secretion by the odontoblasts follows alkaline phosphatase and collagen secretion. The expression of mRNA for these markers is believed to increase during the period of cell culture (D'Souza, Cavender et al. 1997; Couble, Farges et al. 2000; Yokose, Kadokura et al. 2000). The primary objective was to detect the presence or absence of these odontoblastic markers. As the test is qualitative and not quantitative, the results would not allow for a more robust interpretation. To answer this question and also further identify these cells as possessing the odontoblastic phenotype, we examined the expression of cell surface markers and the previously tested odontoblast markers using qPCR techniques. When compared to a commercial mesenchymal cell population (Figure 3.7b – B), there were significantly higher levels of CD44 mRNA expressed by the SCi- and PEx-isolates. This trend was reversed in the case of CD45 mRNA expression (Figure 3.7b – B). These findings on the basis of work by other groups which have defined odontoblast cell populations as being CD44-positive and CD45-negative, demonstrate the phenotypic identity of the isolated cells (Gronthos, Mankani et al. 2000; Gronthos, Brahim et al. 2002; Jo, Lee et al. 2007; Karaöz, Doğan et al. 2010; Atari, Gil-Recio et al. 2012). Further supporting this was the quantitative demonstration of ALP, COL-1, DSPP and DMP-1 mRNA expression levels, which were only greater than mRNA levels seen in mesenchymal controls (Figure 3.7b – C, D, E, F). In the next chapter, the timing of the secretion of these markers is observed and described. At this point, the data obtained



indicates that the cells possess the odontoblastic phenotype. From the findings described thus far, the following conclusions can be made:

- (1) Cells can be successfully isolated by any of the three methods studied. The most superior however, would be the “Single Cell” isolation technique as the functionality of the isolated cells in downstream tests showed to be better than the other methods. While the pulpal explant outgrowth technique seemed relatively easier to perform, the data obtained did show a higher dead cell count that seemed to unfavourably affect the proliferation and mineralisation activities of the cells. The Inverted Crown method may have the advantage of having a population of “only odontoblasts”, as these would be the cell types lining the pulp chamber walls. However, because the cells at that age might be post mitotic, there would be increase in cell death owing to a reduced ability to proliferate thus negating any long term usefulness in further experimentation. The cells cultured by all three isolation methods appeared to have little or no differences morphologically suggesting that the means of isolation may not have an influence on this.
  
- (2) The choice of an RNA extraction method for processing the cells is dependent on the efficiency of the method in yielding good quantities of pure RNA. Both Trizol and Hybrid methods generated RNA yields greater than 100ng/μl. There was a 1.5 to 5.3-fold increase in concentrations between the two methods across the three cell groups, with the SCI-isolates show the greatest increase. The effect of the concentrations seemed to show more on the absorbance readings for the 260nm and 230nm ratios. The ratio of absorbance at 260nm and 280nm assesses the purity of the nucleotide mix in the RNA (guanine, adenine, cytosine and uracil). Both the Trizol and Hybrid methods proved to be the efficient as the results were within in a desired range of 1.9 – 2.2. The 260nm and 230nm ratios assess for the presence of contaminants which may be introduced during the process of isolation and absorb at 230nm. The reagent used in the Trizol method contains the organic solvent phenol, which absorbs ultraviolet radiation at 230nm (and also at 270nm), which we speculate, may be responsible for the low A260/A230 ratios seen in the

results (0.360 – 0.960). However, other sources of contamination such as protein carry over from the earlier cell lysis phases may contribute as well. However, our data suggests that the Hybrid method, which has a more robust series of RNA washes to eliminate contamination, is the more efficient of the two methods.

Within the scope of this study, it can be assumed that the Single Cell isolation technique is the most appropriate for culturing cells from the dental pulp. These dental pulp cells (DPCs) have demonstrated markers of the odontoblastic phenotype and have also shown a potential for proliferation and mineralization by way of the MTS and ALP assays (Gronthos, Mankani et al. 2000; Gronthos, Brahim et al. 2002; Liu, Gronthos et al. 2006; Karaöz, Doğan et al. 2010). The next phase of the work focuses on the determination of the odontoblast cell character of these isolated cells (using only the SCi-isolation method).

# Optimisation of the odontoblast cell culture model

---

4

## Optimization of the odontoblast cell culture model

### 4.1 Introduction

In the previous chapter, a preliminary characterization of cells derived from the extirpated human dental pulp samples was performed to obtain dental pulp cells (DPCs), which showed features of an odontoblastic phenotype. In conditioned culture media, isolated dental pulp stem cells (DPSCs) have the potential to differentiate into adipocytes, neuron-like cells and odontoblasts (Gronthos, Mankani et al. 2000; Gronthos, Brahim et al. 2002; Batouli, Miura et al. 2003; Laino, d'Aquino et al. 2005; Liu, Gronthos et al. 2006; Huang, Chen et al. 2008; Huang, Chen et al. 2009). Studies carried out in human bone marrow fibroblasts, murine marrow stromal cells and later in rat dental pulp stem cells, suggest that the choice of a differentiation pathway (by the pulpal derived cells) following induction through clonogenic methods is dependent on the presence or absence of transcription factors such as runt-related transcription factor 2 (runx2) or core binding factor 1 (cbfa-1) (Chen, Gu et al. 2002; Chen, Rani et al. 2005; Chen, Gluhak-Heinrich et al. 2009; Wojtowicz, Templeman et al. 2010). The transfection of murine stromal cells with the peroxisome proliferator activated receptor gamma (PPAR $\gamma$ -1) has been shown to induce the adipogenic differentiation of these cells through the suppression of Runx2/Cbfa-1 (Lecka-Czernik, Gubrij et al. 1999). Both transcription factors are involved in the differentiation of odontoblasts as murine studies have demonstrated that they regulate DSPP expression which is required for the mineralization activities of the odontoblast cell (Chen, Rani et al. 2005). It was in this context that the nucleic acid expression profiles of the DPSCs was examined to determine if the cells were solely odontoblastic or expressed a non-odontoblastic profile. This would also serve as an examination of the efficacy of media used to induce the odontoblastic differentiation of the isolated cells.

Another consideration in the development of cell culture models is cell sustainability for extended periods of time allowing for long-term studies. In a two-dimensional culture system such as that used in this study, the viability of the DPCs is highly dependent on the nature of their immediate environment. With serial passaging there is the potential of a change in the odontoblast-specific fate of subsequent DPC

progeny. This view is supported by studies that indicate that sub-optimal culture conditions have the potential to cause de-differentiation along non-odontoblastic lineages as a result of serial cell passaging (d'Aquino, Graziano et al. 2007; Stevens, Zuliani et al. 2008). Periodic changes of the culture media during the test periods prevent the build up of waste products following the exhaustion of glucose, serum and other nutrients present in the media. However, the influence of culture media constituents such as glucose and serum can have significant effects on the DPSCs metabolic activity. Serum (FBS) contains mineral supplements such as calcium and phosphate (which are both present in the DMEM culture media) and dexamethasone which promote cell proliferation, as well as cytokines and growth factors (such as fibroblast growth factor) that aid cell proliferation (Boskey and Roy 2008). Odontoblast cell metabolism is influenced by the concentration of glucose available in the culture system. Studies carried out by Valikangas and colleagues using odontoblasts derived from human pulpal cells, demonstrated that increasing the concentration of glucose (ranges 19mM - 24.75mM approximately) in the odontoblast culture media, caused a reduction in the synthesis of collagen type 1, a requirement for the mineralization of dentine (Valikangas, Pekkala et al. 2001). The proliferation of these cells exposed to increased amounts of glucose was also shown to be markedly decreased (Valikangas, Pekkala et al. 2001). However, more recent work carried out on animal and human derived stem cell cultures have indicated the opposite, showing an increase in cell proliferation in the presence of elevated glucose levels (tested levels were between 5.5mM and 24.75mM approximately) (Follmar, Decroos et al. 2006; Mischen, Follmar et al. 2008). For the purposes of this particular study, the commercial media formulations used were acquired from Sigma-Aldrich®, containing glucose concentrations ranging between 5.5mM (1g/L) which is roughly equivalent to normal blood glucose levels *in vivo*, and 55mM (10g/L) (which would be well beyond human diabetic levels of > 16mM)(Dyson, Kelly et al. 2011).

To determine the influence of glucose on DPC proliferation and metabolism in our study, the glucose levels used in the assessment of DPC behaviour were 1mM and 4.5mM. Also varied, was the concentration of serum (FBS) for each of the glucose concentrations (5, 10 and 20%). While the glucose end-point values chosen were lower

than the concentrations evaluated by the previously mentioned groups (Follmar, Decroos et al. 2006; Mischen, Follmar et al. 2008), the aim in this study was to optimise the chosen culture conditions for the isolated DPCs and monitor the effects of varying the concentrations of glucose and serum would have on their behaviour in culture. This was to be assessed by examining the proliferative activity of the cells over a 21-day period. In addition, the clonogenic potential of the DPCs was assessed in order to provide additional information about the proliferative capacity of the cells over six passages. Furthermore, assays were performed to measure amounts of total cellular DNA in experimental DPC groups (which will be described in later sections) following exposure to varied concentrations of glucose and serum thus reflecting the proliferative status of the examined DPCs.

The literature, however, shows little evidence to support continued function (cell proliferation and mineralization) of these dental pulp stem cells for periods extending past two years post cryopreservation (Papaccio, Graziano et al. 2006). Attempts to obtain cultures of human cells have been successful in the main, although often they only have limited proliferative potential (Dirac and Bernardis 2003). The death of these cells is mostly due to oncogenic stress, as a result of an increased number of cell divisions (Dirac and Bernardis 2003; Ohtani, Yamakoshi et al. 2010; Haigis and Sweet-Cordero 2011). As cell division progresses, there is a shortening of telomeres, which causes cellular instability and activates an arrest of cell division. These telomeres are complexes of DNA and protein, which are located at the ends of chromosomes and are “omitted” from a semi conservative process of eukaryotic cell division by the DNA polymerases (Chan and Blackburn 2004; Epel, Blackburn et al. 2004). The reason for this is the inability of the DNA polymerases to synthesize DNA in the 3’ to 5’ direction (they are only able to do so in the 5’ to 3’ direction), causing the loss of any sequences at the end of the chromosomes (Watson and Crick 1993; Watson and Crick 2003). The generalised effect of this process of telomere shortening in human tissues is ageing. The *in vitro* consequence is cellular senescence, which has been attributed to oxidative culture stress, as well as the growth suppressing proteins such as p16 and p53 (Olovniko.Am 1973; Epel, Blackburn et al. 2004; Ohtani, Yamakoshi et al. 2010). The protein p53 controls the senescence of damaged or mutated cells by functioning as a

transcription factor in a negative feedback loop mechanism with a wide range of genes such as those responsive to oxidative stress (for example, p-53-induced gene 3, Pig3) (Polyak, Xia et al. 1997), cycle regulators (for example, G0/G1 regulatory switch gene G0S8) (Siderovski, Heximer et al. 1994), matrix proteins (collagen and actin) and cell surface receptors (tyrosine-protein kinase receptor, Eck) (Zhao, Gish et al. 2000). The function of p53 has also been linked to an “adaptive” cell cycle arrest in transformed mouse fibroblast cells in the presence of low glucose culture conditions through the phosphorylation of an adenosine monophosphate dependent kinase, AMPK (Feng, Hu et al. 2007). Its activity has also been described as dependent on the presence of p16, which is a damage response protein (Beausejour, Krtolica et al. 2003) that shares a senescence inducing pathway with the tumour suppressor protein retinoblastoma protein (pRb), responsible for regulating the G1-S cell cycle entry and exit barrier – a significant point for cell differentiation (Burkhart and Sage 2008).

The maintenance of telomere length of cells in culture is dependent on the expression of human telomerase reverse transcriptase (hTERT) (Bodnar, Ouellette et al. 1998; Carney, Tahara et al. 2002). This gene encodes the catalytic subunit of a protein complex known as telomerase, which permits the addition of telomeric DNA repeat sequences during cell division (Greider and Blackburn 1987; Greider 2006). The activity of hTERT while present in normal somatic cells, is up regulated in human neoplastic cells (Kim, Piatyszek et al. 1994). Research groups who have used a combination of viral oncogenes have demonstrated uninhibited cell division, these allow for the ectopic expression of the telomerase enzyme to successfully establish human cell lines with increased periods of cell growth. Protein products of Simian Virus 40 (SV40) or retroviral vectors have been used to transduce the hTERT gene into human cell lines (Kamata, Fujimoto et al. 2004; Galler, Schweikl et al. 2006; Böker, Yin et al. 2008). This deactivates the p53 pathway and immortalizes the cells (Harvey and Levine 1991; Shay, Pereira-Smith et al. 1991). How this occurs is not entirely clear. In studies using human mammary epidermal cells, the exogenous introduction of hTERT was shown to have led to the activation of the pro-growth gene epidermal fibroblast growth factor receptor and the repression of the activity of the pro-apoptotic gene TRAIL (tumour necrosis factor –related apoptosis inducing ligand (Smith, Collier et al. 2003). Following

this, work carried out on chronic lymphocytic leukaemia cells from human subjects showed that some cells cultured in the presence of basic fibroblast growth factor, bFGF showed a down regulation of p53 activity as well as an increased growth of the neoplastic cells (Romanov, James et al. 2005). This finding was attributed to the up regulation of the p53 –inhibitory gene Mdm2 as well as the impairment of p21, another senescence-associated gene linked to p53 activity (Riley, Sontag et al. 2008; Lars-Gunnar 2011).

A disadvantage, however, with performing such a procedure (transduction), is that in some human cell lines there is the possibility of developing tumour cells (Dickson, Hahn et al. 2000). There is also the suggestion that the expression of p16 may still prevent further cell division as its function is not dependent on telomerase expression (Kiyono, Foster et al. 1998). Hence, in order understand the effect that ectopic telomerase expression might have on preventing cellular senescence and prolonging DPC longevity in culture, a retroviral vector was used in this study to deliver a cloned human telomerase reverse transcriptase gene (hTERT) into the DPCs. The continued expression of genes characteristic of the odontoblastic phenotype in the transfected DPCs (tDPCs) was determined and compared to non-transfected DPCs (nDPCs). This experimental work has been published (Egbuniwe O 2011). In summary, the experimental objectives are:

- Examine the mRNA profile of the isolated cells for the odontoblastic phenotype
- Determine efficacy of media and culture conditions
- immortalize the cells to aid longevity to allow for further experimental work
- With the use of FACS analysis, demonstrate the isolation by cell culture of a homogenous cell population



## 4.2 Materials and methods

All reagents, including cell culture media were purchased from Sigma-Aldrich® unless otherwise noted. The cells used in the culture studies were resuscitated from previously cryopreserved stocks (see Section 2.13).

### 4.2.1 Population doubling studies

For this part of the experiments, population-doubling studies were used to assess the growth capabilities of the cells. The DPCs were divided into two groups corresponding to the glucose concentrations (1mM and 4.5mM) of the growth media formulations. Following a 12- 24 hr. period of conditioning in supplemented media, the cells were seeded at a density of  $1 \times 10^4$  cells per ml of appropriate experimental group media. Using a TC10™ Automated Cell Counter (Bio-Rad, USA) and a TC10™ trypan blue exclusion dye, counts for cell proliferation were performed on cell cultures established from the 1mM and 4.5mM cell culture groups (as described in Section 2.2). The cell numbers were counted on days 0, 3, 7, 14, 28, 42 and 56. The growth rate of the cells and cumulative population doubling was calculated by using the formula proposed by Huang et al (Huang, Shagramanova et al. 2006). The media was changed every 3 days in between counts in order to minimize cell disturbances.

### 4.2.2 Serum content of cell culture media

Parallel experiments were set up to test the effect of serum content (fetal calf serum, FCS) in the supplemented growth media on the DPCs at three concentrations: 5%, 10% and 20% in each of the two experimental groups described in Section 4.2.1. Using a TC10™ Automated Cell Counter (Bio-Rad, USA) and a TC10™ Trypan blue exclusion dye as described in Chapter 2 (Section 2.2), cell counts were performed at days 1, 7, 14 and 21. Media changes were performed every three days.

### 4.2.3 Glucose content of cell culture media

The DPCs were cultured in supplemented media at a density of  $1 \times 10^5$  cells per ml and divided into two groups corresponding to the glucose concentrations (1mM and 4.5mM) of the growth media. Following cell seeding in 24-well plates, the DNA content of the DPCs was examined using the method of Rao and colleagues (Rao and Otto 1992) as described in Chapter 2 (Section 2.1.4) with prepared DNA standards. The fluorescence readings (excitation at 355nm and emission at 460nm) were measured using a fluorimetric reader (Chameleon, Hidex, Finland). The cell lysates used for the experiment were obtained at days 7, 14 and 21 of the cell culture and commercial mesenchymal stem cells were used as controls (mesenchymal cell DNA content from 1000 cell equivalents were used as controls). The experimental condition specific media was replaced every three days between experiments to minimize cell disturbance.

### 4.2.4 RT-PCR to demonstrate multi-lineage potential of DPCs

The resuscitated DPCs were cultured for 1 passage and the total RNA was extracted and quantified as described in Chapter 2 (Section 2.1.10, 2.1.11). Following this, cDNA was synthesized using 1 $\mu$ g of the purified RNA. Markers were chosen to test the expression of mRNA representative of adipogenic (peroxisome proliferator-activated receptor gamma, PPAR $\gamma$ -1 and sex determining region Y-box 9, Sox9) and neurogenic lineages (beta-3-tubulin,  $\beta$ 3T, enolase-2, en-2 and nestin), as well as those of embryonic stem cell markers (runt-related transcription factor 2, Runx2 and core binding factor 1, Cbfa-1). The list of primer sequences (including sizes in base pairs) used in the PCR analysis is provided in Table 2-1 (See section 2.9). Glyceraldehyde 3-phosphate dehydrogenase (GAPDH) was the housekeeping gene used to normalise this series of experiments.

#### 4.2.5 DPC transduction

The retroviral vector containing the cloned human telomerase reverse transcriptase (hTERT) gene, pBabe-puro-hTERT (Figure 4.1) (Counter, Hahn et al. 1998), was a kind gift from Dr J.M. Funes (University College London Cancer Institute). A concentration of  $1 \times 10^4$  DPCs were plated in each well of a 24-well plate. This was followed by exposure to the hTERT retrovirus that was added to DMEM/S growth media, for 24 hours. After 24 hours the virus was removed and replaced with DMEM/S growth media for a further 72 – 90 hour period at 37°C in a humidified incubator. This was followed by selection using 1µg/ml puromycin (Sigma) for between 7 - 14 days. The cells were then expanded over 1 passage. Eighty per cent of these expanded cells were used for the rest of this study and are referred to as tDPCs (transformed dental pulp cells).

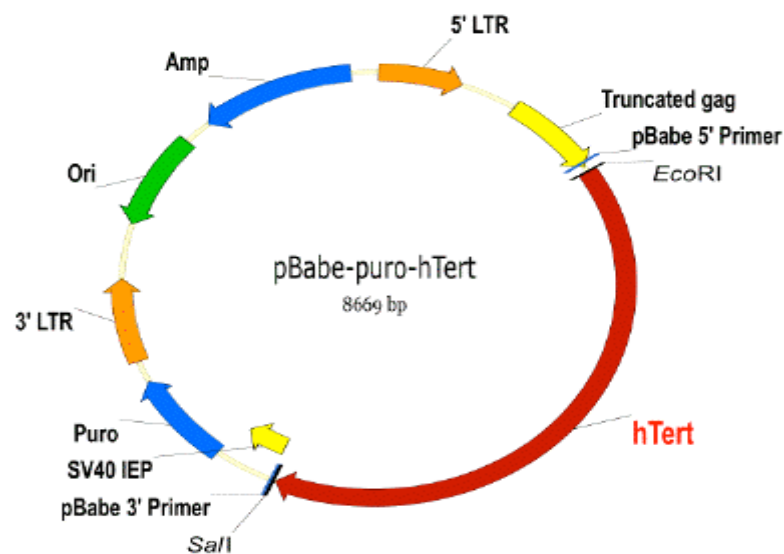


Figure 4:1: The map of the pBabe-puro-hTERT gene designed for use in humans. The hTERT insert size is 3500 base pairs (bp) and the pBabe-puro backbone size is 5169 base pairs (bp). The 5' sequencing primer is pBabe 5' and the 3' sequencing primer is pBabe-3'. The 5'- and 3' cloning sites are *EcoRI* and *SalI* respectively. The plasmid was designed to confer resistance to ampicillin, and the selection marker to determine its uptake was puromycin (Counter, Hahn et al. 1998).

#### 4.2.6 TRAP (telomere repeat amplification protocol) assay

Telomerase activity was determined using a TRAPeze<sup>®</sup>XL Telomerase Detection Kit (Millipore™). The cells were pelleted, washed in PBS and dissolved in 200 µl of 1 × CHAPS lysis buffer. After a 30 min incubation period on ice, the cell samples were centrifuged at 12,000 g for 20 mins at 4°C. 160µl from each of the sample supernatants were collected for protein content analysis using a standard by Bicinchoninic acid protein assay. 2µl of the cell-extract (approximately 2.5 µg protein/sample supernatant) was added to a 48µl reaction solution consisting of 5 × TRAPeze<sup>®</sup>XL reaction mix, a cloned Taq polymerase (Sigma-Aldrich<sup>®</sup>) and distilled water. A 1000 cell equivalents of telomerase positive cell extract (provided with the kit) was used as a positive control. Heat inactivated samples, a sample with Taq polymerase and a sample without telomerase, were used as negative controls. The tubes containing the mixture were incubated at 30 °C for 30 mins in a thermocycler block. This was followed by a 4-step PCR at 94 °C for 30 seconds, 59 °C for 30 seconds, 72 °C for 1 min (36 cycles), a 72 °C for 3 mins extension step, 55 °C for 25 mins and a 4°C incubation phase. During the PCR process, generated products (from test samples) and an internal control product, (a constituent of the reaction buffer provided in the kit) were amplified by fluorescein- and sulphorhadamine-labelled reverse primers respectively (provided with the kit). These generated fluorescence emissions directly proportional to the amount of generated TRAP products. The 50µl PCR reaction product for each sample was transferred into a black walled 96-well plate containing 150µl of 10nM Tris-HCl/0.15M NaCl/2mM MgCl<sub>2</sub> buffer (pH 7.4). Using a fluorescent plate reader, fluorescence was measured for each sample using excitation/emission parameters (in line with the manufacturers' protocol) for fluorescein, F (485nm/534nm) and sulforhodamine, R (584nm/610nm).

#### 4.2.7 Beta-galactosidase staining

Using a Senescence Cells Histochemical Kit (Sigma-Aldrich<sup>®</sup>), the activity of β-galactosidase, a marker of cellular senescence was investigated in tDPSCs and compared to nDPSCs. Cells from both cell groups (nDPSCs and tDPSCs) were seeded in

6-well plates at a density  $1 \times 10^4$  cells/well and cultured in DMEM/S (high glucose media) for 48 hours. The culture media was aspirated after this time and the monolayers of cells were washed in PBS, fixed for 6-7 mins (room temperature) in a 1 x 20% formaldehyde/2% glutaraldehyde buffer (Sigma-Aldrich®). A 10ml staining mixture made up of 0.25ml (40mg/ml) of X-gal solution (Sigma-Aldrich®); 0.125ml of 400mM of potassium ferrocyanide (Sigma-Aldrich®); 0.125ml of 400mM of potassium ferricyanide (Sigma-Aldrich®), 1ml 10xs Staining solution (Sigma-Aldrich®) and 8.5ml of ultrapure water, was prepared immediately before use. After three washes, the cells were incubated at 37°C in an oven with the freshly prepared  $\beta$ -galactosidase senescence associated stain solution. The staining of cells was observed under a fluorescence microscope after 4hrs and 12hrs.

#### 4.2.8 Gene detection using reverse transcription polymerase chain reaction

At passage 6, when the tDPCs had attained 80% confluency, the total RNA content was isolated using methods earlier outlined in Chapter 3 (Section 3.1.9). Primer sequences for the hTERT gene were designed for use in the transcription of its cDNA from mRNA. The chosen sequences were tested as described in Chapter 2 (Section 2.9) and ordered from Sigma-Aldrich when deemed satisfactory. Other sequences also designed were those for odontoblastic differentiation markers (alkaline phosphatase (ALP), collagen I (Col-1), dentine matrix protein (DMP-1), dentine sialophosphoprotein (DSPP)) and oncogenic markers associated with senescence (p16, p21 and p53). Glyceraldehyde 3-phosphate dehydrogenase (GAPDH) was the housekeeping gene used to normalise for RNA expression in this experiment.

#### 4.2.9 DNA content assay

Following cell seeding at  $1 \times 10^4$  cells/well in 24-well plates, the DNA content of tDPSCs and nDPSCs was examined using the method of Rao and colleagues (Rao and Otto 1992): three cycles of freezing – thawing at -80°C and 37°C respectively; 100 $\mu$ l aliquots of each cell group was then transferred to a 96 well-plate; 100 $\mu$ l Hoechst

33258 (Sigma®) fluorimetric dye was added to each well; fluorescence was measured at an excitation of 355nm and emission wavelength of 450nm on a plate reader (Chameleon™, Hidex, Finland). DNA standards (Sigma®) were prepared and the DNA assay was performed in parallel for standardization. The cell lysates used for the experiment were taken at days 1, 3 and 7 of the cell culture and the experiment was performed using triplicate samples.

#### **4.2.10 Alkaline phosphatase assay**

The nDPCs and tDPCs were seeded in 24-well plates at a density  $1 \times 10^4$  cells/well and on days 1, 3, and 7, the growth media was removed from designated wells and the cells were washed with PBS. Cell lysates were collected for each time point as described in Section 2.3 of Chapter 2. Using a 96 well plate, 50µl of the cell lysates and the ALP reaction buffer was pipetted into an appropriate well. The absorbance was measured at a wavelength of 405nm with a spectrophotometer (Opsys MR Microplate reader) after 5 mins.

#### **4.2.11 Immunocytochemistry**

Visualization experiments were performed using a FITC-conjugated phalloidin antibody (1/1000) and a collagen type 1 antibody (1/100) (AbCam) to analyse the actin microfilament cytoskeletal protein and the expression of collagen type 1 (col-1). The cells (nDPSCs and tDPSCs) were cultured to 70% confluence in 6-well plates and following the experimental protocols described in section 2.6, the cells were fixed with 4% paraformaldehyde in PBS and incubated with primary antibody, phalloidin/collagen type 1 at 37°C for 1 hour. Control wells were incubated without phalloidin/collagen type 1. The nuclei in both experimental groups were counterstained with DAPI for 10 mins. The cells were washed before viewing. The plates were visualised using a Leica DMRE upright confocal microscope (Leica Microsystems Heidelberg GmbH).

#### 4.2.12 Fluorescence activated cell sorting (FACS)

Using flow cytometric methods for the analysis of surface proteins, adherent monolayers of tDPSCs were seeded at concentrations of  $2 \times 10^6$  cells/ml (in  $175\text{cm}^3$  culture flasks) and harvested at two time points: passage 5 (early tDPSCs) and passage 36 (late tDPSCs). After collecting the cells, they were centrifuged with FACS buffer (PBS + 2% FCS) at 1350 rpm for 5 mins and re-suspended in 1ml of sterile PBS/FCS. The cells were pipetted into 5ml polypropylene tubes and centrifuged at 1200 rpm for 7 mins. The supernatant was aspirated and the cell pellet was washed once more and resuspended in  $100\mu\text{l}$  FACS buffer. The resuspended cells were stained with  $1\mu\text{l}/\text{test}$  of fluorescent aqua dye (Live/Dead fixable aqua dead cell stain kit, Invitrogen, Cat No.L34957) for the exclusion of dead cells and incubated at room temperature (protected from light) for 30mins. After incubation, the cells were washed once in 1ml sterile PBS (500g for 5mins), re-suspended in  $100\mu\text{l}$  FACS buffer and incubated with  $0.5\text{mg}/\text{ml}$  of the primary conjugated antibodies (CD13 (amino peptidase N), CD44 (lymphocyte homing associated cell adhesion molecule), CD73 (integrin  $\beta 5$ ), CD90 (Thy-1), CD146 (melanoma cell adhesion molecule) and CD166 (vascular cell adhesion molecule)) listed in Table 3-1 for 30 mins on ice (protected once again from light). This incubation was performed in parallel with matching conjugate isotype controls (according to antibody class and species). The cells were sorted using BD FACSCANTO II flow cytometer (Becton Dickinson, CA, USA) by collecting  $\geq 10,000$  events and the data was analysed using FACS DiVa Software (Becton Dickinson, CA, USA).

Antibody	Fluorescent conjugate	Species / Immunoglobulin class	Commercial source
<b>CD13</b>	PE	Mouse IgG1, $\kappa$	BD Cat No 555749
<b>CD44</b>	PE	Mouse IgG <sub>1</sub> , $\kappa$	BD Cat No 550989
<b>CD73</b>	PE	Mouse IgG <sub>1</sub> , $\kappa$	BD Cat No 550257
<b>CD90</b>	FITC	Mouse IgG <sub>1</sub> , $\kappa$	BD Cat No 555595
<b>CD146</b>	PE	Mouse IgG <sub>1</sub> , $\hat{\mu}$	BD Cat No 550315
<b>CD166</b>	PE	Mouse IgG <sub>1</sub> , $\kappa$	BD Cat No 559263

Table 4:1: Conjugated antibodies used in the fluorescence-activated cell sorting of the tDPSCs. PE –Phycoerythrin; FITC – Fluorescein isothiocyanate. All the antibodies used showed cross-reactivity for human protein.

#### 4.2.13 Reverse transcription-quantitative polymerase chain reactions

This series of experiments was performed to investigate the maintenance of an odontoblastic lineage after transfection with the hTERT gene. The transformed DPSCs (tDPSCs) were seeded at concentrations of  $1 \times 10^6$  cells/ml (in  $75\text{cm}^3$  culture flasks) and harvested every 10 passages between two time points: passage 10 (early tDPSCs) and passage 60 (late tDPSCs). Four phenotypic markers were chosen to monitor the cells: alkaline phosphatase (ALP), collagen I (COL-1), dentine sialophosphoprotein (DSPP), and dentine matrix protein 1 (DMP1). The RT-qPCR methodology used in these experiments has been described in section 2.12. The list of primer sequences (including sizes in base pairs) used in the qPCR analysis is provided in Table 2-2 (See Section 2.13). Beta actin was used as a reference gene to normalise for RNA expression.

#### 4.2.14 Statistical analysis

All experiments were run in triplicate to ensure reproducibility. The analyses of the data were determined using one-way ANOVA. The ANOVA analyses were examined post hoc by Bonferroni's post-test. GraphPad Prism® was used to carry out statistical analysis. The  $p$  value for statistical significance was set at  $*p < 0.05$ ,  $**p < 0.01$  and  $***p < 0.001$ .



### 4.3 Results

#### 4.3.1 Population doubling studies

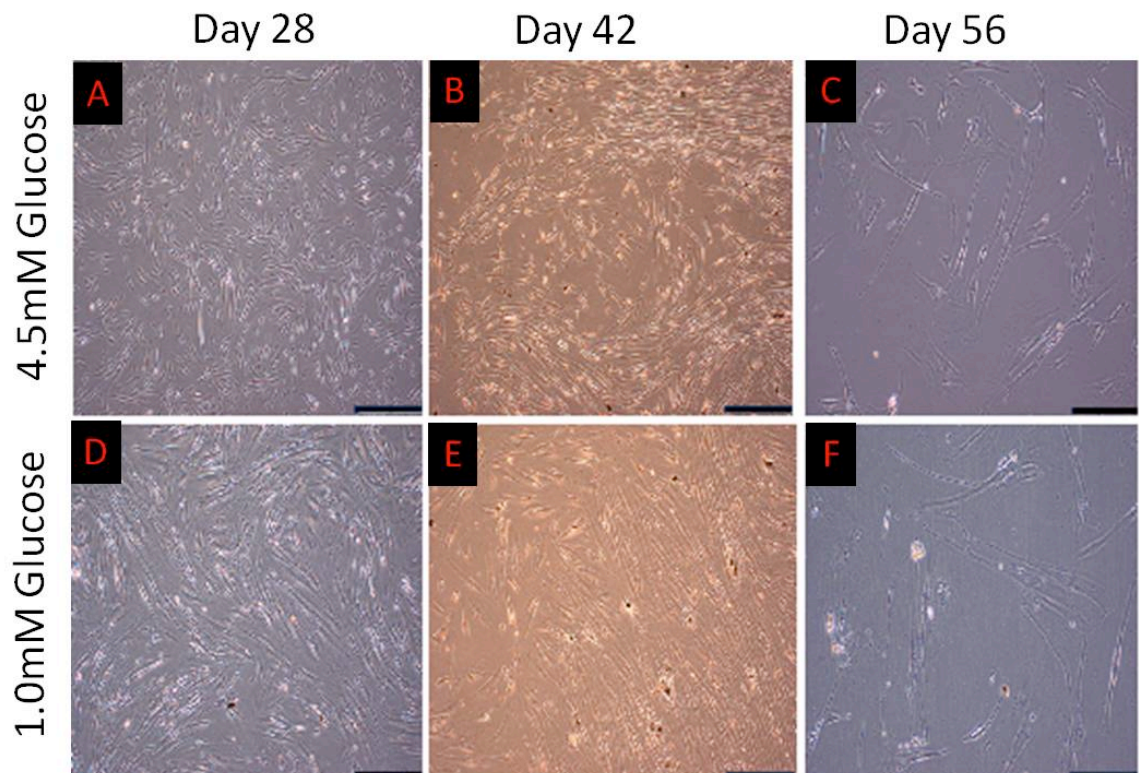
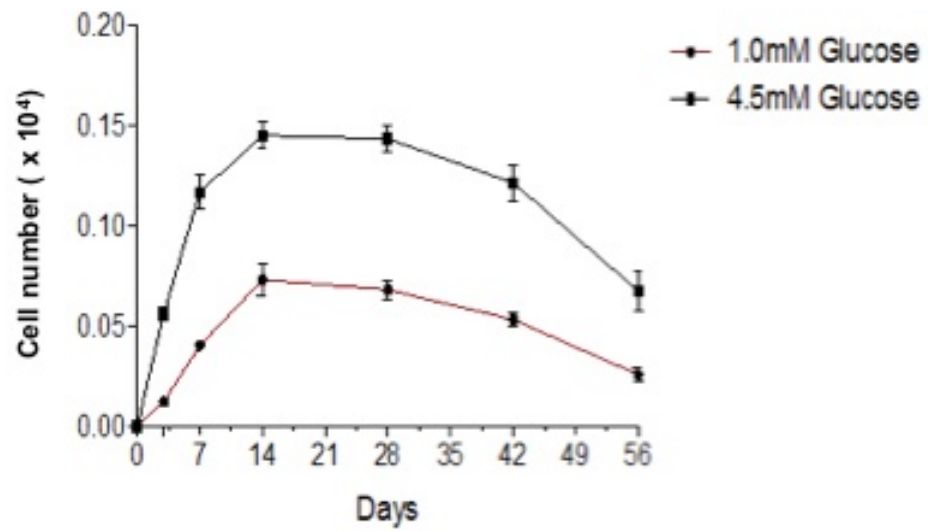


Figure 4:2 Population doubling assessed in DPSCs cultured in media containing 1.0mM and 4.5mM concentrations of glucose over six culture passages spanning a 56-day period (n=5). Scale bars in A, B, D, E = 40 microns. C, F = 100 microns.

With the plating of an equal number of cells in 1.0mM and 4.5mM glucose containing media, the influence of the different media formulations on cell growth was investigated. The *in vitro* expansion of the cells was observed over six passages (Day 0 – 56). The cells in the low glucose media formulation showed population doubling times that were 1.19-fold lower than those of the DPSCs in the high glucose formulations. This was based on calculations using the following formulae: Population doubling (PD) =  $3.33 \times \log_{10} (N_{\text{END}}/N_{\text{START}})$ . Population doubling time ( $\text{PD}^{\text{T}}$ ) =  $\text{Time} (N_{\text{END}} - N_{\text{START}})/\text{PD}$ . (N = Cell number). These differences in growth rates became particularly pronounced between days 7 and 14 (Passage 6 -7,  $p = 0.014$ ). By day 28, there was a reduction in cell population in both groups, with a drop in  $\text{PD}^{\text{T}}$  values (-0.3). Phase contrast images of the cells at day 28 and 42 show a reduction in cell numbers with images at day 56 showing an increase in cell size (Figure 4.2).

#### 4.3.2 Serum content and glucose concentration studies

To determine the optimum amounts of serum (in combination with low and high glucose concentrations) required in the DPC culture media, equal populations of the cells were seeded in three serum-concentration groups. The data obtained showed that the variations in serum concentrations did not cause any significant changes in cell numbers between the low glucose and high glucose groups for each serum-concentration groupings at days 1 and 7 (See Figure 4.3). Cell numbers were consistently higher at days 14 and 21 in both glucose culture environments at serum concentrations of 10% and 20%.

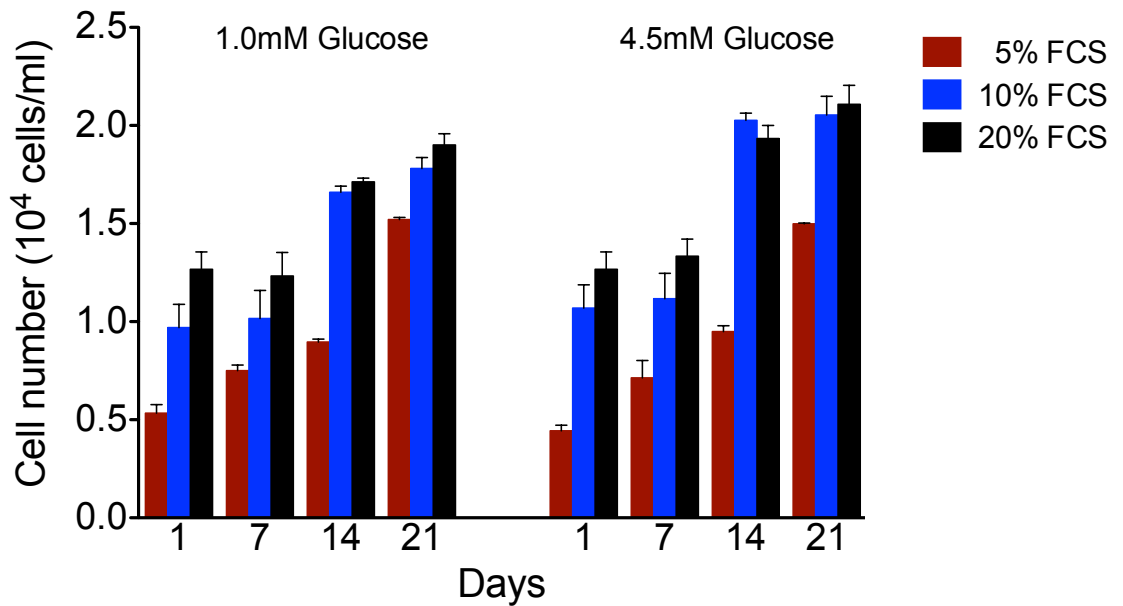


Figure 4:3 Cell populations of DPCs exposed to 1.0mM and 4.5mM glucose concentrations were counted over 21 days. In each of the experimental groups, the cells in different sub-groups were cultured in 5%, 10% and 20% concentrations of fetal calf serum (FCS). (n=7 per sub-group).

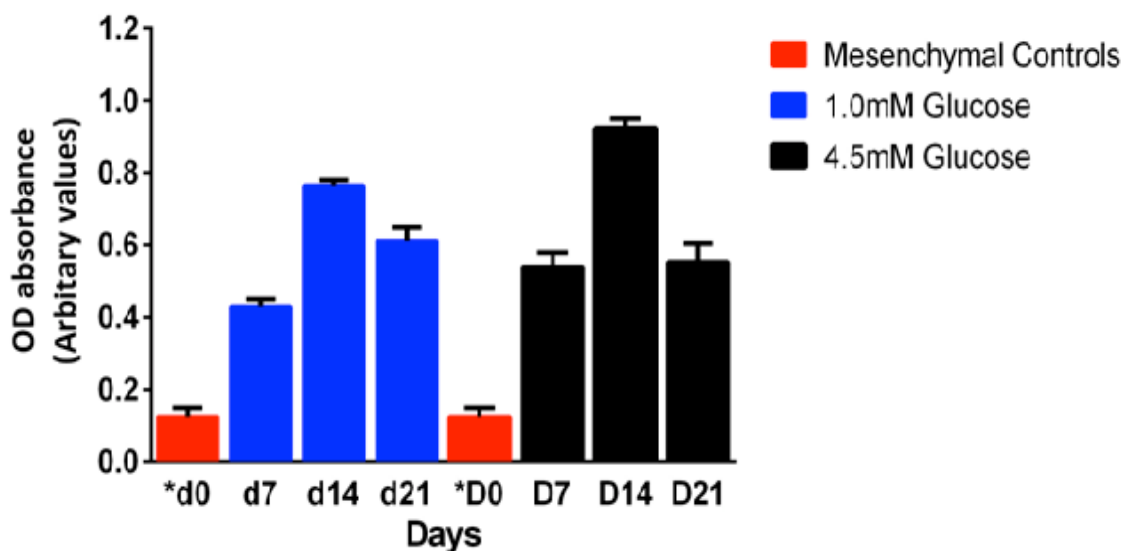


Figure 4:4 Analysis of the influence of glucose concentrations (1.0mM and 4.5mM) on cell proliferation over a 21-day period in DPCs. Mesenchymal controls (\*D0) were used. The values are means of the optical absorbance readings at 490nm  $\pm$  SE and the data was analysed using one-way ANOVA and post hoc Bonferroni's test: \* $p < 0.05$ , \*\*  $< 0.01$ , \*\*\*  $< 0.001$ . (n = 7, \*d0 Vs d14 - \*\* $< 0.01$ ; \*D0 Vs D14 - \*\* $< 0.01$ ).

Following these observations, the optical density (OD) absorbance readings of DNA activity was carried out on DPCs and control MSCs using 10% FBS in low and high glucose containing culture media. The proliferation of the 2 groups of DPCs showed a similar increase from day 7 to 14 in both low glucose (1.0mM) and high glucose (4.5mM) growth media formulations (See Figure 4.4). The OD absorbance readings were found to be higher at day 14 in the DPCs cultured in the high glucose containing media but not significantly so. In both groups, a non-significant drop in absorbance readings was observed at day 21 following maximum values measured at day 14.

### 4.3.3 RT-PCR analysis of DPCs: before and after transduction

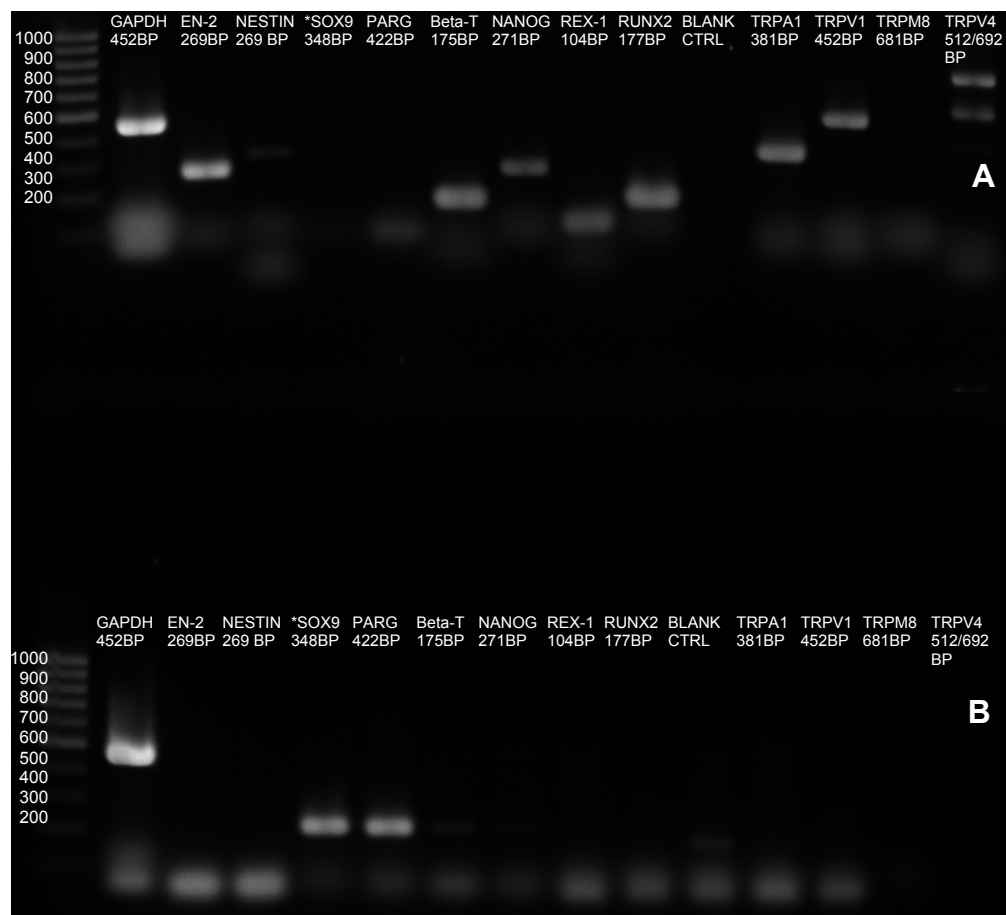


Figure 4:5 RT-PCR was used to identify the expression of non-odontoblastic and transcription factors in human dental pulp cell populations (A). Mesenchymal cells were run as a control (B) GAPDH served as an internal control.

To confirm the odontoblastic phenotype of the resuscitated DPCs, the cells were examined for the expression of mRNA profiles representative of adipogenic and neural phenotypes as well as transcription factors without the induction of lineage-specific differentiation. The data shows (See Figure 4.5A) no bands for SOX9 and PPAR $\gamma$  (adipogenic markers) and marked expression of EN-2 and  $\beta$ 3T (neural markers) and NANOG, REX-1 and RUNX-2 (transcription factors). The expression of nestin, another neural marker was not found.

Following the introduction of hTERT, the presence of its mRNA in the tDPCs was confirmed using RT-PCR. There was a visible expression in the tDPCs (Figure 4.6B) and a faint band present in the nDPCs (Figure 4.6A). Also investigated was the presence of odontoblastic differentiation markers DMP-1 and DSPP and transcription factor cbfa-1 (Figure 4.7A). The expression of mRNA for these markers was more prominent in the tDPCs (Figure 4.7B) compared to the nDPCs (Figure 4.7A). One of the DSPP primers was tested against mesenchymal cells (MyDSPP) as a control for specificity in both DPSC cell lines and no visible bands were seen.

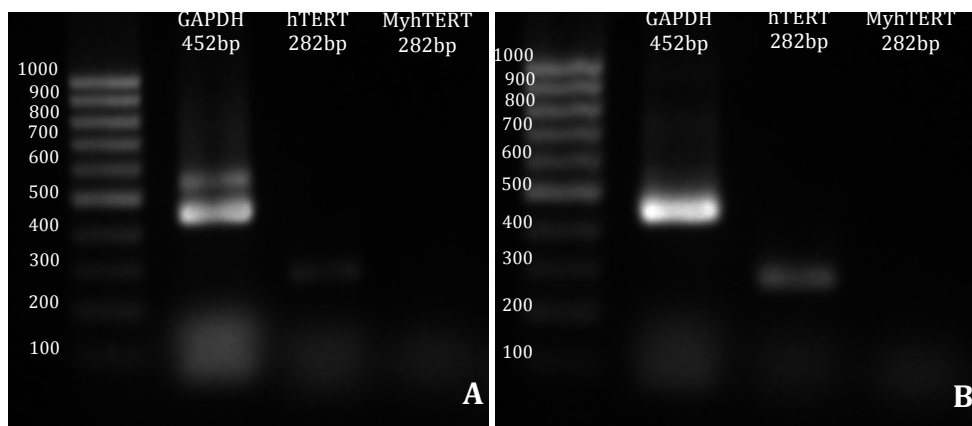


Figure 4:6: The identification of the hTERT expression profile in tDPSCs (B) following retroviral transduction. No hTERT band was visible in the nDPSCs (A). GAPDH was used as an internal control. No visible bands were observed in mesenchymal controls (MyhTERT).



Figure 4: 7: The cells maintained an odontoblastic phenotype as evidenced by the presence of mRNA expression for DMP-1, DSPP and Cbfa-1 in nDPCs (A) and tDPCs (B). There was no visible expression of DSPP in mesenchymal controls (MyDSPP). GAPDH was used as an internal control.

#### 4.3.4 TRAP assay readings

Equivalents of 500 and 1000 cells were made using cell extracts of tDPSCs, nDPSCs, and telomerase-positive and telomerase-negative samples (Figure 4.7). The fluorescence was measured and showed a significant change in the fluorescence ratio ( $\Delta FI/\Delta R$ ) values for tDPSCs at 500 and 1000 cell equivalents. The telomerase-positive extracts showed  $\Delta FI/\Delta R$  values indicative of telomerase activity at 500 cell equivalents.  $\Delta FI/\Delta R$  values for nDPSCs at 500 and 1000 cell equivalents were zero and less than 1 per cent of the telomerase positive cells respectively, indicating a low level of telomerase activity. This would suggest background levels of telomerase activity in nDPSCs in keeping with the faint expression bands detected on mRNA levels by PCR (Figure 4.6). Telomerase-negative samples showed a zero  $\Delta FI/\Delta R$  at 500 cell equivalents.

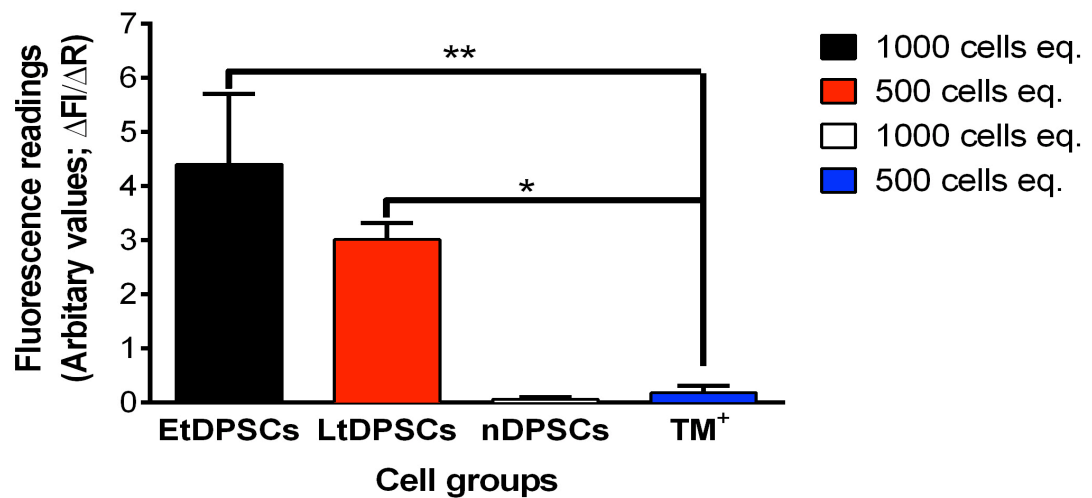


Figure 4:8. Following the introduction of hTERT, relative fluorescent readings were used to analyse telomerase expression in early (EtDPSCs) and late (LtDPSCs) passage cells and nDPSCs. Telomerase positive cells (TM+) provided in the assay kit, were used as controls. The data was analysed using one-way ANOVA and post hoc Bonferroni's test: (Mean  $\pm$  SD,  $n=4$ ;  $*p < 0.05$ ,  $** < 0.01$ ,  $*** < 0.001$ ).

#### 4.3.5 Beta galactosidase staining

DPSCs undergoing senescence showed a blue peri-nuclear stain indicating positivity for  $\beta$ -galactosidase (at a pH of 6.5) activity in these cells (Figure 4.9a). The early passage tDPSCs (passage 6) did not stain for  $\beta$ -galactosidase (Figure 4.9aC). A few late passage tDPSCs (passage 30) and a significant number of nDPSCs (passage 30) showed  $\beta$ -galactosidase activity (Figure 4.9b). The cells were re-plated after the experiment and there was a failure of the positively staining nDPSCs to proliferate.

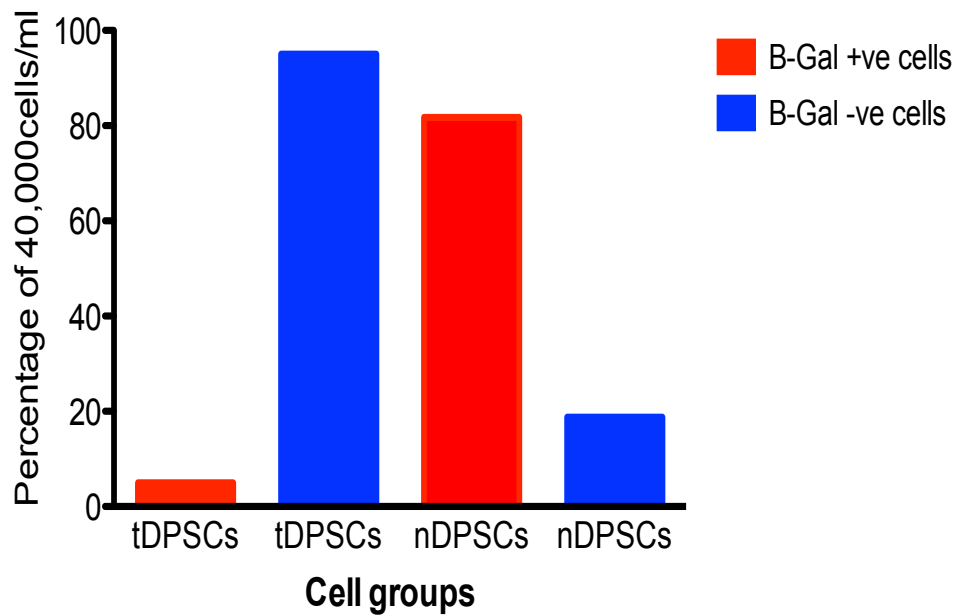
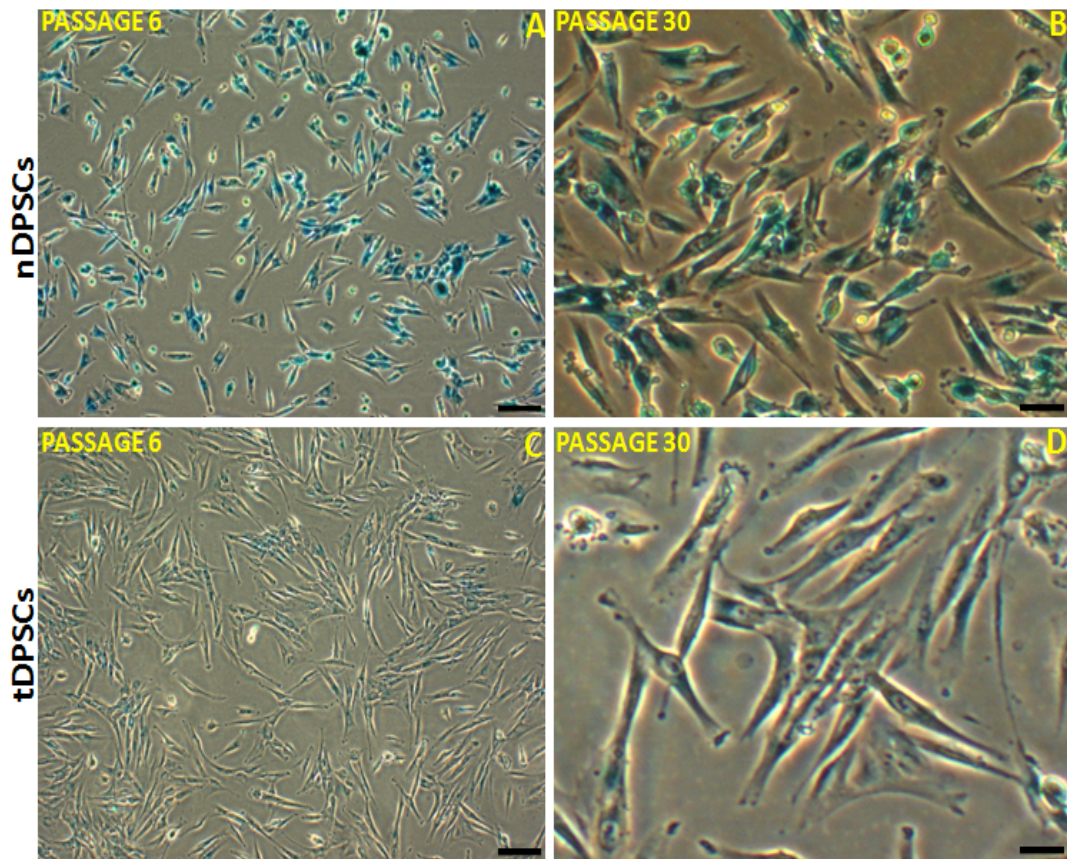


Figure 4:9a. Beta-galactosidase staining in cultured nDPSCs and tDPSCs. Scale bar in A and C = 100x magnification; B and D = x200 microns magnification. Figure 4:9b shows graphical representation of early passage nDPSCs (passage 6) that showed > 80% positive beta galactosidase staining. This positive staining was only seen in the tDPSCs at passage 30, with < 10% positivity. Positive staining was absent after re-plating tDPSCs.



#### 4.3.6 Evaluation of DNA content and ALP activity after transduction

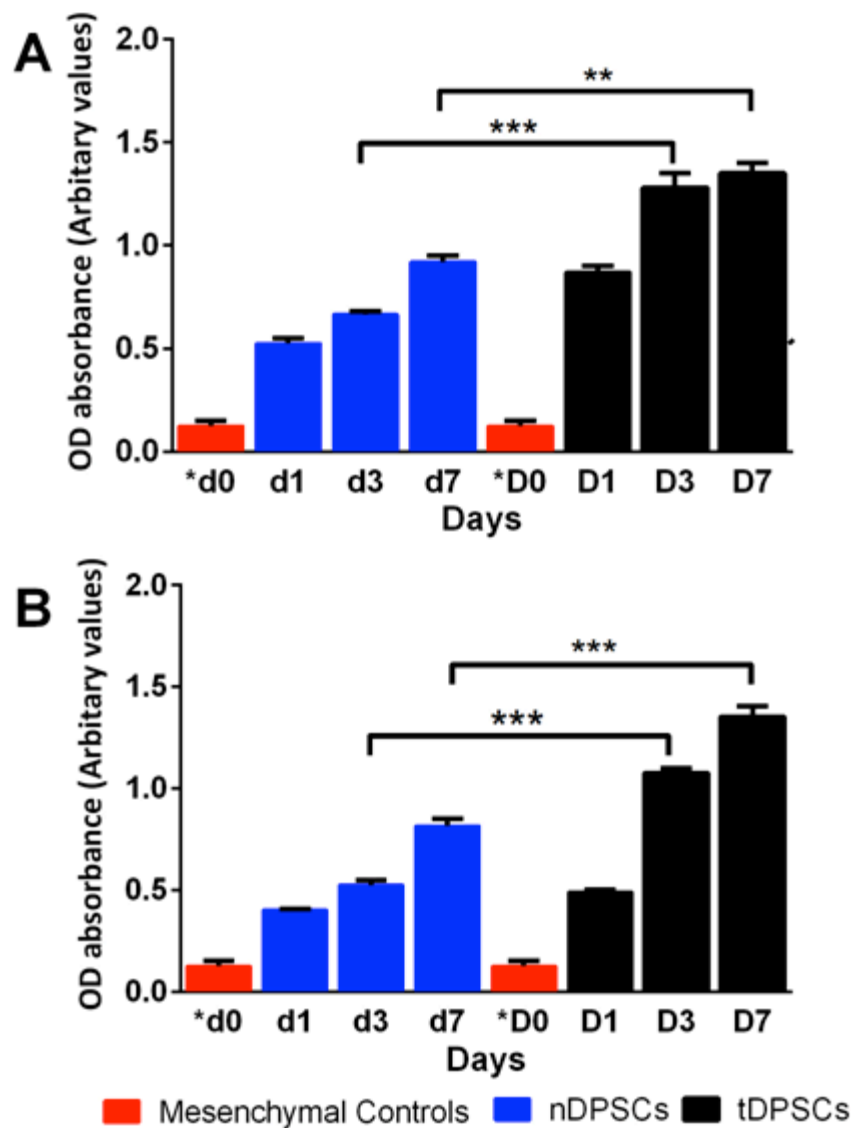


Figure 4:10. Analyses of cell proliferation (B – DNA assay) and cell mineralization (A- ALP assay) in cultured tDPSCs and nDPSCs. Mesenchymal controls (\*D0) were used in all experiments. The values are means of the optical density absorbance readings at 490nm. The data was analysed using one-way ANOVA and post hoc Bonferroni's test: (Mean  $\pm$  SD, n=4; \* $p$  < 0.05, \*\* < 0.01, \*\*\* < 0.001; Figure 4:10A: \*d0 Vs d7 - \* < 0.05; \*D0 Vs D7 - \*\* < 0.01; Figure4: 10B: \*d0 Vs d7 - \* < 0.05; \*D0 Vs D7 - \*\* < 0.01).

The proliferative and mineralising activities of the tDPSCs demonstrated significant increases as seen in Figure 4.10. There was a steady increase in the total proliferative activity of the tDPSCs in comparison to the nDPSCs as the optical density absorbance readings show (Figure 4.10B), over the 7-day test period. The tDPSC-DNA

content was significantly high on days 3 and 7 in comparison to the mesenchymal 1000 cell equivalent controls. This trend was mirrored by the tDPSC-ALP activity as seen in Figure 4:10A.

#### **4.3.7 Analysis of cytoskeletal structure by fluorescence microscopy**

The morphology of tDPSCs and nDPSCs was analysed microscopically. Using a fluorescent-labelled phalloidin, the actin filaments of tDPSCs and nDPSCs were observed. In both cell groups, there was an identical pattern of parallel fibre orientation (Figure 4.11). This was mainly in the cytoplasmic areas of the visualised cells, transversing the nucleus of the spindle-like cells. Both cell groups appeared to assume spindle-like morphology as depicted by the optical phase contrast microphotograph image in Figure 4.11. Corroborating these findings were immunofluorescent staining of tDPSCs and nDPSCs for collagen-1. Once again, a heterogeneous morphology typified by the appearance of spindle-like shaped cells with extensive cellular processes was seen in tDPSCs and nDPSCs (Figure 4.13). This spindle-like phenotype is consistent with the normal growth morphology as observed in Chapter 2 (Section 2.2.4).

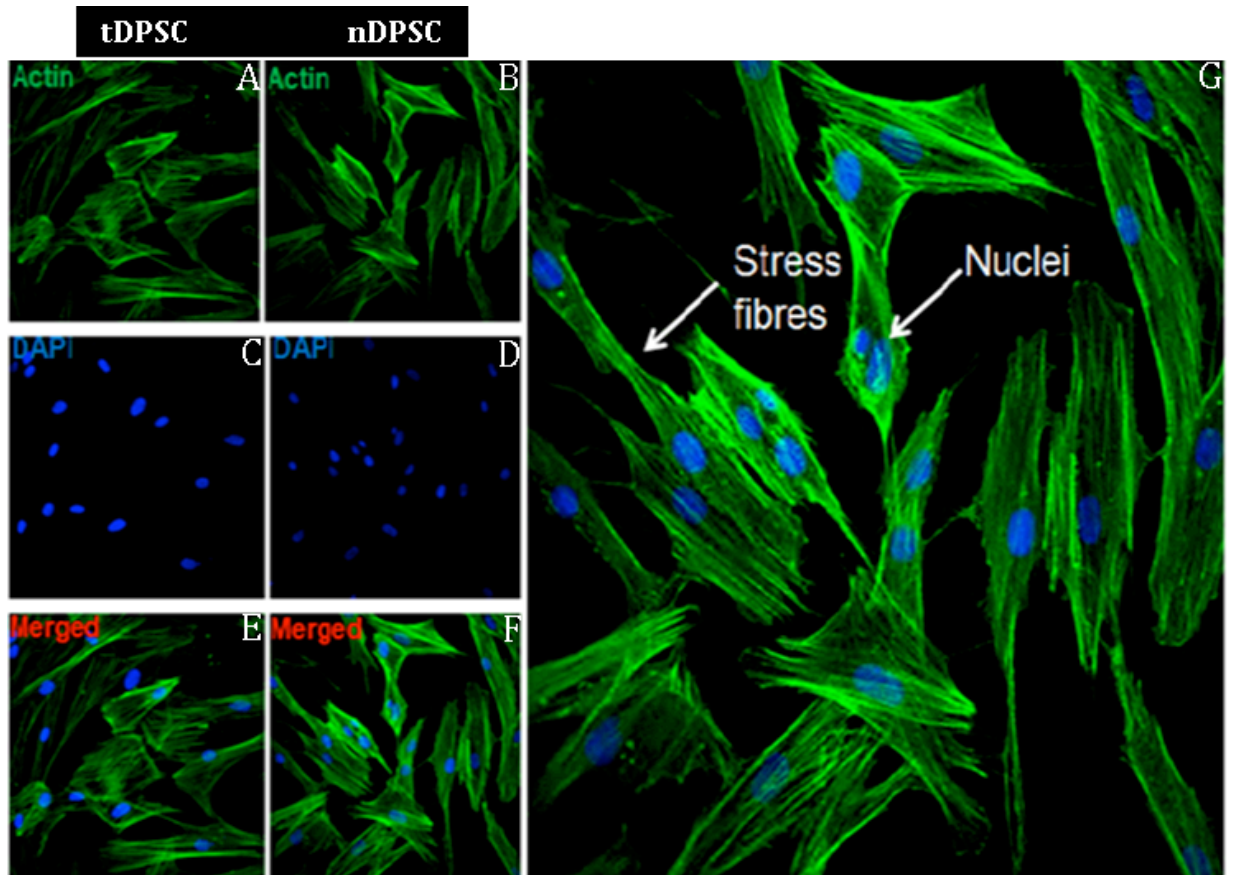


Figure 4:11. Optical phase contrast images showing the spindle-like structure of the tDPSCs and nDPSCs with centrally placed DAPI-positive nuclei under phase contrast microscopy (x400 microns).

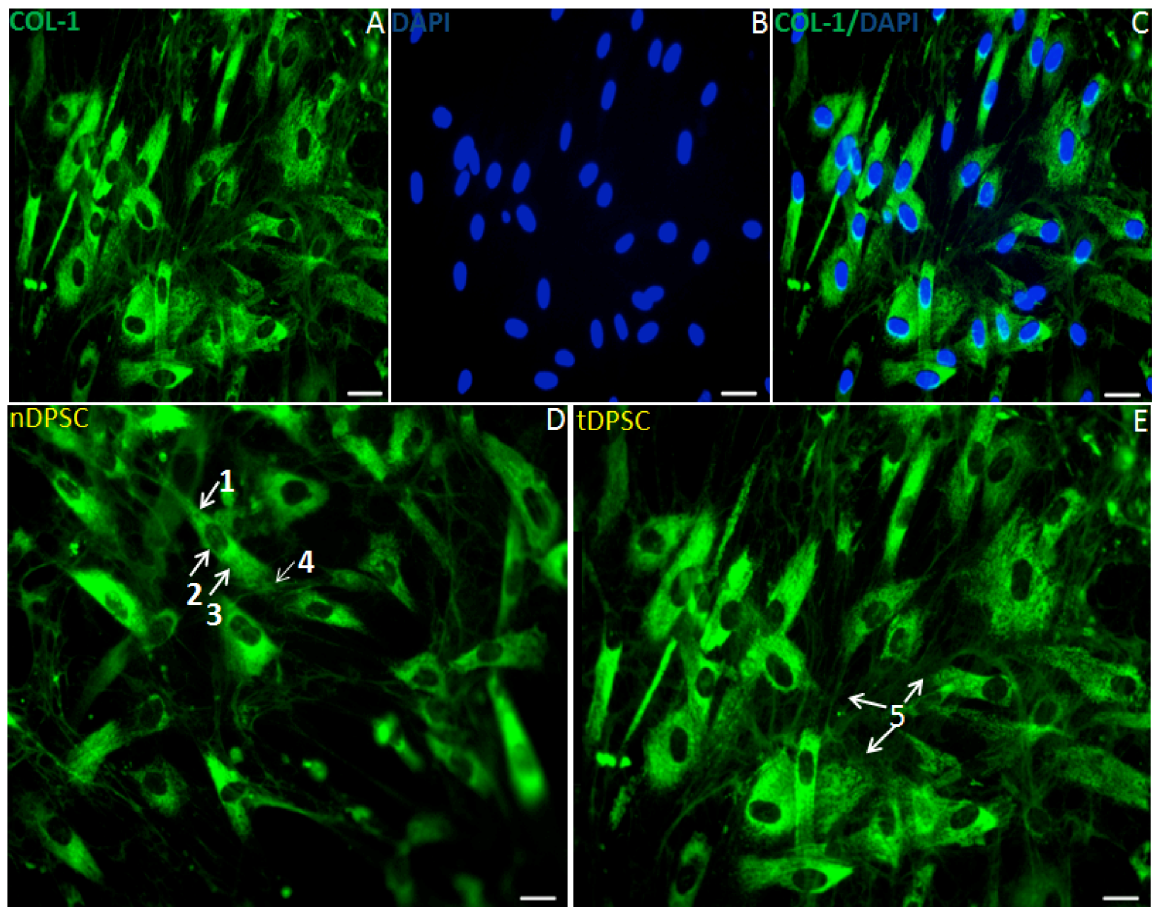


Figure 4:12 Collagen-1/DAPI staining of cultured nDPSCs and tDPSCs. The pattern of expression in both cell groups is almost identical. The heterogeneous spindle-shape morphology of both cell groups consists of: 1-Proximal pole, 2-Nuclear region 3-Sub nuclear area, 4-Intercellular process, and 5- High density of intercellular processes. (Scale bar = x400 microns).

#### 4.3.8 Stem cell markers

To characterize the effect of the transfection of the nDPSCs with hTERT, flow cytometric analysis was performed to at two time points: passage 6 (early) and passage 60 (late) and demonstrated the continued expression of stem cell surface markers associated with cells of a mesenchymal origin. The panel of surface markers investigated were CD13, CD44, CD73, CD90, CD146 and CD166. The experimental evidence obtained demonstrated a strong expression CD13, CD90, CD44 and CD73, which were maintained in both early and late passaged tDPSCs (Figures 4.13 – 4.18). The early tDPSCs were weakly positive for CD146 (11.21%) and this was markedly reduced in the late tDPSCs (1.85%) (Figure 4.18). Approximately 68.38% of the early

tDPSCs examined for CD166 expression were positive and this dropped to 23.72%, showing a reduced CD166 expression over 60 passages (Figure 4.19). The expression of these markers is summarised in the table below.

<b>Marker</b>	<b>Role</b>	<b>Early (%)</b>	<b>Late (%)</b>
<b>CD 13</b>	Mesenchymal marker	100	99.99
<b>CD 44</b>	Mesenchymal marker	94.80	91.90
<b>CD 73</b>	Mesenchymal marker	93.57	75.22
<b>CD 90</b>	Mesenchymal marker	99.69	98.24
<b>*CD 146</b>	Perivascular cell marker	11.21	1.85
<b>*CD 166</b>	Adhesion molecule	68.38	23.72

Table 4:2: Stem marker expression in tDPSCs over 60 passages. \* - CD markers tested as negative controls for the odontoblastic phenotype.

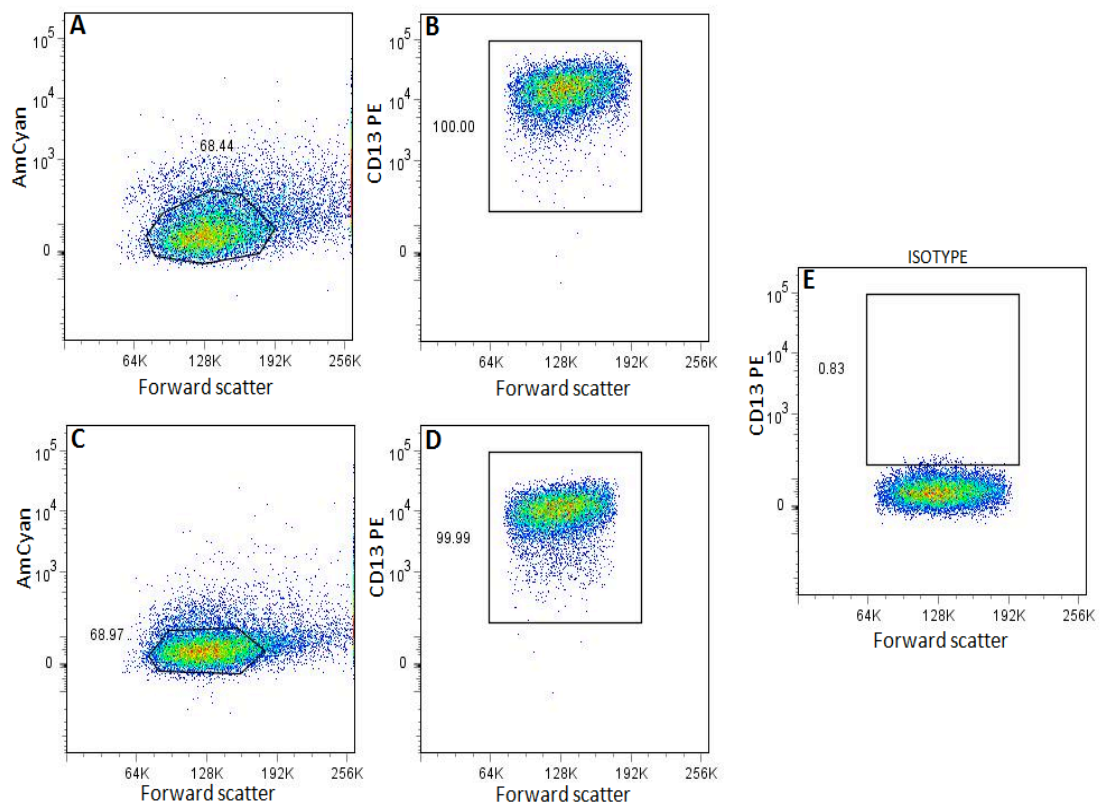


Figure 4:13: Isolation of CD13-positive tDPSCs by FACS. Forward scatter – AmCyan gate was applied on early passage (A, B) and late passage (C, D) tDPSCs to discriminate viable tDPSCs. A forward scatter-CD13 gate was applied on the viable tDPSCs to detect tDPSCs positive for this stem cell marker. Forward scatter – CD13 gate was applied on a commercial isotype control (E) to establish baseline criteria for selective gating. The number of events in (B) 100% and (D) 99.99% is representative of encircled area of cell staining seen in (A) 68.44% and (C) 68.97%.

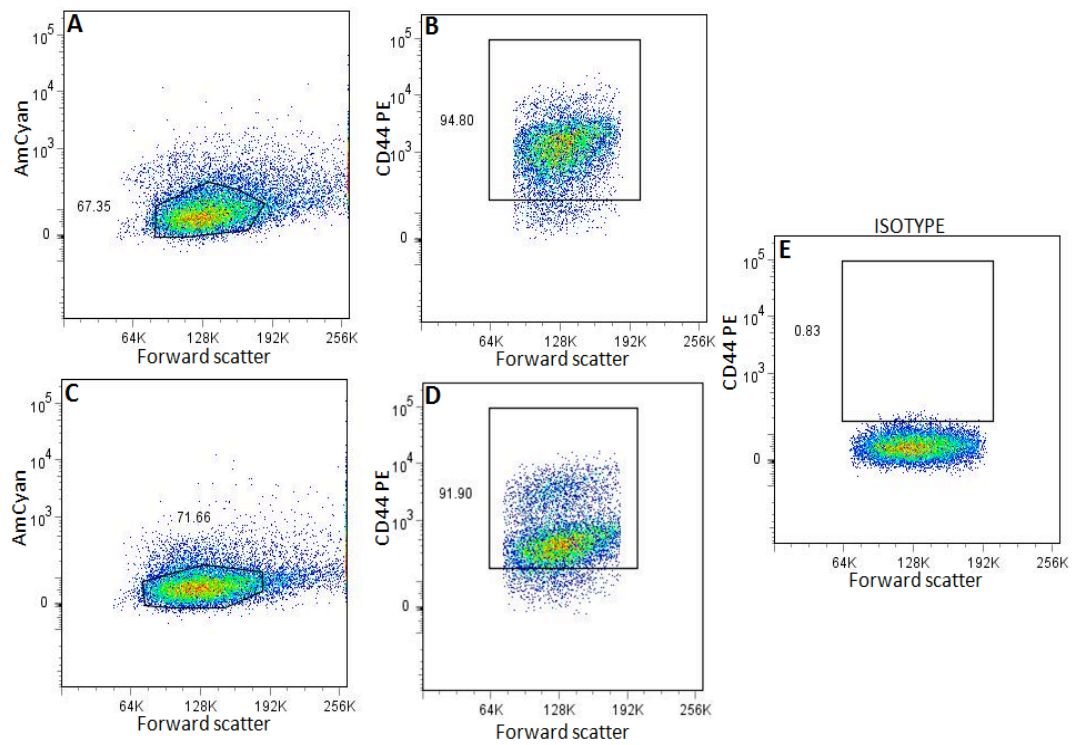


Figure 4:14: Isolation of CD44-positive tDPSCs by FACS. Forward scatter – AmCyan gate was applied on early passage (A, B) and late passage (C, D) tDPSCs to discriminate viable tDPSCs. Forward scatter-CD44 gate was applied on the viable tDPSCs to detect CD44-positive tDPSCs. Forward scatter – CD44 gate was applied on a commercial isotype control (E) to establish gating parameters used. The number of events in (B) 94.80% and (D) 91.90% is representative of encircled area of cell staining seen in (A) 67.35% and (C) 71.66%.

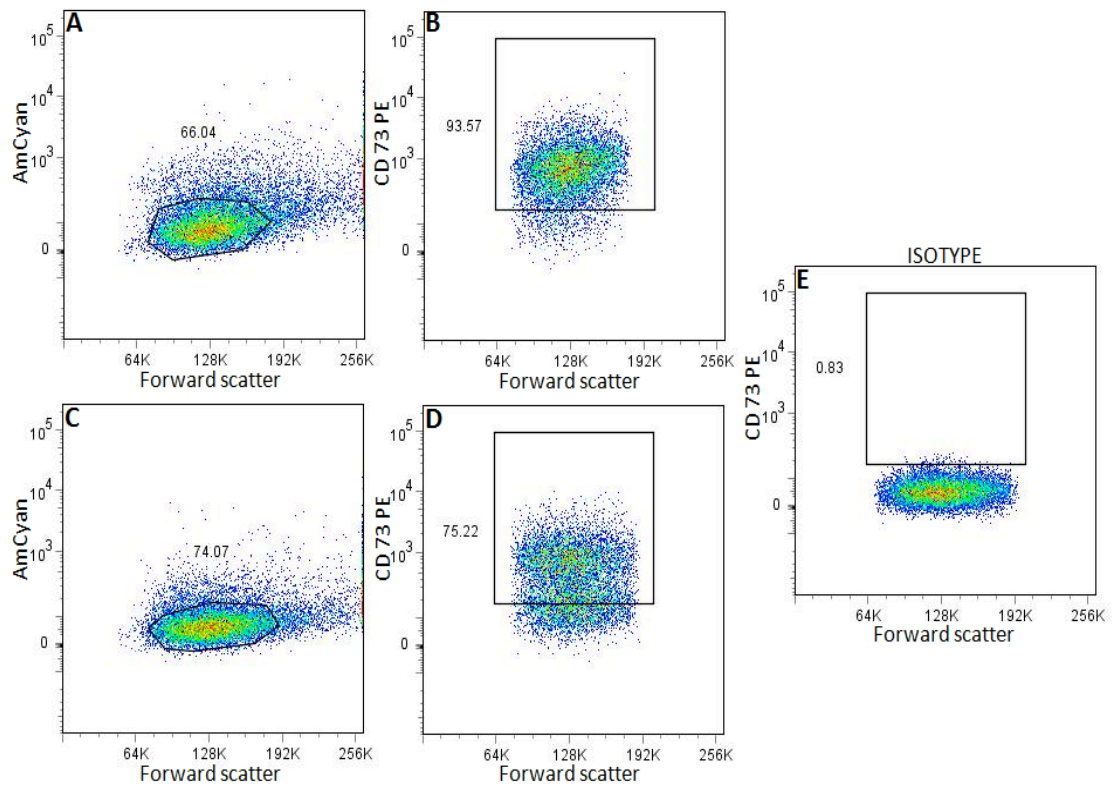


Figure 4:15: Isolation of CD73-positive tDPSCs by FACS. Forward scatter – AmCyan gate was applied on early passage (A, B) and late passage (C, D) tDPSCs to discriminate viable tDPSCs. Forward scatter-CD73 gate was applied on the viable tDPSCs to detect CD73-positive tDPSCs. Forward scatter – CD73 gate was applied on a commercial isotype control (E) to establish gating parameters used. The number of events in (B) 93.57% and (D) 75.22% is representative of encircled area of cell staining seen in (A) 66.04% and (C) 74.07%.



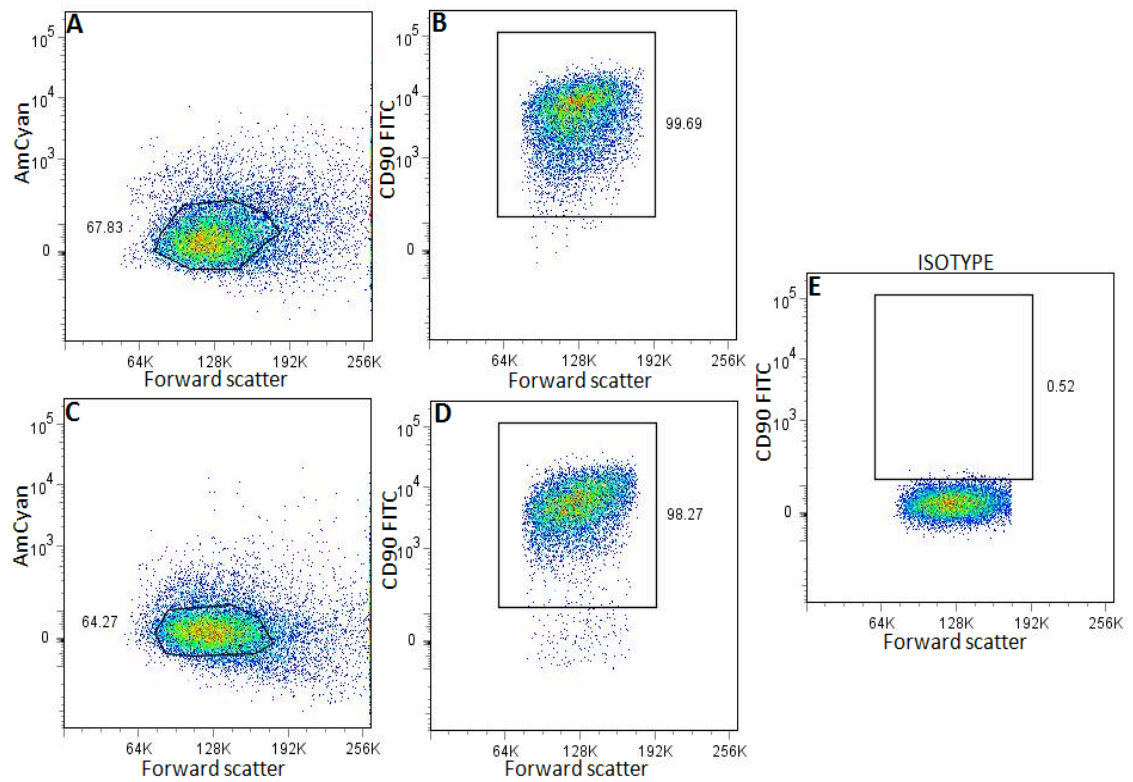


Figure 4:16: Isolation of CD90-positive tDPSCs by FACS. Forward scatter – AmCyan gate was applied on early passage (A, B) and late passage (C, D) tDPSCs to discriminate viable tDPSCs. Forward scatter-CD90 gate was applied on the viable tDPSCs to detect CD90-positive tDPSCs. Forward scatter – CD90 gate was applied on a commercial isotype control (E) to establish gating parameters used. The number of events in (B) 99.69% and (D) 98.27% is representative of encircled area of cell staining seen in (A) 67.83% and (C) 64.27%.

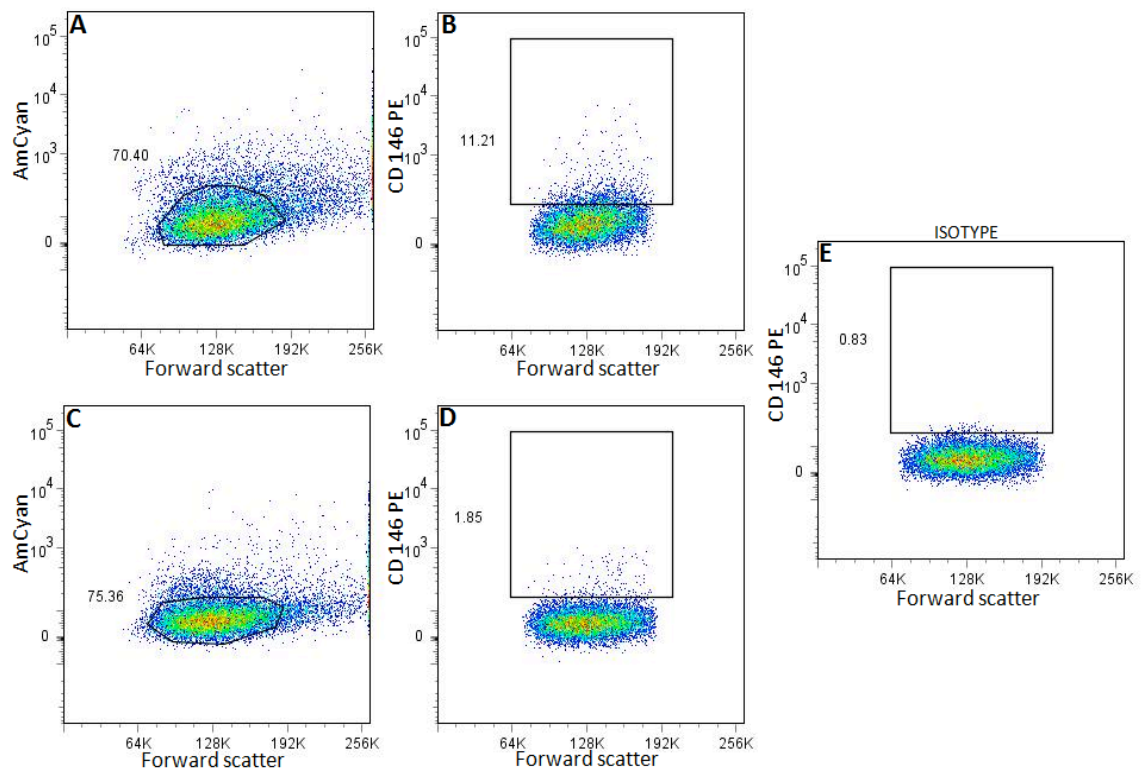


Figure 4:17: Isolation of CD146-positive tDPSCs by FACS. Forward scatter – AmCyan gate was applied on early passage (A, B) and late passage (C, D) tDPSCs to discriminate viable tDPSCs. Forward scatter-CD146 gate was applied on the viable tDPSCs to detect CD146-positive tDPSCs. Forward scatter – CD146 gate was applied on a commercial isotype control (E) to establish gating parameters used. The number of events in (B) 11.21% and (D) 1.85% is representative of encircled area of cell staining seen in (A) 70.40% and (C) 75.36%.

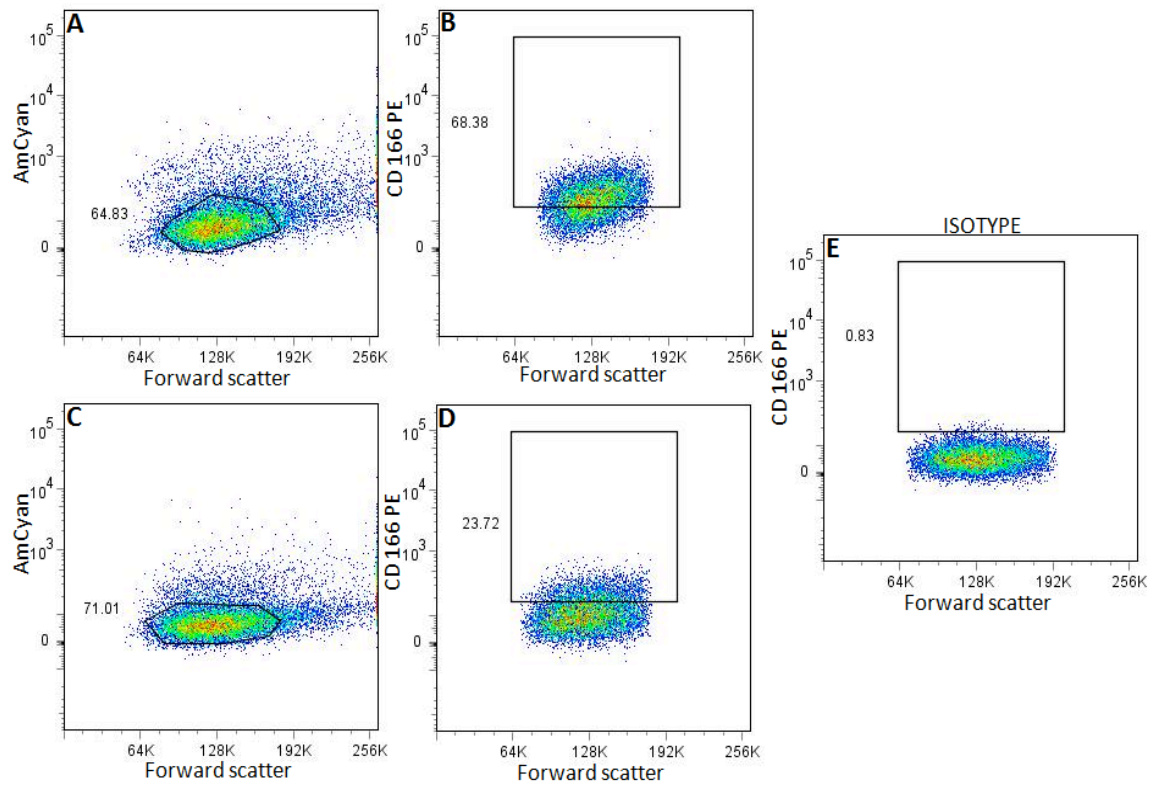


Figure 4:18: Isolation of CD166-positive tDPSCs by FACS. Forward scatter – AmCyan gate was applied on early passage (A, B) and late passage (C, D) tDPSCs to discriminate viable tDPSCs. Forward scatter-CD166 gate was applied on the viable tDPSCs to detect CD166-positive tDPSCs. Forward scatter – CD166 gate was applied on commercial isotype control (E) to establish gating parameters used. The number of events in (B) 68.38% and (D) 23.72% is representative of encircled area of cell staining seen in (A) 64.83% and (C) 71.01%.

### 4.3.9 Quantitative real time PCR results

#### 4.3.9.1 Standard curves for the designed primer sets

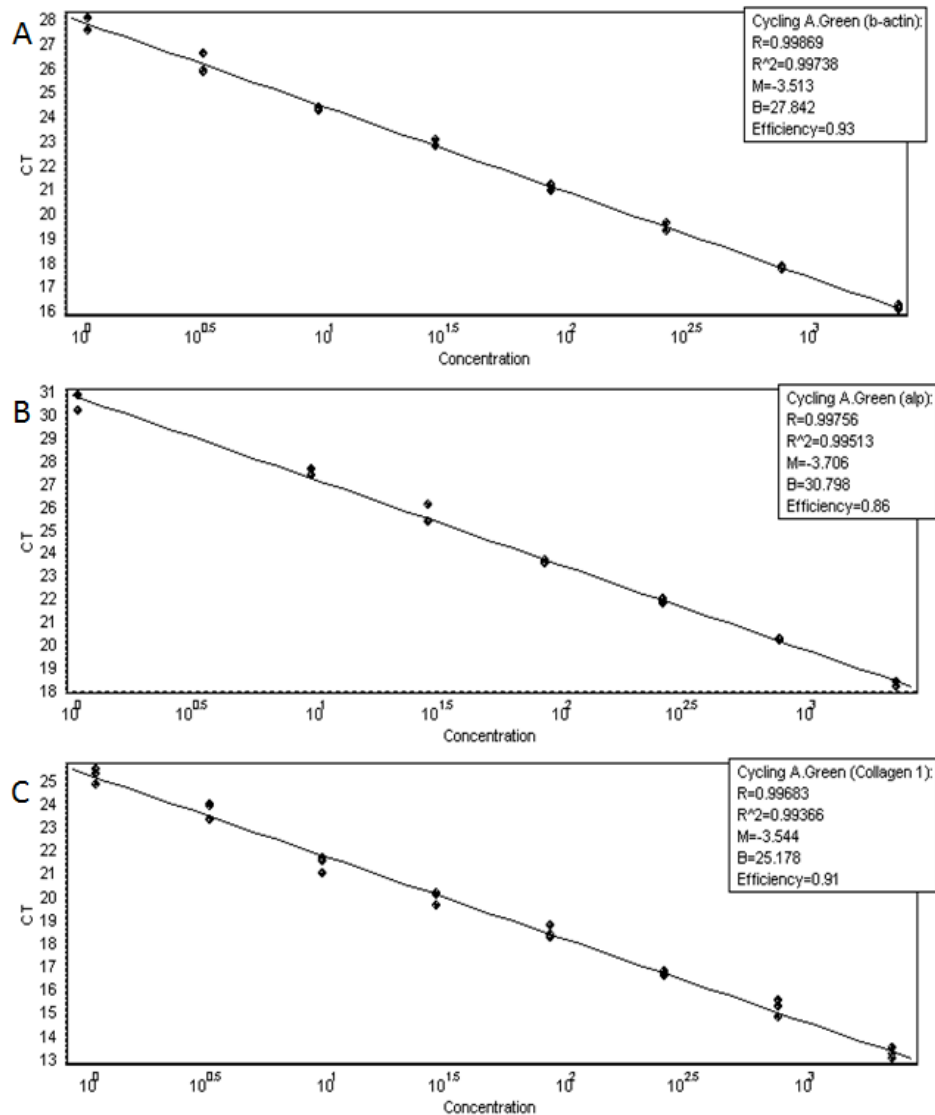


Figure 4: 19: Standard curve of the real time RT-PCR assays for B-actin (A), ALP (B), COL-1 (C). Ten-fold dilutions of plasmid DNA prior to amplification were used ranging from  $1 \times 10^0$  to  $1 \times 10^4$  copies (indicated on the y-axis) with the CT values represented on the x-axis. Sensitivity of the primers against the tDPSCs was tested in duplicates as demonstrated by the gel at the bottom left of Figure 4.21. The co-efficient of determination (R<sup>2</sup>) is indicated on the graphs. The CT values for the primers were: B-actin (27.842), ALP (30.798) and COL-1 (25.178).

The standard curves for  $\beta$ -actin, ALP, COL-1, DMP-1 and DSPP (odontogenic markers), and p16 and p53 (oncogenic markers) were generated using serially diluted

cDNA ranging from  $1 \times 10^0$  to  $1 \times 10^4$  copies. The standard curves generated were able to detect cDNA expression down to  $10^{3.5}$  copies (Figures 3.19 – 3.21) and demonstrated linear regressions ( $R^2$ ), which ranged between 0.988 - 0.996 (Figures 3.19 – 3.21). The cycle threshold values obtained in these experiments demonstrated strong ( $C_T \leq 27$ ) and moderate ( $C_T$  between 30 and 37) positive results, indicating the presence of the target nucleic acids.

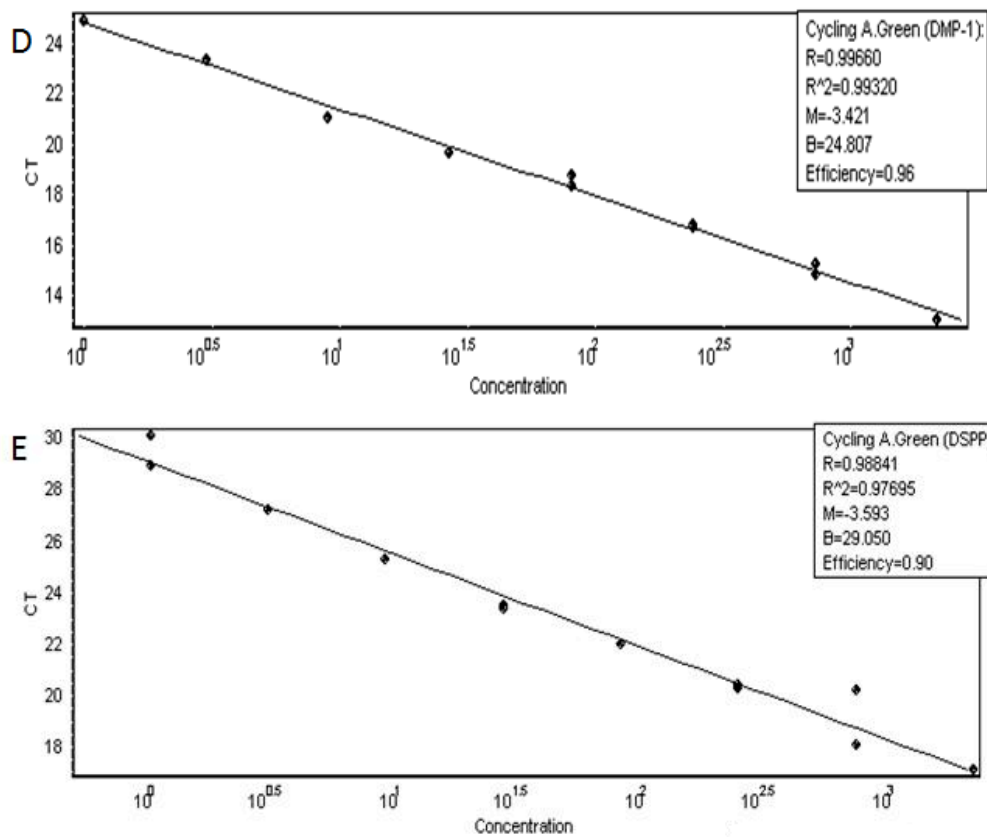


Figure 4:20: Standard curve of the real time RT-PCR assays for DMP-1 (D) and DSPP-1(E). Ten-fold dilutions of plasmid DNA prior to amplification were used ranging from  $1 \times 10^0$  to  $1 \times 10^4$  copies (indicated on the y-axis) with the CT values represented on the x-axis. Sensitivity of the primers against the tDPSCs was tested in duplicates as demonstrated by the gel at the bottom left of Figure 4.21. The co-efficient of determination ( $R^2$ ) is indicated on the graphs. The CT values for the primers were: DMP-1 (24.807) and DSPP (29.050).

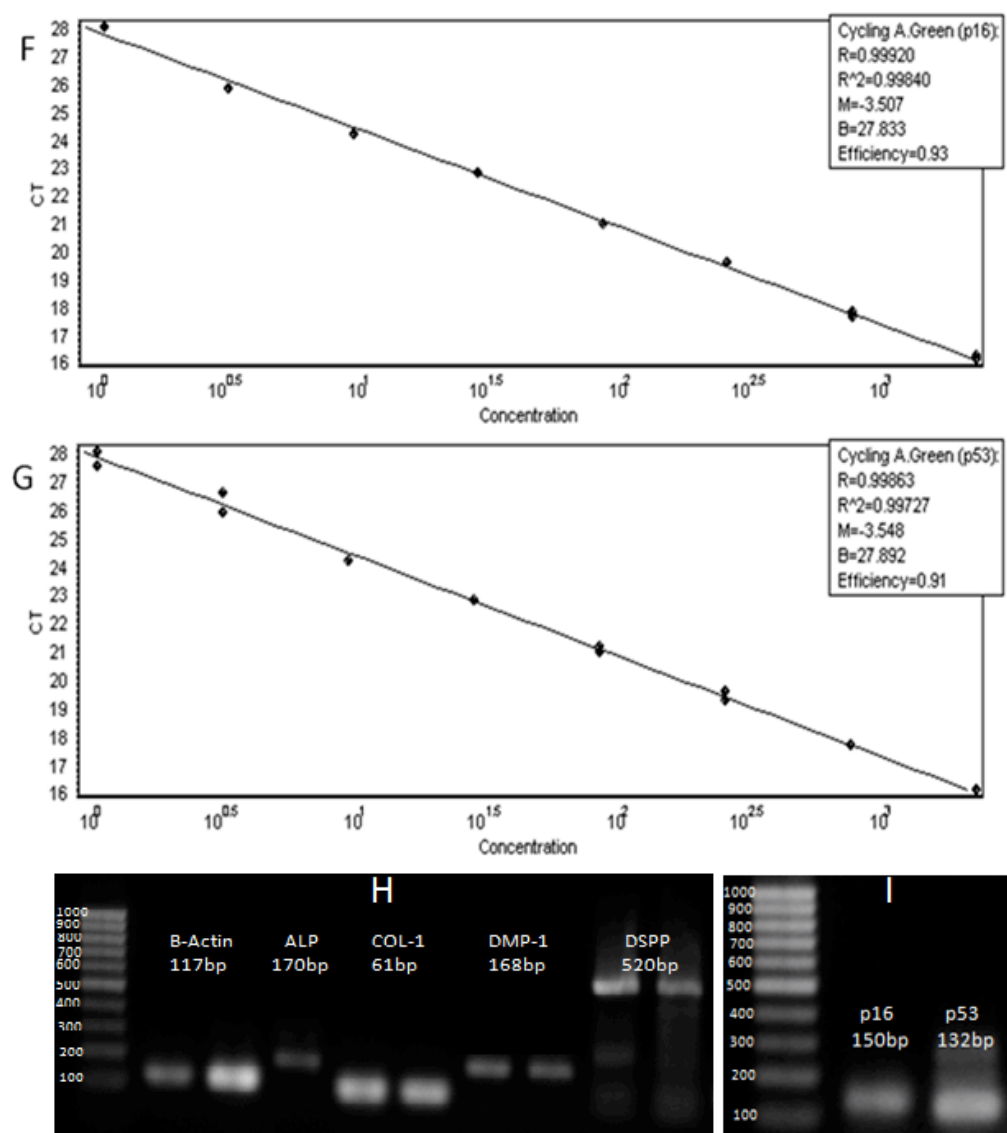


Figure 4:21: Standard curve of the real time RT-PCR assays for p16 (F) and p53 (G). Ten-fold dilutions of plasmid DNA prior to amplification were used ranging from  $1 \times 10^0$  to  $1 \times 10^4$  copies (indicated on the y-axis) with the CT values represented on the x-axis. Sensitivity of the primers against the tDPSCs was tested in duplicates as demonstrated by the gel (I) at the bottom right of the figure. The co-efficient of determination ( $R^2$ ) is indicated on the graphs. The CT values for the primers were: p16 (27.833) and p53 (27.892).

These values were in keeping with the optimization parameters outlined in the SybrGreen protocol (the ideal efficiencies of the reaction range from at least 90% to 105%, while the assay reproducibility should be approximately 0.998). To demonstrate the integrity of the primers used, at the end of the reaction the PCR products were retrieved and run on agarose gels. There was an expression of single bands in each

lane for the tested primers ( $\beta$ -actin, ALP, COL-1, DMP-1 DSPP, p16 and p53) (Figure 4.21H and 3.21I).

#### **4.3.10 Expression of odontoblastic and oncogenic markers**

The mRNA expression of odontoblastic markers ALP, COL-1, DMP-1 and DSPP was evaluated in populations of tDPSCs spanning 60 passages. The baselines used as measures of comparison for the levels of mRNA expression of these markers were those demonstrated by the nDPSCs at passage 5, which were run at the same time (Passage n5 in Figure 4.22A-E). ALP mRNA expression levels were significantly elevated at passages 40 and 50 in comparison to those of the passage n5 cells (Figure 4.22A). While the expression levels of COL-1 mRNA were higher than the demonstrated baseline levels, there were no statistical indications of significance at any of the measured time points (Figure 4.22B). The mRNA expression profiles of the odontoblast-specific markers, DMP-1 and DSPP showed a fairly similar pattern, demonstrating significant elevations at passages 40, 50 and 60 in comparison nDPSC expression at passage n5 (Figure 4.23C and D). Using the expression levels demonstrated by the nDPSC passage n5 cells as the baseline for a comparative analysis, the effect of the retroviral transduction on the expression of oncogenic markers, p16 and p53 was investigated in the tDPSCs.

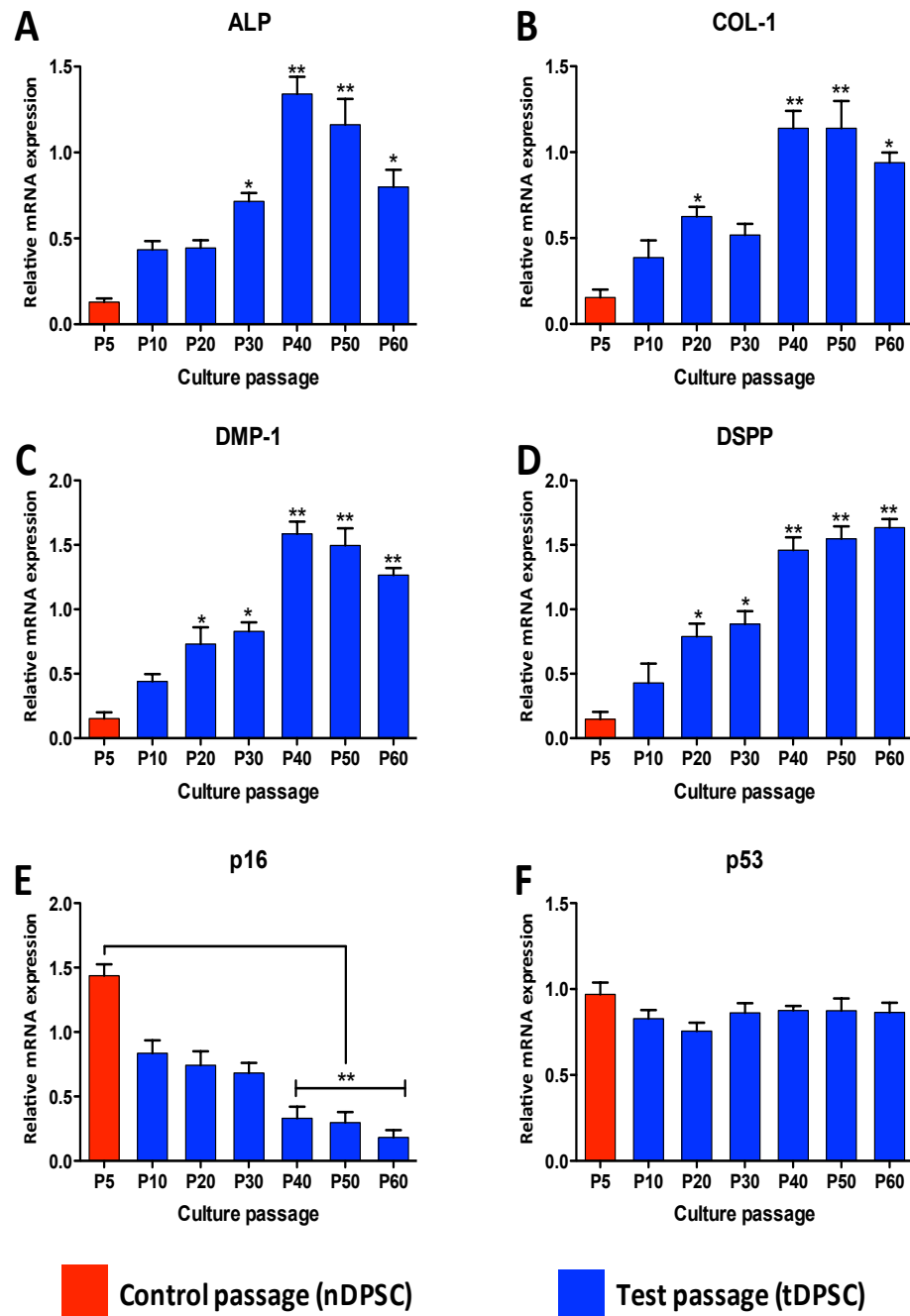


Figure 4:22 Expression of odontoblast mineralization markers ALP (A) and COL-1 (B), odontoblast differentiation markers DMP-1(C) and DSPP (D) and, oncogenic markers p16 (E) and p53 (F) in nDPSC (passage n5 and tDPSCs, passage 10 – 60) was determined by real-time qPCR. Values are reported as relative fold change in cDNA concentration, which were normalised to the housekeeping gene. The data are represented as the mean  $\pm$  S.E of triplicate experiments (technical replicates) with significance differences measured between the cell groups by one-way ANOVA and post hoc Bonferroni's test (\* $p < 0.05$ , \*\* $p < 0.01$ , \*\*\* $p < 0.001$ ).



The p16 expression showed a down-regulation starting passage 10 to significantly lower levels by passage 50 and 60 (Figure 4.22E). The p53 expression profile from passage 10 to passage 60 was quite different to this. The highest levels were observed in the passage n5 cells however; there were no significant changes in expression as noted with p16.

#### 4.4 Discussion

The objectives of these studies were aimed at evaluating the *in vitro* odontoblastic phenotype of the isolated DPCS, the influence of the glucose and serum concentrations in the growth media on the behaviour of the DPCs in culture and finally, the role of retroviral transfection in prolonging the life span of the DPCs to enable sustainability for future use.

The results suggest a loss of the multi-lineage capacity of the DPSCs following odontoblastic induction. There was no detection of the mRNA transcripts encoding adipogenic markers SOX9 and PPAR $\gamma$ , thus suggesting an absence of any adipogenic capabilities in the DPCs. There was no evidence to demonstrate the presence of the neuronal marker nestin; as opposed to the brighter bands detected for the other neuronal markers EN-2 and  $\beta$ 3T. The continued presence of mRNA transcripts for these neurogenic markers is in keeping with previous work on human DPCs, which continued to show a similar transcript profile in DPCs when cultured in non-neurogenic media (Davidson 1994; Gronthos, Brahim et al. 2002; Arthur, Rychkov et al. 2008). The theory proposed is that the continued expression of these neurogenic markers allows for the switch to a neurogenic profile in the presence of the appropriate inductive cues (Arthur, Rychkov et al. 2008). This is an interesting proposition when the expression of the transcription factors (Cbfa-1/RUNX-2) and embryonic stem cell marker (REX-1) are considered. The continued expression of Rex-1 as seen in this study is keeping with the possibility that this pluripotency associated gene maybe become involved in cell behaviour and function at a later date, as demonstrated in studies carried out on embryonic stem cells (Tamaoki, Takahashi et al. 2010). The agarose gels bands in this study also indicated the presence of mRNA transcripts encoding for both transcription factors. Animal studies have demonstrated that the transcription factor Runx2 /Cbfa-1, expressed as a member of the RUNX family (Durst and Hiebert 2004; Ito 2004), is an essential transcription factor for bone and tooth development (Ducy, Zhang et al. 1997; D'Souza, Aberg et al. 1999; Ducy and Karsenty 1999; Miyazaki, Kanatani et al. 2008; Wen, Tao et al. 2010). Gronthos and colleagues also showed that the differentiation of post-natal DPCS, allowing for the formation of reparative dentine, was under the control of Runx2 (Gronthos, Mankani et al. 2000). Following this,

Miyazaki et al suggested that Runx2 is required for the inhibition of the terminal differentiation of the odontoblasts in mice (Miyazaki, Kanatani et al. 2008). This suggests that the presence of Runx2 as seen in this study, allows for the continued proliferation of the odontoblast-induced differentiating DPSCs in culture. Studies carried out in mice have shown that isoforms of the Runx2/cbfa-1 transcripts are required as binding sites for the odontogenic specific marker DSPP (Chen, Gu et al. 2002), which is also strongly expressed in these cells (Chapter 3). This highlights the importance of these markers to *in vitro* odontoblastic differentiation and would support the proposition in this study that the DPSCs had assumed an odontoblastic phenotype. Work performed by Isenmann and colleagues on human mesenchymal stem cell populations, derived from bone, implied that the presence of Cbfa1 down-regulated the expression of telomerase, thus allowing for the terminal osteogenic differentiation of the stem cells (Isenmann, Cakouros et al. 2007). In this study a similar scenario is suggested, as the DPSCs continue to express early (ALP) and late markers (DMP-1 and DSPP) associated with the formation of the extra-cellular dentine matrix – they demonstrated typical features of terminally differentiated odontoblasts – following the introduction of hTERT (Linde 1989; Linde and Goldberg 1993; Narayanan, Srinivas et al. 2001). The expression of mRNA transcripts for Rex-1, an embryonic stem cell marker demonstrates the pluripotential nature of the DPSCs (i.e. the “stem cells of neural crest origin” feature is not entirely lost) (d'Aquino, Tirino et al. 2011). These findings all confirm that the isolated DPSCs possess an odontoblastic phenotype and that the presence of the tested non-odontoblastic phenotypic markers, alludes to a nascent ability of sub populations within the isolated cells, to differentiate along those pathways in the presence of the appropriate inductive cues.

The induction of the lineage specific differentiation of stem cells is dependent on the presence of growth promoting cues that would stimulate the cells to do so in favourable conditions (Mischen, Follmar et al. 2008). Mischen and colleagues suggested that stem cell proliferation was directly influenced by the metabolic culture conditions as their work demonstrated the differentiation of human adipose –derived stem cells into cells of an osteogenic profile with a reduction in glucose concentrations in the media formulations (Mischen, Follmar et al. 2008). This supports the premise

that the proliferation and maturation of a cell line is dependent on the presence of adequate amounts of energy (Deorosan and Nauman 2011). In our study, the effects of variations in the glucose and serum content of media formulations in a two – dimensional culture system, on DPSC proliferation and metabolism was investigated. Variations in the concentrations of glucose and serum in growth media have been shown to have an effect on the proliferation of stem cells in culture (Follmar, Decroos et al. 2006; Deorosan and Nauman 2011), with both groups showing results which demonstrated greater increases in the metabolic activity of the cells (as evidenced by increased lactate production), following increases in glucose concentration of the culture media. This would suggest that the glucose content plays more of a role in determining the metabolic state of the cells.

Our findings in this study showed a significant increase in the proliferative activity of the DPSCs cultured in high glucose-containing media (as evidenced by total DNA) when compared to the low glucose-containing media. These findings were supported by the results of the population doubling studies, which indicated that the high glucose formulations provided a better growth media option for DPSC cultures. The serum concentration chosen based on the results was 10% as the cell numbers indicated a greater effect than the 5% serum concentration. There were no noted differences, however, between the effects of 10% and 20% serum concentrations within the low and high glucose media experimental groups. A 10% serum concentration was chosen for the further experimental work performed in this study. These results provide the basis for the establishment of a model for further studies to be carried out, to investigate the metabolic preferences (aerobic or anaerobic) of the DPSCs in culture and possible effects on the maintenance of the odontoblastic phenotype. However, it has been proposed that physiologically the use of a high glucose content media can cause an overproduction of oxygen radicals thus contributing to genetic damage and senescence of the cell line(Deorosan and Nauman 2011). This informed the decision to carry out senescence studies.

The immortalization of human dental cells has been previously described and studies have demonstrated that transfected cells are able to avoid the normal senescence program and hence extend the life span of the cells (Counter, Hahn et al.

1998). A literature review demonstrated that several authors have successfully transformed and immortalized these cells, having obtained them from a variety of oral sources. Kamata and colleagues in 2004 carried out a series of transformation studies using cells from human dental papilla, dental pulp, periodontal ligament and gingival fibroblasts (Kamata, Fujimoto et al. 2004). In 2007, Kitagawa and co-workers also successfully immortalized dental pulp cells (Kitagawa, Ueda et al. 2007). In 2005 Fujita and colleagues immortalized periodontal ligament cells (Fujita, Otsuka-Tanaka et al. 2005).

In this study we used the HIV retroviral packaging system to explore the possibility of establishing an immortalised hDPSC cell line, which would circumvent normal programmed senescence and maintain its usefulness as a tool for further study of cellular activity. The detection of hTERT expression at mRNA levels following induction in a variety of cell lines has been widely reported (Kamata, Fujimoto et al. 2004; Kang, Kameta et al. 2004; Kitagawa, Ueda et al. 2007). The presence of hTERT mRNA was successfully demonstrated in this study following transfection of the tDPSCs with the hTERT gene. Also, the telomerase activity in tDPSCs was 30 - 60 times greater than in nDPSCs (Figure 4.8). Also demonstrated was perpetual cell growth over 60 passages, whilst maintaining characteristics of differentiation and phenotypic cellular identity, in line with literature-defined parameters for a successful immortalization of dental pulp stem cells (continued cell proliferation and mineralization). There was evidence to support continued odontoblastic differentiation, as demonstrated by the relative mRNA expression levels for DMP-1 and DSPP (Figure 4.23). This corroborates the typical features of odontoblasts in culture (Gronthos, Mankani et al. 2000; Gronthos, Brahim et al. 2002; Kitagawa, Ueda et al. 2007; Karaöz, Doğan et al. 2010). The genetic expression of ALP and COL-1 (Gronthos, Mankani et al. 2000; Gronthos, Brahim et al. 2002), in addition to the mineralization activities of the tDPSCs demonstrated by data from the ALP assays further supported a lack of change in cellular characteristics, as demonstrated by the morphology and cytoskeletal organisation of the cell (see Figure 4.22). In addition, the non-transduced DPSCs (nDPSCs), demonstrated a very high degree of  $\beta$ -galactosidase associated senescence activity (Figure 4.9a and 3.9b), a feature absent from a vast majority of the transduced

DPSCs (tDPSCs), even at a late passage, owing to the introduction of hTERT into these cells.

To further support the DPSC phenotype investigations we examined the expression of cell surface markers. The results demonstrated the maintenance (across 50 passages) of the mesenchymal specific markers CD13, 44, 73 and 90, similar to stem-like DPSC surface marker profiles described by other groups (Gronthos, Mankani et al. 2000; Gronthos, Brahim et al. 2002; Jo, Lee et al. 2007; Karaöz, Doğan et al. 2010). While the expression of CD146 and CD166 has been demonstrated by another group over 10 passages (Karaöz, Doğan et al. 2010), the investigation of expression over a much longer period of time (50 passages) in this study revealed a reduced expression of these two surface markers. CD166 has been described as being present in undifferentiated mesenchymal cell populations with a loss of expression occurring with the assumption of a more defined phenotypic identity by the cells in culture (Arai, Ohneda et al. 2002); a situation clearly mirrored in this study.

With the prolongation of the life span of the DPSCs, the possible effects of transfection on the silencing of senescence-associated factors (oncoproteins) were also considered. hTERT has long been associated with oncoproteins such as p16 and p53 owing to the link between these proteins and telomerase activity (Beausejour, Krtolica et al. 2003; Liu, Dakic et al. 2008; Haferkamp, Tran et al. 2009; Tao, Lv et al. 2009). In this study, using real time quantitative PCR techniques, a link between the introduction of exogenous hTERT and mRNA expression of p16 was examined. The presence of p16 has been attributed to unfavourable culture conditions (Wright and Shay 2000). Also noteworthy is its inverse relationship with the aging and proliferation of some cell types (Chimenti, Kajstura et al. 2003; Torella, Rota et al. 2004). It is uncertain if the alteration of the pathways controlled by any of the oncoproteins examined is solely dependent on the functional presence of hTERT (Kiyono, Foster et al. 1998). The collective opinion of some research groups is that this “down-regulation” of p16 activity may be promoted by the arresting of senescence of DPSCs owing to the introduction of exogenous hTERT which promotes p53 activity in certain human cell types (Kiyono, Foster et al. 1998; Dickson, Hahn et al. 2000; Migliaccio, Amacker et al. 2000; de Jonge, Woolthuis et al. 2009; Tao, Lv et al. 2009).

This would suggest that the molecular mechanisms that control the senescence of the DPSCs are dependent on possible interactions between p16, p53 and telomerase (Lars-Gunnar 2011). The induction of senescence in human tissue derived cell lines has been described as being able to occur through a number of mechanisms. Studies on human keratinocytes have demonstrated that the expression of hTERT is linked to the resistance to p16-induced senescence (Dickson, Hahn et al. 2000). Following this, there have been indications to suggest that these keratinocytes did undergo senescence following an increase in p53 expression that was dependent on the presence of hTERT (Rheinwald, Hahn et al. 2002). This shared control of cellular senescence between p16 and p53 has also been shown in human mammary epithelial cells (Kiyono, Foster et al. 1998). Bhatia and colleagues immortalized human prostate cells using hTERT and transduced the cells with retroviral vectors encoding a p16 short hairpin RNA (to silence p16 gene expression). They demonstrated an increase in lifespan of the cells in culture and at the point of senescence (passage 39) observed that there was no expression of p16, and very high levels of p53 (Bhatia, Jiang et al. 2008).

It is my opinion that while telomere erosion during cell replication may trigger p53-senescence functions, p16 may be the determinant of continued DPSC proliferation in culture. The expression of p16 dropped significantly by passage 60 of the tDPSC cultures while p53 remained virtually unchanged for the time points of the study (Figure 4.24). There was no demonstrated loss of telomerase activity in the transformed cells (as the transfection caused an increase) (Figure 4.6 – 4.9) thus suggesting the telomeres remained intact. A recent study in mouse odontoblast-like cells has indicated that the senescence seen in these cells is reversibly associated with increases in p16 expression following the loss of the chromatin remodelling protein, Bmi-1 (Mehrazarin, Oh et al. 2011), one of many transcription factors that regulates p16 function (Park, Morrison et al. 2004; Kim and Sharpless 2006). It is possible that the presence of ectopic hTERT in the DPSC cultures described in this thesis, may have induced a change to the transcriptional regulation of p16 allowing for the development of an ability to maintain phenotypic characteristics of odontoblasts and circumvent senescence. (This is a theory that will be subject to further experimental validation).

The summation of this section of experimental work is that we have developed an immortalised human dental pulp stem cell line with odontoblastic lineage differentiation that can be used for studying the metabolism and differentiation of odontoblasts.



# Transient receptor channel expression and function in odontoblasts

---

5

## Transient receptor channel expression and function in odontoblasts

### 5.1 Introduction

Transient receptor potential (TRP) ion channels had been already described as “direct” mediators of mechanical and thermal nociception in other human cell types such as ear hair cells (Corey, Garcia-Anoveros et al. 2004), and in bladder mucosal cells (Miyamoto, Mochizuki et al. 2009). One of the primary objectives of this project was to analyse the gene expression for these sensory channels in the derivatives of human pulp cells (odontoblasts).

By way of animal studies, some of these TRP channels (TRPV1, TRPA1 and TRPM8) have already been shown to be expressed in dental primary afferent neurones suggesting a possible role in the sensation of noxious thermal stimulation in dental tissues (Park, Kim et al. 2006). This group of thermosensitive cation channels (TRPV1, TRPA1 and TRPM8) were also described as transducers of dental pain as they were expressed in trigeminal nerve fibres and were suggested to be *directly* activated by the stimuli that produced tooth pain (Renton, Yiangou et al. 2003; Zanutto, Merrill et al. 2007). This would suggest that direct thermal transduction is involved in dental pain sensation and thus completely contradict the hydrodynamic theory in which all painful stimuli are perceived as a result of changes in hydraulic pressures in the dentinal tubules. In 2010 and 2011, the molecular and functional expression of these thermosensitive TRP channels in cultured fibroblasts and odontoblast-like cells derived from human pulpal tissue was analysed by El Karim and colleagues (El Karim, Linden et al. 2010; El Karim, Linden et al. 2011), demonstrating increases in transient calcium movements through these TRP channels that could be blocked by TRP channel-specific antagonists. Information available in the literature regarding the expression of mechanosensitive TRP channels in the human dental pulp such as TRPV4 is unfortunately rather thin. Early in 2011, a group in Spain used immunohistochemical techniques to demonstrate TRPV4 expression in human odontoblasts (Solé-Magdalena, Revuelta et al. 2011). Prior to this TRPV4 expression had only been demonstrated in the trigeminal neurons of mice and cultured rat odontoblasts (Liedtke and Friedman

2003; Son, Yang et al. 2009). The findings of Solé-Magdalena and colleagues support the hypothesis proposed in this thesis, which suggests that the molecular expression of TRPV4 in human tooth pulp tissues is a plausible experimental objective and can be demonstrated in cultured human odontoblasts derived from these tissues. While the findings of Solé-Magdalena et al demonstrating TRPV4-positive odontoblast expression came to light during the course of this study, the investigations performed in this thesis have built on this. The work has analysed the function of TRPV4 transcripts, alongside the molecular expression of these proteins in the cultured human odontoblast cells, and now shows evidence of functional TRPV4 channels in human odontoblasts.

Following the supposition among some researchers that there is some degree of overlap in the functions of different classes of the TRP channels as the thermosensitive TRPA1 also respond to mechanical stimulation (Muraki, Iwata et al. 2003; Barritt and Rychkov 2005), the responses of TRPV1, TRPA1 and TRPM8 receptors to chemical stimulation in both human pulp tissues and cultured odontoblasts was also considered in our studies. We first began by studying the gene expression of TRPA1, TRPM8, TRPV1 and TRPV4 channels in the cultured odontoblasts using PCR and qPCR techniques. Using appropriate TRP channel agonists, the cultured odontoblast cell responses were investigated by means of ratiometric  $Ca^{2+}$  imaging with the highly sensitive dye Fura-2. Following up on the indirect concept of nociceptive transduction by the odontoblasts introduced in Chapter 1 (Section 1.6.2), we also performed ATP release experiments following exposure of the cultured tDPSCs to TRP channel agonists and antagonists.

In Chapter 1, the role of the neuropeptide substance P (SP) in the pulpal inflammatory process post-injury was discussed. Pain arising from tooth damage (secondary to caries, hypersensitivity, drilling or orthodontic movements) has been demonstrated to be associated with an increase in the expression of SP (Awawdeh, Lundy et al. 2002; Caviedes-Bucheli, Gutierrez-Guerra et al. 2007; Caviedes-Bucheli, Azuero-Holguin et al. 2011; Caviedes-Bucheli, Moreno et al. 2011). Work by Kido and colleagues demonstrated the presence of NK1R and NK2R in rat odontoblasts with the former having a higher affinity for SP and being expressed to a higher degree in the odontoblast cell processes (Kido, Ibuki et al. 2005). In human pulpal tissue, the

expression of both NK1R and NK2R has been demonstrated, however, there is no direct evidence of the more specific of the two receptors for SP (Caviedes-Bucheli, Gutierrez-Guerra et al. 2007). The presence of these receptors in the pulp allows for the pro-inflammatory activities of SP (Section 1.6.2) leading to a self-perpetuating cycle of increased SP release and resultant inflammation. An added effect of SP release is the increase in cell proliferation, which has been shown (in adult rat osteoblasts and rat neural progenitor cells) to be dependent on the presence of NK1R (Goto, Nakao et al. 2007; Park, Yan et al. 2007). Prior to these findings, direct links between its ability to mobilize calcium and promote cell proliferation were demonstrated in studies on rat myocardial fibroblasts (Kumaran and Shivakumar 2002). An interesting point, however, is that some animal studies have suggested the co-localization of the TRP channels (TRPA1, TRPV1 and TRPM8) with the SP receptors (NK1R) in neurons from murine dorsal root ganglions (Tominaga, Caterina et al. 1998; Amaya, Oh-Hashi et al. 2003; Bae, Oh et al. 2004; Bautista, Siemens et al. 2007; Zhang, Cang et al. 2007). An increase in TRPV1 activity following the application of exogenous SP has been demonstrated in rat DRG neurones, which was inhibited by the introduction of an inhibitor for the epsilon isoform of protein kinase C (PKC $\epsilon$ ) (Zhang, Cang et al. 2007). It is possible that TRPV1 activity might be modulated by the phosphorylation activities of PKC (Cesare and McNaughton 1996; Cesare, Dekker et al. 1999; Premkumar and Ahern 2000), as is interestingly the case with the activity of NK1R (Khawaja and Rogers 1996), which as we pointed out earlier, the literature suggests is co-localised with TRP channels (TRPV1). While there is also evidence to suggest the PKC-associated desensitization of TRPM8 (Abe, Hosokawa et al. 2006) and PKC-associated sensitization of TRPV4 (Grant, Cottrell et al. 2007) activity, there is no evidence in the current literature suggestive of PKC-modulated activity of TRPA1 (Roufogalis, Armati et al. 2011).

In Chapter 1, a connection between SP and increased calcium in odontoblast cells was described. SP stimulates the formation of inositol triphosphate, a product of hydrolysis of phosphatidylinositol 4,5-bisphosphate (into diacylglycerol and inositol triphosphate) which functions as a second messenger in the mobilization of intracellular calcium (Berridge and Irvine 1984). By means of interactions with G and q proteins, the tachykinin receptors NK1R and NK2R activate the phosphatidylinositol 4,5-bisphosphate hydrolysis pathway (Khawaja and Rogers 1996). The ability of SP to

increase cation conductance through animal cell membranes has been demonstrated in rat dorsal root ganglia (Weinreich, Moore et al. 1997). In another study using guinea pigs, Moore and colleagues demonstrated increased inward currents across ganglion neuronal membranes and elevated intracellular calcium levels, following the application of SP (Moore, Taylor et al. 1999). In studies on human embryonic kidney cells transfected with another class of TRP channels, the human TRPC3 channels, exposure to SP was shown to lead to increases in calcium transients (Oh, Gover et al. 2003). In 2010, Naono-Nakayama and colleagues undertook behavioural studies in rats and demonstrated modulated scratching responses in these animals after the intrathecal administration of agonists for TRPA1 (enhanced), TRPM8 (suppressed) and TRPV1 (enhanced) following pre-exposure to SP (Naono-Nakayama, Sunakawa et al. 2010). This suggests that TRP channel activity in human odontoblasts might be modulated by the release of SP. It was in this context that the relationship between SP and tDPSC proliferation, and TRPA1, TRPM8, TRPV1 and TRPV4 expression in cultured human odontoblasts was investigated in this thesis, following the molecular and functional analysis of the expression of these TRP channels. Gene expression for the tachykinin receptors NK1R and NK2R (and TRP channels) in the tDPSCs was evaluated using qPCR techniques. The presence of mRNA transcripts for the tachykinin receptors in the odontoblasts would suggest that SP could modulate their activity.

## Materials and methods

All reagents, including cell culture media were purchased from Sigma-Aldrich® unless otherwise noted. The cells used in the culture work were resuscitated from previously cryopreserved stocks (see Section 2.13).

### 5.2.1 (A) Detection of TRP channels in human whole pulp samples

Whole pulp tissues were extirpated from the extracted human teeth (n = 4) and placed in flat-bottomed falcon tubes containing 400 $\mu$ l of Trizol solution. Using a tissue homogenizer, the pooled pulp tissues were broken down vigorously, leaving a homogenate with an even consistency. RNA was then extracted and quantified as described in Chapter 2 (Section 2.1.10, 2.1.11). Using 1 $\mu$ g of the purified (pooled) RNA, cDNA was synthesized and primer sequences were designed to test for the expression of mRNA representative of the TRP channels (A1, M8, V1 and V4) and odontoblast marker DSPP. GAPDH was run as the housekeeping gene to normalise this experiment. The list of primer sequences (including sizes in base pairs) used in the PCR analysis is provided in Table 2-1 (See Section 2.9).

### 5.2.1 (B) Identification of TRP channels and neuropeptide receptors in nDPSCs and tDPSCs

The nDPSCs were resuscitated and cultured for 1 passage and the total RNA was extracted and quantified as described in Chapter 2 (Section 2.1.10, 2.1.11). Using 1 $\mu$ g of the purified RNA, cDNA was synthesized and primer sequences were designed to test for the expression of mRNA representative of the TRP channels (A1, M8, V1 and V4) and substance P (SP) receptors, neurokinin-1 and neurokinin-2. The list of primer sequences (including sizes in base pairs) used in the PCR analysis is provided in Table 2-1 (See Section 2.9). mRNA from Chinese hamster ovary (CHO) cells transfected with mTRPM8 was used as an external control in the identification of TRPM8 and was a kind gift from Jack Bircher, Wolfson Centre for Age-Related Diseases, King's College London. Glyceraldehyde 3-phosphate dehydrogenase (GAPDH) was the housekeeping gene used to normalise this series of experiments.

### 5.2.2 Investigation of long-term TRP channel expression

This series of experiments was performed to investigate the maintenance of the TRP channel expression profile after transfection with the hTERT gene. The transformed DPSCs (tDPSCs) were seeded at concentrations of  $1 \times 10^6$  cells/ml (in  $75\text{cm}^3$  culture flasks) and harvested every 10 passages between two time points: passage 10 (early tDPSCs) and passage 60 (late tDPSCs). The RT-qPCR methodology used in these experiments has been described in section 2.12. The list of primer sequences (including sizes in base pairs) used in the qPCR analysis is provided in Table 2-2 (See Section 2.13).  $\beta$ -actin was used as a reference gene to normalise RNA expression and analysed using the Rotor-Gene 6000 Series Software (version 1.7.87) and GraphPad Prism<sup>®</sup>. The reference values used in these experiments were mRNA levels in whole pulp lysates (WPL).

Experiments to determine the effects of the exogenous application of SP on TRP channel expression were performed simultaneously. Resuscitated tDPSCs (Passage 9) were divided into three experimental groups (A – C) and the culture media in each group was supplemented with the addition of substance P (SP) as described in Section 5.2.3. Following this, first strand DNA synthesis was performed on isolated RNA samples from these tDPSC cell cultures at Passage 12 and the cDNA obtained ( $25\mu\text{l}$ ) was used to carry out real-time qPCR reactions for TRPA1, TRPV1 and TRPV4. The previously described experimental conditions and methods of data analysis were also followed. The forward and reverse primers used are shown in Table 2-2. The reference values used in these experiments were mRNA levels in tDPSCs (Passage 12) without SP ( $\text{P12}^{\text{-SP}}$ ).

### 5.2.3 Measurement of intracellular $[\text{Ca}^{2+}]_i$ in cultured odontoblasts

Cultured tDPSCs were used for the  $\text{Ca}^{2+}$  imaging experiments after 18-24 hours in Dulbecco's modified Eagle's medium DMEM (Pharmakine<sup>®</sup>) supplemented with 10% fetal bovine serum, FBS,  $2.5 \times 1000$  U/ml penicillin and 2.5mg/ml streptomycin and then conditioned by adding  $50\mu\text{g/ml}$  ascorbic acid, 10mM  $\beta$ -glycerol phosphate and  $10^{-7}\text{M}$  dexamethasone. The cultures were incubated at  $37^\circ\text{C}$  in an atmosphere of 95%

O<sub>2</sub> and 5% CO<sub>2</sub>. Following this, the cells were incubated in buffer (Hanks' Balanced Salt Solution with 10mM glucose, 10mM HEPES, pH 7.4) with Fura-2-AM (2μM) and probenecid (1mM) for 60 min at 37°C. Coverslips were washed and mounted in an open chamber. Test compounds allyl isothiocyanate (100μM), GSK1016790A (GSK) (1μM), icilin (1μM), KCl (50mM) and capsaicin (1μM) were diluted to required concentrations in buffer and applied to the odontoblast cells by continuous perfusion at 37°C. The fluorescence readings of individual cells were measured at 340 nm and 380 nm excitation, and 510nm emission using microscope based imaging system (PTI, Ford, UK), with one image pair collected every second. The exposure to 1μM ionomycin (an ionophore which stimulates calcium transport across cell membranes) was used to confirm the viability of the cells. Responses were measured as the change in the 340/380nm emission ratio from an averaged baseline ratio and cells that showed a ratio change  $\geq 0.2$  from the baseline were defined as responders. The schematic of the sequential application of the test compounds is shown in Figure 5.1 below.

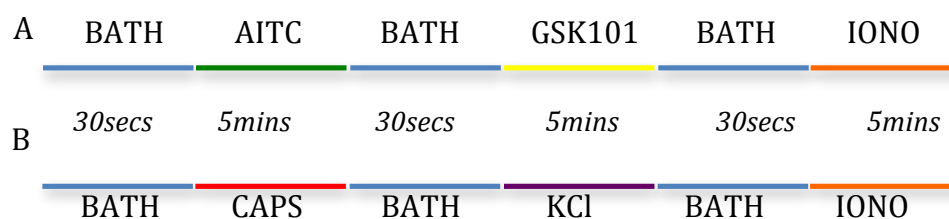


Figure 5.1: A shows the order of application of test compounds allyl isothiocyanate (AITC), a TRPA1 agonist and GSK1016790A, a commercial TRPV4 agonist (Thorneloe, Sulpizio et al. 2008). The preceding bath phases represent cell response baselines periods during which the cultured cells were perfused for 30 seconds with Hanks buffered solution (HBBS). B shows the application of test compounds icilin, a TRP A1/M8 agonist and capsaicin, a TRPV1 agonist.

In separate experiments, tDPSCs were plated and grown until confluence in black-bottomed 96-well plates (Corning, Corning, NY). The cells were loaded in buffer (Hanks' Balanced Salt Solution with 10mM glucose, 10mM HEPES, pH 7.4) with Fura-2-AM (2μM) and probenecid (1mM) for  $\approx$ 60mins. Using a Flexstation (Molecular Devices, Sunnyvale, CA), fluorescence was measured at 90 second-intervals, using excitation



wavelengths of 340 and 380 nm and an emission of 520 nm. TRP channel agonists and antagonists (see Table 5-1) were added after  $\approx 20$  secs. Concentration-response curves were generated by fitting the data with a 4-parameter sigmoidal curve (variable slope) equation using the GraphPad Prism software:  $y = \text{Bottom} + (\text{Top} - \text{Bottom}) / (1 + 10^{-(\log \text{EC50} - x) * \text{Hill-Slope}})$ , where  $x = \log(\text{concentration})$ .

TRP channel	Agonist	Antagonist
TRPA1	Allyl isothiocyanate (AITC)	HC030031
	Cinnamaldehyde	
TRPV1	Capsaicin	
TRPM8	Icilin	
TRPV4	GSK1016790A	HC067047
	Hypotonic solution	

Table 5-1: Tested TRP channel agonists and antagonists.

#### 5.2.4 Measurement of ATP release

Using tDPSCs culture in 4-well plates (CellStar<sup>®</sup>), the concentration of ATP released was measured with a luciferase assay kit (CellTiter-Glo<sup>®</sup> Assay, Promega). When the cells had become fully confluent, volumes of 500 $\mu$ M of 12.5% DMSO-in-DPSC culture media solution, or culture media containing concentrations of TRP channel agonists, which were 500 $\mu$ M AITC (TRPA1), 500 $\mu$ M cinnamaldehyde (TRPA1 agonist), 500nM GSK1016790A (TRPV4) and 40% hypotonic solution (TRPV4), were added to each well. After 15 mins incubation periods at 37 $^{\circ}$ C, 100 $\mu$ l samples of media were collected from these wells for luminescence measurements in a

spectrophotometric plate reader (FluroStar Optima: BMG Labtech). The samples collected from the cells exposed to DMSO were used as comparative basal measurements.

### 5.3 Results

#### 5.3.1 RT-PCR analysis of TRP channel expression

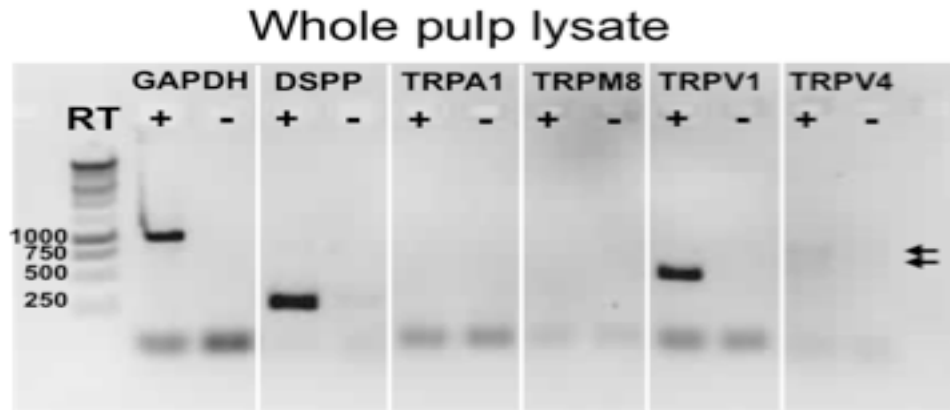


Figure 5:2: The gel shows the identification of TRPV1 and DSPP expression in the whole pulp lysate. GAPDH was used as an internal control. Arrows indicate predicted size of TRPV4 mRNA.



Figure 5:3: (A) demonstrates the identification of the TRP (A1, V1, M8 and V4) expression profile in nDPSCs before retroviral transduction. (B) Shows positive bands for TRPA1, V1 and V4 in tDPSCs at passages 6 (first group of TRP bands) and 30 (second group of TRP bands). GAPDH was used as an internal control. The encircled genes have been discussed in Chapter 4. The underlined mesenchymal stem cells were run in gel B as part of an unrelated experiment to test a beta actin primer.

The cells were examined for the expression of mRNA profiles for TRP channels (TRPA1, TRPV1, TRPM8 and TRPV4) as well as that representative of SP receptors

(NK1R and NK2R). The data shows no bands for TRPM8 were detected in either nDPSCs or tDPSCs (See Figure 5.2A, B). The presence of mRNA for TRPA1, TRPV1 and TRPV4 was detected in these cells. To confirm the specificity of the primers for TRPM8, a positive control experiment was performed using mRNA from Chinese hamster ovary (CHO) cells transfected with mouse TRPM8. The CHO-TRPM8 cell mRNA demonstrated the efficacy of the TRPM8 primers used in this study as there was a strong band present when it was run in parallel with nDPSC and tDPSC mRNA (Figure 5.3A, B). Expression of mRNA for tachykinin receptors NK1R and NK2R was detected in both nDPSCs and tDPSCs (Figure 5.3A, B). The presence of two phenotypic markers for the odontoblast phenotype (ALP and COL-1) was also tested as an internal control, and expression of both was identified.

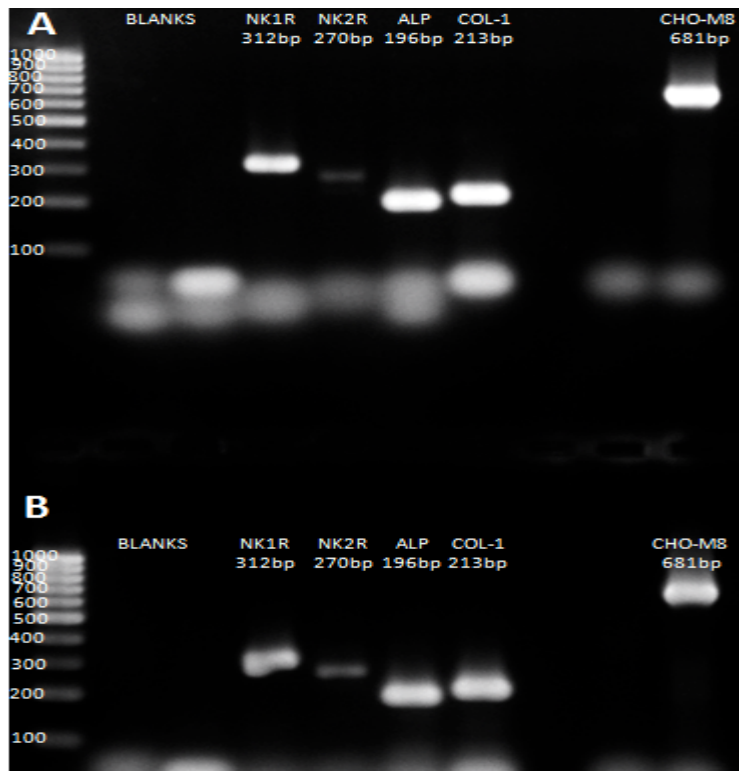


Figure 5:4: The identification of the substance P receptors NK1R and NK2R in nDPSCs (A) and tDPSCs (B). The efficacy of the TRP M8 primer was confirmed as positive bands were seen with control Chinese hamster ovary (CHO) cell RNA. ALP and COL-1 were run as controls.

## 5.3.2 Quantitative gene expression of TRP channels and neuropeptide receptors

### 5.3.2.1 Sensitivity and specificity of the primers

To demonstrate the sensitivity of the primers used in the quantitative analysis of gene expression, standard curves were generated for  $\beta$ -actin, TRPA1, TRPV1, TRPV4, NK1R and NK2R (SP receptors). The standard curves generated demonstrated coefficient of determination values ( $R^2$ ), which ranged between from 0.877 to 0.996 (Figures 5.4A-E). The cycle threshold values obtained in these experiments demonstrated strong ( $C_T \leq 27$ ) and moderate ( $C_T$  between 30 and 37) positive results, indicating the presence of the target nucleic acids. The integrity of the primers used was demonstrated by running the PCR end products on agarose gels. There was an expression of single bands in each lane for the tested primers ( $\beta$ -actin, TRPA1, TRPV1, TRPV4, and NK2R).



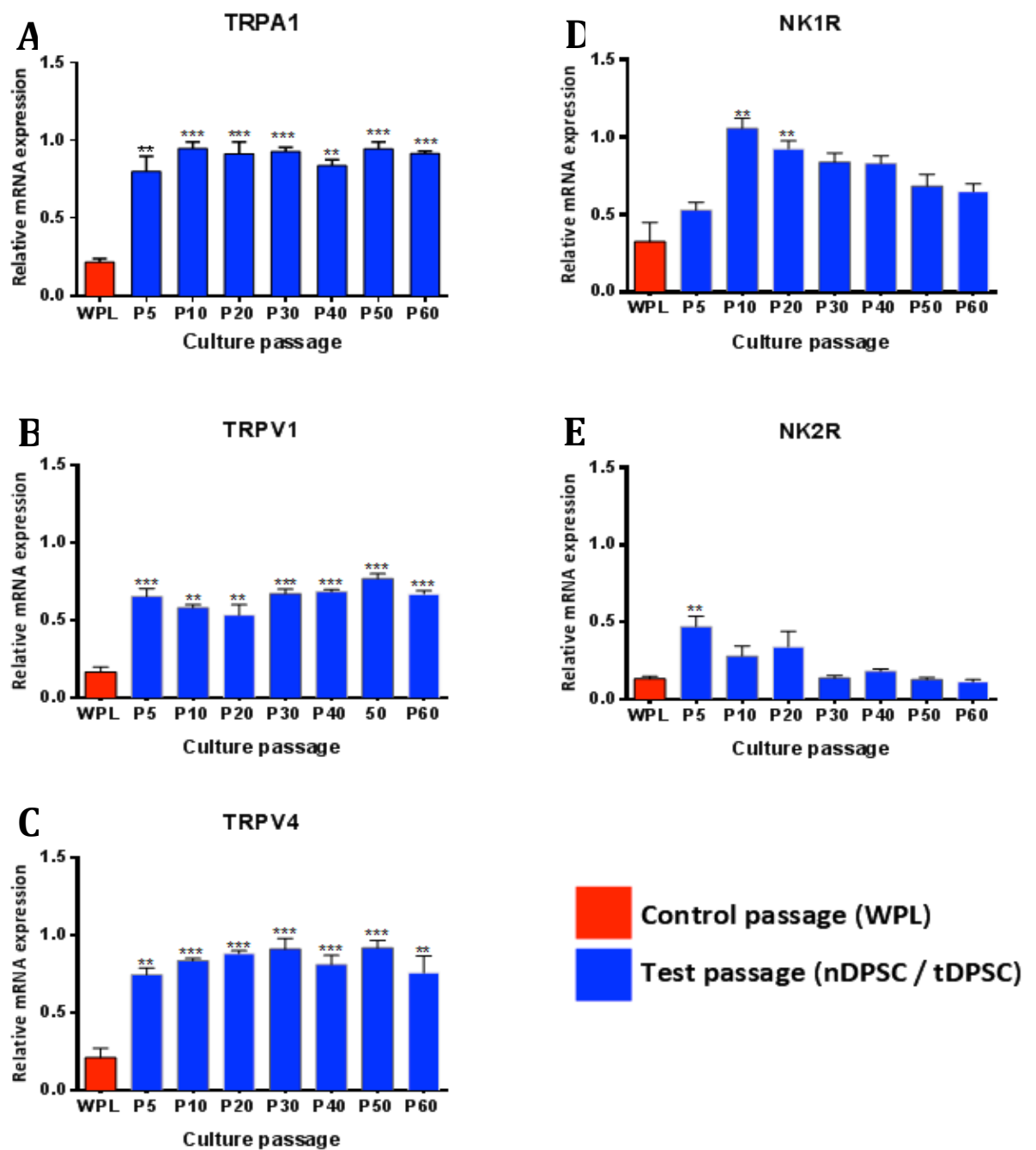


Figure 5:6: Gene expression levels of TRP channels TRPA1 (A), TRPV1 (B) and TRPV4 (C) and substance P receptors NK1R (E) and NK2R (F) in WPL, nDPSC (passage n5) and tDPSCs, (passage 10 – 60) was determined by real-time qPCR. Values are reported as relative fold change in cDNA transcription which were normalised to the housekeeping gene. The data is represented as mean  $\pm$  S.E, with significance differences measured between WPL (control) and the different time points (P5 – P60) by one-way ANOVA and post hoc Bonferroni's test. (\*\* $p < 0.01$ , \*\*\* $p < 0.001$ ).

The mRNA expression of TRP channels TRPA1, TRPV1 and TRPM8 was analysed in populations of tDPSCs spanning 60 passages and compared to the levels of mRNA expression of these markers seen in nDPSCs at passage 5. The data presented in Figure 5.5A-C demonstrates no statistically significant evidence of any difference(s) in the expression of TRPA1, V1 or V4 at any of the measured time points. The mRNA expression levels of the NK1R was higher at passages 10 – 40 of the tDPSCs when compared to the nDPSC expression levels at passage 5. There was a significant down-regulation of tDPSC-NK1R expression between passage 10 and 60 (Figure 5.5D). The NK2R gene expression profile was found to be lower than that of the comparative baseline (passage n5) at passages 10 and 20 (Figure 5.5E). This trend continues all through to passage 60 (becoming statistically significant at passages 30, 40, 50 and 60).

### 5.3.3 Identification of odontoblast TRP channels through $\text{Ca}^{2+}$ imaging

To identify the type of TRP channels present in the cultured tDPSCs, the effects of selective chemical agonists on these cells were investigated using calcium imaging. The application of 100 $\mu\text{M}$  AITC and 1 $\mu\text{M}$  GSK1016790A caused increases in  $[\text{Ca}^{2+}]_i$  suggesting the activation of TRPA1 and V4 channels (Figure 5.6). A response to AITC was observed in the tDPSCs with 36% of a total number of 125 tested cells showing a mean ratio change of  $0.407 \pm 0.05$  (n=6) (Figure 5.7A, B).



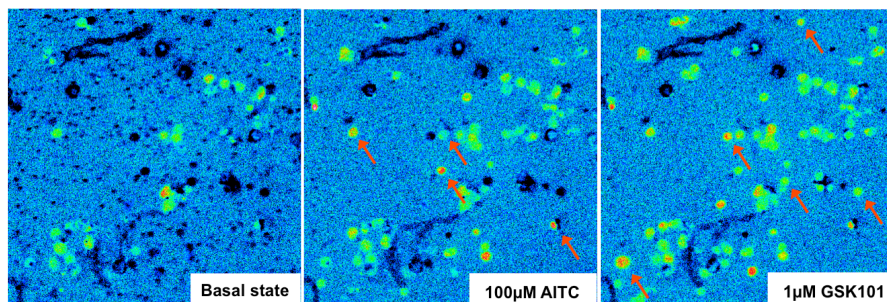
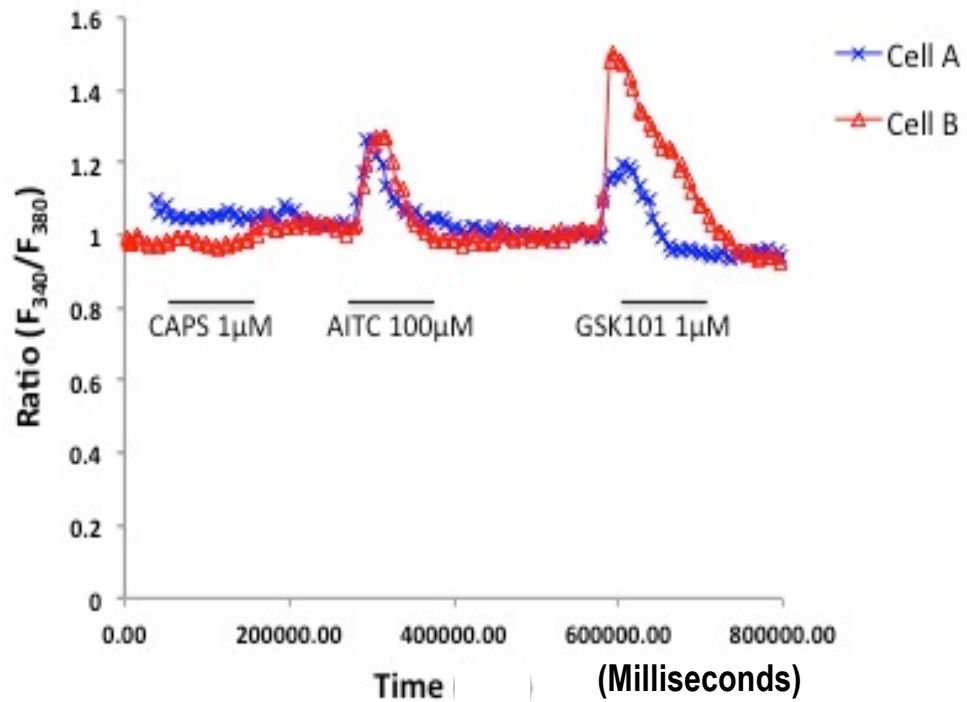


Figure 5:7:  $[Ca^{2+}]_i$  imaging by the application of chemical stimuli (agonists) for thermosensitive and mechanosensitive TRP channels in the cultured tDPSCs. There were no spikes observed following the application of capsaicin while two consecutive sets of spikes were evoked in response to AITC and GSK1016790A respectively. tDPSCs in which the application of these two agonists produced a change in  $[Ca^{2+}]_i$  are highlighted by the red arrows in images below the graph.

Similarly, 29.6% of the 125 tDPSCs observed accounted for the response to GSK1016790A, demonstrating a mean ratio change of  $0.42 \pm 0.016$  ( $n=6$ ) (Figure 5.7A, B). There were no observed responses following the application of  $1\mu\text{M}$  capsaicin by the tDPSCs. To test for the presence of tDPSC- $K^+$  channels, effects following the application of  $50\text{mM}$  KCl were observed. All of the 125 tDPSCs showed a response,

with a mean ratio change of  $-0.1712 \pm 0.02$  (n=3) (Figure 5.7 A, B). In all experiments, 1 $\mu$ M ionomycin served as a control for cell viability and the mean ratio changes observed were  $0.331 \pm 0.02$  (in 125 tDPSCs tested, n=6).

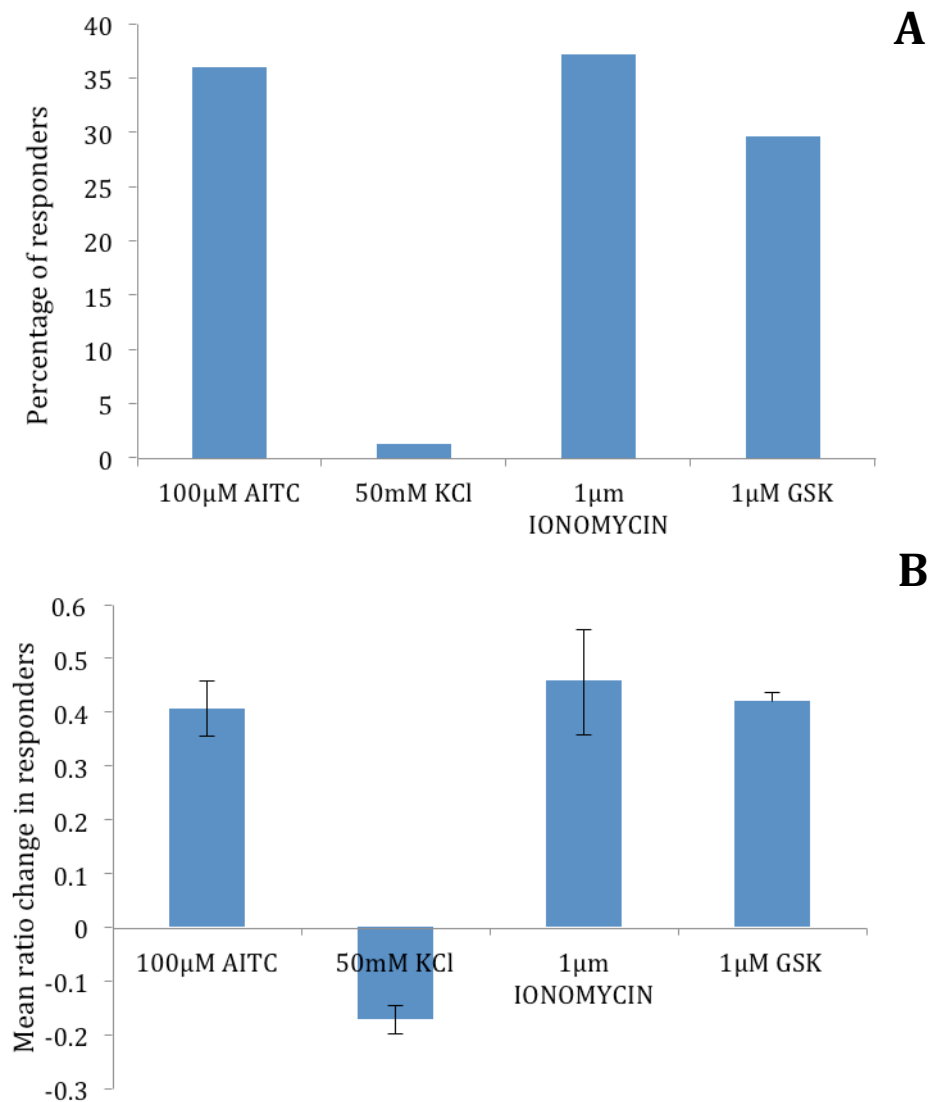


Figure 5:8: (A) Percentage of responders (cells that showed a ratio change  $\geq 0.2$  from the averaged baseline) to changes in  $[Ca^{2+}]_i$  following the application of selective TRP channels agonists in the cell populations tested. (B) Mean ratio changes demonstrated by the responders in this study. Error bars demonstrate the standard error from the mean.

The results obtained in the Flexstation assays showed increases in  $[Ca^{2+}]_i$  that were concentration-dependent, following exposure of the tDPSCs to the TRP channel agonists AITC, cinnamaldehyde and GSK1016790A, as well as hypotonic solution of decreasing osmolarity (292mOsm/l (0%) – 175mOsm/l (40%)) (Figure 5.8 A - D). The estimated  $EC_{50}$  values and Hill-Slope coefficients were  $6.67 \pm 1.34\mu\text{M}/1.4 \pm 0.7$  for AITC ( $n = 4$ ),  $32.33 \pm 1.33\mu\text{M}/1.5 \pm 0.5$  for cinnamaldehyde ( $n = 4$ ), and  $31.78 \pm 1.35\text{nM}/1.6 \pm 0.6$  for GSK1016790A (concentration = 0 – 1000nM;  $n = 6$ ) (Figure 5.8A, C). A similar

trend of concentration-dependent  $[Ca^{2+}]_i$  responses was observed secondary to the exposure of the cells to increasingly hypotonic solution (0 – 40%, n = 4) (Figure 5.8B). There were no observed capsaicin and icilin induced  $[Ca^{2+}]_i$  responses in experiments that were run in parallel (n = 4) (Figure 5.8E, F). Flexstation TRP channel antagonist assays were also performed to demonstrate the inhibition of the activated TRP channels (TRPA1 and V4) (Figure 5.9A - D). The tDPSCs were exposed to the TRPA1 (AITC and cinnamaldehyde) and TRPV4 agonists (GSK1016790A and 40% hypotonic solution) for 10mins following the application of the corresponding antagonists. The estimated  $IC_{50}$  values observed were  $116.2 \pm 1.56nM$  for HC067047 against 200nM GSK1016790A activity (n = 4),  $19.53 \pm 1.82\mu M$  for HC030031 against 200 $\mu M$  AITC activity (n = 4) and  $7.17 \pm 1.33\mu M$  for HC030031 against 200 $\mu M$  cinnamaldehyde activity (n = 4). The complete inhibition of 200 $\mu M$  AITC and 200 $\mu M$  cinnamaldehyde activity by HC030031 was not achieved. There was no apparent inhibition of 40% hypotonic solution activity by HC067047.

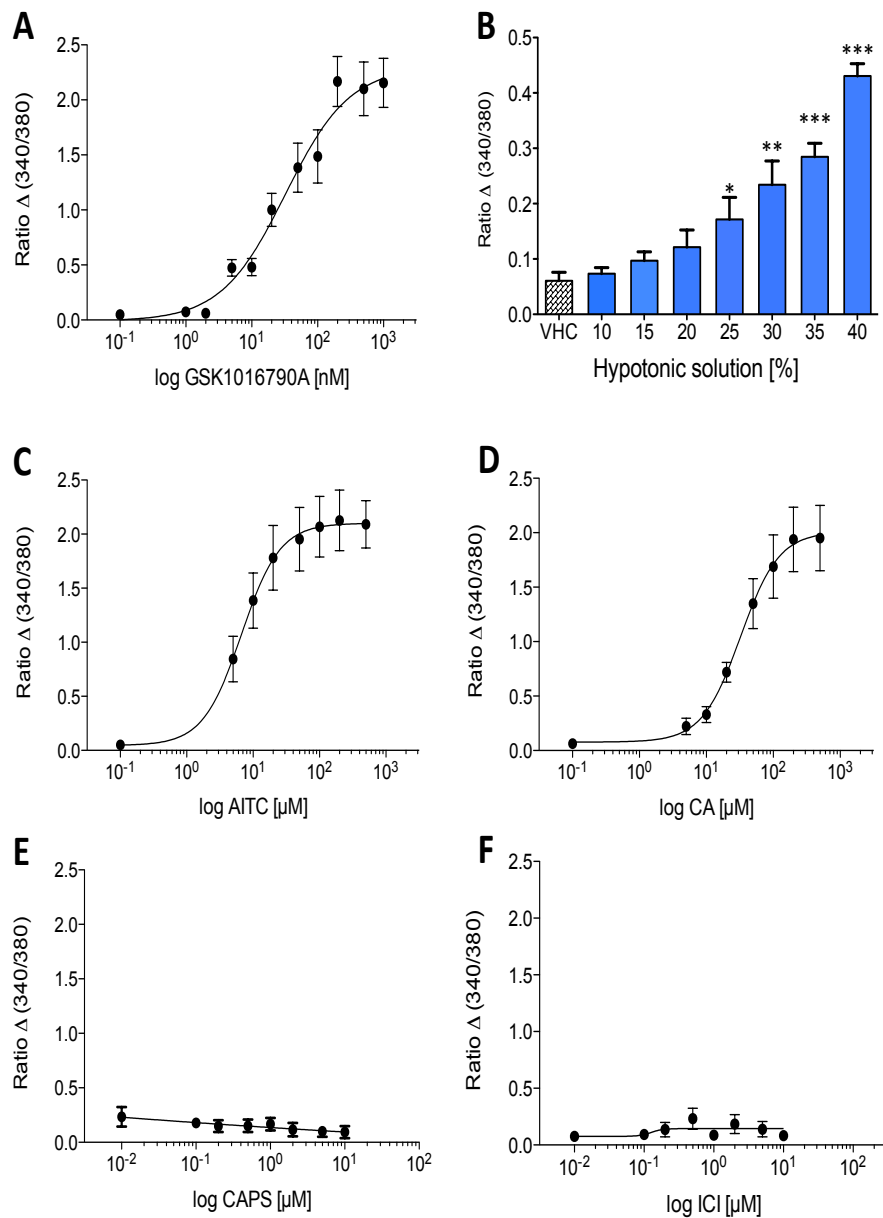


Figure 5:9: Dose-response curves for (A) GSK1016790A, (B) hypotonic solution, (C) allyl isothiocyanate, AITC, (D) cinnamaldehyde, CA, (E) capsaicin, CAPS, (F) icilin, ICI measured in cultured tDPSCs. The data points in each response plot are representative of mean responses (measurements of the emission ratios of Fura-2 as indicators of  $[Ca^{2+}]_i$  transients,  $n=6$ ) at tested concentrations for each agonist. The tDPSCs showed very poor responses to the TRPV1 agonist, capsaicin (E) and TRPM8, agonist icilin (F) in contrast to the responses seen with the other agonists (TRPA1 – AITC and CA, and TRPV4 – GSK1016790A). There is also a concentration-dependent effect of hypotonicity on tDPSC-TRPV4 as evidenced by the observed  $[Ca^{2+}]_i$  responses, ( $n=4$ , VHC = isotonic solution) (B). The column plot data points are represented as mean  $\pm$  S.E, with significance differences measured between VHC (control) and the different percentages of hypotonic solution by one-way ANOVA and post hoc Bonferroni's test. (\*\*\*)  $p < 0.001$ , (\*\*)  $p < 0.01$  and (\*)  $p < 0.05$ ).

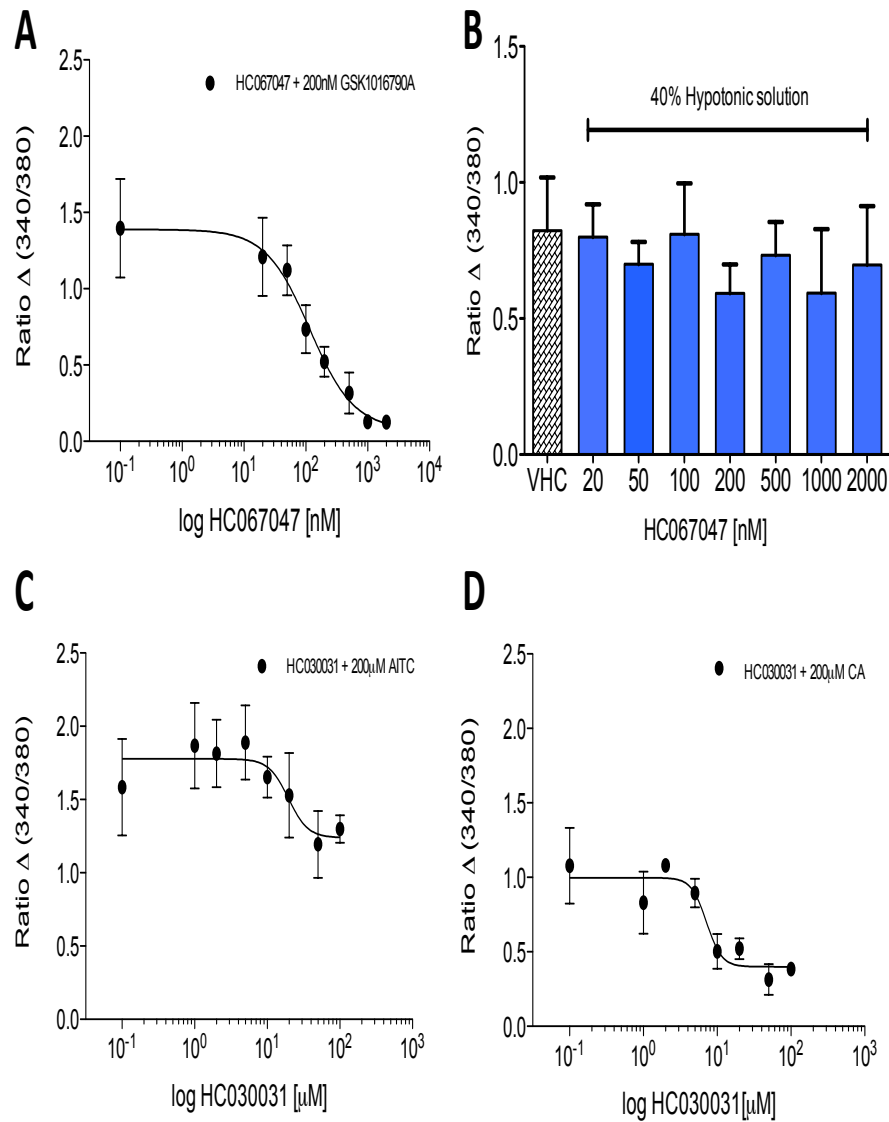


Figure 5:10: Concentration-dependent inhibition of  $[Ca^{2+}]_i$  responses by TRPV4 antagonist HC067047 to 200nM GSK1016790A, (n=4) (A), TRPA1 antagonist HC030031 to 200 $\mu$ M AITC, (n=4) (C) and 200 $\mu$ M cinnamaldehyde, (n=4) (D). Exposure to TRPV4 antagonist does not significantly inhibit the effect of tDPS C pre-exposure to 40% hypotonic solution, (n=3, VHC = isotonic solution) (B). The data points in each of the response plots are representative of mean responses at tested concentrations for each antagonist. The column plot data points are represented as mean  $\pm$  S.E, with significance differences measured between VHC (control) and the different percentages of hypotonic solution by one-way ANOVA and post hoc Bonferroni's test. (\*\*\*)  $p < 0.001$ , (\*\*)  $p < 0.01$  and (\*)  $p < 0.05$ ).

### 5.3.4 TRP channel induced ATP release

The data obtained from the luciferase-assays shows that a significant amount of ATP release was induced by TRPA1 agonist AITC ( $p = 0.0323$ ,  $n = 5$ ) while exposure of the tDPSCs to cinnamaldehyde, GSK1016790A and 40% hypotonic solution did not show any significant changes to ATP release in these experiments (Figure 5.10A- D).

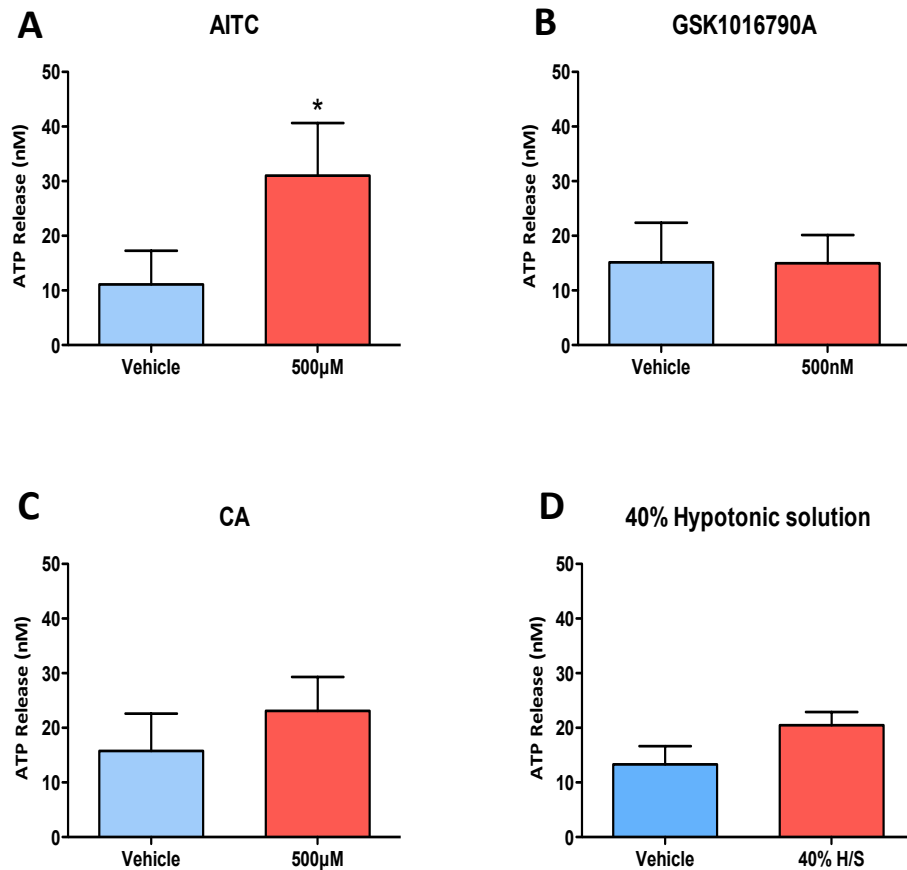


Figure 5:11: TRP channel agonist evoked ATP release by tDPSCs. Significant increases in ATP release was induced by (A) AITC ( $n=5$ ), while (C) cinnamaldehyde ( $n=5$ ), TRPV4 agonists GSK1016790A ( $n=5$ ) (B) and (D) hypotonic solution ( $n=4$ ) failed to induce significant increases in ATP release. The data is represented as mean  $\pm$  S.E and a Student t test was performed to compare for significant differences between the vehicle (control) and the respective TRP agonists ( $*p < 0.05$ ).

### 5.3.5 Effects of SP on TRP channel expression and activity

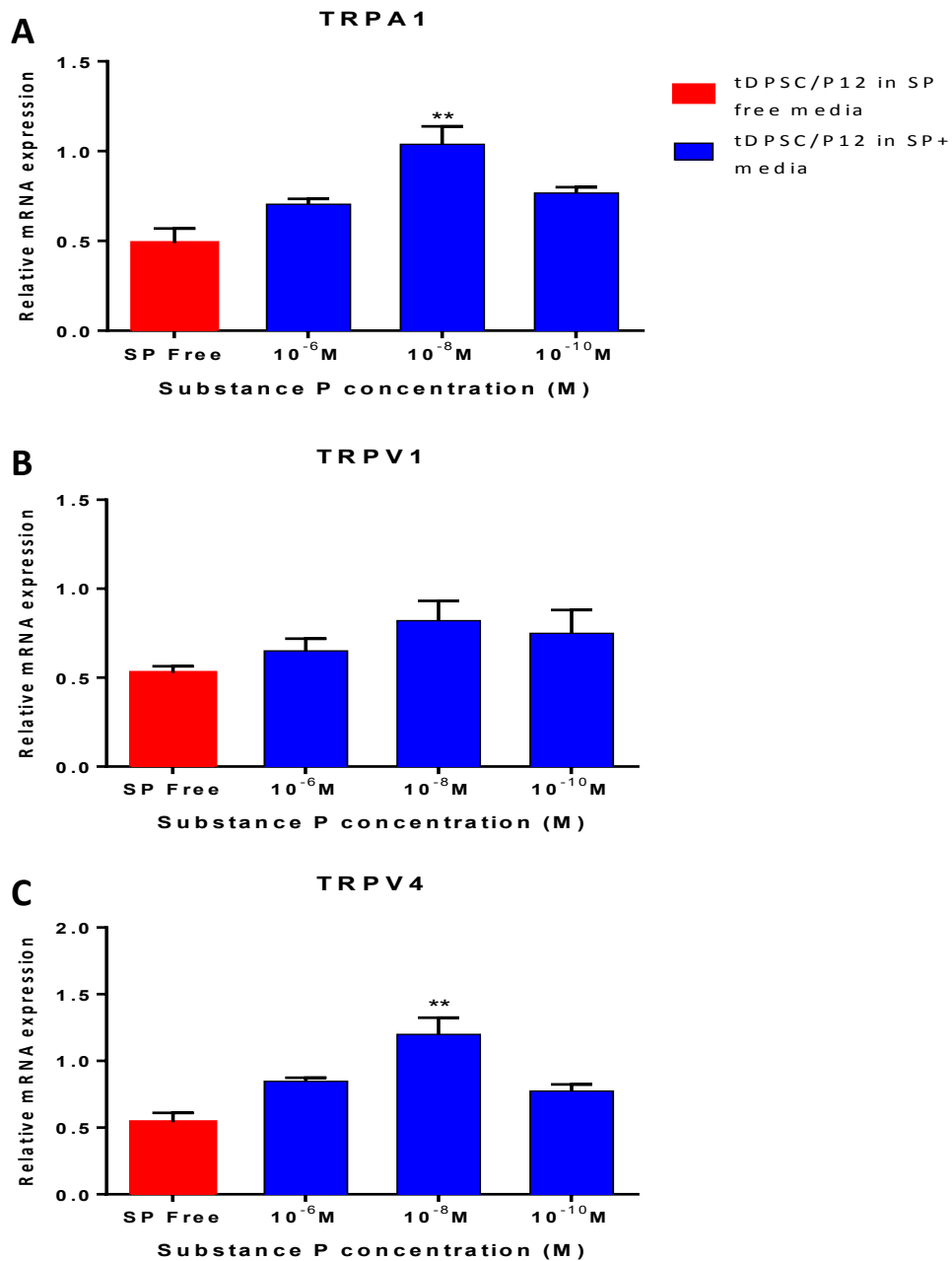


Figure 5:12: The relationship between TRP channel expression levels and variations in concentrations of SP added to tDPSC cell cultures at passage 12 (tDPSC-p12/SP<sup>+</sup>). Expression levels of tDPSC mRNA at passage 12 cultures unexposed to SP (tDPSC-p12/SP<sup>-</sup>) were used as comparative baselines. (B, C). The addition of 10<sup>-8</sup>M SP showed a significant increase in mRNA expression levels in TRPA1 and V4. The data is represented as mean ± S.E, with significance differences measured between SP free samples (control) and the respective concentrations of SP, by one-way ANOVA and post hoc Bonferroni's test (\*\*\**p* < 0.001, \*\**p* < 0.01 and \**p* < 0.05).



Following the addition of SP ( $10^{-6}$ M,  $10^{-8}$ M and  $10^{-10}$ M) for 2 hours to the tDPSC cultures, the mRNA expression of TRPA1, V1 and V4 was evaluated in populations of tDPSCs at passage 12. The baselines used as measures of comparison for the levels of mRNA expression of the TRP channels were those measured in the tDPSCs at passage 12 without exposure to concentrations of SP (tDPSC-p12/SP free media in Figure 5:11). TRPV1 mRNA expression levels were not significantly elevated with the addition of  $10^{-6}$ M and  $10^{-8}$ M SP to the tDPSC cultures. TRPA1 and V4 mRNA expression levels in the tDPSC-p12/SP<sup>+</sup> cultures were significantly elevated ( $p < 0.05$ ) at  $10^{-8}$ M of SP in comparison to the tDPSC-p12/SP<sup>-</sup> cultures (Figure 5:11A, C).

## 5.4 Discussion

In this section, the experimental objectives were the quantitative and qualitative evaluation of TRP channels expression and function in the DPSCs. Additionally, SP-responsive tachykinin receptors (NK1R and NK2R) expression in the tDPSCs, and the effect of SP on the expression of TRP channels was studied.

### 5.4.1 TRP channel expression

RT-PCR experiments to identify TRP channel expression in the nDPSCs and tDPSCs showed the presence of mRNA profiles at the predicted sizes for TRPA1, V1 and V4. The data obtained also suggested the absence of TRPM8 expression in both the nDPSCs and tDPSCs; a finding, which was confirmed by the simultaneous testing for mRNA in TRPM8-positive CHO cells. This strongly suggests that the cells of the odontoblast phenotype isolated in this study do not show any expression of TRPM8. This TRP channel transcript profile (TRPA1-positive, V1-positive, V4-positive and M8-negative) was maintained by the cells all through the period of investigation, which demonstrated that the process of transfection (described in Chapter 4) had no effect on the continued gene expression of these channels by the tDPSCs. The presence of TRPA1, V1 and V4 channels in cultured human odontoblasts as demonstrated in this thesis is in keeping with the work carried out by other groups (El Karim, Linden et al. 2010; Solé-Magdalena, Revuelta et al. 2011). The difference however, is the absence of evidence for TRPM8 gene expression. While differences in experimental methodologies (cell sourcing and transfection as described in chapters 3 and 4 during which we found no RNA or functional response) for obtaining the tDPSCs in this study may account for this, there is another possible explanation. As the expression of TRPM8 has been demonstrated in peripheral nerve endings in the human dental pulp (Alvarado, Perry et al. 2007), and not in the odontoblasts themselves, it is possible that the detection of cold sensations might not involve the individual odontoblast cells. This does not agree with the hydrodynamic theory, which had suggested that there were no direct cold sensations detected by the odontoblasts and dentinal fluid movements induced by cooling temperatures might cause any perceived responses. It was proposed that the outward movement of dentinal fluid following cold stimulation activates mechanoreceptors by causing sufficient stresses on the nerve endings

(Brannstrom and Astrom 1964; Brannstrom 1986; Andrew and Matthews 2000); a theory that was successfully demonstrated by the thermo-mechanical model designed by Lin and colleagues which showed an increase in outward dentinal fluid flow rates following the application of cold stimuli (0-5°C)(Lin, Liu et al. 2011). Prior to the emergence of the Lin-model, other groups had demonstrated that intradental mechano-nociceptors were not as sensitive to the directional changes of dentinal fluid flow when compared to thermo-nociceptors (Andrew and Matthews 2000; Julius and Basbaum 2001). This would imply that while dental pain perception is by all accounts, largely dependent on fluid mechanics within the dentinal tubules, the thermosensitive nociceptor (such as the TRPV1 channel for example) plays a role in the detection of nociceptive stimuli.

#### **5.4.2 Analysis of TRP channel function by single cell imaging**

Following the establishment of the TRP channel expression in the tDPSCs, investigations on channel functionality were performed in this study using ratiometric calcium imaging. The results demonstrated that the tDPSCs expressed the thermo-sensitive TRPA1 channel by way of responses to the TRPA1 agonist, AITC (Story, Peier et al. 2003; Bandell, Story et al. 2004; Cavanaugh, Simkin et al. 2008). TRPV4 mRNA amplification earlier demonstrated in the tDPSCs was supported by the demonstration of influx of Ca<sup>2+</sup> in response to its corresponding agonist, GSK1016790A (Thorneloe, Sulpizio et al. 2008), demonstrating the presence of functional TRPV4 in the tDPSCs. While TRPV1 mRNA expression was demonstrated by PCR techniques, the measured responses from the tDPSCs to the TRPV1 channel agonist capsaicin (Caterina, Schumacher et al. 1997) suggest an absence of function in these cells as there was a failure to evoke calcium transients above the established experimental threshold levels (described in Section 5.2.4). The 1µM concentration of capsaicin used in this study is above EC<sub>50</sub> (concentration producing 50% of the maximum response) values successfully determined in calcium imaging experiments on human TRPV1 receptor-expressing cells performed by three separate groups (0.29 ± 0.05µM; (McNamara, Randall et al. 2005; de Jonge, Woolthuis et al. 2009) and 0.25 ± 0.04µM;(Smart, Jerman et al. 2001)). Demonstrations of capsaicin-induced calcium transients in both animal

and human TRPV1-positive culture systems using this supra-threshold concentration are also evident in the literature (Smart, Jerman et al. 2001; McNamara, Randall et al. 2005; Park, Kim et al. 2006; Riera, Menozzi-Smarrito et al. 2009; Cavanaugh, Chesler et al. 2011). It was in this context that a positive capsaicin response was expected in this study, so the “absence” of TRPV1 response in the tDPSCs was puzzling. The only other successful demonstration of TRPV1 activation in human odontoblast-like cells in culture using this technique was performed using 10 $\mu$ M capsaicin ( $\Delta [Ca^{2+}]_i = 0.2$ ), the effects of which were blocked using 10 $\mu$ M of the TRPV1 antagonist, capsazepine (El Karim, Linden et al. 2010). While it may be suggested that the use of a transfected cell line in this study might have influenced TRPV1 function (El Karim and colleagues used non-transfected passages 4 – 6 of human odontoblast-like pulp cells), there is no evidence in the literature to support this assumption. TRPV1 expression and function has been demonstrated in immortalised animal and human cell lines, suggesting the absence of a controlling influence by the transfection process (Reilly, Taylor et al. 2003; Mergler, Valtink et al. 2010; Chaudhury, Bal et al. 2011). In light of this, it is our opinion that the tDPSCs in this study may express a TRPV1 RNA splice variant which is capsaicin-insensitive; a variant whose expression has been identified in murine DRG sensory neurones (Wang, Hu et al. 2004) as well as demonstrated in *Xenopus* oocyte cells (Lu, Henderson et al. 2005). While the human TRPV1b splice variant is missing an exon region of approximately 60 amino acids and did not show a deletion of its “capsaicin-binding site (Jordt and Julius 2002), the later study to characterize this cloned variant showed that it formed heteromeric complexes with TRPV1 thereby negatively regulating its function in both animal (mouse DRG sensory neurones) and human cells (embryonic kidney cells) (in which its expression was investigated) (Vos, Neelands et al. 2006). In regards to the findings in this study and our supposition that the tDPSC-TRPV1 may be a capsaicin-insensitive variant, we cannot conclude that there would be an absence of a response to other TRPV1-activating stimuli such as heat or decreased pH levels as we did not perform any experiments testing these parameters. Work by Sudbury and colleagues on isolated mice magnocellular neurosecretory neurons, suggests that an N-terminal variant of TRPV1 that is capsaicin-insensitive, enables mechano/osmosensation and thermosensation (Sudbury, Ciura et al. 2010). The proposed explanation for this was based on the observations

made by Suzuki and colleagues in rat kidney cell studies that the expression of a construct made up of transmembrane segments of TRPV1 and the cytoplasmic carboxyl termini of TRPV4 can allow for detection of hypertonicity (Suzuki, Sato et al. 1999). Alternatively, we could hypothesize that the absence of TRPV1 proteins might result from the non-translation of its mRNA, a phenomenon that could (as broadly described by Rastinejad and Blau (Rastinejad and Blau 1993) alter the phenotypic features of a cell such as tDPSC-TRPV1 responsiveness in this case. The presence of TRPV1 mRNA but absence of functional V1 proteins could also indicate a level of expression below the detection threshold. A recently described means of sensitive gene targeting which couples reporter molecule expression to the promoter region of a gene of interest (and has been shown to be effective in the mapping of TRPV1 expression in murine DRGs and trigeminal ganglia (TG), especially in regions of low expression)(Cavanaugh, Chesler et al. 2011) could be used to corroborate the functional absence of tDPSC-TRPV1 as shown in our studies. This would of course be impossible in human subjects and might require the use of animal subjects genetically modified to express for this human tDPSC-TRPV1 variant.

The RT-PCR results showed the absence of the thermosensitive TRPM8 which responds to cool temperatures ( $\leq 28^{\circ}\text{C}$ )(Clapham 2003; Chuang, Neuhausser et al. 2004). This was validated by the calcium imaging studies the results of which demonstrated an absence of responses to icilin, an agonist which activates both TRPA1 and M8 (McKemy, Neuhausser et al. 2002), although the TRPA1 channel to a lesser extent (Story, Peier et al. 2003). While some groups have been able to detect the presence of the mRNA for the TRPM8 channel in cells derived from human pulp tissue (fibroblasts and odontoblasts), (El Karim, Linden et al. 2010; El Karim, Linden et al. 2011), it is not entirely clear as to why TRPM8 expression was not detected in this study. The  $1\mu\text{M}$  concentration used to investigate tDPSC-TRPM8 icilin-responses in this study is close to the  $\text{EC}_{50}$  values demonstrated by McKemy and colleagues in TRPM8 receptor-expressing cells ( $0.36 \pm 0.03\mu\text{M}$ ) (McKemy, Neuhausser et al. 2002), as was the  $100\mu\text{M}$  concentration of AITC to demonstrate TRPA1 functionality ( $\text{EC}_{50} = 64.5 \pm 3.12\mu\text{M}$  (Hinman, Chuang et al. 2006).

### 5.4.3 tDPSC K<sup>+</sup> channel expression

Electrophysiological *in vitro* studies on cultured human odontoblasts have demonstrated the presence of calcium-dependent mechanosensitive K<sup>+</sup> channels in these cells (Basbaum, Bautista et al. 2009). To examine the functional contribution of these ion channels to tDPSC-response to potassium depolarization, we performed Ca<sup>2+</sup> imaging experiments using 50mM KCl, to which as the results indicate (Figure 5:7A, B), a maximum number of responders (125 tested tDPSCs). Our observations suggest that the exposure to K<sup>+</sup> decreased [Ca<sup>2+</sup>]<sub>i</sub> transients. The possible explanations for the efflux of Ca<sup>2+</sup> ions which coincides with the opening of the Ca<sup>2+</sup> channels could either be due to the presence of the TRP channel agonists used in this study (AITC or GSK1016790A for example) or, the depolarizing effects of KCl that extrudes some Ca<sup>2+</sup> ions. These results argue against a direct role for these K<sub>Ca</sub> channels in mechanosensitivity as proposed by Magloire et al (Magloire, Lesage et al. 2003). It would also suggest (based on a concept described by Hermanstynne and colleagues in their work on pulpal nerves in rats) that while the K<sub>Ca</sub> channels are present in the tDPSCs, their sensitization might be modulated by the intensity of the stimuli (Truini, Padua et al. 2009). While the data we obtained is not reflective of chemical stimulation of the K<sub>Ca</sub> channels, we believe that our findings can be corroborated in future work, by the measurement of [K<sup>+</sup>]<sub>i</sub> transients through K<sub>Ca</sub> channels following voltage-dependent or mechanical/osmotic stimulation of the tDPSCs in patch clamp experiments.

### 5.4.4 Analyses of TRP channel activation and inhibition

To validate the findings of our microscope-based calcium imaging studies, we performed further fluorescence measurements of intracellular [Ca<sup>2+</sup>]<sub>i</sub> levels of the tDPSCs using the Flexstation system. The data yielded the following observations:

#### (1) TRPA1

There was a clear demonstration of concentration-dependent relationships for AITC and cinnamaldehyde confirming the activation of the tDPSC-TRPA1 channel (Figure 5:8 C, D). The data also demonstrated that AITC is a more potent TRPA1 agonist as indicated by its concentration-response profile (EC<sub>50</sub>=

6.67 ± 1.34µM; Hill-Slope coefficient = 1.4 ± 0.7) in comparison to that of cinnamaldehyde (EC<sub>50</sub> of 32.33 ± 1.33µM; Hill-Slope coefficient = 1.5 ± 0.5). The 5-fold difference in TRPA1 activation by both agonists used in our study (AITC= EC<sub>50</sub> of 6.67 ± 1.34µM and cinnamaldehyde =EC<sub>50</sub> of 32.33 ± 1.33µM), also suggests a stronger AITC binding affinity for TRPA1. This would be in keeping with evidence in the literature, which also suggests that both AITC and cinnamaldehyde activate TRPA1 in the same manner - through the covalent modification of N-terminal cysteines and lysines (Willis 1985; Bandell, Story et al. 2004; Hinman, Chuang et al. 2006). Following this, using single concentrations of AITC (200µM) and cinnamaldehyde (200µM), we then performed blockade experiments with TRPA1 channel antagonist HC030031. Our results illustrated the partial inhibition of TRPA1 activation by AITC and cinnamaldehyde with HC030031, as evidenced by decreased [Ca<sup>2+</sup>]<sub>i</sub> responses at 1, 2, 5 and 100µM HC030031(Figure 5:9 C,D). The partial blockade of cinnamaldehyde-induced TRPA1 activation by HC030031 demonstrated more of a concentration-dependent profile with an IC<sub>50</sub> of 7.12 ± 1.34µM, (AITC-induced TRPA1 activation; IC<sub>50</sub> of 19.53 ± 1.82µM) and suggests that HC030031 is a more potent antagonist of cinnamaldehyde-induced TRPA1 sensitization or, that at high concentrations of AITC, HC030031 can block other targets besides TRPA1.

## (2) TRPV4

The activation of the tDPSC-TRPV4 channels by GSK1016790A was also concentration-dependent (Figure 5:9A). In a similar context, the measured response of the tDPSCs to the application of graded concentrations of hypotonic solution also illustrated sensitivity. The observed hypotonicity-induced [Ca<sup>2+</sup>]<sub>i</sub> responses were significant, with peak responses following the application of 40% hypotonic solution ( $p^{***}= 0.001$ ) (Figure 5:8B). Initially thought, was that this might be linked to TRPV4 channel activation, in keeping with work done by other groups, which demonstrated that the TRPV4 channel is responsive to changes in hypo- and hypertonicity (Liedtke and Friedman 2003; Vriens, Watanabe et al. 2004; Todd 2010). However, the data from the

inhibition experiments showed otherwise. TRPV4 activation by GSK1016790A was completely abolished by 2 $\mu$ M HC067047 in a concentration-dependent manner as shown in Figure 5:9A ( $IC_{50}$  of  $116.1 \pm 1.56$ nM). Conversely, only a partial abolition of 40% hypotonic solution induced TRPV4 activation was demonstrated by altered  $[Ca^{2+}]_i$  responses following the application of 20 - 500nM HC067047 (Figure 5:9B). The inability of HC067047 to completely antagonize tDPSC-TRPV4 following hypotonic stimulation suggests that GSK1016790A- and hypotonic stimulation of the TRPV4 do not operate via the same  $Ca^{2+}$  influx activation pathways, or that hypotonic challenge can activate channels other than TRPV4. TRPV4 has always been described as a polymodal channel with various groups showing its activation following hypotonic stimulation to be dependent on different pathways such as the activation of the tyrosine kinase (Julius and Basbaum 2001) or the phospholipase  $A_2$  pathway (Vriens, Watanabe et al. 2004). Most recently, work carried out by Jin and colleagues on mouse cortical duct cells showed that GSK1016790A-TRPV4 activation was stable, dose-dependent and independent of the influence of extracellular  $Ca^{2+}$  unlike hypotonicity-induced TRPV4 activation which showed a transient dependency on extracellular  $Ca^{2+}$  (Todd 2010)..

### (3) TRPM8 and TRPV1

There were no responses generated by capsaicin (TRPV1) and icilin (TRPM8), even at maximum concentrations of 10 $\mu$ M capsaicin and 10 $\mu$ M icilin (Figure 5:8 E, F). This confirmed our initial findings that showed non-responsive tDPSC-TRPV1 and the absence of TRPM8 expression by the tDPSCs.

In summation, only the GSK1016790A-induced TRPV4 activity showed a complete inhibition following application of its antagonist HC067047.

#### **5.4.5 TRP channel-evoked ATP release**

Following our earlier supposition in Chapter 1 that the odontoblasts might also have an intermediary role in the nociception through the release of a chemical



mediator such as ATP, we performed ATP-release experiments. The data obtained showed that TRPA1 agonist AITC evoked significant levels of ATP release by the tDPSCs (Figure 5:10A). It could be suggested that the previously observed  $[Ca^{2+}]_i$  responses mediated by this agonist might be directly linked to the evoked ATP release as studies in guinea pig and human respiratory tissues have demonstrated that TRPA1 stimulation induces ATP release in response to reactive oxidative species (ROS) (Treede 1999). For the purposes of our findings in this study, the data can be corroborated by for instance, the measurement of ATP release by the tDPSCs following inhibition by a TRPA1 antagonist, such as HC030031. Unfortunately owing to time constraints, we were unable to undertake these additional experiments. In a similar vein, there was no significant ATP release evoked by TRPA1 activation following stimulation by cinnamaldehyde and TRPV4 activation with GSK1016790A and 40% hypotonic solution stimulation (Figure 5:10B, C and D). This would suggest that the absence of an effect of TRPA1 and V4 activation by these agonists on ATP release.

#### 5.4.6 tDPSC expression of tachykinin receptors

We were able to demonstrate a functional correlation between the activation of tachykinin receptors (NK1R and NK2R) and expression of mRNAs TRPA1, V1 and V4. Previous work has demonstrated the expression of the tachykinin receptors NK1R and NK2R, in rat oral tissue (Fristad, Vandevska-Radunovic et al. 1999; Fristad, Vandevska-Radunovic et al. 2003). Using radio immunoassay techniques, Caviedes-Bucheli and colleagues also demonstrated the presence of these receptors in human pulpal tissues (Caviedes-Bucheli, Muñoz et al. 2008). However, the problem was that the technique used did not allow for a clear distinction between the receptors identified. In this study, we used a different approach. The presence of mRNA for both the NK1 and NK2 receptors was demonstrated by RT-PCR. The relative mRNA expression levels of both SP receptors was analysed over 60 passages using qPCR demonstrating the continued expression of both receptors by the tDPSCs with a much lower level of NK2 receptor mRNA expression (Figure 5.5D, E). Following the establishment of a TRP channel transcript profile (described earlier), we were able to show a significant modulation of TRPA1 and V4 mRNA expression following pre-exposure to selected concentrations of

SP ( $10^{-8}$ M) (Figure 5.5A, C). This demonstrated responsiveness to SP, a well-documented tachykinin peptide released following noxious stimulation (Awawdeh, Lundy et al. 2002; Caviedes-Bucheli, Gutierrez-Guerra et al. 2007; Caviedes-Bucheli, Muñoz et al. 2008; Caviedes-Bucheli, Azuero-Holguin et al. 2011; Caviedes-Bucheli, Moreno et al. 2011) and would also suggest a possible regulatory relationship between SP and TRPA1-TRPV4 expression (and perhaps function).

#### 5.4.8 Summary

The data obtained in this study clearly shows the expression of functional TRPA1 and TRPV4 channels in the DPSCs. There is a lack of experimental evidence in the literature to show a definitive “relationship” between the odontoblasts and nerve fibres. However, the role of the odontoblast in the detection of noxious stimuli sounds is plausible as studies showing the expression of ion channels in the human odontoblast cell membrane have been published (Magloire, Lesage et al. 2003; Allard, Magloire et al. 2006; El Karim, Linden et al. 2010; Gibbs, Melnyk et al. 2011; Solé-Magdalena, Revuelta et al. 2011). The demonstration of tDPSC-TRPA1 and V4 functionality in this study (both of which have been shown to exhibit mechano-sensory features in studies on murine DRGs (Brierley, Castro et al. 2011) and rat odontoblasts (Son, Yang et al. 2009)), and the demonstration of mechano-sensory proteins expressed by odontoblasts by other research groups (such as TREK-1  $K^+$  channels (Magloire, Lesage et al. 2003), stretch-activated  $K^+$  channels (Allard, Couble et al. 2000) and acid sensing ion channels, ASICs (Solé-Magdalena, Revuelta et al. 2011)), supports the supposition outlined in the introduction section of this chapter, that the nociceptive function of the odontoblast is primarily mechano-sensation. The demonstrated increase in relative tDPSC-mRNA expression for TRPA1, V1 and V4 following the application of SP lends credence to this hypothesis. SP as part of the neurogenic inflammation response process is released from SP-containing nerve fibres which supply pulpal vasculature (Rodd and Boissonade 2000; Rodd and Boissonade 2003), causing an increase in pulpal blood flow, permeability and ultimately contributing to the exudation of fluids and increased interstitial tissue pressure (Vongsavan and Matthews 1992; Heyeraas, Kim et al. 1994; Holzer 1998). It has also

been suggested that there is an associated increase in outward dentinal fluid flow (Vongsavan and Matthews 1992; Matthews and Vongsavan 1994; Lin, Luo et al. 2011). It is our opinion that this sequence of events may be linked to the proposed mechanosensory functions of the tDPSC-TRPA1/TRPV4, especially TRPV4 whose role as a transducer of osmotic pressure (direct stretch activation or via the action of fatty acid metabolites) as well as its response to mechanical hyperalgesia associated with inflammation is well documented.

# General discussions and conclusions

---

6

## General discussions and conclusions

### 6.1 Summary

The primary objective of the work presented in this thesis has been to demonstrate the expression of sensory transducer proteins by human odontoblasts, which are involved in mechano-nociception. The currently accepted paradigm of dental pain is that dentinal fluid movements induced by external stimuli are detected by mechanoreceptors present on dental sensory neurons. This theory of an “indirect” detection of external stimuli in concert with the non-neuronal odontoblast cell population in the dental pulp is a supposition based on the location of the odontoblasts at the dentine-pulp border. The projection of the odontoblast processes into the dentinal tubules places them in close proximity to nerve fibre endings present in the dentinal tubules, where both structures are surrounded by dentinal fluid (Brannstrom and Astrom 1964; Närhi, Jyväsjärvi et al. 1992; Byers and Närhi 1999; Maurin, Couble et al. 2004). The mechanical displacement of the dentinal fluid in these tubules is thought to lead to the generation of pain sensations and transduced to the unmyelinated sensory nerve endings (Avery and Rapp 1959; Brannstrom and Astrom 1972).

While there is little evidence to suggest any synaptic communication between the odontoblasts and these nerve endings (Alfaqeeh and Anil 2011), a number of research groups have published data that describes the expression of selective sodium, potassium and calcium cation channels, which may be involved in this mechano-transductive process (Davidson 1993; Davidson 1994; Allard, Magloire et al. 2006; Magloire, Couble et al. 2009). Studies performed on non-dental animal and human tissues also describe how the influx of calcium cations causes the depolarisation of aggregations of trans-membrane protein domains which have been described as transient receptor potential (TRP) channels (Caterina, Schumacher et al. 1997; Clapham 2003; Story, Peier et al. 2003; Ramsey 2006). The expression of different classes of these TRP channels has been demonstrated in murine dental afferent neurones (Park, Kim et al. 2006), as well as in human dental tissues (El Karim, Linden et al. 2010; El Karim, Linden et al. 2011; Gibbs, Melnyk et al. 2011; Solé-Magdalena,

Revuelta et al. 2011). Our data shows the expression of the mechano-sensitive TRP channels TRPA1 and TRPV4 by the odontoblast-like cells as well as the novel demonstration of TRPV4 function. This lends further support to the mechanical stimulation based premise of the hydrodynamic theory.

## 6.2 Suggested modifications to experimental techniques

While the work presented here has identified a population of odontoblast-like cells derived from dental pulp, it is important to note that there are other methodologies that could DPC isolation and characterization. Following the sieving of pulp tissue lysates as described in Chapter 3, the use of fibronectin-coated culture plates in plating the cells, which has been described as an effective cell colony selection technique by Waddington and colleagues (Waddington, Youde et al. 2009) could have been adopted. The premise for this supposition is evident in the literature as fibronectin (a matrix protein) as demonstrated by Sottile and colleagues in mouse embryo cells influences cell adhesion and growth *in vitro* (Sottile and Chandler 2005). There is also still scope for further analysis as with the suggested existence of stem cell niches within the dental pulp (Sloan and Waddington 2009; Waddington, Youde et al. 2009), the identification of the exact location of these niches would aid in the direct sourcing and isolation of dental pulp stem cell populations. Work recently published on dental pulp cell isolation in mice described the targeting of Wnt-1 marked cells, which were of neural crest origin and showed characteristics of the odontoblast phenotype (Zartman, McWhorter et al. 2002). This might be a more efficient means of niche-specific DPC isolation from the pulp.

Downstream experiments to determine cell survival rates such as DNA activity assays are limited as formation of fluorescent complexes between DAPI and DNA are dependent on the amount of adenine-thymine and guanine-cytosine content (Katouziansafadi, Cremet et al. 1989). As there is no effective means of determining percentage of nucleotide material left in cell the after lysis by the freeze-thaw method described in Chapters 2 and 3, there is room for error in measurements. While the methods we used were relatively consistent, a more up-to date method would be the

use of 5-bromo-2'-deoxyuridine (BrdU)-labeling to not only monitor cell proliferation but also aid in niche identification (Halvorsen, Beattie et al. 2000; Jeon, Kang et al. 2011). In terms of future work the latter is of particular interest considering that the choice of adult third molars in this study as a source for the DPSCs was informed by the need to have access to a developmentally young pool of undifferentiated progenitor cells (Gronthos, Mankani et al. 2000; Liu, Gronthos et al. 2006; Tirino, Paino et al. 2011).

Senescent cells have been described as possessing phenotypic features such as an increased cell size, distinctive flat morphology, wide changes in gene expression, and activity of senescence-associated  $\beta$ -galactosidase (Ball and Levine 2005; Itahana, Campisi et al. 2007). While our studies did demonstrate the latter, following immortalization it would have been interesting to have had performed telomere length analysis to determine if the expression of the senescent phenotype was linked to telomere shortening. This is owing to evidence in other cell types which has shown the presence of telomere-independent senescence (Ball and Levine 2005) as well as the failure of hTERT transfection to prevent senescence (Halvorsen, Beattie et al. 2000). There is also recent evidence suggestive of other senescence pathways in dental pulp cells isolated from human teeth that are more linked to oxidative culture stress and p53 expression, and are attenuated by non-hTERT methodologies (Choi, Lee et al. 2012). In the context of the work presented in this thesis, while the methodology employed in this study did not allow for telomere length assessment, the use of chemiluminescent assays for example has successfully being used to demonstrate telomere in cells isolated from the dental pulp (Jeon, Kang et al. 2011) and can be employed in future experimental work to drive this aspect of the study further.

Finally, the presented data in this thesis on the studied TRP channels provides concrete evidence of tDPSC-TRPA1 and tDPSC-TRPV4 functional expression. To get a clearer impression of the polymodal nature of these TRP channels as well as the underlying mechanism of channel activation, it would be interesting to investigate the influences of other candidate stimuli such as pH changes, stretch and temperature changes on their activities. We had earlier suggested that ATP might act as a

nociceptive “secondary messenger” in the process of response to noxious stimuli. Early work on TRPV1 channels in rat bladders and TRPV4 in mouse urothelial tissues has identified ATP release, following channel activation which caused bladder contractile responses via the activation of P2X3 receptors on sensory neurones (Dubner R 1978; Svensson P 2004). There is evidence in the literature to support this theory as data from mouse urothelial cell studies demonstrated the modulation of afferent nerve impulses in response to ATP release secondary to TRPV1 channel activity (Sessle 2000). Our preliminary investigations into the effects of the agonist-induced activity of the tDPSC-TRPA1 channels demonstrated evidence of ATP release, findings which were in keeping with those presented by other research groups following work on animal and human tissues (Treede 1999; Basbaum, Bautista et al. 2009). To develop a better understanding of the roles of TRP channel activation in the nociceptive response process, investigation of tDPSC-TRPA1 and –TRPV4 antagonist-modulated ATP release would be the next step as it would shed more light on the proposed secondary messenger role of ATP. It is our opinion that the demonstration of an absence of evidence suggestive of tDPSC-TRPM8 mRNA expression and the demonstration of a capsaicin-insensitive tDPSC-TRPV1 RNA splice variant is an area for further research. Owing to the polymodal nature of TRPV1 channel activation (Caterina, Schumacher et al. 1997; Caterina, Rosen et al. 1999), it would most probably focus on the testing of TRPV1 channel modulation by changes in tDPSC-cell membrane currents by means of electrophysiological studies (patch-clamp experiments) and as well as the influence of temperature-driven tDPSC-TRPV1 activity.

### **6.3 Pain associated gene expression in painful and non painful pulps**

One of the primary features of odontoblast-like cells is the production of the protective barrier of reparative dentine following destruction of the outer hull of enamel by caries (Smith, Scheven et al. 2012). The role of odontoblasts in the development of inflammatory responses (induced by caries) through the production of chemokines and cytokines has been demonstrated in *in vitro* human odontoblast culture models (Durand, Flacher et al. 2006). These chemokines and cytokines are involved in the activation of immune system cells (such as neutrophils, macrophages,



natural killer cells) and may modulate both central and peripheral pain processing by sensitizing nociceptors through inflammatory mediators (Sessle 2000) and / or direct sensory nerve sensitization (Svensson P 2004). Some of these identified in odontoblasts include cytokines such as IL1b and TNFa (Treede 1999; Sessle 2005), and the chemokines, CCL2 and CXCL2 (Sessle 2005). As part of a preliminary study, to form the basis for future work, we analyzed inflammatory mediator profiles of human teeth, using custom-made gene array cards. The objective was to identify significant transcriptional changes in “pain-associated” gene expression in pain-free and painful pulps obtained from extracted adult teeth of consenting patients. This would provide a guide for further investigations of the roles played by these upregulated genes in the modulation of dental pain perception.

The microarray analyses considered the expression of inflammatory chemokines and cytokines in twelve human pulp samples obtained from extracted painful (n=6) and non-painful (n=6) teeth. The transcript data obtained was normalised to the means of the house keeping genes used and the fold change values are representative of relative changes in transcript levels between the painful and non-painful samples. The relative changes in transcript levels were measured from CT values (These are fluorescent readings taken at predefined threshold set within the exponential amplification phase of microarray PCR, where 1 unit CT value represents a doubling of target transcript. This means that a lower CT value denotes a higher level of gene expression). The methodology and analysis for these experiments were adapted from work by Dawes and colleagues (Dawes, Calvo et al. 2011). From this microarray screening, the data obtained (Table 5:2) showed the mean fold changes of the tested transcripts, with 13 genes down-regulated (underlined), 49 genes up-regulated and 30 genes which showed no signs of transcriptional regulation (represented by the zero values).

### **6.3b Microarray findings**

With the identification of TRP channel expression in human dental pulp, the next question would be if an increase in TRP channel expression would mean an increase in pain. This might give an indication of the contributory roles they play in the generation of responses to noxious stimuli. In earlier sections, we presented data

showing a significant modulation of TRPA1 and V4 function following the introduction of exogenous SP, suggesting an alteration of TRP channel function in the odontoblast cells. Some groups have demonstrated the altered expression of TRPV1 in trigeminal sensory neurons, which has been tentatively suggested as contributing to neuropathic (Biggs, Yates et al. 2007; Kim, Park et al. 2008) and inflammatory (Morgan, Rodd et al. 2005) oral pain states. The odontoblasts are considered the first line of defence against bacterial ingress into the dentine from the oral cavity by virtue of their anatomical position at the dentine-pulp border. The odontoblasts also express proteins which code for Toll-like receptors such as TLRs 2-9, which have been demonstrated in human odontoblast cell cultures (Durand, Flacher et al. 2006; Farges, Keller et al. 2009) and are thought to aid the immune response process (Takeda, Kaisho et al. 2003). These TLRs mediate the secretion of chemokines and cytokines which attract and activate cells (such as neutrophils and macrophages) involved in the inflammatory response (Zlotnik and Yoshie 2000; Yoshie, Imai et al. 2001) in which the dilation of pulpal blood vessels and fluid exudation into surrounding tissue spaces. It has been suggested that this fluid build-up could put pressure on pulpal nerve endings (C. Yu 2007). A wide range of inflammatory mediators have been shown to increase in bacteria-infected odontoblast-like cell culture systems, some of these include the C-C chemokine ligands CCL2 and CCL7 (Durand, Flacher et al. 2006; Farges, Keller et al. 2009), CCL20 (Takahashi, Nakanishi et al. 2008), CXCL2 and CXCL10 (Durand, Flacher et al. 2006), interleukins 1L $\beta$  (Horst, Horst et al. 2011), IL2 (Rauschenberger, Bailey et al. 1997), IL8 (Levin, Rudd et al. 1999) and tumour necrosis factor TNF- $\alpha$  (Kokkas, Goulas et al. 2007) which all influence the process of immune responses within pulpal tissue. Human odontoblast cell cultures studies have demonstrated that the exogenous application of TGF-B1 (which is involved in the repair of the dentine following injury) inhibits the expression of some of these inflammatory cytokines such as IL-8 and TNF-A as well as TLR2, TLR4. It is possible that with a shift in homeostatic balance towards uncontrolled inflammation as would occur in pulpitis, that there might be a generation of inflammatory pressure-induced nociceptive responses. It is possible therefore that some of these mediators may indirectly sensitize the TRP channels, which may then in turn be responsible for the detection of painful stimuli. The most likely candidates in the pulp would be the mechanosensitive TRP channels (such as TRPV4) owing to

accumulation of exudates in surrounding tissues which could put pressure on the odontoblasts and cause stretch activation of these channels (as demonstrated in mouse urothelium cells where the TRPV4 channels responded to bladder filling (Everaerts, Vriens et al. 2010; Janssen, Hoenderop et al. 2011). Earlier work considering the role of TRP channels in inflammation done by Ceppa and colleagues on inflamed mice pancreatic cells, demonstrated a 2-fold increase in c-fos positive dorsal horn neurons between positions T8 and T10, illustrating the activation of pain signalling pathways arising from the mice pancreas (Ceppa, Cattaruzza et al. 2010). This cerulein-induced response (cerulein is a decapeptide used to induce pancreatic inflammation in experimental animals (Lerch and Adler 1994)) was much greater in TRPA1 and V4-wild type mice in comparison to TRPA1 and V4-knockouts used in this study. This gives further support to the possible role of the TRP channels in inflammatory pressure-induced nociception.

From the microarray data we obtained in this study, only one of the down-regulated inflammatory gene transcripts, IL5 showed a  $\leq -2$  fold change and 5 of the up-regulated transcripts showed a  $\geq +2$  fold change (BDNF, CCL8, CCL18, IL28A, IL31 and IL34) (Table 5:2). In a recent study by Farges et al (using human pulp samples), there was no evidence to demonstrate any meaningful transcriptional change (up-regulation or down-regulation) of IL5 which would suggest that it may not be involved in the pulpal inflammatory response (Farges, Carrouel et al. 2011). However, in the same year, Horst and colleagues showed a  $\geq +2$  fold up regulation in IL5 expression in RNA extracted from odontoblast layer cells of carious teeth (Horst, Horst et al. 2011). It is possible that differences in experimental methodologies may account for the variable expression of this cytokine. Based on our findings, those of other groups and its demonstrated role in the pathogenesis of allergic diseases such as allergic rhinitis and asthma (it is responsible for eosinophil and mast cell activation) in animal studies (Shen, Ochkur et al. 2003), it is possible that it may not play a major role in the development of a response to noxious stimuli in the human pulp. While CCL8 was the only up-regulated pro-inflammatory gene in this study that has been previously demonstrated in human odontoblast cell cultures (Horst, Horst et al. 2011), most

interesting was the up-regulation of IL34. This cytokine is involved in osteoclastogenesis (bone remodelling), and the differentiation of monocytes and

GENE	NON-PAINFUL HUMAN PULPS						PAINFUL HUMAN PULPS					
	1	2	3	4	5	6	1	2	3	4	5	6
ACTB	16.8	18.4	17.5	16.8	18.2	18.7	15.7	17.4	17.4	20.8	18.4	19.1
B2M	20.3	19.1	19.0	19.2	19.3	19.8	16.5	19.2	18.5	23.6	20.1	20.8
GAPDH	17.8	18.3	17.6	17.4	18.2	18.6	16.0	17.7	17.4	21.5	18.4	19.0
18S	13.3	13.1	13.2	13.1	13.4	13.5	13.9	13.1	13.0	14.1	13.6	13.8
GENE	1	2	3	4	5	6	1	2	3	4	5	6
*CCL8	38	33.3	33.1	38	36.8	38	29.2	32.1	32.3	38	38	38
*CCL18	38	38	37.6	38	35.9	33.0	38	38	38	38	32.1	32.7
*IL34	33.7	25.6	24.8	31.0	33.2	31.4	22.5	25.4	24.8	33.5	29.9	38
*IL28A	38	38	38	38	36.4	37.3	38	38	38	38	33.5	35.0
*IL31	38	38	38	38	38	36.3	38	34.7	38	38	36.1	33.8
*BDNF	34.8	33.7	31.0	38	33.6	34.3	29.0	32.0	31.5	38	32.3	33.5
IL1B	38	34.7	35.1	38	36.2	35.3	30.6	35.0	34.3	38	36.6	34.9
CCL27	34.0	33.8	33.6	35.4	35.8	35.2	30.7	33.4	33.0	38	38	35.9
CCL4	38	38	35.3	35.5	35.0	36.2	38	34.9	38	38	34.6	38
CCL3	33.0	38	38	33.5	29.0	28.7	34.0	38	38	38	27.5	28.3
IRPV4	28.0	27.1	26.0	27.0	31.9	30.8	24.3	26.1	26.5	32.0	31.6	31.8
GENE	1	2	3	4	5	6	1	2	3	4	5	6
CCL26	33.7	35.3	38	33.8	34.0	36.2	34.1	37.2	36.7	38	33.8	34.9
EDN1	24.2	25.7	24.8	23.9	28.1	29.8	22.8	24.6	24.8	28.8	29.4	30.6
IL12A	26.9	31.0	29.0	27.4	30.2	31.9	27.3	29.4	29.9	32.7	30.4	31.6
XCL1.XCL2	38	28.3	38	36.5	37.7	30.4	33.5	32.0	38	38	32.7	38
IL11	26.9	29.3	28.5	26.0	29.7	31.2	25.8	28.7	28.6	32.0	30.2	32.0
IL12B	35.8	31.4	36.3	33.7	35.4	38	32.9	35.0	35.1	36.4	38	38
IL1A	38	28.8	38	35.9	32.5	38	31.6	33.9	34.1	38	35.5	38
CSF3	38	38	38	36.0	38	35.2	36.9	38	38	38	35.9	38
IL18	27.4	38	34.3	34.6	38	38	35.2	38	38	36.7	25.6	38
*IL5	25.4	26.0	33.2	38	34.8	38	38	36.2	38	38	34.4	38
IRPA1	25.7	26.3	25.1	24.6	26.9	25.8	23.4	25.8	25.3	31.4	25.5	26.4

Table 5-2: Raw Ct values for the four housekeeping genes (highlighted in yellow: glyceraldehyde 3-phosphate dehydrogenase GAPDH, 18s, beta-actin ACTB and beta-2-microglobulin B2M), and ten of the highest up-regulated (underlined) and down-regulated (italicised) inflammation mediating genes. CCL: chemokine (CC-motif) ligand/IL: Interleukin/BDNF: Brain derived neurotrophic factor/CXCL: chemokine (CXC-motif) ligand/EDN1: Endothelin-1/ CSF: Colony stimulating factor. NA: Not detected.  $\geq 50\%$  CT expression for each inflammatory mediator was used to define gene expression (\* =  $\geq +2$ - fold change/# =  $\leq -2$  fold change).

GENE	SEQUENCE
CCL8	Forward: TATCCAGAGGCTGGAGAGCTAC Reverse: TGGAATCCCTGACCCATCTCTC
CCL18	Forward: GTTGACTATTCTGAAACCAGCCC Reverse: GTCGCTGATGTATTTCTGGACCC
IL34	Forward: CCAAGGTGGAATCCGTGTTGTC Reverse: CACCTCACAGTCCTGCCAGTTT
IL28A	Forward: TCGCTTCTGCTGAAGGACTGCA Reverse: CCTCCAGAACCTTCAGCGTCAG
IL31	Forward: CGTCCGTTTACTACGACCAAGTG Reverse: GGCAGCGTGAATTCTGGGACA
BDNF	Forward: CATCCGAGGACAAGGTGGCTTG Reverse: GCCGAACCTTCTGGTCCTCATC

Table 5-3: List of primer sequences of the upregulated transcripts

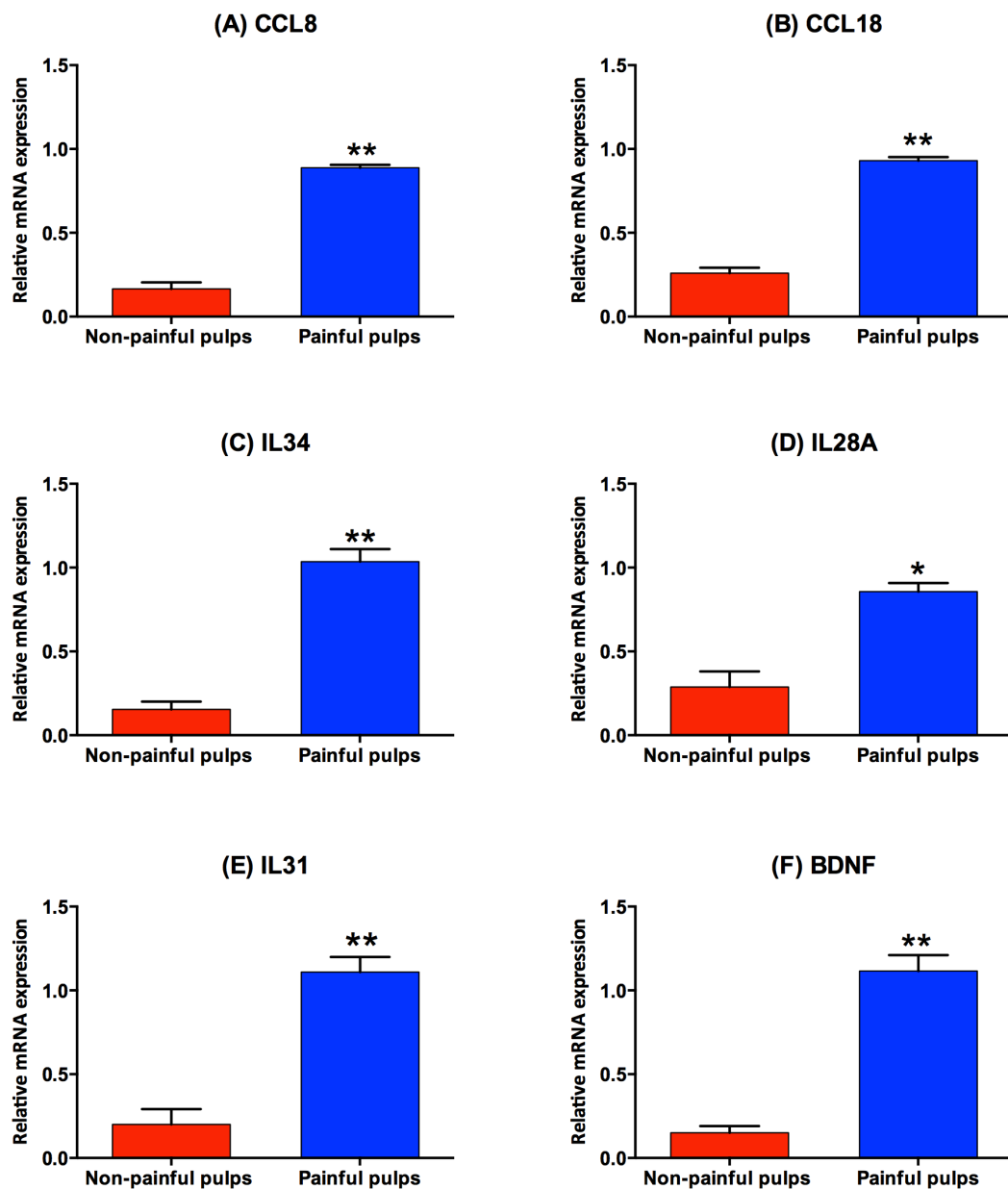


Figure 5:13: Validation of up-regulated transcripts as measured by the microarray cards with real-time qPCR. Values are reported as relative fold change in cDNA transcription, which were normalised to the housekeeping gene. The data is represented as mean  $\pm$  S.E and a Student t test was performed to compare for significant differences between the non-painful pulps (control) and the painful pulps for the respective transcripts (\* $p < 0.05$ , \*\* $p < 0.01$ ,  $n=3$ ).

myeloid cells (which are important to the innate immune response process)(Chen, Buki et al. 2011). The classical pro inflammatory cytokines IL-1 $\beta$  and BDNF, while expressing fold changes less than two-fold, were up-regulated in this study as well, findings corroborated by work done by other groups (Durand, Flacher et al. 2006; Farges, Keller et al. 2009; Farges, Carrouel et al. 2011; Horst, Horst et al. 2011). We would like to state that this microarray data is representative of preliminary experimental work and as part of future experiments, it would be interesting to study the effects of the subject transcripts (the up-regulated cytokines) on TRP channel expression and function. While the increase in the relative expression for 6 of the top up-regulated inflammatory mediators using qPCR was demonstrated in pulp samples (n=3) (Fig 5.13), owing to small number of tested samples this is an aspect of the experimental work that needs to be further expanded upon.

## 6.4 Conclusions

The findings presented in this thesis show the expression of pain-related receptors and channels in immortalised human DPSCs, which express odontoblastic markers. This *in vitro* work highlights the successful isolation and transformation of the DPSCs from human pulpal tissue samples without the introduction of untoward phenotypic features. The novel demonstration of the functional tDPSC-TRPV4 channel alongside the detection of tDPSC-TRPA1 function in the tDPSCs is the beginning of the research geared at the establishing a better understanding of the pathophysiology of dental pain and hypersensitivity.

# References

---

**7**

---

## References

- (2011). "The Adult Dental Health Survey 2009." Primary Dental Care **18**(3): 99-100.
- Abe, J., H. Hosokawa, et al. (2006). "Ca<sup>2+</sup>-Dependent Pkc Activation Mediates Menthol-Induced Desensitization of Transient Receptor Potential M8." Neuroscience Letters **397**(1-2): 140-144.
- About, I., M. J. Bottero, et al. (2000). "Human Dentin Production in Vitro." Experimental Cell Research **258**(1): 33-41.
- Ahlquist, M., O. Franzen, et al. (1994). "Dental Pain Evoked by Hydrostatic Pressures Applied to Exposed Dentin in Man: A Test of the Hydrodynamic Theory of Dentin Sensitivity." J Endod **20**(3): 130-134.
- Alessandri-Haber, N., E. Joseph, et al. (2005). "Trpv4 Mediates Pain-Related Behavior Induced by Mild Hypertonic Stimuli in the Presence of Inflammatory Mediator." Pain **118**(1-2): 70-79.
- Alfaqeeh, S. A. and S. Anil (2011). "Osteocalcin and N-Telopeptides of Type I Collagen Marker Levels in Gingival Crevicular Fluid During Different Stages of Orthodontic Tooth Movement." Am J Orthod Dentofacial Orthop **139**(6): e553-559.
- Alge, D. L., D. Zhou, et al. (2010). "Donor-Matched Comparison of Dental Pulp Stem Cells and Bone Marrow-Derived Mesenchymal Stem Cells in a Rat Model." J Tissue Eng Regen Med **4**(1): 73-81.
- Allard, B., M. L. Couble, et al. (2000). "Characterization and Gene Expression of High Conductance Calcium-Activated Potassium Channels Displaying Mechanosensitivity in Human Odontoblasts." Journal of Biological Chemistry **275**(33): 25556-25561.
- Allard, B., H. Magloire, et al. (2006). "Voltage-Gated Sodium Channels Confer Excitability to Human Odontoblasts: Possible Role in Tooth Pain Transmission." J. Biol. Chem. **281**(39): 29002-29010.
- Alvarado, L. T., G. M. Perry, et al. (2007). "Trpm8 Axonal Expression Is Decreased in Painful Human Teeth with Irreversible Pulpitis and Cold Hyperalgesia." Journal of Endodontics **33**(10): 1167-1171.
- Amaya, F., K. Oh-Hashi, et al. (2003). "Local Inflammation Increases Vanilloid Receptor 1 Expression within Distinct Subgroups of Drg Neurons." Brain Research **963**(1-2): 190-196.
- Andrew, D. and B. Matthews (2000). "Displacement of the Contents of Dentinal Tubules and Sensory Transduction in Intradental Nerves of the Cat." The Journal of Physiology **529**(3): 791-802.
- Arai, F., O. Ohneda, et al. (2002). "Mesenchymal Stem Cells in Perichondrium Express Activated Leukocyte Cell Adhesion Molecule and Participate in Bone Marrow Formation." Journal of Experimental Medicine **195**(12): 1549-1563.
- Armstrong, P. B. and M. T. Armstrong (1984). "A Role for Fibronectin in Cell Sorting." Journal of Cell Science **69**(1): 179-197.
- Arthur, A., G. Rychkov, et al. (2008). "Adult Human Dental Pulp Stem Cells Differentiate toward Functionally Active Neurons under Appropriate Environmental Cues." Stem Cells **26**(7): 1787-1795.
- Atari, M., C. Gil-Recio, et al. (2012). "Dental Pulp of the Third Molar: A New Source of Pluripotent-Like Stem Cells." Journal of Cell Science **125**(14): 3343-3356.
- Aubin, J. E., F. Liu, et al. (1995). "Osteoblast and Chondroblast Differentiation." Bone **17**(2): S77-S83.



- Avery, J. K. and R. Rapp (1959). "An Investigation of the Mechanism of Neural Impulse Transmission in Human Teeth." *Oral surgery, oral medicine, and oral pathology* **12**(2): 190-198.
- Awawdeh, L., F. T. Lundy, et al. (2002). "Quantitative Analysis of Substance P, Neurokinin a and Calcitonin Gene-Related Peptide in Pulp Tissue from Painful and Healthy Human Teeth." *Int Endod J* **35**: 30 - 36.
- Bae, Y. C., J. M. Oh, et al. (2004). "Expression of Vanilloid Receptor Trpv1 in the Rat Trigeminal Sensory Nuclei." *Journal of Comparative Neurology* **478**(1): 62-71.
- Ball, A. J. and F. Levine (2005). "Telomere-Independent Cellular Senescence in Human Fetal Cardiomyocytes." *Aging Cell* **4**(1): 21-30.
- Bandell, M., G. M. Story, et al. (2004). "Noxious Cold Ion Channel Trpa1 Is Activated by Pungent Compounds and Bradykinin." *Neuron* **41**(6): 849-857.
- Barritt, G. and G. Rychkov (2005). "Trps as Mechanosensitive Channels." *Nat Cell Biol* **7**(2): 105-107.
- Basbaum, A. I., D. M. Bautista, et al. (2009). "Cellular and Molecular Mechanisms of Pain." *Cell* **139**(2): 267-284.
- Batouli, S., M. Miura, et al. (2003). "Comparison of Stem-Cell-Mediated Osteogenesis and Dentinogenesis." *Journal of Dental Research* **82**(12): 976-981.
- Bautista, D. M., S. E. Jordt, et al. (2006). "Trpa1 Mediates the Inflammatory Actions of Environmental Irritants and Proalgesic Agents." *Cell* **124**(6): 1269-1282.
- Bautista, D. M., J. Siemens, et al. (2007). "The Menthol Receptor Trpm8 Is the Principal Detector of Environmental Cold." *Nature* **448**(7150): 204-208.
- Beausejour, C. M., A. Krtolica, et al. (2003). "Reversal of Human Cellular Senescence: Roles of the P53 and P16 Pathways." *EMBO J* **22**(16): 4212-4222.
- Beguekirk, C., A. J. Smith, et al. (1992). "Effects of Dentin Proteins, Transforming Growth-Factor Beta-1 (Tgf-Beta-1) and Bone Morphogenetic Protein-2 (Bmp2) on the Differentiation of Odontoblast Invitro." *International Journal of Developmental Biology* **36**(4): 491-503.
- Bellinger, D. L., D. Lorton, et al. (1996). "The Significance of Vasoactive Intestinal Polypeptide (Vip) in Immunomodulation." *Advances in Neuroimmunology* **6**(1): 5-27.
- Bender, I. B. (2000). "Pulpal Pain Diagnosis--a Review." *Journal of Endodontics* **26**(3): 175-179.
- Beneng, K., T. Renton, et al. (2010). "Cannabinoid Receptor Cb1-Immunoreactive Nerve Fibres in Painful and Non-Painful Human Tooth Pulp." *Journal of Clinical Neuroscience* **17**(11): 1476-1479.
- Beneng, K., T. Renton, et al. (2010). "Sodium Channel Na(V)1.7 Immunoreactivity in Painful Human Dental Pulp and Burning Mouth Syndrome." *Bmc Neuroscience* **11**.
- Berchtold, M., H. Brinkmeier, et al. (2000). "Calcium Ion in Skeletal Muscle: Its Crucial Role for Muscle Function, Plasticity, and Disease." *Physiol Rev* **80**: 1215 - 1265.
- Berridge, M. J. and R. F. Irvine (1984). "Inositol Trisphosphate, a Novel 2nd Messenger in Cellular Signal Transduction." *Nature* **312**(5992): 315-321.
- Bhatia, B., M. Jiang, et al. (2008). "Critical and Distinct Roles of P16 and Telomerase in Regulating the Proliferative Life Span of Normal Human Prostate Epithelial Progenitor Cells." *Journal of Biological Chemistry* **283**(41): 27957-27972.
- Biggs, J. (1999). "What the Student Does: Teaching for Enhanced Learning." *Higher Education Research & Development* **18**(1): 57-75.
- Biggs, J. E., J. M. Yates, et al. (2007). "Changes in Vanilloid Receptor 1 (Trpv1) Expression Following Lingual Nerve Injury." *European Journal of Pain* **11**(2): 192-201.
- Birder, L. A. and E. R. Perl (1994). "Cutaneous Sensory Receptors." *Journal of Clinical Neurophysiology* **11**(6): 534-552.
- Bleicher, F., M. L. Couble, et al. (1999). "Sequential Expression of Matrix Protein Genes in Developing Rat Teeth." *Matrix Biology* **18**(2): 133-143.

- Bleicher, F., H. Magloire, et al. (2008). Reelin and Odontogenesis
- Reelin Glycoprotein. S. H. Fatemi, Springer New York: 279-290.
- Bluteau, G., H. U. Luder, et al. (2008). "Stem Cells for Tooth Engineering." European Cells & Materials **16**: 1-9.
- Bodnar, A. G., M. Ouellette, et al. (1998). "Extension of Life-Span by Introduction of Telomerase into Normal Human Cells." Science **279**(5349): 349-352.
- Böker, W., Z. Yin, et al. (2008). "Introducing a Single-Cell-Derived Human Mesenchymal Stem Cell Line Expressing Htert after Lentiviral Gene Transfer." Journal of Cellular and Molecular Medicine **12**(4): 1347-1359.
- Bongenhielm, U., A. Hægerstrand, et al. (1995). "Effects of Neuropeptides on Growth of Cultivated Rat Molar Pulp Fibroblasts." Regulatory Peptides **60**(2-3): 91-98.
- Bonica, J. J. (1981). "Pain." Triangle **20**(1-2): 1-6.
- Boskey, A., L. Spevak, et al. (2000). "Dentin Sialoprotein (Dsp) Has Limited Effects on in Vitro Apatite Formation and Growth." Calcified Tissue International **67**(6): 472-478.
- Boskey, A. L. and R. Roy (2008). "Cell Culture Systems for Studies of Bone and Tooth Mineralization." Chemical Reviews **108**(11): 4716-4733.
- Bosshardt, D. D., S. Zalzal, et al. (1998). "Developmental Appearance and Distribution of Bone Sialoprotein and Osteopontin in Human and Rat Cementum." The Anatomical Record **250**(1): 13-33.
- Brain, S. D., T. J. Williams, et al. (1985). "Calcitonin Gene-Related Peptide Is a Potent Vasodilator." Nature **313**(5997): 54-56.
- Brannstrom, M. (1986). "The Hydrodynamic Theory of Dentinal Pain - Sensation in Preparations, Caries, and the Dentinal Crack Syndrome." Journal of Endodontics **12**(10): 453-457.
- Brannstrom, M. and A. Astrom (1964). "Study on Mechanism of Pain Elicited from Dentin." Journal of Dental Research **43**(4): 619-&.
- Brannstrom, M. and A. Astrom (1972). "Hydrodynamics of Dentine - Its Possible Relationship to Dentinal Pain." International Dental Journal **22**(2): 219-&.
- Brierley, S. M., J. Castro, et al. (2011). "Trpa1 Contributes to Specific Mechanically Activated Currents and Sensory Neuron Mechanical Hypersensitivity." The Journal of Physiology **589**(14): 3575-3593.
- Buckley, S., J. Coleman, et al. (2009). "The Educational Effects of Portfolios on Undergraduate Student Learning: A Best Evidence Medical Education (Beme) Systematic Review. Beme Guide No. 11." Medical teacher **31**(4): 282-298.
- Burkhardt, D. L. and J. Sage (2008). "Cellular Mechanisms of Tumour Suppression by the Retinoblastoma Gene." Nature Reviews Cancer **8**(9): 671-682.
- Butler, W. T. (1998). "Dentin Matrix Proteins." European Journal of Oral Sciences **106**: 204-210.
- Butler, W. T. and H. Ritchie (1995). "The Nature and Functional-Significance of Dentin Extracellular-Matrix Proteins." International Journal of Developmental Biology **39**(1): 169-179.
- Byers, M. R. (1984). "Dental Sensory Receptors." International Review of Neurobiology **25**: 39-94.
- Byers, M. R. and W. K. Dong (1983). "Autoradiographic Location of Sensory Nerve-Endings in Dentin of Monkey Teeth." Anatomical Record **205**(4): 441-454.
- Byers, M. R. and M. V. O. Narhi (1999). "Dental Injury Models: Experimental Tools for Understanding Neuroinflammatory Interactions and Polymodal Nociceptor Functions." Critical Reviews in Oral Biology & Medicine **10**(1): 4-39.
- Byers, M. R., H. Suzuki, et al. (2003). "Dental Neuroplasticity, Neuro-Pulpal Interactions, and Nerve Regeneration." Microscopy Research and Technique **60**(5): 503-515.
- C. Yu, P. A. (2007). "An Overview of the Dental Pulp: Its Functions and Responses to Injury." Australian Dental Journal **52**(s1): S4-S6.

- Calland, J. W., S. E. Harris, et al. (1997). "Human Pulp Cells Respond to Calcitonin Gene-Related Peptide in Vitro." *Journal of Endodontics* **23**(8): 485-489.
- Calvo, C. F., G. Chavanel, et al. (1992). "Substance-P Enhances IL-2 Expression in Activated Human T-Cells." *Journal of Immunology* **148**(11): 3498-3504.
- Campero, M., J. Serra, et al. (2001). "Slowly Conducting Afferents Activated by Innocuous Low Temperature in Human Skin." *Journal of Physiology-London* **535**(3): 855-865.
- Carney, S. A., H. Tahara, et al. (2002). "Immortalization of Human Uterine Leiomyoma and Myometrial Cell Lines after Induction of Telomerase Activity: Molecular and Phenotypic Characteristics." *Lab Invest* **82**(6): 719-728.
- Caterina, M. J., T. A. Rosen, et al. (1999). "A Capsaicin-Receptor Homologue with a High Threshold for Noxious Heat." *Nature* **398**(6726): 436-441.
- Caterina, M. J., M. A. Schumacher, et al. (1997). "The Capsaicin Receptor: A Heat-Activated Ion Channel in the Pain Pathway." *Nature* **389**(6653): 816-824.
- Caton, J., P. Bringas, et al. (2007). "Establishment and Characterization of an Immortomouse-Derived Odontoblast-Like Cell Line to Evaluate the Effect of Insulin-Like Growth Factors on Odontoblast Differentiation." *Journal of Cellular Biochemistry* **100**(2): 450-463.
- Cavanaugh, D. J., A. T. Chesler, et al. (2011). "Trpv1 Reporter Mice Reveal Highly Restricted Brain Distribution and Functional Expression in Arteriolar Smooth Muscle Cells." *The Journal of Neuroscience* **31**(13): 5067-5077.
- Cavanaugh, E. J., D. Simkin, et al. (2008). "Activation of Transient Receptor Potential A1 Channels by Mustard Oil, Tetrahydrocannabinol and Ca<sup>2+</sup> Reveals Different Functional Channel States." *Neuroscience* **154**(4): 1467-1476.
- Caviedes-Bucheli, J., N. Arenas, et al. (2005). "Calcitonin Gene-Related Peptide Receptor Expression in Healthy and Inflamed Human Pulp Tissue." *International Endodontic Journal* **38**(10): 712-717.
- Caviedes-Bucheli, J., M. M. Azuero-Holguin, et al. (2011). "Effect of Experimentally Induced Occlusal Trauma on Substance P Expression in Human Dental Pulp and Periodontal Ligament." *Journal of Endodontics* **37**(5): 627-630.
- Caviedes-Bucheli, J., J. E. Gutierrez-Guerra, et al. (2007). "Substance P Receptor Expression in Healthy and Inflamed Human Pulp Tissue." *International Endodontic Journal* **40**(2): 106-111.
- Caviedes-Bucheli, J., J. O. Moreno, et al. (2011). "The Effect of Orthodontic Forces on Calcitonin Gene-Related Peptide Expression in Human Dental Pulp." *Journal of Endodontics* **37**(7): 934-937.
- Caviedes-Bucheli, J., H. R. Muñoz, et al. (2008). "Neuropeptides in Dental Pulp: The Silent Protagonists." *Journal of Endodontics* **34**(7): 773-788.
- Ceppa, E., F. Cattaruzza, et al. (2010). "Transient Receptor Potential Ion Channels V4 and A1 Contribute to Pancreatitis Pain in Mice." *Am J Physiol Gastrointest Liver Physiol* **299**(3): G556-571.
- Cesare, P., L. V. Dekker, et al. (1999). "Specific Involvement of Pkc-E in Sensitization of the Neuronal Response to Painful Heat." *Neuron* **23**(3): 617-624.
- Cesare, P. and P. McNaughton (1996). "A Novel Heat-Activated Current in Nociceptive Neurons and Its Sensitization by Bradykinin." *Proceedings of the National Academy of Sciences* **93**(26): 15435-15439.
- Chai, Y., X. Jiang, et al. (2000). "Fate of the Mammalian Cranial Neural Crest During Tooth and Mandibular Morphogenesis." *Development* **127**(8): 1671-1679.
- Chan, S. and E. H. Blackburn (2004). "Telomeres and Telomerase." *Philosophical Transactions of the Royal Society of London Series B-Biological Sciences* **359**(1441): 109-121.
- Chaudhury, S., M. Bal, et al. (2011). "Akap150-Mediated Trpv1 Sensitization Is Disrupted by Calcium/Calmodulin." *Molecular Pain* **7**(1): 34.

- Chen, S., J. Gluhak-Heinrich, et al. (2009). "Runx2, Osx, and Dspp in Tooth Development." Journal of Dental Research **88**(10): 904-909.
- Chen, S., T. T. Gu, et al. (2002). "Spatial Expression of Cbfa1/Runx2 Isoforms in Teeth and Characterization of Binding Sites in the Dspp Gene." Connective Tissue Research **43**(2-3): 338-344.
- Chen, S., S. Rani, et al. (2005). "Differential Regulation of Dentin Sialophosphoprotein Expression by Runx2 During Odontoblast Cytodifferentiation." Journal of Biological Chemistry **280**(33): 29717-29727.
- Chen, Z., K. Buki, et al. (2011). "The Critical Role of Il-34 in Osteoclastogenesis." Plos One **6**(4).
- Chéry-Croze (1983). "Painful Sensation Induced by a Thermal Cutaneous Stimulus." Pain **17**(2): 109-137.
- Chimenti, C., J. Kajstura, et al. (2003). "Senescence and Death of Primitive Cells and Myocytes Lead to Premature Cardiac Aging and Heart Failure." Circulation Research **93**(7): 604-613.
- Choi, Y. J., J. Y. Lee, et al. (2012). "Cell-Penetrating Superoxide Dismutase Attenuates Oxidative Stress-Induced Senescence by Regulating the P53-P21(Cip1) Pathway and Restores Osteoblastic Differentiation in Human Dental Pulp Stem Cells." Int J Nanomedicine **7**: 5091-5106.
- Chuang, H. H., W. M. Neuhausser, et al. (2004). "The Super-Cooling Agent Icilin Reveals a Mechanism of Coincidence Detection by a Temperature-Sensitive Trp Channel." Neuron **43**(6): 859-869.
- Clapham, D. E. (2003). "Trp Channels as Cellular Sensors." Nature **426**(6966): 517-524.
- Cooper, P. R., Y. Takahashi, et al. (2010). "Inflammation-Regeneration Interplay in the Dentine-Pulp Complex." J Dent **38**(9): 687-697.
- Corey, D. P., J. Garcia-Anoveros, et al. (2004). "Trpa1 Is a Candidate for the Mechanosensitive Transduction Channel of Vertebrate Hair Cells." Nature **432**(7018): 723-730.
- Corey, D. P., J. Garcia-Anoveros, et al. (2004). "Trpa1 Is a Candidate for the Mechanosensitive Transduction Channel of Vertebrate Hair Cells." Nature **432**(7018): 723-730.
- Couple, M. L., J. C. Farges, et al. (2000). "Odontoblast Differentiation of Human Dental Pulp Cells in Explant Cultures." Calcified Tissue International **66**(2): 129-138.
- Counter, C. M., W. C. Hahn, et al. (1998). "Dissociation among in Vitro Telomerase Activity, Telomere Maintenance, and Cellular Immortalization." Proceedings of the National Academy of Sciences **95**(25): 14723-14728.
- Counter, C. M., W. C. Hahn, et al. (1998). "Dissociation among in Vitro Telomerase Activity, Telomere Maintenance, and Cellular Immortalization." Proceedings of the National Academy of Sciences of the United States of America **95**(25): 14723-14728.
- Couve, E. (1986). "Ultrastructural-Changes During the Life-Cycle of Human Odontoblasts." Archives of Oral Biology **31**(10): 643-651.
- Cross, K. J., N. L. Huq, et al. (2005). "Protein Dynamics of Bovine Dentin Phosphophoryn." Journal of Peptide Research **66**(2): 59-67.
- d'Aquino, R., A. Graziano, et al. (2007). "Human Postnatal Dental Pulp Cells Co-Differentiate into Osteoblasts and Endotheliocytes: A Pivotal Synergy Leading to Adult Bone Tissue Formation." Cell Death and Differentiation **14**(6): 1162-1171.
- d'Aquino, R., V. Tirino, et al. (2011). "Human Neural Crest-Derived Postnatal Cells Exhibit Remarkable Embryonic Attributes Either in Vitro or in Vivo." European Cells & Materials **21**: 304-316.
- D'Souza, R. N., T. Aberg, et al. (1999). "Cbfa1 Is Required for Epithelial-Mesenchymal Interactions Regulating Tooth Development in Mice." Development **126**(13): 2911-2920.
- D'Souza, R. N., A. Cavender, et al. (1997). "Gene Expression Patterns of Murine Dentin Matrix Protein 1 (Dmp1) and Dentin Sialophosphoprotein (Dspp) Suggest Distinct

- Developmental Functions in Vivo." *Journal of Bone and Mineral Research* **12**(12): 2040-2049.
- Darian-Smith, I., K. O. Johnson, et al. (1979). "Warm Fibers Innervating Palmar and Digital Skin of the Monkey - Responses to Thermal Stimuli." *Journal of Neurophysiology* **42**(5): 1297-1315.
- Davidson, R. M. (1993). "Potassium Currents in Cells Derived from Human Dental-Pulp." *Archives of Oral Biology* **38**(9): 803-811.
- Davidson, R. M. (1994). "Neural Form of Voltage-Dependent Sodium Current in Human Cultured Dental-Pulp Cells." *Archives of Oral Biology* **39**(7): 613-620.
- Davis, K. D. (1998). "Cold-Induced Pain and Prickle in the Glabrous and Hairy Skin." *Pain* **75**(1): 47-57.
- Davis, K. D. and G. E. Pope (2002). "Noxious Cold Evokes Multiple Sensations with Distinct Time Courses." *Pain* **98**(1-2): 179-185.
- Dawes, J. M., M. Calvo, et al. (2011). "Cxcl5 Mediates Uvb Irradiation-Induced Pain." *Science Translational Medicine* **3**(90): 90ra60.
- de Jonge, H. J. M., C. M. Woolthuis, et al. (2009). "Paradoxical Down-Regulation of P16(Ink4a) Mrna with Advancing Age in Acute Myeloid Leukemia." *Aging-Ur* **1**(11): 949-953.
- Delmas, P., J. Z. Hao, et al. (2011). "Molecular Mechanisms of Mechanotransduction in Mammalian Sensory Neurons." *Nature Reviews Neuroscience* **12**(3): 139-153.
- Deorosan, B. and E. A. Nauman (2011). "The Role of Glucose, Serum, and Three-Dimensional Cell Culture on the Metabolism of Bone Marrow-Derived Mesenchymal Stem Cells." *Stem Cells International* **2011**.
- Dheda, K., J. F. Huggett, et al. (2005). "The Implications of Using an Inappropriate Reference Gene for Real-Time Reverse Transcription Pcr Data Normalization." *Analytical Biochemistry* **344**(1): 141-143.
- Dhima, M., V. C. Petropoulos, et al. (2012). "Dental Students, Perceptions of Dental Specialties and Factors Influencing Specialty and Career Choices." *Journal of Dental Education* **76**(5): 562-573.
- Dhopatkar, A. A., A. J. Sloan, et al. (2005). "British Orthodontic Society, Chapman Prize Winner 2003. A Novel in Vitro Culture Model to Investigate the Reaction of the Dentine-Pulp Complex to Orthodontic Force." *J Orthod* **32**(2): 122-132.
- Dickson, M. A., W. C. Hahn, et al. (2000). "Human Keratinocytes That Express Htert and Also Bypass a P16ink4a-Enforced Mechanism That Limits Life Span Become Immortal yet Retain Normal Growth and Differentiation Characteristics." *Mol. Cell. Biol.* **20**(4): 1436-1447.
- Dirac, A. M. G. and R. Bernards (2003). "Reversal of Senescence in Mouse Fibroblasts through Lentiviral Suppression of P53." *Journal of Biological Chemistry* **278**(14): 11731-11734.
- Dubner R, S. B., Storey AT. (1978). *The Neural Basis of Oral and Facial Function*. New York, Plenum Press.
- Ducy, P. and G. Karsenty (1999). "Transcriptional Control of Osteoblast Differentiation." *Endocrinologist* **9**(1): 32-35.
- Ducy, P., R. Zhang, et al. (1997). "Osf2/Cbfa1: A Transcriptional Activator of Osteoblast Differentiation." *Journal of Bone and Mineral Research* **12**: P202-P202.
- Durand, S. H., V. Flacher, et al. (2006). "Lipoteichoic Acid Increases Tlr and Functional Chemokine Expression While Reducing Dentin Formation in in Vitro Differentiated Human Odontoblasts." *The Journal of Immunology* **176**(5): 2880-2887.
- Durst, K. L. and S. W. Hiebert (2004). "Role of Runx Family Members in Transcriptional Repression and Gene Silencing." *Oncogene* **23**(24): 4220-4224.
- Dyson, P. A., T. Kelly, et al. (2011). "Diabetes Uk Evidence-Based Nutrition Guidelines for the Prevention and Management of Diabetes." *Diabetic Medicine* **28**(11): 1282-1288.

- Egbuniwe O, I. B., Funes JM, Grant AD, Renton T, Di Silvio L. (2011). P16/P53 Expression and Telomerase Activity in Immortalized Human Dental Pulp Cells. Cell Cycle. **10**: 3912 - 3919.
- Eisenberger, N. I. and M. D. Lieberman (2004). "Why Rejection Hurts: A Common Neural Alarm System for Physical and Social Pain." Trends in Cognitive Sciences **8**(7): 294-300.
- El Karim, I. A., G. J. Linden, et al. (2011). "Human Dental Pulp Fibroblasts Express the "Cold-Sensing" Transient Receptor Potential Channels Trpa1 and Trpm8." Journal of Endodontics **37**(4): 473-478.
- El Karim, I. A., G. J. Linden, et al. (2010). "Human Odontoblasts Express Functional Thermo-Sensitive Trp Channels: Implications for Dentin Sensitivity." Pain In Press, Corrected Proof.
- Entwistle, N. (1997). "Reconstituting Approaches to Learning: A Response to Webb." Higher Education **33**(2): 213-218.
- Entwistle, N., H. Tait, et al. (2000). "Patterns of Response to an Approaches to Studying Inventory across Contrasting Groups and Contexts." European Journal of Psychology of Education **15**(1): 33-48.
- Epel, E. S., E. H. Blackburn, et al. (2004). "Accelerated Telomere Shortening in Response to Life Stress." Proceedings of the National Academy of Sciences of the United States of America **101**(49): 17312-17315.
- Everaerts, W., J. Vriens, et al. (2010). "Functional Characterization of Transient Receptor Potential Channels in Mouse Urothelial Cells." American Journal of Physiology-Renal Physiology **298**(3): F692-F701.
- Farges, J.-C., F. Carrouel, et al. (2011). "Cytokine Production by Human Odontoblast-Like Cells Upon Toll-Like Receptor-2 Engagement." Immunobiology **216**(4): 513-517.
- Farges, J.-C., J.-F. Keller, et al. (2009). "Odontoblasts in the Dental Pulp Immune Response." Journal of Experimental Zoology Part B: Molecular and Developmental Evolution **312B**(5): 425-436.
- Farges, J. C., J. F. Keller, et al. (2009). "Odontoblasts in the Dental Pulp Immune Response." Journal of Experimental Zoology Part B-Molecular and Developmental Evolution **312B**(5): 425-436.
- Feng, Z., W. Hu, et al. (2007). "The Regulation of Ampk B1, Tsc2, and Pten Expression by P53: Stress, Cell and Tissue Specificity, and the Role of These Gene Products in Modulating the Igf-1-Akt-Mtor Pathways." Cancer Research **67**(7): 3043-3053.
- Fisher, L. W. and N. S. Fedarko (2003). "Six Genes Expressed in Bones and Teeth Encode the Current Members of the Sibling Family of Proteins." Connective Tissue Research **44**: 33-40.
- Follmar, K. E., F. C. Decroos, et al. (2006). "Effects of Glutamine, Glucose, and Oxygen Concentration on the Metabolism and Proliferation of Rabbit Adipose-Derived Stem Cells." Tissue Engineering **12**(12): 3525-3533.
- Fried, K., U. Bongenhielm, et al. (2001). "Nerve Injury-Induced Pain in the Trigeminal System." Neuroscientist **7**(2): 155-165.
- Fried, K., B. J. Sessle, et al. (2011). "The Paradox of Pain from Tooth Pulp: Low-Threshold "Algoneurons"?" Pain **152**(12): 2685-2689.
- Friedenstein, A., G. JF, et al. (1976). "- Fibroblast Precursors in Normal and Irradiated Mouse Hematopoietic Organs." - Exp Hematol. 1976 Sep;4(5):267-74.(- 0301-472X (Print)): T - ppublish.
- Fristad, I., V. Vandevska-Radunovic, et al. (2003). "Nk1, Nk2, Nk3 and Cgrp1 Receptors Identified in Rat Oral Soft Tissues, and in Bone and Dental Hard Tissue Cells." Cell and Tissue Research **311**(3): 383-391.
- Fristad, I., V. Vandevska-Radunovic, et al. (1999). "Neurokinin-1 Receptor Expression in the Mature Dental Pulp of Rats." Archives of Oral Biology **44**(2): 191-195.

- Fry, H. (2009). A Handbook for Teaching and Learning in Higher Education: Enhancing Academic Practice, Routledge.
- Fujita, T., Y. Otsuka-Tanaka, et al. (2005). "Establishment of Immortalized Clonal Cells Derived from Periodontal Ligament Cells by Induction of the Htert Gene." Journal of Oral Science **47**(4): 177-184.
- Galler, K. M., H. Schweikl, et al. (2006). "Human Pulp-Derived Cells Immortalized with Simian Virus 40 T-Antigen." European Journal of Oral Sciences **114**(2): 138-146.
- Gibbs, J. L., J. L. Melnyk, et al. (2011). "Differential Trpv1 and Trpv2 Channel Expression in Dental Pulp." Journal of Dental Research **90**(6): 765-770.
- Giulietti, A., L. Overbergh, et al. (2001). "An Overview of Real-Time Quantitative Pcr: Applications to Quantify Cytokine Gene Expression." Methods **25**(4): 386-401.
- Gold, J. I., K. A. Belmont, et al. (2007). "The Neurobiology of Virtual Reality Pain Attenuation." CyberPsychology & Behavior **10**(4): 536-544.
- Goldberg, M., D. Septier, et al. (1995). "Dental Mineralization." International Journal of Developmental Biology **39**(1): 93-110.
- Goldberg, M. and A. J. Smith (2004). "Cells and Extracellular Matrices of Dentin and Pulp: A Biological Basis for Repair and Tissue Engineering." Critical Reviews in Oral Biology & Medicine **15**(1): 13-27.
- Goldberg, M. and M. Takagi (1993). "Dentin Proteoglycans - Composition, Ultrastructure and Functions." Histochemical Journal **25**(11): 781-806.
- Gorter de Vries, I., D. Coomans, et al. (1988). "Immunocytochemical Localization of Osteocalcin in Human and Bovine Teeth." Calcified Tissue International **43**(2): 128-130.
- Goto, T., K. Nakao, et al. (2007). "Substance P Stimulates Late-Stage Rat Osteoblastic Bone Formation through Neurokinin-1 Receptors." Neuropeptides **41**(1): 25-31.
- Grant, A. D., G. S. Cottrell, et al. (2007). "Protease-Activated Receptor 2 Sensitizes the Transient Receptor Potential Vanilloid 4 Ion Channel to Cause Mechanical Hyperalgesia in Mice." The Journal of Physiology **578**(3): 715-733.
- Greider, C. W. (2006). "Telomerase Rna Levels Limit the Telomere Length Equilibrium." Cold Spring Harbor Symposia on Quantitative Biology **71**: 225-229.
- Greider, C. W. and E. H. Blackburn (1987). "The Telomere Terminal Transferase of Tetrahymena Is a Ribonucleoprotein Enzyme with 2 Kinds of Primer Specificity." Cell **51**(6): 887-898.
- Gronroos, M., T. Reunala, et al. (1996). "Influence of Selective Nerve Fiber Blocks on Argon Laser-Induced Thermal Pain in the Human Skin." Neuroscience Letters **211**(2): 143-145.
- Gronthos, S., A. Arthur, et al. (2011). "A Method to Isolate and Culture Expand Human Dental Pulp Stem Cells." Methods Mol Biol **698**: 107-121.
- Gronthos, S., J. Brahim, et al. (2002). "Stem Cell Properties of Human Dental Pulp Stem Cells." J Dent Res **81**(8): 531-535.
- Gronthos, S., M. Mankani, et al. (2000). "Postnatal Human Dental Pulp Stem Cells (Dpscs) in Vitro and in Vivo." Proc Natl Acad Sci U S A **97**(25): 13625-13630.
- Gronthos, S., M. Mankani, et al. (2000). "Postnatal Human Dental Pulp Stem Cells (Dpscs) in Vitro and Invivo." Proceedings of the National Academy of Sciences of the United States of America **97**(25): 13625-13630.
- Guler, A. D., H. S. Lee, et al. (2002). "Heat-Evoked Activation of the Ion Channel, Trpv4." Journal of Neuroscience **22**(15): 6408-6414.
- Haegerstrand, A., C. J. Dalsgaard, et al. (1990). "Calcitonin Gene-Related Peptide Stimulates Proliferation of Human Endothelial-Cells." Proceedings of the National Academy of Sciences of the United States of America **87**(9): 3299-3303.
- Haferkamp, S., S. L. Tran, et al. (2009). "The Relative Contributions of the P53 and Prb Pathways in Oncogene Induced Melanocyte Senescence." Aging-Us **1**(6): 542-556.

- Hahn, C. L. and F. R. Liewehr (2007). "Innate Immune Responses of the Dental Pulp to Caries." Journal of Endodontics **33**(6): 643-651.
- Haigis, K. M. and A. Sweet-Cordero (2011). "New Insights into Oncogenic Stress." Nat Genet **43**(3): 177-178.
- Hallin, R. G., H. E. Torebjork, et al. (1982). "Nociceptors and Warm Receptors Innervated by C-Fibers in Human-Skin." Journal of Neurology Neurosurgery and Psychiatry **45**(4): 313-319.
- Halvorsen, T. L., G. M. Beattie, et al. (2000). "Accelerated Telomere Shortening and Senescence in Human Pancreatic Islet Cells Stimulated to Divide in Vitro." J Endocrinol **166**(1): 103-109.
- Hargreaves, K. M., J. Q. Swift, et al. (1994). "Pharmacology of Peripheral Neuropeptide and Inflammatory Mediator Release." Oral Surgery, Oral Medicine, Oral Pathology **78**(4): 503-510.
- Harrison, J. L. K. and K. D. Davis (1999). "Cold-Evoked Pain Varies with Skin Type and Cooling Rate: A Psychophysical Study in Humans." Pain **83**(2): 123-135.
- Harvey, D. M. and A. J. Levine (1991). "P53 Alteration Is a Common Event in the Spontaneous Immortalization of Primary Balb/C Murine Embryo Fibroblasts." Genes & Development **5**(12B): 2375-2385.
- He, G. and A. George (2004). "Dentin Matrix Protein 1 Immobilized on Type I Collagen Fibrils Facilitates Apatite Deposition in Vitro." Journal of Biological Chemistry **279**(12): 11649-11656.
- Healey, M. and A. Jenkins (2000). "Kolb's Experiential Learning Theory and Its Application in Geography in Higher Education." Journal of Geography **99**(5): 185-195.
- Helke, C. J., C. A. Sasek, et al. (1991). "Tachykinins in Autonomic Control-Systems - the Company They Keep." Annals of the New York Academy of Sciences **632**: 154-169.
- Henry, M. (2011). "Odontoblast and Dentin Thermal Sensitivity." Pain **152**(10): 2191-2192.
- Hensel, H. and A. Iggo (1971). "Analysis of Cutaneous Warm and Cold Fibres in Primates." Pflugers Archiv-European Journal of Physiology **329**(1): 1-&.
- Hensel, H. and Y. Zotterman (1951). "The Effect of Menthol on the Thermoreceptors." Acta Physiologica Scandinavica **24**(1): 27-34.
- Heyeraas, K. J., S. C. Kim, et al. (1994). "Effect of Electrical Tooth Stimulation on Blood-Flow, Interstitial Fluid Pressure and Substance-P and Cg Rp-Immunoreactive Nerve-Fibers in the Low Compliant Cat Dental-Pulp." Microvascular Research **47**(3): 329-343.
- Hildebrand, C., K. Fried, et al. (1995). "Teeth and Tooth Nerves." Progress in Neurobiology **45**(3): 165-222.
- Hinman, A., H.-h. Chuang, et al. (2006). "Trp Channel Activation by Reversible Covalent Modification." Proceedings of the National Academy of Sciences **103**(51): 19564-19568.
- Hirotoni, H., N. A. Tuohy, et al. (2004). "The Calcineurin/Nuclear Factor of Activated T Cells Signaling Pathway Regulates Osteoclastogenesis in Raw264.7 Cells." Journal of Biological Chemistry **279**(14): 13984-13992.
- Hoad, R. and E. Theaker (2003). "Providing Support for Problem-Based Learning in Dentistry: The Manchester Experience." European Journal of Dental Education **7**(1): 3-12.
- Holyfield, L. J., K. A. Bolin, et al. (2005). "Use of Computer Technology to Modify Objective Structured Clinical Examinations." Journal of Dental Education **69**(10): 1133-1136.
- Holzer, P. (1998). "Neurogenic Vasodilatation and Plasma Leakage in the Skin." General Pharmacology **30**(1): 5-11.
- Horst, O. V., J. A. Horst, et al. (2011). "Caries Induced Cytokine Network in the Odontoblast Layer of Human Teeth." Bmc Immunology **12**.



- Huang, A. H. C., Y. K. Chen, et al. (2009). "Isolation and Characterization of Human Dental Pulp Stem/Stromal Cells from Nonextracted Crown-Fractured Teeth Requiring Root Canal Therapy." *Journal of Endodontics* **35**(5): 673-681.
- Huang, A. H. C., Y. K. Chen, et al. (2008). "Isolation and Characterization of Dental Pulp Stem Cells from a Supernumerary Tooth." *Journal of Oral Pathology & Medicine* **37**(9): 571-574.
- Huang, G. T., S. Gronthos, et al. (2009). "Mesenchymal Stem Cells Derived from Dental Tissues Vs. Those from Other Sources: Their Biology and Role in Regenerative Medicine." *J Dent Res* **88**(9): 792-806.
- Huang, G. T. J., K. Shagramanova, et al. (2006). "Formation of Odontoblast-Like Cells from Cultured Human Dental Pulp Cells on Dentin in Vitro." *Journal of Endodontics* **32**(11): 1066-1073.
- Huang, G. T. J., W. Sonoyama, et al. (2006). "In Vitro Characterization of Human Dental Pulp Cells: Various Isolation Methods and Culturing Environments." *Cell and Tissue Research* **324**(2): 225-236.
- Hume, W. R. and W. L. Massey (1990). "Keeping the Pulp Alive - the Pharmacology and Toxicology of Agents Applied to Dentin." *Australian Dental Journal* **35**(1): 32-37.
- IASP. (1994). from ([http://www.iasp-pain.org/AM/Template.cfm?Section=Pain\\_Defi.](http://www.iasp-pain.org/AM/Template.cfm?Section=Pain_Defi.))
- Ikeda, H. and H. Suda (2003). "Sensory Experiences in Relation to Pulpal Nerve Activation of Human Teeth in Different Age Groups." *Archives of Oral Biology* **48**(12): 835-841.
- Imai, H., N. Osumi-Yamashita, et al. (1996). "Contribution of Early-Emigrating Midbrain Crest Cells to the Dental Mesenchyme of Mandibular Molar Teeth in Rat Embryos." *Developmental Biology* **176**(2): 151-165.
- Irvine, J. H. (1988). "Root Surface Sensitivity: A Review of Aetiology and Management." *Journal of the New Zealand Society of Periodontology*(66): 15-18.
- Isenmann, S., D. Cakouros, et al. (2007). "Htert Transcription Is Repressed by Cbfa1 in Human Mesenchymal Stem Cell Populations." *Journal of Bone and Mineral Research* **22**(6): 897-906.
- Itahana, K., J. Campisi, et al. (2007). "Methods to Detect Biomarkers of Cellular Senescence: The Senescence-Associated Beta-Galactosidase Assay." *Methods Mol Biol* **371**: 21-31.
- Ito, Y. (2004). "Oncogenic Potential of the Runx Gene Family: 'Overview'." *Oncogene* **23**(24): 4198-4208.
- Jansen, I., R. Uddman, et al. (1986). "Localization and Effects of Neuropeptide-Y, Vasoactive Intestinal Polypeptide, Substance-P, and Calcitonin Gene Related Peptide in Human Temporal Arteries." *Annals of Neurology* **20**(4): 496-501.
- Janssen, D. A. W., J. G. Hoenderop, et al. (2011). "The Mechanoreceptor Trpv4 Is Localized in Adherence Junctions of the Human Bladder Urothelium: A Morphological Study." *The Journal of Urology* **186**(3): 1121-1127.
- Jeon, B. G., E. J. Kang, et al. (2011). "Comparative Analysis of Telomere Length, Telomerase and Reverse Transcriptase Activity in Human Dental Stem Cells." *Cell Transplant* **8**(10).
- Jo, Y. Y., H. J. Lee, et al. (2007). "Isolation and Characterization of Postnatal Stem Cells from Human Dental Tissues." *Tissue Engineering* **13**(4): 767-773.
- Johnsen, D. C., J. Harshbarger, et al. (1983). "Quantitative Assessment of Neural Development in Human Premolars." *Anatomical Record* **205**(4): 421-429.
- Jordt, S. E. and D. Julius (2002). "Molecular Basis for Species-Specific Sensitivity to "Hot" Chili Peppers." *Cell* **108**(3): 421-430.
- Julius, D. and A. I. Basbaum (2001). "Molecular Mechanisms of Nociception." *Nature* **413**(6852): 203-210.
- Jyvasjarvi, E. and K. D. Kniffki (1987). "Cold Stimulation of Teeth - a Comparison between the Responses of Cat Intradental a-Delta and C-Fibers and Human Sensation." *Journal of Physiology-London* **391**: 193-207.

- Kamata, N., R. Fujimoto, et al. (2004). "Immortalization of Human Dental Papilla, Dental Pulp, Periodontal Ligament Cells and Gingival Fibroblasts by Telomerase Reverse Transcriptase." *Journal of Oral Pathology & Medicine* **33**(7): 417-423.
- Kang, M. K., A. Kameta, et al. (2004). "Senescence Occurs with Htert Repression and Limited Telomere Shortening in Human Oral Keratinocytes Cultured with Feeder Cells." *Journal of Cellular Physiology* **199**(3): 364-370.
- Karaöz, E., B. Doğan, et al. (2010). "Isolation and in Vitro Characterisation of Dental Pulp Stem Cells from Natal Teeth." *Histochemistry and Cell Biology* **133**(1): 95-112.
- Katouziansafadi, M., J. Y. Cremet, et al. (1989). "Limitation of DNA-4',6-Diamidine-2-Phenylindole Assay in the Presence of an Excess of Transfer-Rna." *Analytical Biochemistry* **176**(2): 416-419.
- Kawanami, Y., Y. Morimoto, et al. (2009). "Calcitonin Gene-Related Peptide Stimulates Proliferation of Alveolar Epithelial Cells." *Respiratory Research* **10**.
- Kettunen, P., I. Karavanova, et al. (1998). "Responsiveness of Developing Dental Tissues to Fibroblast Growth Factors: Expression of Splicing Alternatives of Fgfr1, -2, -3, and of Fgfr4; and Stimulation of Cell Proliferation by Fgf-2, -4, -8, and -9." *Developmental Genetics* **22**(4): 374-385.
- Khawaja, A. M. and D. F. Rogers (1996). "Tachykinins: Receptor to Effector." *International Journal of Biochemistry & Cell Biology* **28**(7): 721-738.
- Kido, M. A., T. Ibuki, et al. (2005). "Immunocytochemical Localization of the Neurokinin 1 Receptor in Rat Dental Pulp." *Archives of Histology and Cytology* **68**(4): 259-265.
- Kim, H. Y., C.-K. Park, et al. (2008). "Differential Changes in Trpv1 Expression after Trigeminal Sensory Nerve Injury." *Journal of Pain* **9**(3): 280-288.
- Kim, N. W., M. A. Piatyszek, et al. (1994). "Specific Association of Human Telomerase Activity with Immortal Cells and Cancer." *Science* **266**(5193): 2011-2015.
- Kim, S. and J. Dorscherkim (1989). "Hemodynamic Regulation of the Dental-Pulp in a Low Compliance Environment." *Journal of Endodontics* **15**(9): 404-408.
- Kim, S., J. E. Dorscherkim, et al. (1989). "Quantitative Assessment of Microcirculation in the Rat Dental-Pulp in Response to Alpha-Adrenergic and Beta-Adrenergic Agonists." *Archives of Oral Biology* **34**(9): 707-712.
- Kim, W. Y. and N. E. Sharpless (2006). "The Regulation of Ink4/Arf in Cancer and Aging." *Cell* **127**(2): 265-275.
- KincyCain, T. and K. L. Bost (1997). "Substance P-Induced Il-12 Production by Murine Macrophages." *Journal of Immunology* **158**(5): 2334-2339.
- Kishi, Y., N. Shimozato, et al. (1989). "Vascular Architecture of Cat Pulp Using Corrosive Resin Cast under Scanning Electron-Microscope." *Journal of Endodontics* **15**(10): 478-483.
- Kitagawa, M., H. Ueda, et al. (2007). "Immortalization and Characterization of Human Dental Pulp Cells with Odontoblastic Differentiation." *Archives of Oral Biology* **52**(8): 727-731.
- Kiyono, T., S. A. Foster, et al. (1998). "Both Rb/P16ink4a Inactivation and Telomerase Activity Are Required to Immortalize Human Epithelial Cells." *Nature* **396**(6706): 84-88.
- Klee, C. B., H. Ren, et al. (1998). "Regulation of the Calmodulin-Stimulated Protein Phosphatase, Calcineurin." *Journal of Biological Chemistry* **273**(22): 13367-13370.
- Kochukov, M. Y., T. A. McNearney, et al. (2006). "Thermosensitive Trp Ion Channels Mediate Cytosolic Calcium Response in Human Synoviocytes." *American Journal of Physiology - Cell Physiology* **291**(3): C424-C432.
- Kokkas, A. B., A. Goulas, et al. (2007). "Irreversible but Not Reversible Pulpitis Is Associated with up-Regulation of Tumour Necrosis Factor-Alpha Gene Expression in Human Pulp." *International Endodontic Journal* **40**(3): 198-203.
- Kolb, A. Y. and D. A. Kolb (2009). "Experiential Learning Theory: A Dynamic, Holistic Approach to Management Learning, Education and Development." *The Sage handbook of management learning, education and development*: 42-68.

- Kolb, D. A. (1984). The Experiential Learning: Experience as the Source of Learning and Development. The Process of Experiential Learning: 21.
- Kulkarni, G. V., B. Chen, et al. (2000). "Promotion of Selective Cell Attachment by the Rgd Sequence in Dentine Matrix Protein 1." Archives of Oral Biology **45**(6): 475-484.
- Kumaran, C. and K. Shivakumar (2002). "Calcium- and Superoxide Anion-Mediated Mitogenic Action of Substance P on Cardiac Fibroblasts." American Journal of Physiology - Heart and Circulatory Physiology **282**(5): H1855-H1862.
- Laino, G., R. d'Aquino, et al. (2005). "A New Population of Human Adult Dental Pulp Stem Cells: A Useful Source of Living Autologous Fibrous Bone Tissue (Lab)." Journal of Bone and Mineral Research **20**(8): 1394-1402.
- Laino, G., A. Graziano, et al. (2006). "An Approachable Human Adult Stem Cell Source for Hard-Tissue Engineering." J Cell Physiol **206**(3): 693-701.
- Lakshmipathy, U. and C. Verfaillie (2005). "Stem Cell Plasticity." Blood Reviews **19**(1): 29-38.
- Lars-Gunnar, L. (2011). "Oncogene- and Tumor Suppressor Gene-Mediated Suppression of Cellular Senescence." Seminars in Cancer Biology **21**(6): 367-376.
- Lecka-Czernik, B., I. Gubrij, et al. (1999). "Inhibition of Osf2/Cbfa1 Expression and Terminal Osteoblast Differentiation by Ppar $\gamma$ 2." Journal of Cellular Biochemistry **74**(3): 357-371.
- Lerch, M. M. and G. Adler (1994). "Experimental Animal Models of Acute Pancreatitis." Int J Pancreatol **15**(3): 159-170.
- Lesot, H., S. Lisi, et al. (2001). "Epigenetic Signals During Odontoblast Differentiation." Advances in Dental Research **15**(1): 8-13.
- Levin, L. G., A. Rudd, et al. (1999). "Expression of Il-8 by Cells of the Odontoblast Layer in Vitro." European Journal of Oral Sciences **107**(2): 131-137.
- Liao, H. H., C. Brandsten, et al. (1998). "Osteonectin Rna and Collagen Alpha 1(I) Rna in the Developing Rat Maxilla." European Journal of Oral Sciences **106**: 418-423.
- Liedtke, W. and J. M. Friedman (2003). "Abnormal Osmotic Regulation in Trpv4(-/-) Mice." Proceedings of the National Academy of Sciences of the United States of America **100**(23): 13698-13703.
- Light, A. R. and E. R. Perl (1979). "Spinal Termination of Functionally Identified Primary Afferent Neurons with Slowly Conducting Myelinated Fibers." J Comp Neurol **186**(2): 133-150.
- Lin, M., S. Liu, et al. (2011). "Analysis of Thermal-Induced Dentinal Fluid Flow and Its Implications in Dental Thermal Pain." Archives of Oral Biology **56**(9): 846-854.
- Lin, M., Z. Y. Luo, et al. (2011). "Fluid Mechanics in Dentinal Microtubules Provides Mechanistic Insights into the Difference between Hot and Cold Dental Pain." Plos One **6**(3): e18068.
- Linde, A. (1989). "Dentin Matrix Proteins - Composition and Possible Functions in Calcification." Anatomical Record **224**(2): 154-166.
- Linde, A. (1995). "Dentin Mineralization and the Role of Odontoblasts in Calcium Transport." Connective Tissue Research **33**(1-3): 163-170.
- Linde, A. and M. Goldberg (1993). "Dentinogenesis." Critical Reviews in Oral Biology and Medicine **4**(5): 679-728.
- Linde, A. and T. Lundgren (1995). "From Serum to the Mineral Phase. The Role of the Odontoblast in Calcium Transport and Mineral Formation." International Journal of Developmental Biology **39**(1): 213-222.
- Liu, B. Y., K. Y. Hui, et al. (2003). "Thermodynamics of Heat Activation of Single Capsaicin Ion Channels Vr1." Biophysical Journal **85**(5): 2988-3006.
- Liu, H., S. Gronthos, et al. (2006). "Dental Pulp Stem Cells." Adult Stem Cells **4**19: 99-113.
- Liu, X. F., A. Dakic, et al. (2008). "Cell-Restricted Immortalization by Human Papillomavirus Correlates with Telomerase Activation and Engagement of the Htert Promoter by Myc." Journal of Virology **82**(23): 11568-11576.

- Livak, K. J. and T. D. Schmittgen (2001). "Analysis of Relative Gene Expression Data Using Real-Time Quantitative Pcr and the 2(T)(-Delta Delta C) Method." *Methods* **25**(4): 402-408.
- Loken, L. S., J. Wessberg, et al. (2009). "Coding of Pleasant Touch by Unmyelinated Afferents in Humans." *Nature Neuroscience* **12**(5): 547-548.
- Lotz, M., J. H. Vaughan, et al. (1988). "Effect of Neuropeptides on Production of Inflammatory Cytokines by Human-Monocytes." *Science* **241**(4870): 1218-1221.
- Lu, G., D. Henderson, et al. (2005). "Trpv1b, a Functional Human Vanilloid Receptor Splice Variant." *Molecular Pharmacology* **67**(4): 1119-1127.
- Lucarz, A. and G. Brand (2007). "Current Considerations About Merkel Cells." *European Journal of Cell Biology* **86**(5): 243-251.
- Lundgren, T. and A. Linde (1997). "Voltage-Gated Calcium Channels and Nonvoltage-Gated Calcium Uptake Pathways in the Rat Incisor Odontoblast Plasma Membrane." *Calcified Tissue International* **60**(1): 79-85.
- Lundquist, P., T. Lundgren, et al. (2000). "Na<sup>+</sup>/Ca<sup>2+</sup> Exchanger Isoforms of Rat Odontoblasts and Osteoblasts." *Calcified Tissue International* **67**(1): 60-67.
- Luukko, K., I. H. Kvinnsland, et al. (2005). "Tissue Interactions in the Regulation of Axon Pathfinding During Tooth Morphogenesis." *Developmental Dynamics* **234**(3): 482-488.
- MacDougall, M., J. Dong, et al. (2006). "Molecular Basis of Human Dentin Diseases." *American Journal of Medical Genetics Part A* **140A**(23): 2536-2546.
- Macdougall, M., T. T. Gu, et al. (1998). "Identification of a Novel Isoform of Mouse Dentin Matrix Protein 1: Spatial Expression in Mineralized Tissues." *Journal of Bone and Mineral Research* **13**(3): 422-431.
- Mackenzie, R. A., D. Burke, et al. (1975). "Fiber Function and Perception During Cutaneous Nerve Block." *Journal of Neurology Neurosurgery and Psychiatry* **38**(9): 865-873.
- Magloire, H., M. L. Couble, et al. (2004). "Odontoblast Primary Cilia: Facts and Hypotheses." *Cell Biology International* **28**(2): 93-99.
- Magloire, H., M. L. Couble, et al. (2009). "Odontoblast: A Mechano-Sensory Cell." *Journal of Experimental Zoology Part B-Molecular and Developmental Evolution* **312B**(5): 416-424.
- Magloire, H., F. Lesage, et al. (2003). "Expression and Localization of Trek-1 K<sup>+</sup> Channels in Human Odontoblasts." *Journal of Dental Research* **82**(7): 542-545.
- Martinek, N., J. Shahab, et al. (2007). "Is Sparc an Evolutionarily Conserved Collagen Chaperone?" *Journal of Dental Research* **86**(4): 296-305.
- Masella, R. S. and M. Meister (2006). "Current Concepts in the Biology of Orthodontic Tooth Movement." *Am J Orthod Dentofacial Orthop* **129**(4): 458-468.
- Mason, W. T. and P. W. Strike (2003). "See One, Do One, Teach One--Is This Still How It Works? A Comparison of the Medical and Nursing Professions in the Teaching of Practical Procedures." *Med Teach* **25**(6): 664-666.
- Massey, W. L. K., D. M. Romberg, et al. (1993). "The Association of Carious Dentin Microflora with Tissue Changes in Human Pulpitis." *Oral Microbiology and Immunology* **8**(1): 30-35.
- Matthews, B. and N. Vongsavan (1994). "Interactions between Neural and Hydrodynamic Mechanisms in Dentin and Pulp." *Archives of Oral Biology* **39**: S87-S95.
- Matthews, B. and N. Vongsavan (1994). "Interactions between Neural and Hydrodynamic Mechanisms in Dentine and Pulp." *Arch Oral Biol* **39 Suppl**: 87S-95S.
- Maurin, J.-C., M.-L. Couble, et al. (2004). "Expression and Localization of Reelin in Human Odontoblasts." *Matrix Biology* **23**(5): 277-285.
- Maurin, J. C., M. L. Couble, et al. (2004). "Expression and Localization of Reelin in Human Odontoblasts." *Matrix Biology* **23**(5): 277-285.
- McCabe, M., J. Davis, et al. (2005). "Regulation of DNA Methyltransferase 1 by the Prb/E2f1 Pathway." *Cancer Res* **65**(9): 3624 - 3632.

- McKemy, D. D., W. M. Neuhauser, et al. (2002). "Identification of a Cold Receptor Reveals a General Role for Trp Channels in Thermosensation." *Nature* **416**(6876): 52-58.
- McNamara, F. N., A. Randall, et al. (2005). "Effects of Piperine, the Pungent Component of Black Pepper, at the Human Vanilloid Receptor (Trpv1)." *British Journal of Pharmacology* **144**(6): 781-790.
- Mehrazarin, S., J. E. Oh, et al. (2011). "Impaired Odontogenic Differentiation of Senescent Dental Mesenchymal Stem Cells Is Associated with Loss of Bmi-1 Expression." *Journal of Endodontics* **37**(5): 662-666.
- Melzack, R., T. J. Coderre, et al. (1999). Pain and Neuroplasticity. *Neuronal Plasticity: Building a Bridge from the Laboratory to the Clinic*. J. Grafman and Y. Christen: 35-52.
- Melzack, R. and P. D. Wall (1965). "Pain Mechanisms - a New Theory." *Science* **150**(3699): 971-&.
- Mengel, M. K. C., A. E. Stiefenhofer, et al. (1993). "Pain Sensation During Cold Stimulation of the Teeth: Differential Reflection of A $\delta$  and C Fibre Activity?" *Pain* **55**(2): 159-169.
- Mergler, S., M. Valtink, et al. (2010). "Trpv Channels Mediate Temperature-Sensing in Human Corneal Endothelial Cells." *Experimental Eye Research* **90**(6): 758-770.
- Mesgouez, C., M. Oboeuf, et al. (2006). "Ultrastructural and Immunocytochemical Characterization of Immortalized Odontoblast Mo6-G3." *International Endodontic Journal* **39**(6): 453-463.
- Migliaccio, M., M. Amacker, et al. (2000). "Ectopic Human Telomerase Catalytic Subunit Expression Maintains Telomere Length but Is Not Sufficient for Cd8+ T Lymphocyte Immortalization." *The Journal of Immunology* **165**(9): 4978-4984.
- Minke, B. (1977). "Drosophila Mutant with a Transducer Defect." *Biophysics of Structure and Mechanism* **3**(1): 59-64.
- Mischen, B. T., K. F. Follmar, et al. (2008). "Metabolic and Functional Characterization of Human Adipose-Derived Stem Cells in Tissue Engineering." *Plastic and Reconstructive Surgery* **122**(3): 725-738.
- Miyamoto, T., T. Mochizuki, et al. (2009). "The Expression of Transient Receptor Potential (Trp) V4, A1, and V1 in the Human Bladder Mucosa of Normal and Bladder Outlet Obstruction. - a Novel Mechanism in the Obstruction-Induced Bladder Overactivity." *Neurourology and Urodynamics* **28**(7): 872-873.
- Miyazaki, T., N. Kanatani, et al. (2008). "Inhibition of the Terminal Differentiation of Odontoblasts and Their Transdifferentiation into Osteoblasts in Runx2 Transgenic Mice." *Archives of Histology and Cytology* **71**(2): 131-146.
- Montell, C., L. Birnbaumer, et al. (2002). "The Trp Channels, a Remarkably Functional Family." *Cell* **108**(5): 595-598.
- Moore, K. A., G. E. Taylor, et al. (1999). "Serotonin Unmasks Functional Nk-2 Receptors in Vagal Sensory Neurones of the Guinea-Pig." *Journal of Physiology-London* **514**(1): 111-124.
- Morgan, C. R., H. D. Rodd, et al. (2005). "Vanilloid Receptor 1 Expression in Human Tooth Pulp in Relation to Caries and Pain." *Journal of Orofacial Pain* **19**(3): 248-260.
- Morrison, I., L. S. Loken, et al. (2011). "Reduced C-Afferent Fibre Density Affects Perceived Pleasantness and Empathy for Touch." *Brain* **134**: 1116-1126.
- Munger, B. L. and C. Ide (1988). "The Structure and Function of Cutaneous Sensory Receptors." *Archives of Histology and Cytology* **51**(1): 1-34.
- Muraki, K., Y. Iwata, et al. (2003). "Trpv2 Is a Component of Osmotically Sensitive Cation Channels in Murine Aortic Myocytes." *Circulation Research* **93**(9): 829-838.
- Nanci, A. and A. R. T. Cate (2008). *Ten Cate's Oral Histology: Development, Structure, and Function*, Mosby Elsevier.
- Naono-Nakayama, R., N. Sunakawa, et al. (2010). "Differential Effects of Substance P or Hemokinin-1 on Transient Receptor Potential Channels, Trpv1, Trpa1 and Trpm8, in the Rat." *Neuropeptides* **44**(1): 57-61.

- Narayanan, K., R. Srinivas, et al. (2001). "Differentiation of Embryonic Mesenchymal Cells to Odontoblast-Like Cells by Overexpression of Dentin Matrix Protein 1." Proceedings of the National Academy of Sciences **98**(8): 4516-4521.
- Närhi, M., E. Jyväsjärvi, et al. (1992). "Role of Intradental a- and C-Type Nerve Fibres in Dental Pain Mechanisms." Proceedings of the Finnish Dental Society. Suomen Hammaslaakariseuran toimituksia **88 Suppl 1**: 507-516.
- Närhi, M., H. Yamamoto, et al. (1994). "The Neurophysiological Basis and the Role of Inflammatory Reactions in Dentine Hypersensitivity." Archives of Oral Biology **39, Supplement(0)**: S23-S30.
- Närhi, M. V. O., T. J. Hirvonen, et al. (1982). "Responses of Intradental Nerve Fibres to Stimulation of Dentine and Pulp." Acta Physiologica Scandinavica **115**(2): 173-178.
- Newble, D. I. and K. Jaeger (1983). "The Effect of Assessments and Examinations on the Learning of Medical Students." Medical Education **17**(3): 165-171.
- Nicol, D. J. and D. Macfarlane, Dick (2006). "Formative Assessment and Self-Regulated Learning: A Model and Seven Principles of Good Feedback Practice." Studies in higher education **31**(2): 199-218.
- Nilius, B. and T. Voets (2005). "Trp Channels: A Tr(1)P through a World of Multifunctional Cation Channels." Pflugers Archiv-European Journal of Physiology **451**(1): 1-10.
- Nishikawa, S. and H. Kitamura (1987). "Microtubules, Intermediate Filaments, and Actin-Filaments in the Odontoblast of Rat Incisor." Anatomical Record **219**(2): 144-151.
- Niv, D. and M. Devor (2006). "Refractory Neuropathic Pain: The Nature and Extent of the Problem." Pain Practice **6**(1): 3-9.
- Nuttall, N. M., J. G. Steele, et al. (2001). "Adult Dental Health Survey: The Impact of Oral Health on People in the Uk in 1998." Br Dent J **190**(3): 121-126.
- Oh, E. J., T. D. Gover, et al. (2003). "Substance P Evokes Cation Currents through Trp Channels in Hek293 Cells." Journal of Neurophysiology **90**(3): 2069-2073.
- Ohtani, N., D. Mann, et al. (2009). "Cellular Senescence Its Role in Tumor Suppression and Aging." Cancer Science **100**: 792 - 797.
- Ohtani, N., K. Yamakoshi, et al. (2010). "Real-Time in Vivo Imaging of P16ink4a Gene Expression: A New Approach to Study Senescence Stress Signaling in Living Animals." Cell Division **5**(1): 1.
- Ohtani, N., Z. Zebedee, et al. (2001). "Opposing Effects of Ets and Id Proteins on P16ink4a Expression During Cellular Senescence." Nature **409**: 1067 - 1070.
- Oka, S., K. Oka, et al. (2007). "Cell Autonomous Requirement for Tgf-Beta Signaling During Odontoblast Differentiation and Dentin Matrix Formation." Mechanisms of Development **124**(6): 409-415.
- Okazaki, J., G. Embery, et al. (1999). "Adsorption of Glycosaminoglycans onto Hydroxyapatite Using Chromatography." Biomaterials **20**(4): 309-314.
- Olgart, L. (1974). "Excitation of Intradental Sensory Units by Pharmacological Agents." Acta Physiologica Scandinavica **92**(1): 48-55.
- Olgart, L., T. Hokfelt, et al. (1977). "Localization of Substance P-Like Immunoreactivity in Nerves in Tooth-Pulp." Pain **4**(2): 153-159.
- Olovniko, Am (1973). "Theory of Marginotomy - Incomplete Copying of Template Margin in Enzymic-Synthesis of Polynucleotides and Biological Significance of Phenomenon." Journal of Theoretical Biology **41**(1): 181-190.
- Orchardson, R. and D. G. Gillam (2006). "Managing Dentin Hypersensitivity." Journal of the American Dental Association **137**(7): 990-998.
- Orenuga, O. O. and O. O. da Costa (2006). "Characteristics and Study Motivation of Clinical Dental Students in Nigerian Universities." Journal of Dental Education **70**(9): 996-1003.
- Orsini, G., A. Ruggeri, et al. (2008). "Immunohistochemical Localization of Dentin Matrix Protein 1 in Human Dentin." European Journal of Histochemistry **52**(4): 215-220.

- Ortega, S., M. Malumbres, et al. (2002). "Cyclin D-Dependent Kinases, Ink4 Inhibitors and Cancer." *Biochim Biophys Acta* **1602**: 73 - 87.
- Oshima, S. and M. Watanabe (2012). "Elevated Expression of Calcineurin Subunits During Active Mineralization of Developing Mouse Molar Teeth." *European Journal of Oral Sciences* **120**(5): 386-394.
- Oyarzun, A., H. Rathkamp, et al. (2000). "Immunohistochemical and Ultrastructural Evaluation of the Effects of Phosphoric Acid Etching on Dentin Proteoglycans." *European Journal of Oral Sciences* **108**(6): 546-554.
- Özok, A. R., M.-K. Wu, et al. (2002). "Effect of Perfusion with Water on Demineralization of Human Dentin in Vitro." *Journal of Dental Research* **81**(11): 733-737.
- Paine, M. L., W. Luo, et al. (2005). "Dentin Sialoprotein and Dentin Phosphoprotein Overexpression During Amelogenesis." *Journal of Biological Chemistry* **280**(36): 31991-31998.
- Papaccio, G., A. Graziano, et al. (2006). "Long-Term Cryopreservation of Dental Pulp Stem Cells (Sbp-Dpscs) and Their Differentiated Osteoblasts: A Cell Source for Tissue Repair." *Journal of Cellular Physiology* **208**(2): 319-325.
- Papagerakis, P., A. Berdal, et al. (2002). "Investigation of Osteocalcin, Osteonectin, and Dentin Sialophosphoprotein in Developing Human Teeth." *Bone* **30**(2): 377-385.
- Park, C.-K., M. S. Kim, et al. (2006). "Functional Expression of Thermo-Transient Receptor Potential Channels in Dental Primary Afferent Neurons: Implication for Tooth Pain." *J. Biol. Chem.* **281**(25): 17304-17311.
- Park, E.-S., H.-S. Cho, et al. (2009). "Proteomics Analysis of Human Dentin Reveals Distinct Protein Expression Profiles." *Journal of Proteome Research* **8**(3): 1338-1346.
- Park, I.-K., S. J. Morrison, et al. (2004). "Bmi1, Stem Cells, and Senescence Regulation." *The Journal of Clinical Investigation* **113**(2): 175-179.
- Park, S. W., Y. P. Yan, et al. (2007). "Substance P Is a Promoter of Adult Neural Progenitor Cell Proliferation under Normal and Ischemic Conditions." *Journal of Neurosurgery* **107**(3): 593-599.
- Pashley, D. H. (1990). "Mechanisms of Dentin Sensitivity." *Dental Clinics of North America* **34**(3): 449-473.
- Patel, T., S. H. Park, et al. (2003). "Substance P Induces Interleukin-8 Secretion from Human Dental Pulp Cells." *Oral Surgery, Oral Medicine, Oral Pathology, Oral Radiology, and Endodontics* **96**(4): 478-485.
- Pau, A. and C. D. Allen (2011). "Self-Reported Oral Health Status of Adults Resident in Medway, Kent in 2009." *Primary Dental Care* **18**(4): 173-180.
- Pau, A., R. Croucher, et al. (2005). "Development and Validation of a Dental Pain-Screening Questionnaire." *Pain* **119**(1-3): 75-81.
- Pau, A., R. E. Croucher, et al. (2007). "Demographic and Socio-Economic Correlates of Dental Pain among Adults in the United Kingdom, 1998." *British Dental Journal* **202**(9).
- Peier, A. M., A. Moqrich, et al. (2002). "A Trp Channel That Senses Cold Stimuli and Menthol." *Cell* **108**(5): 705-715.
- Perl, E. R. (1996). "Cutaneous Polymodal Receptors: Characteristics and Plasticity." *Polymodal Receptor - a Gateway to Pathological Pain* **113**: 21-37.
- Polyak, K., Y. Xia, et al. (1997). "A Model for P53-Induced Apoptosis." *Nature* **389**(6648): 300-305.
- Polycarpou, N., Y. L. Ng, et al. (2005). "Prevalence of Persistent Pain after Endodontic Treatment and Factors Affecting Its Occurrence in Cases with Complete Radiographic Healing." *International Endodontic Journal* **38**(3): 169-178.
- Premkumar, L. S. and G. P. Ahern (2000). "Induction of Vanilloid Receptor Channel Activity by Protein Kinase C." *Nature* **408**(6815): 985-990.

- Price, P. A., A. A. Otsuka, et al. (1976). "Characterization of a Gamma-Carboxyglutamic Acid-Containing Protein from Bone." Proceedings of the National Academy of Sciences of the United States of America **73**(5): 1447-1451.
- Ramsey, I. S. (2006). An Introduction to Trp Channels. Annual Review of Physiology. Palo Alto, Annual Reviews. **68**: 619-647.
- Ranly, D. M., H. F. Thomas, et al. (1997). "Osteocalcin Expression in Young and Aged Dental Pulp as Determined by Rt-Pcr." Journal of Endodontics **23**(6): 374-377.
- Rao, J. and W. R. Otto (1992). "Fluorimetric DNA Assay for Cell Growth Estimation." Analytical Biochemistry **207**(1): 186-192.
- Rastinejad, F. and H. M. Blau (1993). "Genetic Complementation Reveals a Novel Regulatory Role for 3' Untranslated Regions in Growth and Differentiation." Cell **72**(6): 903-917.
- Rauschenberger, C. R., J. C. Bailey, et al. (1997). "Detection of Human Il-2 in Normal and Inflamed Dental Pulp." Journal of Endodontics **23**(6): 366-370.
- Reader, A. and D. W. Foreman (1981). "An Ultrastructural Quantitative Investigation of Human Intradental Innervation." J Endod **7**: 493 - 499.
- Reilly, C. A., J. L. Taylor, et al. (2003). "Capsaicinoids Cause Inflammation and Epithelial Cell Death through Activation of Vanilloid Receptors." Toxicological Sciences **73**(1): 170-181.
- Renton, T., Y. Yiangou, et al. (2003). "Capsaicin Receptor Vr1 and Atp Purinoceptor P2x3 in Painful and Nonpainful Human Tooth Pulp." J Orofac Pain **17**: 245 - 250.
- Rheinwald, J. G., W. C. Hahn, et al. (2002). "A Two-Stage, P16ink4a- and P53-Dependent Keratinocyte Senescence Mechanism That Limits Replicative Potential Independent of Telomere Status." Molecular and Cellular Biology **22**(14): 5157-5172.
- Riera, C. E., C. Menozzi-Smarrito, et al. (2009). "Compounds from Sichuan and Melegueta Peppers Activate, Covalently and Non-Covalently, Trpa1 and Trpv1 Channels." British Journal of Pharmacology **157**(8): 1398-1409.
- Riley, T., E. Sontag, et al. (2008). "Transcriptional Control of Human P53-Regulated Genes." Nat Rev Mol Cell Biol **9**: 402 - 412.
- Rodd, H. D. and F. M. Boissonade (2000). "Substance P Expression in Human Tooth Pulp in Relation to Caries and Pain Experience." Eur J Oral Sci **108**: 467 - 474.
- Rodd, H. D. and F. M. Boissonade (2003). "Immunocytochemical Investigation of Neurovascular Relationships in Human Tooth Pulp." Journal of Anatomy **202**(2): 195-203.
- Rodd, H. D. C. R. M., ; P.F. Day,; F.M. Boissonade, (2007). "Pulpal Expression of Trpv1 in Molar Incisor Hypomineralisation.(Clinical Report)." European Archives of Paediatric Dentistry. European Academy of Paediatric Dentistry **8**: 184-188.
- Romanov, V. V., C. H. James, et al. (2005). "Basic Fibroblast Growth Factor Suppresses P53 Activation in the Neoplastic Cells of a Proportion of Patients with Chronic Lymphocytic Leukaemia." Oncogene **24**(45): 6855-6860.
- Roufogalis, B., P. Armati, et al. (2011). Protein Kinase C Modulation of Thermo-Sensitive Transient Receptor Potential Channels: Implications for Pain Signaling.
- Ruch, J. V., H. Lesot, et al. (1995). "Odontoblast Differentiation." International Journal of Developmental Biology **39**(1): 51-68.
- Sacerdote, P. and L. Levrini (2012). "Peripheral Mechanisms of Dental Pain: The Role of Substance P." Mediators Inflamm **2012**: 951920.
- Sasaki, T. and P. R. Garant (1996). "Structure and Organization of Odontoblasts." Anatomical Record **245**(2): 235-249.
- Sattari, M., M. A. Mozayeni, et al. (2010). "Substance P and Cgrp Expression in Dental Pulp with Irreversible Pulpitis." Australian Endodontic Journal **36**(2): 59-63.
- Schepers, R. J. and M. Ringkamp (2010). "Thermoreceptors and Thermosensitive Afferents." Neuroscience and Biobehavioral Reviews **34**(2): 177-184.



- Schoenebeck, B., H. J. Hartschen, et al. (2009). "Molecular Characterization of Human Impacted Third Molars: Diversification of Compartments." *Cells Tissues Organs* **189**(5): 356-370.
- Seal, R. P., X. D. Wang, et al. (2009). "Injury-Induced Mechanical Hypersensitivity Requires C-Low Threshold Mechanoreceptors." *Nature* **462**(7273): 651-655.
- Sessle, B. J. (2000). "Acute and Chronic Craniofacial Pain: Brainstem Mechanisms of Nociceptive Transmission and Neuroplasticity, and Their Clinical Correlates." *Crit Rev Oral Biol Med* **11**(1): 57-91.
- Sessle, B. J. (2005). "Peripheral and Central Mechanisms of Orofacial Pain and Their Clinical Correlates." *Minerva Anestesiol* **71**(4): 117-136.
- Shay, J. W., O. M. Pereira-Smith, et al. (1991). "A Role for Both Rb and P53 in the Regulation of Human Cellular Senescence." *Experimental Cell Research* **196**(1): 33-39.
- Shen, H. H. H., S. I. Ochkur, et al. (2003). "A Causative Relationship Exists between Eosinophils and the Development of Allergic Pulmonary Pathologies in the Mouse." *Journal of Immunology* **170**(6): 3296-3305.
- Shiba, H., Y. Mouri, et al. (2003). "Enhancement of Alkaline Phosphatase Synthesis in Pulp Cells Co-Cultured with Epithelial Cells Derived from Lower Rabbit Incisors." *Cell Biol Int* **27**(10): 815-823.
- Shibukawa, Y. and T. Suzuki (2003). "Ca<sup>2+</sup> Signaling Mediated by Ip<sub>3</sub>-Dependent Ca<sup>2+</sup> Releasing and Store-Operated Ca<sup>2+</sup> Channels in Rat Odontoblasts." *Journal of Bone and Mineral Research* **18**(1): 30-38.
- Siderovski, D. P., S. P. Heximer, et al. (1994). "A Human Gene Encoding a Putative Basic Helix-Loop-Helix Phosphoprotein Whose Messenger-Rna Increases Rapidly in Cycloheximide-Treated Blood Mononuclear-Cells." *DNA and Cell Biology* **13**(2): 125-147.
- Sloan, A. J. and R. J. Waddington (2009). "Dental Pulp Stem Cells: What, Where, How?" *International Journal of Paediatric Dentistry* **19**(1): 61-70.
- Smart, D., J. C. Jerman, et al. (2001). "Characterisation Using Flipr of Human Vanilloid Vr1 Receptor Pharmacology." *European Journal of Pharmacology* **417**(1-2): 51-58.
- Smith, A. J., N. Cassidy, et al. (1995). "Reactionary Dentinogenesis." *Int J Dev Biol* **39**(1): 273-280.
- Smith, A. J. and H. Lesot (2001). "Induction and Regulation of Crown Dentinogenesis: Embryonic Events as a Template for Dental Tissue Repair?" *Critical Reviews in Oral Biology & Medicine* **12**(5): 425-437.
- Smith, A. J., B. A. Scheven, et al. (2012). "Dentine as a Bioactive Extracellular Matrix." *Arch Oral Biol* **57**(2): 109-121.
- Smith, L. L., H. A. Collier, et al. (2003). "Telomerase Modulates Expression of Growth-Controlling Genes and Enhances Cell Proliferation." *Nat Cell Biol* **5**(5): 474-479.
- Sodek, J. and S. M. Mandell (1982). "Collagen-Metabolism in Rat Incisor Predentine Invivo - Synthesis and Maturation of Type-I, Alpha-1(I) Trimer, and Type-V Collagens." *Biochemistry* **21**(9): 2011-2015.
- Solé-Magdalena, A., E. G. Revuelta, et al. (2011). "Human Odontoblasts Express Transient Receptor Protein and Acid-Sensing Ion Channel Mechanosensor Proteins." *Microscopy Research and Technique* **74**(5): 457-463.
- Son, A. R., Y. M. Yang, et al. (2009). "Odontoblast Trp Channels and Thermo/Mechanical Transmission." *Journal of Dental Research* **88**(11): 1014-1019.
- Sottile, J. and J. Chandler (2005). "Fibronectin Matrix Turnover Occurs through a Caveolin-1-Independent Process." *Molecular Biology of the Cell* **16**(2): 757-768.
- Stevens, A., T. Zuliani, et al. (2008). "Human Dental Pulp Stem Cells Differentiate into Neural Crest-Derived Melanocytes and Have Label-Retaining and Sphere-Forming Abilities." *Stem Cells and Development* **17**(6): 1175-1184.

- Stevens, A., T. Zuliani, et al. (2008). "Human Dental Pulp Stem Cells Differentiate into Neural Crest-Derived Melanocytes and Have Label-Retaining and Sphere-Forming Abilities." *Stem Cells Dev* **17**(6): 1175-1184.
- Story, G. M., A. M. Peier, et al. (2003). "Anktm1, a Trp-Like Channel Expressed in Nociceptive Neurons, Is Activated by Cold Temperatures." *Cell* **112**(6): 819-829.
- Stucky, C. L., A. E. Dubin, et al. (2009). "Roles of Transient Receptor Potential Channels in Pain." *Brain Research Reviews* **60**(1): 2-23.
- Sudbury, J. R., S. Ciura, et al. (2010). "Osmotic and Thermal Control of Magnocellular Neurosecretory Neurons--Role of an N-Terminal Variant of Trpv1." *Eur J Neurosci* **32**(12): 2022-2030.
- Suzuki, M., J. Sato, et al. (1999). "Cloning of a Stretch-Inhibitable Nonselective Cation Channel." *J Biol Chem* **274**(10): 6330-6335.
- Svensson P, S. B. (2004). *Orofacial Pain*. Copenhagen, Quintessence.
- Svinicki, M. D. and W. J. McKeachie (2011). *McKeachie's Teaching Tips: Strategies, Research, and Theory for College and University Teachers*, Wadsworth Publishing Company.
- Takahashi, K., T. Nakanishi, et al. (2008). "Ccl20 Production Is Induced in Human Dental Pulp Upon Stimulation by Streptococcus Mutans and Proinflammatory Cytokines." *Oral Microbiology and Immunology* **23**(4): 320-327.
- Takayanagi, H. (2007). "The Role of Nfat in Osteoclast Formation." *Annals of the New York Academy of Sciences* **1116**(1): 227-237.
- Takeda, K., T. Kaisho, et al. (2003). "Toll-Like Receptors." *Annual Review of Immunology* **21**: 335-376.
- Tamaoki, N., K. Takahashi, et al. (2010). "Dental Pulp Cells for Induced Pluripotent Stem Cell Banking." *Journal of Dental Research* **89**(8): 773-778.
- Tao, Q., B. Lv, et al. (2009). "Immortalization of Ameloblastoma Cells Via Reactivation of Telomerase Function: Phenotypic and Molecular Characteristics." *Oral Oncology* **45**(12): e239-e244.
- Thesleff, I., S. Keranen, et al. (2001). "Enamel Knots as Signaling Centers Linking Tooth Morphogenesis and Odontoblast Differentiation." *Advances in Dental Research* **15**(1): 14-18.
- Thesleff, I. and C. Sahlberg (1996). "Growth Factors as Inductive Signals Regulating Tooth Morphogenesis." *Seminars in Cell & Developmental Biology* **7**(2): 185-193.
- Thorneloe, K. S., A. C. Sulpizio, et al. (2008). "N-((1s)-1-{ 4-((2s)-2-{ (2,4-Dichlorophenyl)Sulfonyl Amino}-3-Hydroxypro Panoyl)-1-Piperazinyl Carbonyl}-3-Methylbutyl)-1-Benzothiophene-2-Carbox Amide (Gsk1016790a), a Novel and Potent Transient Receptor Potential Vanilloid 4 Channel Agonist Induces Urinary Bladder Contraction and Hyperactivity: Part I." *Journal of Pharmacology and Experimental Therapeutics* **326**(2): 432-442.
- Thyagarajan, T., T. Sreenath, et al. (2001). "Reduced Expression of Dentin Sialophosphoprotein Is Associated with Dysplastic Dentin in Mice Overexpressing Transforming Growth Factor-Beta 1 in Teeth." *The Journal of biological chemistry* **276**(14): 11016-11020.
- Tight, M. (2012). *Researching Higher Education*, Open University Press.
- Tirino, V., F. Paino, et al. (2011). "Methods for the Identification, Characterization and Banking of Human Dpscs: Current Strategies and Perspectives." *Stem Cell Reviews and Reports* **7**(3): 608-615.
- Tjäderhane, L., T. Salo, et al. (1998). "A Novel Organ Culture Method to Study the Function of Human Odontoblasts in Vitro: Gelatinase Expression by Odontoblasts Is Differentially Regulated by Tgf-B1." *Journal of Dental Research* **77**(7): 1486-1496.
- Todd, A. J. (2010). "Neuronal Circuitry for Pain Processing in the Dorsal Horn." *Nat Rev Neurosci* **11**(12): 823-836.

- Tokuda, M., R. Miyamoto, et al. (2004). "Substance P Enhances Expression of Lipopolysaccharide-Induced Inflammatory Factors in Dental Pulp Cells." Journal of Endodontics **30**(11): 770-774.
- Tominaga, M. (2007). Nociception and Trp Channels. Handbook of Experimental Pharmacology. V. N. B. Flockerzi. **179**: 489-505.
- Tominaga, M., M. J. Caterina, et al. (1998). "The Cloned Capsaicin Receptor Integrates Multiple Pain-Producing Stimuli." Neuron **21**(3): 531-543.
- Torella, D., M. Rota, et al. (2004). "Cardiac Stem Cell and Myocyte Aging, Heart Failure, and Insulin-Like Growth Factor-1 Overexpression." Circulation Research **94**(4): 514-524.
- Torneck, C. D., K. C. Titley, et al. (1993). "Adhesion of a Resin Composite to Bleached and Unbleached Human Enamel." Journal of Endodontics **19**(3): 112-115.
- Tracey, I. and P. W. Mantyh (2007). "The Cerebral Signature and Its Modulation for Pain Perception." Neuron **55**(3): 377-391.
- Trantor, I. R., H. H. Messer, et al. (1995). "The Effects of Neuropeptides (Calcitonin Gene-Related Peptide and Substance P) on Cultured Human Pulp Cells." Journal of Dental Research **74**(4): 1066-1071.
- Treede, R. D. (1999). "Transduction and Transmission Properties of Primary Nociceptive Afferents." Ross Fiziol Zh Im I M Sechenova **85**(1): 205-211.
- Truini, A., L. Padua, et al. (2009). "Differential Involvement of  $\alpha$ -Delta and  $\alpha$ -Beta Fibres in Neuropathic Pain Related to Carpal Tunnel Syndrome." Pain **145**(1-2): 105-109.
- Tsukamoto, Y., S. Fukutani, et al. (1992). "Mineralized Nodule Formation by Cultures of Human Dental Pulp-Derived Fibroblasts." Archives of Oral Biology **37**(12): 1045-1055.
- Tsumura, M., R. Okumura, et al. (2010). "Ca<sup>2+</sup> Extrusion Via Na<sup>+</sup>-Ca<sup>2+</sup> Exchangers in Rat Odontoblasts." Journal of Endodontics **36**(4): 668-674.
- Tsumura, M., U. Sobhan, et al. (2012). "Trpv1-Mediated Calcium Signal Couples with Cannabinoid Receptors and Sodium-Calcium Exchangers in Rat Odontoblasts." Cell Calcium **52**(2): 124-136.
- Tziafas, D. (1995). "Basic Mechanisms of Cytodifferentiation and Dentinogenesis During Dental-Pulp Repair." International Journal of Developmental Biology **39**(1): 281-290.
- Uddman, R., T. Grunditz, et al. (1986). "Calcitonin Gene Related Peptide - a Sensory Transmitter in Dental Pulps." Scandinavian Journal of Dental Research **94**(3): 219-224.
- Uddman, R., J. Kato, et al. (1999). "Expression of Calcitonin Gene-Related Peptide-1 Receptor Mrna in Human Tooth Pulp and Trigeminal Ganglion." Archives of Oral Biology **44**(1): 1-6.
- Ushiyama, J. (1989). "Gap-Junctions between Odontoblasts Revealed by Transjunctional Flux of Fluorescent Tracers." Cell and Tissue Research **258**(3): 611-616.
- Valikangas, L., E. Pekkala, et al. (2001). "The Effects of High Levels of Glucose and Insulin on Type I Collagen Synthesis in Mature Human Odontoblasts and Pulp Tissue in Vitro." Advances in Dental Research **15**(1): 72-75.
- Vandesompele, J., M. Kubista, et al. (2009). Reference Gene Validation Software for Improved Normalization, Caister Academic Press.
- Voets, T., G. Droogmans, et al. (2004). "The Principle of Temperature-Dependent Gating in Cold- and Heat-Sensitive Trp Channels." Nature **430**(7001): 748-754.
- Voets, T., A. Janssens, et al. (2004). "Outer Pore Architecture of a Ca<sup>2+</sup>-Selective Trp Channel." Journal of Biological Chemistry **279**(15): 15223-15230.
- Vongsavan, N. and B. Matthews (1992). "Changes in the Rate of Fluid-Flow through Exposed Dentin Produced by Sympathetic and Inferior Alveolar Nerve-Stimulation in Anesthetized Cats." Journal of Physiology-London **446**: P209-P209.
- Vos, M. H., T. R. Neelands, et al. (2006). "Trpv1b Overexpression Negatively Regulates Trpv1 Responsiveness to Capsaicin, Heat and Low Ph in Hek293 Cells." Journal of Neurochemistry **99**(4): 1088-1102.

- Vriens, J., H. Watanabe, et al. (2004). "Cell Swelling, Heat, and Chemical Agonists Use Distinct Pathways for the Activation of the Cation Channel Trpv4." Proceedings of the National Academy of Sciences of the United States of America **101**(1): 396-401.
- Waddington, R. J., S. J. Youde, et al. (2009). "Isolation of Distinct Progenitor Stem Cell Populations from Dental Pulp." Cells Tissues Organs **189**(1-4): 268-274.
- Wakisaka, S. and M. Akai (1989). "Immunohistochemical Observation on Neuropeptides around the Blood-Vessel in Feline Dental-Pulp." Journal of Endodontics **15**(9): 413-416.
- Wang, C., H.-Z. Hu, et al. (2004). "An Alternative Splicing Product of the Murine Trpv1 Gene Dominant Negatively Modulates the Activity of Trpv1 Channels." Journal of Biological Chemistry **279**(36): 37423-37430.
- Watanabe, H., J. Vriens, et al. (2002). "Heat-Evoked Activation of Trpv4 Channels in a Hek293 Cell Expression System and in Native Mouse Aorta Endothelial Cells." Journal of Biological Chemistry **277**(49): 47044-47051.
- Watson, J. D. and F. H. C. Crick (1993). "Molecular-Structure of Nucleic-Acids - a Structure for Deoxyribose Nucleic-Acid." Jama-Journal of the American Medical Association **269**(15): 1966-1967.
- Watson, J. D. and F. H. C. Crick (2003). "Molecular Structure of Nucleic Acids - a Structure for Deoxyribose Nucleic Acid (Reprinted from Nature, Vol 171, Pg 737-738, 1953)." Revista De Investigacion Clinica **55**(2): 108-109.
- Weinreich, D., K. A. Moore, et al. (1997). "Allergic Inflammation in Isolated Vagal Sensory Ganglia Unmasks Silent Nk-2 Tachykinin Receptors." Journal of Neuroscience **17**(20): 7683-7693.
- Wen, J., R. Tao, et al. (2010). "Immunolocalization and Expression of Runx2 in Tertiary Dentinogenesis." Hybridoma **29**(3): 195-199.
- Wilfinger, W. W., K. Mackey, et al. (1997). "Effect of Ph and Ionic Strength on the Spectro-Photometric Assessment of Nucleic Acid Purity." Biotechniques **22**(3): 474-&.
- Willis, W. D., Jr. (1985). "The Pain System. The Neural Basis of Nociceptive Transmission in the Mammalian Nervous System." Pain Headache **8**: 1-346.
- Woelfel, J. B. (1990). "Dental Anatomy Its Relevance to Dentistry Fourth Edition." Woelfel, J. B. Dental Anatomy: Its Relevance to Dentistry, Fourth Edition. X+438p. Lea and Febiger: Philadelphia, Pennsylvania, USA; London, England, Uk. Illus. Paper: X+438P.
- Wojtowicz, A. M., K. L. Templeman, et al. (2010). "Runx2 Overexpression in Bone Marrow Stromal Cells Accelerates Bone Formation in Critical-Sized Femoral Defects." Tissue Engineering Part A **16**(9): 2795-2808.
- Wright, W. E. and J. W. Shay (2000). "Telomere Dynamics in Cancer Progression and Prevention: Fundamental Differences in Human and Mouse Telomere Biology." Nat Med **6**(8): 849-851.
- Wu, I. B. and R. A. Schwartz (2008). "Reiter's Syndrome: The Classic Triad and More." J Am Acad Dermatol **59**(1): 113-121.
- Xu, H. X., I. S. Ramsey, et al. (2002). "Trpv3 Is a Calcium-Permeable Temperature-Sensitive Cation Channel." Nature **418**(6894): 181-186.
- Yang, X., J. van den Dolder, et al. (2007). "The Odontogenic Potential of Stro-1 Sorted Rat Dental Pulp Stem Cells in Vitro." Journal of Tissue Engineering and Regenerative Medicine **1**(1): 66-73.
- Yarbrough, D. K., E. Hagerman, et al. (2010). "Specific Binding and Mineralization of Calcified Surfaces by Small Peptides." Calcified Tissue International **86**(1): 58-66.
- Yilmaz, Z., T. Renton, et al. (2007). "Burning Mouth Syndrome as a Trigeminal Small Fibre Neuropathy: Increased Heat and Capsaicin. Receptor Trpv1 in Nerve Fibres Correlates with Pain Score." Journal of Clinical Neuroscience **14**(9): 864-871.

- 
- Yokose, S., H. Kadokura, et al. (2000). "Establishment and Characterization of a Culture System for Enzymatically Released Rat Dental Pulp Cells." Calcified Tissue International **66**(2): 139-144.
- Yoshie, O., T. Imai, et al. (2001). "Chemokines in Immunity." Advances in Immunology, Vol 78 **78**: 57-110.
- Yu, C., Abbott, PV. (2007). "An Overview of the Dental Pulp: Its Functions and Responses to Injury." Australian Dental Journal **52**(s1): S4-S6.
- Yu, J., H. He, et al. (2010). "Differentiation Potential of Stro-1+ Dental Pulp Stem Cells Changes During Cell Passaging." BMC Cell Biol **11**: 32.
- Zakharian, E., C. Cao, et al. (2010). "Gating of Transient Receptor Potential Melastatin 8 (Trpm8) Channels Activated by Cold and Chemical Agonists in Planar Lipid Bilayers." Journal of Neuroscience **30**(37): 12526-12534.
- Zanotto, K. L., A. W. Merrill, et al. (2007). "Neurons in Superficial Trigeminal Subnucleus Caudalis Responsive to Oral Cooling, Menthol, and Other Irritant Stimuli." Journal of Neurophysiology **97**(2): 966-978.
- Zartman, R., A. McWhorter, et al. (2002). "Using Osce-Based Evaluation: Curricular Impact over Time." Journal of Dental Education **66**(12): 1323-1330.
- Zhang, H., C. L. Cang, et al. (2007). "Neurokinin-1 Receptor Enhances Trpv1 Activity in Primary Sensory Neurons Via Pkc $\epsilon$ : A Novel Pathway for Heat Hyperalgesia." Journal of Neuroscience **27**(44): 12067-12077.
- Zhao, R. B., K. Gish, et al. (2000). "Analysis of P53-Regulated Gene Expression Patterns Using Oligonucleotide Arrays." Genes & Development **14**(8): 981-993.
- Zlotnik, A. and O. Yoshie (2000). "Chemokines: A New Classification System and Their Role in Immunity." Immunity **12**(2): 121-127.